INTRODUCTION TO THEORETICAL GEOMECHANICS

Chloé Arson
Georgia Institute of Technology

CONTENTS

PART II   DEFORMATION AND FLOW IN POROUS MEDIA

PART III YIELD AND FAILURE OF GEOMATERIALS

PART IV APPENDICES

GLOSSARY

Irrotational fluid flow

> When individual parcels of a frictionless incompressible fluid initially at rest cannot be caused to rotate, the fluid flow is said to be irrotationnal. Mathematically, the curl of the velocity field is zero.

Newtonian fluid

> Fluid in which the viscous stresses arising from its flow, at every point, are linearly proportional to the local strain rate.

Plastic collapse

> Indefinitely increasing deformations under constant loads.

Representative Elementary Volume

> The minimum volume above which the average field variables of interest do not vary as the volume used for averaging is increased. Noted "REV".

PART I

GEOMECHANICS IN ELASTICITY

CHAPTER 1

REVIEW OF TENSOR ALGEBRA

Physical laws should be independent of the position and orientation of the observer. Therefore, equations that describe physical laws are vector or tensor equations, since vectors and tensors transform from one system to another in such a way that if the vector or tensor equation holds for one coordinate system, it holds for any other coordinate system not moving relative to the first on, i.e. in any other coordinate system in the same reference frame. Invariance in the form of a physical law referred to two frames of reference in accelerated motion relative to each other is more difficult and requires tensors in four-dimensional space-time. In what follows, we provide a brief overview of tensor algebra as it pertains to continuum mechanics. We use the so-called Einstein's notation for repeated indices, so that when an index appears at least twice in an expression, that means that there is a summation over the values of that index. For example, if $i \in [1, ..., n]$ and $j \in [1, ..., m]$:

$$v_i \boldsymbol{e}_i = \sum_{i=1}^{n} v_i \boldsymbol{e}_i \tag{1.1}$$

$$a_{ii} = \sum_{i=1}^{n} a_{ii} \tag{1.2}$$

$$a_{ij} b_{ij} = \sum_{j=1}^{m} \sum_{i=1}^{n} a_{ij} b_{ij} \tag{1.3}$$

1.1 Vectors

In three-dimensional Euclidian space, vectors are physical quantities that possess magnitude and direction and obey certain laws. Scalars, on the other hand, have no direction associated with them, although some scalars may have positive or negative values associated with them. Vectors are conventionally represented by an arrow, which points in the direction associated with the vector and has length proportional to the magnitude of the vector. Typical examples include forces, velocity, and acceleration.

A vector can be noted $\vec{v}$, $\boldsymbol{v}$ or $\underline{v}$. A unit vector is a vector of norm (or length) equal to one. In 3D, a direct orthonormal basis is formed by three orthogonal unit vectors $\underline{e}_1$, $\underline{e}_2$ and $\underline{e}_3$ that are oriented in such a way that the angles $(\underline{e}_1, \underline{e}_2)$, $(\underline{e}_2, \underline{e}_3)$ and $(\underline{e}_3, \underline{e}_1)$ are $+90^o$, where positive is counter-clockwise. A vector $\boldsymbol{v}$ is decomposed as:

$$\boldsymbol{v} = v_1\boldsymbol{e}_1 + v_2\boldsymbol{e}_2 + v_3\boldsymbol{e}_3 \tag{1.4}$$

where the scalars v_1, v_2 and v_3 are called the components of $\boldsymbol{v}$ in directions 1, 2 and 3, respectively. The scalar product between two vectors $\boldsymbol{a}$ and $\boldsymbol{b}$ is noted $\boldsymbol{a} \cdot \boldsymbol{b}$ and is defined as:

$$\boldsymbol{a} \cdot \boldsymbol{b} = \sum_{i=1}^{3} a_i\, b_i\, \boldsymbol{e}_i \tag{1.5}$$

The cross product between two vectors $\boldsymbol{a}$ and $\boldsymbol{b}$ is noted $\boldsymbol{a} \times \boldsymbol{b}$ and is defined as:

$$\boldsymbol{a} \times \boldsymbol{b} = (a_2b_3 - a_3b_2)\boldsymbol{e}_1 + (a_3b_1 - a_1b_3)\boldsymbol{e}_2 + (a_1b_2 - a_2b_1)\boldsymbol{e}_3 \tag{1.6}$$

The vector $\boldsymbol{a} \times \boldsymbol{b}$ is orthogonal to $\boldsymbol{a}$ and $\boldsymbol{b}$ and the vectors $\boldsymbol{a}$, $\boldsymbol{b}$ and $\boldsymbol{a} \times \boldsymbol{b}$ form a direct orthogonal basis. The norm of a vector $\boldsymbol{v}$ can be calculated as:

$$|\boldsymbol{v}| = \sqrt{\boldsymbol{v} \cdot \boldsymbol{v}} \tag{1.7}$$

Below are some remarkable properties of the cross product:

$$\boldsymbol{a} \times (\boldsymbol{b} \times \boldsymbol{c}) = (\boldsymbol{a} \cdot \boldsymbol{c})\boldsymbol{b} - (\boldsymbol{a} \cdot \boldsymbol{b})\boldsymbol{c} \tag{1.8}$$

$$(\boldsymbol{a} \times \boldsymbol{d}) \cdot (\boldsymbol{b} \times \boldsymbol{c}) = (\boldsymbol{a} \cdot \boldsymbol{b})(\boldsymbol{c} \cdot \boldsymbol{d}) - (\boldsymbol{a} \cdot \boldsymbol{c})(\boldsymbol{b} \cdot \boldsymbol{d}) \tag{1.9}$$

The following is known as Jacobi's formula:

$$\boldsymbol{a} \times (\boldsymbol{b} \times \boldsymbol{c}) + \boldsymbol{b} \times (\boldsymbol{c} \times \boldsymbol{a}) + \boldsymbol{c} \times (\boldsymbol{a} \times \boldsymbol{b}) = \boldsymbol{0} \tag{1.10}$$

1.2 Matrices and tensors of order 2

1.2.1 Matrices

1.2.1.1 Basic operations
Matrices of the same order add term by term, i.e.

$$[A] \pm [B] = [C] \tag{1.11}$$

is calculated as:

$$\forall i, j, \quad A_{ij} \pm B_{ij} = C_{ij} \tag{1.12}$$

Matrices must be conformable or else they cannot be multiplied. Matrices A and B are conformable and can be multiplied in the order AB, if the first matrix has the same number of columns as the second matrix has rows. Assuming that A has n columns and B has n rows, the two matrices are then multiplied as follows:

$$[A][B] = [C] \tag{1.13}$$

is calculated as:

$$\forall i, j, \quad \sum_{k=1}^{n} A_{ik} \pm B_{kj} = C_{ij} \tag{1.14}$$

In general, matrix multiplication is non-commutative, i.e.

$$[A][B] \neq [B][A] \tag{1.15}$$

Matrix multiplication is associative, i.e.

$$([A][B])[C] = [A]([B][C]) \tag{1.16}$$

1.2.1.2 Special matrices

A diagonal matrix is a square matrix with nonzero elements only on the main diagonal, i.e. the elements M_{ij} of the diagonal matrix $[M]$ are non-zero if and only if $i = j$. An identity matrix, denoted by $[I]$, is a diagonal matrix with each diagonal element equal to unity. The elements of the identity matrix are δ_{ij}, which is the Kronecker delta: $\delta_{ij} = 1$ if $i = j$ and $\delta_{ij} = 0$ otherwise.

The transpose of a matrix $[M]$ is noted $[M]^T$ is the matrix obtained by interchanging rows and columns, i.e. for all i,j: $M_{ij}^T = M_{ji}$. The transpose of a matrix product is:

$$([M_1][M_2][M_3]...[M_n])^T = [M_n]^T...[M_3]^T[M_2]^T[M_1]^T \tag{1.17}$$

A symmetric matrix is a square matrix with equal elements in the positions symmetrically placed with respect to the main diagonal, i.e. $\forall i, j, \quad M_{ij} = M_{ji}$. A skew or anti-symmetric matrix is such that $\forall i, j, \quad M_{ij} = -M_{ji}$, which implies that the diagonal elements are all zero. We can always substitute a matrix $[A]$ by the summation of a symmetric matrix $[B]$ and an anti-symmetric matrix, as follows:

$$[A] = [B] + [C], \quad [B] = \frac{1}{2}\left([A] + [A]^T\right), \quad [C] = \frac{1}{2}\left([A] - [A]^T\right) \tag{1.18}$$

The inverse $[M]^{-1}$ of a matrix $[M]$ is defined as:

$$[M]^{-1}[M] = [M][M]^{-1} = [I] \tag{1.19}$$

A matrix $[M]$ is said to be orthogonal if:

$$[M]^T[M] = [M][M]^T = [I] \tag{1.20}$$

Therefore, for an orthogonal matrix we have:

$$[M]^T = [M]^{-1} \tag{1.21}$$

1.2.1.3 Determinant of a matrix

A matrix is singular (i.e., non-invertible), if, and only if, its determinant is zero. Geometrically, the determinant can be viewed as the volume scaling factor of the linear transformation described by the matrix. This is also the signed volume of the n-dimensional parallelepiped spanned by the column or row vectors of the matrix. The determinant is positive or negative according to whether the linear mapping preserves or reverses the orientation of n-space [21]. The determinant of a matrix $[A]$ is noted $\det(A)$ or $|A|$. The Leibniz formula for the determinant of an n x n matrix $[A]$ is:

$$\det(A) = \sum_{\sigma \in S_n} (\text{sgn}(\sigma)) \prod_{i=1}^{n} a_{i,\sigma_i} \tag{1.22}$$

Here the sum is computed over all permutations σ of the set $\{1, 2, ..., n\}$. A permutation is a function that reorders this set of integers. The value in the ith position after the reordering σ is denoted by σ_i. For example, for $n = 3$, the original sequence 1, 2, 3 might be reordered to $\sigma = [2, 3, 1]$, with $\sigma_1 = 2$, $\sigma_2 = 3$, and $\sigma_3 = 1$. The set of all such permutations (also known as the symmetric group on n elements) is denoted by S_n. For each permutation σ, $\text{sgn}(\sigma)$ denotes the signature of σ, a value that is +1 whenever the reordering given by σ can be achieved by successively interchanging two entries an even number of times, and -1 whenever it can be achieved by an odd number of such interchanges. For a 2 x 2 matrix $[A]$, it can be shown that:

$$\det(A) = A_{11}A_{22} - A_{12}A_{21} \tag{1.23}$$

For a 3 x 3 matrix, it can be shown that:

$$\det(A) \quad = \quad A_{11} \det \left(\begin{bmatrix} A_{22} & A_{23} \\ A_{32} & A_{33} \end{bmatrix} \right) \tag{1.24}$$

$$-A_{12} \det \left(\begin{bmatrix} A_{21} & A_{23} \\ A_{31} & A_{33} \end{bmatrix} \right) + A_{13} \det \left(\begin{bmatrix} A_{21} & A_{22} \\ A_{31} & A_{32} \end{bmatrix} \right)$$

1.2.1.4 Eigenvalues and eigenvectors

A vector $\boldsymbol{v}$ is an eigenvector of the matrix $[M]$ if:

$$[M]\boldsymbol{v} = \lambda \boldsymbol{v} \tag{1.25}$$

in which λ is a scalar called an eigenvalue of the matrix $[M]$. Equation 1.25 is true if and only if:

$$([M] - \lambda[I])\,\boldsymbol{v} = \boldsymbol{0} \tag{1.26}$$

If the vector $\boldsymbol{v}$ is non zero, equation 1.26 implies that the determinant of the matrix $([M] - \lambda[I])$ is zero:

$$det\left([M] - \lambda[I]\right) = 0 \tag{1.27}$$

By developping the determinant for a 3x3 matrix, we obtain:

$$
det\left([M] - \lambda[I]\right) = det\left(\begin{bmatrix} M_{11} - \lambda & M_{12} & M_{13} \\ M_{21} & M_{22} - \lambda & M_{23} \\ M_{31} & M_{32} & M_{33} - \lambda \end{bmatrix}\right) \tag{1.28}
$$

$$
= (M_{11} - \lambda)\, det\begin{bmatrix} M_{22} - \lambda & M_{23} \\ M_{32} & M_{33} - \lambda \end{bmatrix}
$$

$$
-M_{12}\, det\begin{bmatrix} M_{21} & M_{23} \\ M_{31} & M_{33} - \lambda \end{bmatrix}
$$

$$
+M_{13}\, det\begin{bmatrix} M_{21} & M_{22} - \lambda \\ M_{31} & M_{32} \end{bmatrix}
$$

which can be re-arranged as:

$$
det\left([M] - \lambda[I]\right) = -\lambda^3 + A_1\lambda^2 - A_2\lambda + A_3 \tag{1.29}
$$

in which:

$$
A_1 = M_{11} + M_{22} + M_{33} \tag{1.30}
$$

$$
A_2 = (M_{11}M_{22} - M_{12}M_{21}) + (M_{22}M_{33} - M_{23}M_{32}) + (M_{11}M_{33} - M_{13}M_{31})
$$

$$
A_3 = det[M]
$$

The three coefficients A_1, A_2 and A_3 are frame invariants, and the characteristic equation (equation 1.29) has three real solutions, referred to as eigenvalues (noted λ_1, λ_2 and λ_3). Correspondingly, there are three eigenvectors v_1, v_2 and v_3, which can be found by solving the following equations:

$$
\forall i = 1, 2, 3, \quad [M]v_i = \lambda_i v_i \tag{1.31}
$$

Any sqaure matrix can be transformed to the base of eigen vectors. Noting n_1, n_2 and n_3 the eigenvectors, we have:

$$
\boldsymbol{M} = \lambda_1\, \boldsymbol{n}_1 \otimes \boldsymbol{n}_1 + \lambda_2\, \boldsymbol{n}_2 \otimes \boldsymbol{n}_2 + \lambda_3\, \boldsymbol{n}_3 \otimes \boldsymbol{n}_3 \tag{1.32}
$$

The stress tensor $\boldsymbol{\sigma}$ is often times written in the form of a square matrix. The eigenvalues of the stress matrix ($\lambda_1 = \sigma_1$, $\lambda_2 = \sigma_2$ and $\lambda_3 = \sigma_3$) define the values of the so-called principal stresses. The normalized eigenvectors n_1, n_2 and n_3 define the directions of the principal stresses.

1.2.1.5 *Rotation matrices*
A rotation matrix $[Q]$ is an orthogonal matrix with a determinant equal to unity:

$$
[Q]^T[Q] = [I], \quad [Q][Q]^T = [I], \quad det[Q] = 1 \tag{1.33}
$$

In 2D, the matrix that operates a rotation by an angle θ in a direct orthonormal coordinate system is:
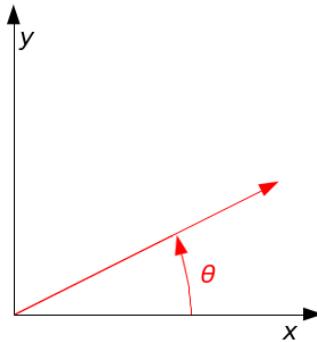
$$\mathcal{R}(\theta) = \begin{pmatrix} \cos\theta & \sin\theta \\ -\sin\theta & \cos\theta \end{pmatrix} \tag{1.34}$$

Figure 1.1 illustrates the transformation operated by $\mathcal{R}(\theta)$. To transform a vector, the following operation is needed:

$$\boldsymbol{v}' = \mathcal{R}(\theta) \cdot \boldsymbol{v} \tag{1.35}$$

To transform a matrix (or a tensor of order 2), the following operation is needed:

$$\boldsymbol{A}' = \mathcal{R}(\theta) \cdot \boldsymbol{A} \cdot \mathcal{R}^T(\theta) \tag{1.36}$$

Figure 1.1 Transformation operated by $\mathcal{R}(\theta)$. Image taken from *Wikipedia*, Jan. 2020.

In a 3D Euclidian space, the following rotation matrices operate rotations about the x, y and z axes respectively:

$$\mathcal{R}_x(\theta) = \begin{pmatrix} 1 & 0 & 0 \\ 0 & \cos\theta & \sin\theta \\ 0 & -\sin\theta & \cos\theta \end{pmatrix} \tag{1.37}$$

$$\mathcal{R}_y(\theta) = \begin{pmatrix} \cos\theta & 0 & -\sin\theta \\ 0 & 1 & 0 \\ \sin\theta & 0 & \cos\theta \end{pmatrix} \tag{1.38}$$

$$\mathcal{R}_z(\theta) = \begin{pmatrix} \cos\theta & \sin\theta & 0 \\ -\sin\theta & \cos\theta & 0 \\ 0 & 0 & 1 \end{pmatrix} \tag{1.39}$$

The rotation matrix that accounts for all three rotations is the product of the three operators above:

$$\mathcal{R}(\alpha, \beta, \gamma) = \mathcal{R}_x(\alpha) \cdot \mathcal{R}_y(\beta) \cdot \mathcal{R}_z(\gamma) \tag{1.40}$$

1.2.2   Tensors of order 2

A second-order tensor is a linear function which associates a vector (say, $\boldsymbol{b}$) to another vector (say, $\boldsymbol{a}$). A second-order tensor is usually noted with a capital letter, as $\boldsymbol{A}$ or $\underline{\underline{A}}$:

$$\boldsymbol{b} = \boldsymbol{A}\left(\boldsymbol{a}\right) \tag{1.41}$$

By definition of linearity, $\boldsymbol{A}$ satisfies:

$$\boldsymbol{A}\left(\lambda\boldsymbol{a}\right) = \lambda\boldsymbol{b} \tag{1.42}$$

in which λ is a scalar; and:

$$\boldsymbol{A}\left(\boldsymbol{a}_1 + \boldsymbol{a}_2\right) = \boldsymbol{b}_1 + \boldsymbol{b}_2 \tag{1.43}$$

if $\boldsymbol{b}_1 = \boldsymbol{A}\left(\boldsymbol{a}_1\right)$ and $\boldsymbol{b}_2 = \boldsymbol{A}\left(\boldsymbol{a}_2\right)$.

A second order tensor $\boldsymbol{A}$ can be represented in a matrix form. For example, in a three-dimensional space:

$$[\boldsymbol{A}] = \begin{bmatrix} A_{11} & A_{12} & A_{13} \\ A_{21} & A_{22} & A_{23} \\ A_{31} & A_{32} & A_{33} \end{bmatrix} \tag{1.44}$$

As a result, matrix properties apply to tensors of order 2. Some of these properties are summarized below.

The transpose of a tensor $\boldsymbol{A}$ of order 2 is noted $\boldsymbol{A}^T$ and is defined as:

$$\forall i, j, \quad A_{ij}^T = A_{ji} \tag{1.45}$$

A tensor $\boldsymbol{A}$ of order 2 is symmetric if, and only if:

$$\boldsymbol{A} = \boldsymbol{A}^T \tag{1.46}$$

A tensor $\boldsymbol{A}$ of order 2 is anti-symmetric (also called "skew") if, and only if:

$$\boldsymbol{A} = -\boldsymbol{A}^T \tag{1.47}$$

A tensor can always be decomposed into a symmetric part $\boldsymbol{A}_s$ and an anti-symmetric part $\boldsymbol{A}_s$ as follows:

$$\boldsymbol{A} = \boldsymbol{A}_s + \boldsymbol{A}_a, \quad \boldsymbol{A}_s = \frac{1}{2}\left(\boldsymbol{A} + \boldsymbol{A}^T\right), \quad \boldsymbol{A}_a = \frac{1}{2}\left(\boldsymbol{A} - \boldsymbol{A}^T\right) \tag{1.48}$$

The tensorial product of two vectors $\boldsymbol{a}$ and $\boldsymbol{b}$ is a second-order tensor noted $\boldsymbol{a} \otimes \boldsymbol{b}$ and defined as:

$$\boldsymbol{a} \otimes \boldsymbol{b} = \begin{bmatrix} a_1b_1 & a_1b_2 & a_1b_3 \\ a_2b_1 & a_2b_2 & a_2b_3 \\ a_3b_1 & a_3b_2 & a_3b_3 \end{bmatrix} \tag{1.49}$$

which can also be noted as:

$$\boldsymbol{a} \otimes \boldsymbol{b} = \left(\sum_{i=1}^{3} a_i\boldsymbol{e}_i\right) \otimes \left(\sum_{j=1}^{3} b_j\boldsymbol{e}_j\right) = \sum_{i=1}^{3}\sum_{j=1}^{3} a_ib_j\boldsymbol{e}_i \otimes \boldsymbol{e}_j = a_ib_j\boldsymbol{e}_i \otimes \boldsymbol{e}_j \tag{1.50}$$

in which we used Einstein's notation in the right-hand side member of the equation. The tensorial product of two tensors of order 2 $\boldsymbol{A}$ and $\boldsymbol{B}$ is a fourth order tensor noted $\boldsymbol{A} \otimes \boldsymbol{B}$ and defined as:

$$\boldsymbol{A} \otimes \boldsymbol{B} = \sum_i \sum_j \sum_k \sum_l A_{ij} B_{kl} \, \boldsymbol{e}_i \otimes \boldsymbol{e}_j \otimes \boldsymbol{e}_k \otimes \boldsymbol{e}_l \tag{1.51}$$

The dot product between two vectors is the scalar product of these two vectors. The dot product between two tensors of order 2 $\boldsymbol{A}$ and $\boldsymbol{B}$ is a tensor of order 2, noted $\boldsymbol{A} \cdot \boldsymbol{B}$ and defined in index notation as:

$$\forall i, j, \quad (\boldsymbol{A} \cdot \boldsymbol{B})_{ij} = \sum_k A_{ik} B_{kj} = A_{ik} B_{kj} \tag{1.52}$$

in which we used Einstein's notation in the right-hand side of the equation above. The dot product can be viewed as a tensorial product in which the last index of the first tensor is "contracted" (or merged) with the first index of the second tensor. As a result, the dot product between a vector $\boldsymbol{v}$ and a tensor of order 2 $\boldsymbol{A}$ is a vector noted $\boldsymbol{v} \cdot \boldsymbol{A}$ and defined in index notation as:

$$\forall i, \quad (\boldsymbol{v} \cdot \boldsymbol{A})_i = \sum_k v_k A_{ki} = v_k A_{ki} \tag{1.53}$$

Similarly, the dot product $\boldsymbol{A} \cdot \boldsymbol{v}$ is defined as:

$$\forall i, \quad (\boldsymbol{A} \cdot \boldsymbol{v})_i = \sum_k A_{ik} v_k = A_{ik} v_k \tag{1.54}$$

in which we used Einstein's notation in the right-hand side of the two equations above. The double-dot product is a double contraction of indices, i.e. the double-dot product of two tensors of order 2 $\boldsymbol{A}$ and $\boldsymbol{B}$ is such that the second index of $\boldsymbol{A}$ is set equal to the first index of $\boldsymbol{B}$, and the first index of $\boldsymbol{A}$ is set equal to the second index of $\boldsymbol{B}$. The double-dot product of two tensors of order 2 $\boldsymbol{A}$ and $\boldsymbol{B}$ is a scalar noted $\boldsymbol{A} : \boldsymbol{B}$ and is defined as:

$$\boldsymbol{A} : \boldsymbol{B} = \sum_{i,j} A_{ij} \, B_{ji} = A_{ij} \, B_{ji} \tag{1.55}$$

in which we used Einstein's notation in the right-hand side of the equation above. We can readily see that:

$$\boldsymbol{A} : \boldsymbol{B} = A_{ij} \, B_{ji} = B_{ji} \, A_{ij} = \boldsymbol{B} : \boldsymbol{A} \tag{1.56}$$

1.3   Higher-order tensors

Let us consider an Euclidian space E endowed with an othronormal base $(\boldsymbol{e}_1, \boldsymbol{e}_2, \boldsymbol{e}_3)$. Any tensor of order 2 $\boldsymbol{A}$ can be decomposed into:

$$\boldsymbol{A} = \sum_{i=1}^3 \sum_{j=1}^3 A_{ij} \, \boldsymbol{e}_i \otimes \boldsymbol{e}_j \tag{1.57}$$

Any tensor of order 2 is a bilinear function of E, i.e., in the equation above, every tensor $A_{ij} \, \boldsymbol{e}_i \otimes \boldsymbol{e}_j$ is linear in $\boldsymbol{e}_i$ and in $\boldsymbol{e}_j$. More generally, a tensor of order p is a p-linear

function of E, i.e. a function that is linear in each of its p arguments. Noting $\mathcal{T}^{(p)}$ a tensor of order p, we have:

$$\mathcal{T}^{(p)}\left(\boldsymbol{e}_{k_1}, \boldsymbol{e}_{k_2}, ..., \boldsymbol{e}_{k_p}\right) = \mathcal{T}_{k_1 k_2 ... k_p} \tag{1.58}$$

or equivalently:

$$\mathcal{T}^{(p)} = \sum_{k_1=1}^{3} \sum_{k_2=1}^{3} ... \sum_{k_p}^{3} \mathcal{T}_{k_1 k_2 ... k_p}\, \boldsymbol{e}_{k_1} \otimes \boldsymbol{e}_{k_2} \otimes ... \otimes \boldsymbol{e}_{k_p} \tag{1.59}$$

A scalar is a tensor of order 0 (for example, mass or temperature). A vector is a tensor of order 1 (for example, displacement, velocity or flux). Stress and strain are tensors of order 2. The stiffness that relates a stress to a strain is a tensor of order 4.

The tensorial product of a tensor $\mathcal{T}^{(p)}$ of order p and of a tensor $\mathcal{T}'^{(q)}$ or order q is a tensor of order $p + q$, noted $\mathcal{T}^{(p)} \otimes \mathcal{T}'^{(q)}$ and defined as:

$$\mathcal{T}^{(p)} \otimes \mathcal{T}'^{(q)} = \tag{1.60}$$

$$\sum_{k_1=1}^{3} \sum_{k_2=1}^{3} ... \sum_{k_p}^{3} \sum_{k_{p+1}}^{3} ... \sum_{k_{p+q}}^{3} \mathcal{T}_{k_1 k_2 ... k_p}\, \mathcal{T}'_{k_{p+1} k_{p+2} ... k_{p+q}}\, \boldsymbol{e}_{k_1} \otimes \boldsymbol{e}_{k_2} \otimes ... \otimes \boldsymbol{e}_{k_p} \otimes \boldsymbol{e}_{k_{p+1}} \otimes ... \otimes \boldsymbol{e}_{k_{p+q}}$$

The dot, double-dot and triple dot products reduce the order of the resulting tensor by, 2, 4 and 6, respectively, by contracting 2, 4 and 6 indices, as follows:

$$\mathcal{T}^{(p)} \cdot \mathcal{T}'^{(q)} = \mathcal{T}_{k_1 k_2 ... k_{p-1} k_i}\, \mathcal{T}'_{k_i k_{p+2} ... k_{p+q}}\, \boldsymbol{e}_{k_1} \otimes \boldsymbol{e}_{k_2} \otimes ... \otimes \boldsymbol{e}_{k_{p-1}} \otimes \boldsymbol{e}_{k_{p+2}} \otimes ... \otimes \boldsymbol{e}_{k_{p+q}} \tag{1.61}$$

$$\mathcal{T}^{(p)} : \mathcal{T}'^{(q)} = \mathcal{T}_{k_1 k_2 ... k_{p-2} k_j k_i}\, \mathcal{T}'_{k_i k_j k_{p+3} ... k_{p+q}}\, \boldsymbol{e}_{k_1} \otimes \boldsymbol{e}_{k_2} \otimes ... \otimes \boldsymbol{e}_{k_{p-2}} \otimes \boldsymbol{e}_{k_{p+3}} \otimes ... \otimes \boldsymbol{e}_{k_{p+q}} \tag{1.62}$$

$$\mathcal{T}^{(p)} \vdots \mathcal{T}'^{(q)} = \mathcal{T}_{k_1 k_2 ... k_{p-3} k_l k_j k_i}\, \mathcal{T}'_{k_i k_j k_l k_{p+4} ... k_{p+q}}\, \boldsymbol{e}_{k_1} \otimes \boldsymbol{e}_{k_2} \otimes ... \otimes \boldsymbol{e}_{k_{p-3}} \otimes \boldsymbol{e}_{k_{p+4}} \otimes ... \otimes \boldsymbol{e}_{k_{p+q}} \tag{1.63}$$

in which we are using Einstein's notation for repeated indices. Higher-order dot products are defined in the same way as the above.

A well-known double-dot product is the one that relates the stress tensor to the strain tensor:

$$\boldsymbol{\sigma} = \mathcal{C} : \boldsymbol{\epsilon} \tag{1.64}$$

In index notation:

$$\forall i, j, \quad \sigma_{ij} = \mathcal{C}_{ijkl}\, \epsilon_{lk} \tag{1.65}$$

in which there is a summation on the k and l indices, according to Einstein's notation. Other interesting results follow.

$$\boldsymbol{e}_i \cdot \mathcal{C} \cdot \boldsymbol{e}_j = \mathcal{C}_{iklj} \boldsymbol{e}_k \otimes \boldsymbol{e}_l \tag{1.66}$$

in which there is a summation on the k and l indices, according to Einstein's notation.

$$(\boldsymbol{e}_i \otimes \boldsymbol{e}_j) : \mathcal{C} : (\boldsymbol{e}_k \otimes \boldsymbol{e}_l) = \mathcal{C}_{ijkl} \tag{1.67}$$

in which there is no summation.

1.4 Differential operations with tensors

1.4.1 Derivative of a scalar function by a tensor

Consider a scalar function ψ that depends on a second-order tensorial variable $\boldsymbol{A}$. Let us assume that ψ is differentiable in terms of the components of $\boldsymbol{A}$. We have:

$$d\psi = \frac{\partial \psi}{\partial A_{ij}} dA_{ij} \tag{1.68}$$

in which Einstein's convention is used for repeated indices. We note:

$$\frac{\partial \psi}{\partial \boldsymbol{A}} = \frac{\partial \psi}{\partial A_{ij}} \boldsymbol{e}_i \otimes \boldsymbol{e}_j \tag{1.69}$$

again, with Eintein's convention for the repeated indices. From equations 1.68 and 1.69, we have:

$$d\psi = \frac{{}^T \partial \psi}{\partial \boldsymbol{A}} : d\boldsymbol{A} \tag{1.70}$$

Equation 1.70 is the intrinsic definition of the derivative of ψ by $\boldsymbol{A}$. Note that the definition takes the same form if $\boldsymbol{A}$ is a first- or higher-order tensor.

1.4.2 Gradient of a tensor field

The gradient of a scalar tensor T is noted $\underline{\nabla} T$ or $grad T$ and is defined to be the vector such that for any unit vector $\underline{n}$, the directional derivative dT/ds in the direction of $\underline{n}$ is given by the scalar product:

$$\frac{dT}{ds} = \underline{\nabla} T \cdot \underline{n} \tag{1.71}$$

The geometric interpretation of the gradient, illustrated in 2D in Figure 1.2, follows from the definition in equation 1.72, if we take $\underline{n}$ as the tangent vector $\underline{t}$ to the level surface $T(x_1, x_2, x_3) = constant$. Then, $dT/ds = 0$ and equation 1.72 implies that:
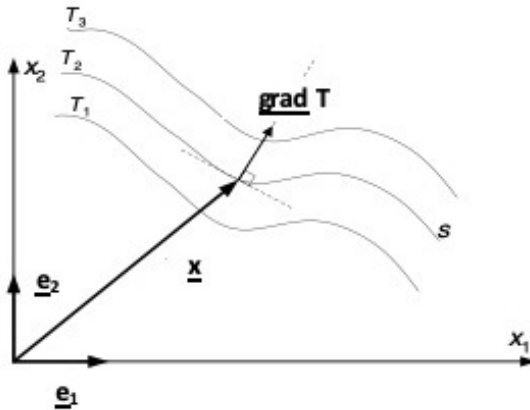
$$\underline{\nabla} T \cdot \underline{t} = 0 \tag{1.72}$$

According to equation 1.72, since the gradient vector is perpendicular to every tangent vector at the point considered, the gradient vector must be normal to the level surface through that point.

Moreover, the rate of change of the function T with respect to distance in the direction $\underline{n}$ of increasing T normal to the surface $T(x_1, x_2, x_3) = constant$, namely $\underline{\nabla} T \cdot \underline{n}$, is equal to $|\underline{\nabla} T|$ since $\underline{\nabla} T$ is parallel to the normal and since $\underline{\nabla} T \cdot \underline{n}$ is positive because $\underline{n}$ was taken as the direction of increasing T. The unit normal vector to the level surface, taken in the direction of increasing T, is therefore given by:

$$\underline{n} = \frac{\underline{\nabla} T}{|\underline{\nabla} T|} \tag{1.73}$$

Other important applications of the gradient in mechanics relate the force vector to the gradient of the potential of a conservative force field, and the velocity vector to the gradient of a velocity potential in irrotational fluid flow.

Figure 1.2   Gradient of a scalar field. Image taken from [2].

Let us now consider a vector field $\underline{\Phi}$, which associates the vector $\underline{\Phi}(\underline{X})$ to the vector $\underline{X}$. Let us assume that the components Φ_i of $\underline{\Phi}$ are differentiable. We have:

$$d\underline{\Phi} = \frac{\partial \underline{\Phi}}{\partial X_j} dX_j = \left(\frac{\partial \underline{\Phi}}{\partial X_j} \otimes \underline{e}_j \right) \cdot \underline{dX} \tag{1.74}$$

Therefore, there exists a tensor of order 2 that relates the differentials $\underline{dX}$ and $d\underline{\Phi}$. That tensor, noted $\underline{\underline{\nabla\Phi}}$, is the gradient of $\underline{\Phi}$:

$$d\underline{\Phi} = \underline{\underline{\nabla\Phi}} \cdot \underline{dX} \tag{1.75}$$

so that:

$$\underline{\underline{\nabla\Phi}} = \frac{\partial \underline{\Phi}}{\partial X_j} \otimes \underline{e}_j = \frac{\partial \Phi_i}{\partial X_j} \underline{e}_i \otimes \underline{e}_j \tag{1.76}$$

Equation 1.76 is the intrinsic definition of the gradient of $\underline{\Phi}$.

Let us now consider a tensor field or order p, $\underline{X} \rightarrow \mathcal{T}^{(p)}(\underline{X})$. The differential of $\mathcal{T}^{(p)}$ is written:

$$d\mathcal{T}^{(p)} = \frac{\partial \mathcal{T}^{(p)}}{\partial X_j} dX_j = \left(\frac{\partial \mathcal{T}^{(p)}}{\partial X_j} \otimes \underline{e}_j \right) \cdot \underline{dX} \tag{1.77}$$

in which Eintein's convention is adopted for repeated indices. The gradient that relates linearly the differentials $d\mathcal{T}^{(p)}$ and $\underline{dX}$ is therefore a tensor of order $p + 1$, intrinsically defined as:

$$d\mathcal{T}^{(p)} = \nabla\left(\mathcal{T}^{(p)} \right) \cdot \underline{dX} \tag{1.78}$$

In the orthonormal base:

$$\nabla\left(\mathcal{T}^{(p)} \right) = \frac{\partial \mathcal{T}^{(p)}}{\partial X_i} \otimes \underline{e}_i \tag{1.79}$$

1.4.3   Divergence of a tensor field

1.4.3.1   *Definition*
Let us consider a tensor $\mathcal{T}^{(p)}$ of order $p \geq 1$. The divergence of $\mathcal{T}^{(p)}$ is noted $div\mathcal{T}^{(p)}$ and

is defined as the contraction of the two last indices of $\nabla \left(\mathcal{T}^{(p)} \right)$. By definition, $div\,\mathcal{T}^{(p)}$ is thus a tensor of order $p - 1$. For example, if $p = 1$:

$$div\underline{T} = \underline{\underline{\nabla T}} : \underline{\underline{I}} = \frac{\partial T_i}{\partial X_j}\delta_{ji} = \frac{\partial T_i}{\partial X_i} \tag{1.80}$$
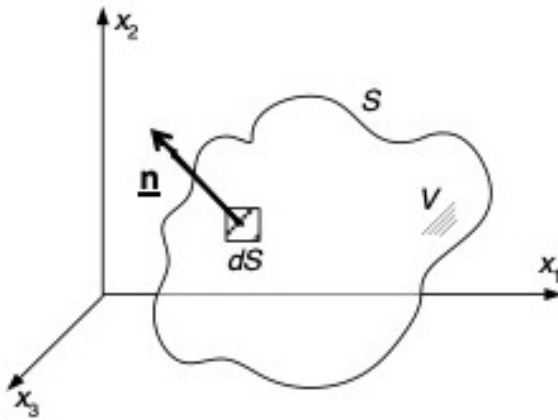
with, as always, Einstein's convention for repeated indices. If $p = 2$:

$$\underline{div} \left(\underline{\underline{T}} \right) = \underline{\underline{\underline{\nabla T}}} : \underline{\underline{I}} = \left(\frac{\partial T_{ij}}{\partial X_k}\underline{e}_i \otimes \underline{e}_j \otimes \underline{e}_k \right) : \left(\delta_{lp}\underline{e}_l \otimes \underline{e}_p \right) = \frac{\partial T_{ij}}{\partial X_k}\delta_{kj}\underline{e}_i = \frac{\partial T_{ij}}{\partial X_j}\underline{e}_i \tag{1.81}$$

1.4.3.2 Divergence theorem

In general, tensors vary from point to point and represent a tensor field, i.e. a tensor function of position. To determine the unknown tensor functions, one needs to derive the differential equations governing the way the stress and deformation vary in the neighborhood of a point and with time. In addition, the constitutive equations (e.g., stress-strain equations) and boundary and initial conditions must be added to obtain a well-defined mathematical problem to solve for the stress and deformation distributions or the displacement or velocity fields.

The differential equations expressing locally the conservation of mass, momentum, and energy are derived from integral forms of the equations of balance expressing fundamental postulates of continuum mechanics. The derivations make use of certain integral transformation formulas, especially the *divergence theorem (Gauss's theorem)*. In the invariant form shown below, this theorem is independent of any choice of coordinates, but it is simpler to present the derivation of Gauss's theorem in terms of rectangular Cartesian components, as shown in Figure 1.3.

Figure 1.3 Outgoing normal vector at an infinitesimal surface element on volume V. Image taken from [2].

The derivation of Gauss's theorem makes use of the following relationship between a volume integral and a surface integral over the bounding surface of the volume. If the scalar field $T(x_1, x_2, x_3)$ has continuous first partial derivatives with respect to the rectangular

Cartesian coordinates x_i, then:

$$\forall i = 1, 2, 3, \quad \oint_S T \, n_i \, dS = \int_V \frac{\partial T}{\partial x_i} dV \tag{1.82}$$

Here the unit vector components n_i are the direction cosines of the outward normal to the surface S at a point in the surface area element dS; the n_i are functions of position on the surface. The restrictions on the surface regularity are not great; it will be sufficient if the surface is piecewise smooth and is topologically such that it clearly defines an inside and an outside. The volume need not be simply connected, provided that the surface integral is extended over all the bounding surfaces, and the outer normal on each is taken to point away from the enclosed volume. It should be possible by inserting a finite number of interior boundaries to display the total volume as the sum of a finite number of volumes each bounded by simple closed surfaces.

If equation 1.82 is written with the three components v_i of a vector $\boldsymbol{v}$ successively substituted for T and the three resulting equations are added, the result is:

$$\oint_S v_i \, n_i \, dS = \int_V \frac{\partial v_i}{\partial x_i} dV \tag{1.83}$$

in the Cartesian form, and:

$$\oint_S \boldsymbol{v} \cdot \boldsymbol{n} \, dS = \int_V div(\boldsymbol{v}) dV \tag{1.84}$$

in the vector form. Equations 1.83 and 1.84 are the *divergence theorem, or Gauss's theorem*, which states that the integral of the outer normal component of a vector over a closed surface is equal to the integral of the divergence of the vector over the volume bounded by the closed surface (subject, of course, to the same kind of restrictions on the continuity of derivatives, etc. as were stated above for the component equations).

Finally, if equation 1.82 is written with the components of a second-order tensor $\boldsymbol{A}$ successively substituted for T, and the corresponding equations are added, we get the following form of the divergence theorem:

$$\oint_S A_{ij} \, n_j \, dS = \int_V \frac{\partial A_{ij}}{\partial x_j} dV \tag{1.85}$$

in Cartesian form and:

$$\oint_S \boldsymbol{A} \cdot \boldsymbol{n} \, dS = \int_V \underline{div\left(\boldsymbol{A}\right)} \, dV \tag{1.86}$$

in tensor form.

1.4.4 Laplacian operator

The Laplacian of a tensor order p $\mathcal{T}^{(p)}$ is noted $\Delta \mathcal{T}^{(p)}$ and is calculated as:

$$\Delta \mathcal{T}^{(p)} = div\left(\nabla \mathcal{T}^{(p)}\right) \tag{1.87}$$

By definition, the Laplacian of $\mathcal{T}^{(p)}$ is a tensor of order $(p + 1) - 1 = p$.

1.4.5 Curl of a vector

The curl of a vector field $\underline{v}$ is noted $\underline{curl}\,(\underline{v})$ or $\mathbf{curl}\,(\mathbf{v})$ and is defined as:

$$\underline{curl}\,(\underline{v}) = \nabla \times \underline{v} \tag{1.88}$$

For example, in a 3D space and in Cartesian coordinates:

$$\underline{curl}\,(\underline{v}) = \left(\frac{\partial v_3}{\partial x_2} - \frac{\partial v_2}{\partial x_3}\right)\underline{e}_1 + \left(\frac{\partial v_1}{\partial x_3} - \frac{\partial v_3}{\partial x_1}\right)\underline{e}_2 + \left(\frac{\partial v_2}{\partial x_1} - \frac{\partial v_1}{\partial x_2}\right)\underline{e}_3 \tag{1.89}$$

1.4.6 Formula sheet: gradient, divergence, Laplacian and curl operators in Cartesian, cylindrical and spherical coordinate systems

Figure 1.4 below provides the expressions of basic operators applied to a vector in all coordinate systems. In the four next pages, these operators are expressed more explicitly for both vectors and scalars. The text is in French, but the formalism is the same as that used in the course.

	Cartesian Coordinates	Cylindrical Coordinates	Spherical Coordinates
Conversion to Cartesian Coordinates		$x = \rho\cos\varphi \quad y = \rho\sin\varphi \quad z = z$	$x = r\cos\varphi\sin\theta \quad y = r\sin\varphi\sin\theta$ $z = r\cos\theta$
Vector A	$A_x i + A_y j + A_z k$	$A_\rho\hat{\rho} + A_\varphi\hat{\varphi} + A_z\hat{z}$	$A_r\hat{r} + A_\theta\hat{\theta} + A_\varphi\hat{\varphi}$
Gradient $\nabla\phi$	$\frac{\partial\phi}{\partial x}i + \frac{\partial\phi}{\partial y}j + \frac{\partial\phi}{\partial z}k$	$\frac{\partial\phi}{\partial\rho}\hat{\rho} + \frac{1}{\rho}\frac{\partial\phi}{\partial\varphi}\hat{\varphi} + \frac{\partial\phi}{\partial z}\hat{z}$	$\frac{\partial\phi}{\partial r}\hat{r} + \frac{1}{r}\frac{\partial\phi}{\partial\theta}\hat{\theta} + \frac{1}{r\sin\theta}\frac{\partial\phi}{\partial\varphi}\hat{\varphi}$
Divergence $\nabla\cdot A$	$\frac{\partial A_x}{\partial x} + \frac{\partial A_y}{\partial y} + \frac{\partial A_z}{\partial z}$	$\frac{1}{\rho}\frac{\partial(\rho A_\rho)}{\partial\rho} + \frac{1}{\rho}\frac{\partial A_\varphi}{\partial\varphi} + \frac{\partial A_z}{\partial z}$	$\frac{1}{r^2}\frac{\partial(r^2 A_r)}{\partial r} + \frac{1}{r\sin\theta}\frac{\partial A_\theta\sin\theta}{\partial\theta}$ $+ \frac{1}{r\sin\theta}\frac{\partial A_\varphi}{\partial\varphi}$
Curl $\nabla \times A$	$\begin{vmatrix} i & j & k \\ \frac{\partial}{\partial x} & \frac{\partial}{\partial y} & \frac{\partial}{\partial z} \\ A_x & A_y & A_z \end{vmatrix}$	$\begin{vmatrix} \frac{1}{\rho}\hat{\rho} & \hat{\varphi} & \frac{1}{\rho}\hat{z} \\ \frac{\partial}{\partial\rho} & \frac{\partial}{\partial\varphi} & \frac{\partial}{\partial z} \\ A_\rho & \rho A_\varphi & A_z \end{vmatrix}$	$\begin{vmatrix} \frac{1}{r^2\sin\theta}\hat{r} & \frac{1}{r\sin\theta}\hat{\theta} & \frac{1}{r}\hat{\varphi} \\ \frac{\partial}{\partial r} & \frac{\partial}{\partial\theta} & \frac{\partial}{\partial\varphi} \\ A_r & rA_\theta & rA_\varphi\sin\theta \end{vmatrix}$
Laplacian $\nabla^2\phi$	$\frac{\partial^2\phi}{\partial x^2} + \frac{\partial^2\phi}{\partial y^2} + \frac{\partial^2\phi}{\partial z^2}$	$\frac{1}{\rho}\frac{\partial}{\partial\rho}\left(\rho\frac{\partial\phi}{\partial\rho}\right) + \frac{1}{\rho^2}\frac{\partial^2\phi}{\partial\varphi^2} + \frac{\partial^2\phi}{\partial z^2}$	$\frac{1}{r^2}\frac{\partial}{\partial r}\left(r^2\frac{\partial\phi}{\partial r}\right) + \frac{1}{r^2\sin\theta}\frac{\partial}{\partial\theta}\left(\sin\theta\frac{\partial\phi}{\partial\theta}\right)$ $+ \frac{1}{r^2\sin^2\theta}\frac{\partial^2\phi}{\partial\varphi^2}$

Figure 1.4 Gradient, divergence, Laplacian and curl of a vector in Cartesian, cylindrical and spherical coordinate systems. Image taken from *calculusandmathematicsformulas.blogspot.com.*

2. Opérateurs

2.1. Coordonnées cartésiennes

B = $(\vec{x}, \vec{y}, \vec{z})$

$\vec{v} = u\vec{x} + v\vec{y} + w\vec{z}$

Gradient :

$$\overrightarrow{grad}\ p = \frac{\partial p}{\partial x}\vec{x} + \frac{\partial p}{\partial y}\vec{y} + \frac{\partial p}{\partial z}\vec{z} \quad \text{est un vecteur.}$$

$$\overline{\overline{grad}}\ \vec{v} = \begin{bmatrix} \overrightarrow{grad}\ u \\ \overrightarrow{grad}\ v \\ \overrightarrow{grad}\ w \end{bmatrix} = \begin{bmatrix} \dfrac{\partial u}{\partial x} & \dfrac{\partial u}{\partial y} & \dfrac{\partial u}{\partial z} \\ \dfrac{\partial v}{\partial x} & \dfrac{\partial v}{\partial y} & \dfrac{\partial v}{\partial z} \\ \dfrac{\partial w}{\partial x} & \dfrac{\partial w}{\partial y} & \dfrac{\partial w}{\partial z} \end{bmatrix} \quad \text{est une matrice.}$$

Divergence :

$$div\ \vec{v} = tr\left(\overline{\overline{grad}}\ \vec{v}\right) = \frac{\partial u}{\partial x} + \frac{\partial v}{\partial y} + \frac{\partial w}{\partial z} \quad \text{est un scalaire.}$$

$$\overrightarrow{div}\left(\overline{\overline{A}}\right) = \begin{pmatrix} div\ \vec{A}_x \\ div\ \vec{A}_y \\ div\ \vec{A}_z \end{pmatrix} = \begin{pmatrix} \dfrac{\partial A_{xx}}{\partial x} + \dfrac{\partial A_{xy}}{\partial y} + \dfrac{\partial A_{xz}}{\partial z} \\ \dfrac{\partial A_{yx}}{\partial x} + \dfrac{\partial A_{yy}}{\partial y} + \dfrac{\partial A_{yz}}{\partial z} \\ \dfrac{\partial A_{zx}}{\partial x} + \dfrac{\partial A_{zy}}{\partial y} + \dfrac{\partial A_{zz}}{\partial z} \end{pmatrix} = \left(\frac{\partial A_{ij}}{\partial x_j}\right)_{i=1,3} \quad \text{est un vecteur.}$$

Laplacien :

$$\Delta p = div\left(\overrightarrow{grad}\ p\right) = \frac{\partial^2 p}{\partial x^2} + \frac{\partial^2 p}{\partial y^2} + \frac{\partial^2 p}{\partial z^2} \quad \text{est un scalaire}$$

$$\Delta\vec{v} = \overrightarrow{div}\left(\overline{\overline{grad}}\ \vec{v}\right) = \begin{pmatrix} \dfrac{\partial^2 u}{\partial x^2} + \dfrac{\partial^2 u}{\partial y^2} + \dfrac{\partial^2 u}{\partial z^2} \\ \dfrac{\partial^2 v}{\partial x^2} + \dfrac{\partial^2 v}{\partial y^2} + \dfrac{\partial^2 v}{\partial z^2} \\ \dfrac{\partial^2 w}{\partial x^2} + \dfrac{\partial^2 w}{\partial y^2} + \dfrac{\partial^2 w}{\partial z^2} \end{pmatrix} = \left(\frac{\partial^2 u_i}{\partial x_j \partial x_j}\right)_{i=1,3} \quad \text{est un vecteur.}$$

Rotationnel :

$$\overrightarrow{rot}\ \vec{v} = \begin{pmatrix} \dfrac{\partial}{\partial x} \\[2mm] \dfrac{\partial}{\partial y} \\[2mm] \dfrac{\partial}{\partial z} \end{pmatrix} \wedge \begin{pmatrix} u \\ v \\ w \end{pmatrix} = \left(\dfrac{\partial w}{\partial y} - \dfrac{\partial v}{\partial z} \right) \vec{x} + \left(\dfrac{\partial u}{\partial z} - \dfrac{\partial w}{\partial x} \right) \vec{y} + \left(\dfrac{\partial v}{\partial x} - \dfrac{\partial u}{\partial y} \right) \vec{z}$$

Taux de déformation :
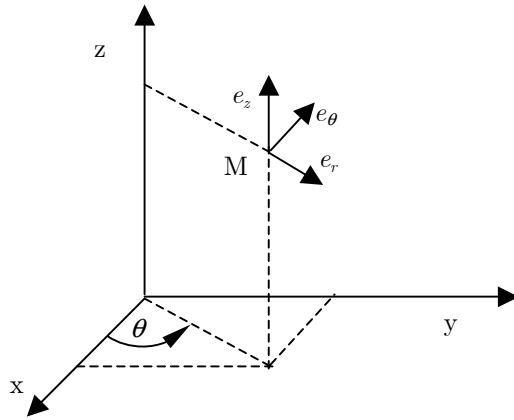
$$\overline{\overline{D}} = \begin{bmatrix} \dfrac{\partial u}{\partial x} & \dfrac{1}{2}\left(\dfrac{\partial u}{\partial y} + \dfrac{\partial v}{\partial x} \right) & \dfrac{1}{2}\left(\dfrac{\partial u}{\partial z} + \dfrac{\partial w}{\partial x} \right) \\[3mm] & \dfrac{\partial v}{\partial y} & \dfrac{1}{2}\left(\dfrac{\partial w}{\partial y} + \dfrac{\partial v}{\partial z} \right) \\[3mm] sym & & \dfrac{\partial w}{\partial z} \end{bmatrix}$$

Remarque :

L'opérateur gradient augmente l'ordre du tenseur, l'opérateur divergence le diminue et le laplacien le laisse inchangé. Le rotationnel ne s'applique qu'à un vecteur.

2.2. Coordonnées cylindriques

$B = \left(\vec{e}_r, \vec{e}_\theta, \vec{e}_z \right)$

$\vec{v} = v_r \vec{e}_r + v_\theta \vec{e}_\theta + v_z \vec{e}_z$

Gradient :

$$\overrightarrow{grad}\ p = \dfrac{\partial p}{\partial r} \vec{e}_r + \dfrac{1}{r} \dfrac{\partial p}{\partial \theta} \vec{e}_\theta + \dfrac{\partial p}{\partial z} \vec{e}_z$$

$$\overline{\overline{grad}}\ \vec{v} = \begin{bmatrix} \dfrac{\partial v_r}{\partial r} & \dfrac{1}{r}\dfrac{\partial v_r}{\partial \theta} - \dfrac{v_\theta}{r} & \dfrac{\partial v_r}{\partial z} \\[2ex] \dfrac{\partial v_\theta}{\partial r} & \dfrac{1}{r}\dfrac{\partial v_\theta}{\partial \theta} + \dfrac{v_r}{r} & \dfrac{\partial v_\theta}{\partial z} \\[2ex] \dfrac{\partial v_z}{\partial r} & \dfrac{1}{r}\dfrac{\partial v_z}{\partial \theta} & \dfrac{\partial v_z}{\partial z} \end{bmatrix}$$

Divergence :

$$div\ \vec{v} = tr\left(\overline{\overline{grad}}\ \vec{v}\right) = \dfrac{\partial v_r}{\partial r} + \dfrac{1}{r}\dfrac{\partial v_\theta}{\partial \theta} + \dfrac{v_r}{r} + \dfrac{\partial v_z}{\partial z}$$

Laplacien :

$$\Delta p = div\left(\overrightarrow{grad}\ p\right) = \dfrac{\partial^2 p}{\partial r^2} + \dfrac{1}{r}\dfrac{\partial p}{\partial r} + \dfrac{1}{r^2}\dfrac{\partial^2 p}{\partial \theta^2} + \dfrac{\partial^2 p}{\partial z^2}$$

Rotationnel :
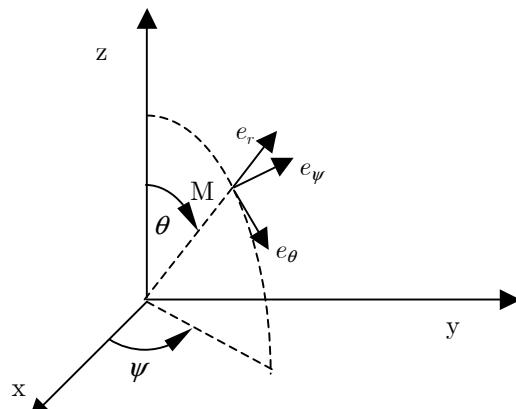
$$\overrightarrow{rot}\ \vec{v} = \left(\dfrac{1}{r}\dfrac{\partial v_z}{\partial \theta} - \dfrac{\partial v_\theta}{\partial z}\right)\vec{e}_r + \left(\dfrac{\partial v_r}{\partial z} - \dfrac{\partial v_z}{\partial r}\right)\vec{e}_\theta + \dfrac{1}{r}\left(\dfrac{\partial(r v_\theta)}{\partial r} - \dfrac{\partial v_r}{\partial \theta}\right)\vec{e}_z$$

Taux de déformation :

$$\overline{\overline{D}} = \begin{bmatrix} \dfrac{\partial v_r}{\partial r} & \dfrac{1}{2}\left(\dfrac{1}{r}\dfrac{\partial v_r}{\partial \theta} - \dfrac{v_\theta}{r} + \dfrac{\partial v_\theta}{\partial r}\right) & \dfrac{1}{2}\left(\dfrac{\partial v_r}{\partial z} + \dfrac{\partial v_z}{\partial r}\right) \\[3ex] & \dfrac{1}{r}\left(\dfrac{\partial v_\theta}{\partial \theta} + \dfrac{v_r}{r}\right) & \dfrac{1}{2}\left(\dfrac{1}{r}\dfrac{\partial v_z}{\partial \theta} + \dfrac{\partial v_\theta}{\partial z}\right) \\[3ex] sym & & \dfrac{\partial v_z}{\partial z} \end{bmatrix}$$

2.3. Coordonnées sphériques

$\mathrm{B} = \left(\vec{e}_r, \vec{e}_\theta, \vec{e}_\psi\right)$

$$\vec{v} = v_r\vec{e}_r + v_\theta\vec{e}_\theta + v_\psi\vec{e}_\psi$$

Gradient :

$$\overrightarrow{grad}\ p = \frac{\partial p}{\partial r}\vec{e}_r + \frac{1}{r}\frac{\partial p}{\partial \theta}\vec{e}_\theta + \frac{1}{r\sin\theta}\frac{\partial p}{\partial \psi}\vec{e}_\psi$$

$$\overline{\overline{grad}}\ \vec{v} = \begin{bmatrix} \dfrac{\partial v_r}{\partial r} & \dfrac{1}{r}\dfrac{\partial v_r}{\partial \theta} - \dfrac{v_\theta}{r} & \dfrac{1}{r\sin\theta}\dfrac{\partial v_r}{\partial \psi} - \dfrac{v_\psi}{r} \\[3mm] \dfrac{\partial v_\theta}{\partial r} & \dfrac{1}{r}\dfrac{\partial v_\theta}{\partial \theta} + \dfrac{v_r}{r} & \dfrac{1}{r\sin\theta}\dfrac{\partial v_\theta}{\partial \psi} - \dfrac{v_\psi\cot\theta}{r} \\[3mm] \dfrac{\partial v_\psi}{\partial r} & \dfrac{1}{r}\dfrac{\partial v_\psi}{\partial \theta} & \dfrac{1}{r\sin\theta}\dfrac{\partial v_\psi}{\partial \psi} + \dfrac{v_r}{r} + \dfrac{v_\theta\cot\theta}{r} \end{bmatrix}$$

Divergence :

$$div\ \vec{v} = tr\left(\overline{\overline{grad}}\ \vec{v}\right) = \frac{1}{r^2}\frac{\partial\left(r^2 v_r\right)}{\partial r} + \frac{1}{r\sin\theta}\frac{\partial\left(v_\theta \sin\theta\right)}{\partial \theta} + \frac{1}{r\sin\theta}\frac{\partial v_\psi}{\partial \psi}$$

Laplacien :

$$\Delta p = div\left(\overrightarrow{grad}\ p\right) = \frac{1}{r^2}\frac{\partial}{\partial r}\left(r^2\frac{\partial p}{\partial r}\right) + \frac{1}{r^2\sin\theta}\frac{\partial}{\partial \theta}\left(\sin\theta\frac{\partial p}{\partial \theta}\right) + \frac{1}{r^2\sin\theta}\frac{\partial^2 p}{\partial \psi^2}$$

Rotationnel :

$$\overrightarrow{rot}\ \vec{v} = \frac{1}{r^2\sin\theta}\left(\frac{\partial}{\partial \theta}\left(r\sin\theta v_\psi\right) - \frac{\partial\left(rv_\theta\right)}{\partial \psi}\right)\vec{e}_r + \frac{1}{r\sin\theta}\left(\frac{\partial v_r}{\partial \psi} - \frac{\partial}{\partial r}\left(r\sin\theta v_\psi\right)\right)\vec{e}_\theta + \frac{1}{r}\left(\frac{\partial(rv_\theta)}{\partial r} - \frac{\partial v_r}{\partial \theta}\right)\vec{e}_\psi$$

Taux de déformation :

$$\overline{\overline{D}} = \begin{bmatrix} \dfrac{\partial v_r}{\partial r} & \dfrac{1}{2}\left(\dfrac{1}{r}\dfrac{\partial v_r}{\partial \theta} - \dfrac{v_\theta}{r} + \dfrac{\partial v_\theta}{\partial r}\right) & \dfrac{1}{2}\left(\dfrac{1}{r\sin\theta}\dfrac{\partial v_r}{\partial \psi} - \dfrac{v_\psi}{r} + \dfrac{\partial v_\psi}{\partial r}\right) \\[3mm] & \dfrac{1}{r}\dfrac{\partial v_\theta}{\partial \theta} + \dfrac{v_r}{r} & \dfrac{1}{2}\left(\dfrac{1}{r\sin\theta}\dfrac{\partial v_\theta}{\partial \psi} + \dfrac{1}{r}\dfrac{\partial v_\psi}{\partial \theta} - \dfrac{v_\psi\cot\theta}{r}\right) \\[3mm] sym & & \dfrac{1}{r\sin\theta}\dfrac{\partial v_\psi}{\partial \psi} + \dfrac{v_r}{r} + \dfrac{v_\theta\cot\theta}{r} \end{bmatrix}$$

PROBLEMS

1.1 Prove equations 1.8, 1.9 and 1.10.

1.2 Prove equations 1.23 and 1.24.

1.3 Find the eigenvalues of $[A]$, and for each eigenvalue, find an eigenvector, where:

$$[A] = \begin{bmatrix} -3 & 15 \\ 3 & 9 \end{bmatrix}$$

1.4 Let us consider an Euclidian space of dimension 3, with the Cartesian coordinate system (e_1, e_2, e_3). In the following, tensors noted in lower case are vectors, tensors noted with capital letters are tensors of order 2 and tensors noted in calligraphic font are tensors of order 4. Develop the following expressions in index notation:

$$\boldsymbol{a} \cdot \mathcal{T} \cdot \boldsymbol{b}, \quad \boldsymbol{a} \otimes \boldsymbol{b} : \mathcal{T}, \quad \mathcal{T} \otimes \boldsymbol{A} \vdots \boldsymbol{B} \otimes \boldsymbol{c}$$

$$\boldsymbol{a} \otimes \boldsymbol{b} : \mathcal{T} : \boldsymbol{c} \otimes \boldsymbol{d}, \quad \mathcal{T} \vdots \boldsymbol{a} \otimes \boldsymbol{b} \otimes \boldsymbol{c} \otimes \boldsymbol{d}$$

1.5 Prove the formulas given in Figure 1.4.

1.6 A force of magnitude F acts in a direction radially away from the axes origin, at a point with coordinates $(a/3, 2b/3, 2c/3)$ on the surface of the ellipsoid of equation:

$$\left(\frac{x_1}{a}\right)^2 + \left(\frac{x_2}{b}\right)^2 + \left(\frac{x_3}{c}\right)^2 = 1$$

Determine the component of the force in the direction normal to the surface.

1.7 In the following, U is a scalar and $\boldsymbol{a}$ is a vector. Prove the following equations:

$$div\left(\boldsymbol{\nabla} U\right) = \Delta U \tag{1.90}$$

$$\boldsymbol{\nabla} \times \left(\boldsymbol{\nabla} U\right) = \boldsymbol{0} \tag{1.91}$$

$$\boldsymbol{\nabla} \cdot \left(\boldsymbol{\nabla} \times \boldsymbol{a}\right) = \boldsymbol{0} \tag{1.92}$$

$$\boldsymbol{\nabla} \times \left(\boldsymbol{\nabla} \times \boldsymbol{a}\right) = \boldsymbol{\nabla}\left(\boldsymbol{\nabla} \cdot \boldsymbol{a}\right) - \Delta \boldsymbol{a} \tag{1.93}$$

1.8 In the following, U and V are scalars and $\boldsymbol{a}$ and $\boldsymbol{b}$ are vectors. Prove the following equations:

$$\boldsymbol{\nabla}\left(U V\right) = V \boldsymbol{\nabla}(U) + U \boldsymbol{\nabla}(V) \tag{1.94}$$

$$\boldsymbol{\nabla} \cdot \left(U \boldsymbol{a}\right) = \boldsymbol{a} \cdot \boldsymbol{\nabla}(U) + U \left(\boldsymbol{\nabla} \cdot \boldsymbol{a}\right) \tag{1.95}$$

$$\boldsymbol{\nabla} \times \left(U \boldsymbol{a}\right) = \boldsymbol{\nabla}(U) \times \boldsymbol{a} + U \left(\boldsymbol{\nabla} \times \boldsymbol{a}\right) \tag{1.96}$$

$$\boldsymbol{\nabla} \cdot \left(\boldsymbol{a} \times \boldsymbol{b}\right) = \boldsymbol{b} \cdot \left(\boldsymbol{\nabla} \times \boldsymbol{a}\right) - \boldsymbol{a} \cdot \left(\boldsymbol{\nabla} \times \boldsymbol{b}\right) \tag{1.97}$$

$$\boldsymbol{\nabla} \times \left(\boldsymbol{a} \times \boldsymbol{b}\right) = \left(\boldsymbol{\nabla} \cdot \boldsymbol{b}\right) \boldsymbol{a} - \left(\boldsymbol{\nabla} \cdot \boldsymbol{a}\right) \boldsymbol{b} + \left(\boldsymbol{b} \cdot \boldsymbol{\nabla}\right) \boldsymbol{a} - \left(\boldsymbol{a} \cdot \boldsymbol{\nabla}\right) \boldsymbol{b} \tag{1.98}$$

$$\boldsymbol{\nabla}\left(\boldsymbol{a} \cdot \boldsymbol{b}\right) = \boldsymbol{a} \times \left(\boldsymbol{\nabla} \times \boldsymbol{b}\right) + \boldsymbol{b} \times \left(\boldsymbol{\nabla} \times \boldsymbol{a}\right) + \left(\boldsymbol{b} \cdot \boldsymbol{\nabla}\right) \boldsymbol{a} + \left(\boldsymbol{a} \cdot \boldsymbol{\nabla}\right) \boldsymbol{b} \tag{1.99}$$

CHAPTER 2

ELEMENTS OF CONTINUUM MECHANICS
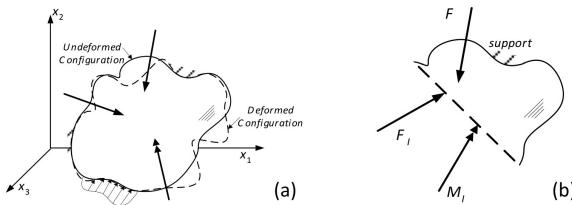
2.1 Basic assumptions and principles of Continuum mechanics

The mechanics of a continuous medium is that branch of mechanics that relates the deformation or flow of solids, liquids, and gases under the influence of external forces. The term continuous refers to the simplifying concept underlying the analysis: we disregard the molecular structure of matter and picture it as being without gaps or empty spaces. We further suppose that all the mathematical functions entering the theory are continuous functions, except possibly at a finite number of interior surfaces separating regions of continuity. This statement implies that the derivatives of the functions are continuous too, if they enter the theory, since all functions entering the theory are assumed continuous. This hypothetical continuous material we call a continuous medium or continuum.

Given a solid body acted upon contact forces (surface forces) applied to the surface of the body/ and or forces acting throughout the body (body forces), the two basic questions that are posed in the study of continuum mechanics are: (i) How are the forces transmitted through the interior of the body? (ii) What are the resulting deformations?

Deformations refer to the differences in the shape and size of the body prior and after the load application, that is, the natural shape and size of the body are in general changed by the application of loads (Figure 2.1.a).

Transmission of the forces refers to the internal force distribution resulting from the application of loads together with the types and locations of the supports. The resultants associated with this internal force distribution can be determined by taking a section through the body (Figure 2.1.b).

Figure 2.1   (a) Undeformed and deformed configurations.   (b) Section showing internal force resultants. Image taken from [2].

The formulation of a solid mechanics problem involves establishing the framework within which the relationship(s) between the loads, the internal forces and the deformations can be determined.

First Basic Element: Equilibrium and Stress. The first element in the formulation of a continuum mechanics problem refers to the requirement that the body or any part of the body is in a state of equilibrium or that the motion is in accordance with Newton's second law. This is one of the basic physical laws that govern any and all solutions to problems in solid mechanics. This basic physical law can be used to establish relationships between the loads and the reactions by drawing a free body diagram (FBD) and requiring the entire body to be in equilibrium. Also, equilibrium equations can be written for portions of the body obtained by sectioning to establish the force resultants acting on a section through the body (internal forces).
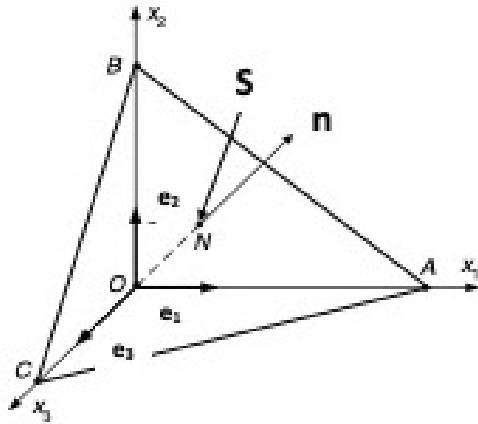
Second Basic Element: Deformation and Strain. The second basic idea of solid mechanics arises in connection with the need to be able to describe the deformations that are associated with the differences in the undeformed and deformed configurations. In the study of statics and dynamics, bodies are generally assumed to be rigid and hence undergo what are termed rigid body motions. The kinematics that is appropriate for discussing the motion of a rigid body deals with translations and rotations. When formulating the kinematics for a deformable body it is also necessary to describe changes in the size of the body and changes in the shape of the body in addition to any rigid body motions that may result.

Third Basic Element: Material behavior. In the first basic element that refers to the state of stress and equilibrium of a body, we introduced the unknown normal and shear stresses acting on the body. In the second element that refers to deformation and strain, the additional unknown variables are the displacements and the strains. The equations relating these unknowns are the strain-displacement relations and equilibrium equations, which are insufficient for the solution of the boundary value problem. Thus, the third basic element introduces the relationship between the kinetic variables (stresses) and the kinematic variables (displacements and strains), thus bringing into balance the number of equations and unknowns. The relationships between the force and displacement variables for a given material are generally referred to as material behavior. This discussion of material behavior will characterize, both qualitatively and quantitatively, the basic responses of different materials to mechanical and thermal inputs by specifying the form of, as well as the constants appearing in, the relations between the force and displacement variables.

2.2 Stress tensor

2.2.1 Lemma of the tetrahedron and definition of Cauchy's stress tensor

Assume that at a point O in a continuous medium a set of rectangular coordinates is drawn, and a free body is chosen in the form of a tetrahedron or triangular pyramid bounded by parts of the three coordinate planes through O and a fourth plane ABC not passing through O, as shown in Figure 2.2. The outward normal to the oblique plane is noted n and the surface traction vector whose direction is positive for the sign convention in continuum mechanics for geomaterials (compression positive), is noted S.

Figure 2.2   Cauchy's tetrahedron. Image taken from [2].

The components of the unit vector normal n are the direction cosines of its direction, i.e.

$$n_1 = cos\left(\widehat{AON}\right), \quad n_2 = cos\left(\widehat{BON}\right), \quad n_3 = cos\left(\widehat{CON}\right) \tag{2.1}$$

Next, we denote the area of the four triangles comprising the surface of the tetrahedron as:

$$A_1 = \mathcal{A}(OBC), \quad A_2 = \mathcal{A}(OCA), \quad A_3 = \mathcal{A}(OAB), \quad A = \mathcal{A}(ABC) \tag{2.2}$$

The altitude ON, of length h, is a leg of the three triangles ANO, BNO and CNO with hypotenuses OA, OB, and OC. Therefore:

$$h = OA\,n_1 = OB\,n_2 = OC\,n_3 \tag{2.3}$$

Finally, the volume of the tetrahedron is one third of the base multiplied by the altitude. Considering each of the four bases in turn, four equivalent expressions for the volume V are obtained:

$$V = \frac{1}{3}h\,A = \frac{1}{3}OA\,A_1 = \frac{1}{3}OB\,A_2 = \frac{1}{3}OC\,A_3 \tag{2.4}$$

From equations 2.3 and 2.4, we have:

$$A_1 = A\,n_1, \quad A_2 = A\,n_2, \quad A_3 = A\,n_3 \tag{2.5}$$

These equations express the fact that three on the faces are projections of the oblique face onto the coordinate planes. We shall now consider the equilibrium of the free body in the three Cartesian coordinate directions. Suppose that the traction $\boldsymbol{S}$ is balanced by three surface distributions of traction $\boldsymbol{T}_1$, $\boldsymbol{T}_2$ and $\boldsymbol{T}_3$, acting on the faces OBC, OCA and OAB respectively. The surface tractions $\boldsymbol{T}_j$ do not necessarily act orthogonal to the faces where they are applied and each have three components T_{1j}, T_{2j} and T_{3j} in directions 1, 2 and 3 of the Cartesian space. As a result, the equilibrium equations are:

$$
\begin{aligned}
S_1\,A &= T_{11}\,A_1 + T_{12}\,A_2 + T_{13}\,A_3 \\
S_2\,A &= T_{21}\,A_1 + T_{22}\,A_2 + T_{23}\,A_3 \\
S_3\,A &= T_{31}\,A_1 + T_{32}\,A_2 + T_{33}\,A_3
\end{aligned}
\tag{2.6}
$$

where S_1, S_2 and S_3 are the components of the surface traction vector $\boldsymbol{S}$ in directions 1, 2 and 3, respectively. From equations 2.5 and 2.6, we have:

$$
\left.
\begin{aligned}
S_1 &= T_{11}\,n_1 + T_{12}\,n_2 + T_{13}\,n_3 \\
S_2 &= T_{21}\,n_1 + T_{22}\,n_2 + T_{23}\,n_3 \\
S_3 &= T_{31}\,n_1 + T_{32}\,n_2 + T_{33}\,n_3
\end{aligned}
\right\} \Rightarrow \forall i = 1,2,3, \quad S_i = T_{ij} n_j
\tag{2.7}
$$

The second-order tensor that associates the surface traction vector $\boldsymbol{S}$ to the unit normal vector $\boldsymbol{n}$ is called Cauchy's stress tensor and it is noted $\boldsymbol{\sigma}$. By construction:

$$
\boldsymbol{\sigma}\,(\boldsymbol{x}, t) \cdot \boldsymbol{n} = \boldsymbol{S}\,(\boldsymbol{x}, t, \boldsymbol{n})
\tag{2.8}
$$

$$
\forall i = 1,2,3, \quad \sigma_{ij}\,(\boldsymbol{x}, t)\,n_j = S_i\,(\boldsymbol{x}, t, \boldsymbol{n})
\tag{2.9}
$$

in which $\boldsymbol{x}$ is the position vector and t is the time variable. The stress component σ_{ij} can physically be understood as the surface force that is applied in the direction of $\boldsymbol{e}_i$ on a surface of normal $\boldsymbol{e}_j$.

2.2.2   Equilibrium of forces - Cauchy's equations of motion

The momentum principle for a collection of particles states that: "the time rate of change of the total momentum of a given set of particles equals the vector sum of all the external forces acting on the particles of the set", provided that Newton's third law of action and reaction governs the internal forces. Consider a given mass of medium, instantaneously occupying a volume V bounded by a surface S and acted upon by an external surface force field $\boldsymbol{t}$ per unit area and by a body forces field $\boldsymbol{b}$ per unit of mass. The rate of change of momentum of the given mass is $\frac{d}{dt}\int_V \rho \boldsymbol{v}\,dV$, in which ρ is the mass density of the material and $\boldsymbol{v}$ is the velocity field of the medium. Then, the momentum balance expressed by the postulate is:

$$
\int_S \boldsymbol{t}\,dS + \int_V \rho \boldsymbol{b}\,dV = \frac{d}{dt}\int_V \rho \boldsymbol{v}\,dV
\tag{2.10}
$$

Introducing the Cauchy stress defined in Equation 2.9 in the above equation, we get:

$$
\forall i = 1,2,3, \quad \int_S \sigma_{ij} n_j\,dS + \int_V \rho b_i\,dV = \frac{d}{dt}\int_V \rho v_i\,dV
\tag{2.11}
$$

Now using the divergence theorem in the first term of the equation above, we obtain:

$$\forall i = 1, 2, 3, \quad \int_S \sigma_{ij} n_j dS \;=\; \int_V div_i \left(\boldsymbol{\sigma} \right) dV \;=\; \int_V \frac{\partial \sigma_{ij}}{\partial x_j} dV \qquad (2.12)$$

Using the Reynolds transport theorem, which states that the time derivative of a volume integral is equal to the volume integral of a time derivative, we obtain:

$$\forall i = 1, 2, 3, \quad \frac{d}{dt} \int_V \rho v_i dV \;=\; \int_V \rho \frac{dv_i}{dt} dV \qquad (2.13)$$

where here, it is assumed that the mass density ρ does not vary over time. Now combining equations 2.11, 2.12 and 2.13, we get:

$$\forall i = 1, 2, 3, \quad \int_V \frac{\partial \sigma_{ij}}{\partial x_j} dV + \int_V \rho b_i dV \;=\; \int_V \rho \frac{dv_i}{dt} dV \qquad (2.14)$$

Equation 2.14 holds for an arbitrary volume V, and consequently at each point. This result yields the Caushy's equations of motion:

$$\forall i = 1, 2, 3, \quad \frac{\partial \sigma_{ij}}{\partial x_j} + \rho b_i \;=\; \rho \frac{dv_i}{dt} \;=\; \rho \frac{d^2 u_i}{dt^2} \qquad (2.15)$$

in which $\frac{d^2 u_i}{dt^2}$ is the acceration field in direction i. If the problem is static, we get:

$$\forall i = 1, 2, 3, \quad \frac{\partial \sigma_{ij}}{\partial x_j} + f_i \;=\; 0 \qquad (2.16)$$

in which $f_i = \rho b_i$ is the body force in direction i per unit of volume.

2.2.3 Equilibrium of moments - symmetry of the stress tensor

In a collection of particles whose interactions are equal, opposite, and collinear forces, the time rate of change of the total moment of momentum for the given collection of particles is equal to the vector sum of the moments of the external forces acting on the system. Using the conservation of momentum equation (equation 2.10) and assuming that the continuum considered is not subjected to any distributed couple, we have:

$$\int_S \boldsymbol{r} \times \boldsymbol{t} dS + \int_V \boldsymbol{r} \times (\rho \boldsymbol{b}) \, dV \;=\; \frac{d}{dt} \int_V \boldsymbol{r} \times (\rho \boldsymbol{v}) \, dV \qquad (2.17)$$

in which $\boldsymbol{r} = x_1 \boldsymbol{e}_1 + x_2 \boldsymbol{e}_2 + x_3 \boldsymbol{e}_3$ is the position vector. In indicial notation:

$$\int_S \overline{e}_{ijk} e_i x_j t_k dS + \int_V \overline{e}_{ijk} e_i x_j \rho b_k dV \;=\; \frac{d}{dt} \int_V \overline{e}_{ijk} e_i x_j \rho v_k dV \qquad (2.18)$$

in which $\overline{e}$ is the third-order permutation tensor, defined as:

$$\forall i, j, k, \quad \overline{e}_{ijk} = \begin{cases} 0 \text{ when two indices are equal} \\ +1 \text{ when the indices are 1,2,3 or an even permutation of 1,2,3} \\ -1 \text{ when the indices are an odd permutation of 1,2,3} \end{cases}$$

$$(2.19)$$

One can show that the components of the permutation tensor can be calculated as follows:

$$\overline{e}_{ijk} = \frac{1}{2}(i-j)(j-k)(k-i) \tag{2.20}$$

Using the stress-traction relationship (Equation 2.9) and the divergence theorem, the first term of Equation 2.18 can be rewritten as:

$$\int_S \overline{e}_{ijk}e_i x_j t_k dS = \int_S \overline{e}_{ijk}e_i x_j \sigma_{kl}n_l dS = e_i \int_V \frac{\partial\left(\overline{e}_{ijk}x_j\sigma_{kl}\right)}{\partial x_l}dV \tag{2.21}$$

$$\int_S \overline{e}_{ijk}e_i x_j t_k dS = e_i \int_V \overline{e}_{ijk}\delta_{jl}\sigma_{kl}dV + e_i \int_V \overline{e}_{ijk}x_j\frac{\partial\sigma_{kl}}{\partial x_l}dV \tag{2.22}$$

Using Reynold's transport theorem, the third term of Equation 2.18 can be rewritten as:

$$\frac{d}{dt}\int_V \overline{e}_{ijk}e_i x_j \rho v_k dV = \int_V \overline{e}_{ijk}e_i\rho\frac{dx_j v_k}{dt}dV = e_i \int_V \overline{e}_{ijk}\rho\left(v_k\frac{dx_j}{dt} + x_j\frac{dv_k}{dt}\right)dV \tag{2.23}$$

Substituting the two equations above into Equation 2.18, one gets:

$$e_i \int_V \overline{e}_{ijk}\sigma_{kj}dV + e_i \int_V \overline{e}_{ijk}x_j\frac{\partial\sigma_{kl}}{\partial x_l}dV \quad + \quad e_i \int_V \overline{e}_{ijk}x_j\rho b_k dV \tag{2.24}$$

$$= e_i \int_V \overline{e}_{ijk}\rho\left(v_k\frac{dx_j}{dt} + x_j\frac{dv_k}{dt}\right)dV$$

Cauchy's equations of motion (Equations 2.15) impose that:

$$\frac{\partial\sigma_{kl}}{\partial x_l} + \rho b_k = \rho\frac{dv_k}{dt} \tag{2.25}$$

Combining the two equations above provides:

$$e_i \int_V \overline{e}_{ijk}\sigma_{kj}dV = e_i \int_V \rho\overline{e}_{ijk}v_k v_j dV \tag{2.26}$$

In the right-hand side of the equation above, $\rho\overline{e}_{ijk}e_i v_j v_k$ is the indicial notation for $\rho\boldsymbol{v}\times\boldsymbol{v}$, which is zero. Therefore, for an arbitrary volume V:

$$e_i \int_V \overline{e}_{ijk}\sigma_{kj}dV = 0 \tag{2.27}$$

Hence, at each point of the volume, we have:

$$\sigma_{23} = \sigma_{32} \text{ if i=1} \tag{2.28}$$
$$\sigma_{31} = \sigma_{13} \text{ if i=2}$$
$$\sigma_{12} = \sigma_{21} \text{ if i=3}$$

This establishes the symmetry of the stress tensor in general, with no assumption of equilibrium or uniformity of the stress distribution. The symmetry of the stress tensor is related to the moment of momentum principle in the general non-polar case (i.e. no assigned traction couples or body forces and no couple stresses) and related to the moment equilibrium condition.

2.2.4   Principal stresses and stress invariants

Stress is a symmetric tensor of order and can thus be represented by a symmetric 3 x 3 matrix. According to Section 1.2.1.4, the eigenvalues of the stress matrix, are the roots of the following characteristic equation:

$$det\left(\sigma_{ij} - \sigma\delta_{ij}\right) = -\sigma^3 + I_1\sigma^2 - I_2\sigma + I_3 \tag{2.29}$$

in which σ is an eigenvalue and in which

$$I_1 = \sigma_{11} + \sigma_{22} + \sigma_{33} = Tr\left(\boldsymbol{\sigma}\right) \tag{2.30}$$

$$I_2 = \left(\sigma_{11}\sigma_{22} - \sigma_{12}^2\right) + \left(\sigma_{22}\sigma_{33} - \sigma_{23}^2\right) + \left(\sigma_{11}\sigma_{33} - \sigma_{13}^2\right) = \frac{1}{2}\left[Tr\left(\boldsymbol{\sigma}\right)^2 - Tr\left(\boldsymbol{\sigma}^2\right)\right]$$

$$I_3 = det\left(\boldsymbol{\sigma}\right)$$

in which Tr is the trace operator (i.e., the sum of the diagonal coefficients of a matrix). The three coefficients I_1, I_2 and I_3 are frame invariants, and they are called the stress invariants.

The characteristic equation is a polynomial of order 3 and therefore, there are three roots σ_1, σ_2 and σ_3 (note that there is only one index, as opposed to the stress tensor components, which are referred to with two indices). The stress eigenvalues are called the principal stress values. The corresponding eigenvectors $\boldsymbol{v}$ are called the principal stress directions. Typically, we order the principal stresses as follows: $\sigma_1 \geq \sigma_2 \geq \sigma_3$. $\sigma_1\boldsymbol{v}_1 \otimes \boldsymbol{v}_1$ is called the major principal stress, $\sigma_3\boldsymbol{v}_3 \otimes \boldsymbol{v}_3$ is called the minor principal stress and $\sigma_2\boldsymbol{v}_2 \otimes \boldsymbol{v}_2$ is called the intermediate principal stress. Since the stress matrix is symmetric, it can be shown that the eivenvectors are orthogonal. It is possible to write the stress tensor as:

$$\boldsymbol{\sigma} = \sigma_1\boldsymbol{v}_1 \otimes \boldsymbol{v}_1 + \sigma_2\boldsymbol{v}_2 \otimes \boldsymbol{v}_2 + \sigma_3\boldsymbol{v}_3 \otimes \boldsymbol{v}_3 \tag{2.31}$$

In other words, the stress matrix is diagonal in the principal base ($\boldsymbol{v}_1$, $\boldsymbol{v}_2$, $\boldsymbol{v}_2$). In the principal stress base, the stress invariants have a simpler expression:

$$I_1 = \sigma_1 + \sigma_2 + \sigma_3 \tag{2.32}$$

$$I_2 = \sigma_1\sigma_2 + \sigma_2\sigma_3 + \sigma_1\sigma_3$$

$$I_3 = \sigma_1\sigma_2\sigma_3$$

The stress tensor is commonly decomposed into a volumetric part, which represents the effects of an isotropic pressure, and a deviatoric part, which represents a state of pure shear. The volumetric part of the stress tensor is its mean value p, times the identity tensor, where:

$$p = \frac{1}{3}Tr\left(\boldsymbol{\sigma}\right) = \frac{1}{3}I_1 \tag{2.33}$$

The deviatoric stress tensor $\boldsymbol{s}$ is defined as the difference between the stress tensor and the volumetric part of the stress tensor:

$$\boldsymbol{s} = \boldsymbol{\sigma} - p\boldsymbol{I} \tag{2.34}$$

Since subtracting a constant normal stress in all directions will not change the principal directions, $\boldsymbol{\sigma}$ and $\boldsymbol{s}$ have the same principal axes. The principal values of the deviatoric stress tensor, s_1, s_2 and s_3, can be found in the same manner as the principal values of the stress tensor, σ_1, σ_2 and σ_3:

$$\det\left(\boldsymbol{s} - s\boldsymbol{I}\right) = 0 \implies s^3 - J_1 s^2 - J_2 s - J_3 = 0 \tag{2.35}$$

in which J_1, J_2 and J_3 are the deviatoric stress invariants:

$$
\begin{aligned}
J_1 &= Tr\left(\boldsymbol{s}\right) = Tr\left(\boldsymbol{\sigma}\right) - 3 \times \frac{1}{3} Tr\left(\boldsymbol{\sigma}\right) = 0 \tag{2.36} \\
J_2 &= -\frac{1}{2}\left(s_{ii}s_{jj} - s_{ij}s_{ij}\right) = \frac{1}{2}s_{ij}s_{ij} \\
J_3 &= \det(\boldsymbol{s})
\end{aligned}
$$

2.2.5   Rotation of the stress tensor

Stress is a tensor field that is expressed at a material point. In 3D, a material point can be thought of as a cube of infinitesimal dimensions. When the faces of the cube are normal to the Cartesian axes $\boldsymbol{e}_x$, $\boldsymbol{e}_y$ and $\boldsymbol{e}_z$, the stress is said to be expressed in the base $(\boldsymbol{e}_x, \boldsymbol{e}_y, \boldsymbol{e}_z)$ and can be written in the form of a 3 x 3 matrix, as follows:

$$[\boldsymbol{\sigma}]_{\boldsymbol{e}_x, \boldsymbol{e}_y, \boldsymbol{e}_z} = \begin{pmatrix} \sigma_{xx} & \sigma_{xy} & \sigma_{xz} \\ \sigma_{xy} & \sigma_{yy} & \sigma_{yz} \\ \sigma_{xz} & \sigma_{yz} & \sigma_{zz} \end{pmatrix} \tag{2.37}$$

in which we used the property of symmetry of the stress tensor. As written, the knowledge of the stress tensor only informs on the stress that is applied on faces that are normal to $\boldsymbol{e}_x$, $\boldsymbol{e}_y$, or $\boldsymbol{e}_z$. For example, that could be the stress at a point P located at a depth h, subjected to the vertical stress $\sigma_{yy} = \gamma h$ and to horizontal stresses σ_{xx} and σ_{zz} (typically calculated from the coefiicent of pressures at rest). Often times, it is necessary to know the state of stress on planes other than those normal to the reference axes. For example, if P is located on a fault that has a certain angle θ compared to the horizontal, then it becomes necessary to calculate the state of stress on a plane that has a normal oriented by an angle θ compared to $\boldsymbol{e}_y$, as illustrated in Figure 2.3. As a result, an operation is needed to calculate the state of stress in a new coordinate system (here, $\boldsymbol{e}'_x = \boldsymbol{e}_{x+\theta}$, $\boldsymbol{e}'_y = \boldsymbol{e}_{y+\theta}$, $\boldsymbol{e}'_z = \boldsymbol{e}_z$). This operation is a rotation by an angle θ about the z-axis, which, according to Subsection 1.2.1.5, is mathematically expressed as:

$$[\boldsymbol{\sigma}]_{\boldsymbol{e}'_x, \boldsymbol{e}'_y, \boldsymbol{e}'_z} = \mathcal{R}_z(\theta)\,[\boldsymbol{\sigma}]_{\boldsymbol{e}_x, \boldsymbol{e}_y, \boldsymbol{e}_z}\,\mathcal{R}_z^T(\theta) \tag{2.38}$$

in which:

$$\mathcal{R}_z(\theta) = \begin{pmatrix} \cos\theta & \sin\theta & 0 \\ -\sin\theta & \cos\theta & 0 \\ 0 & 0 & 1 \end{pmatrix} \tag{2.39}$$
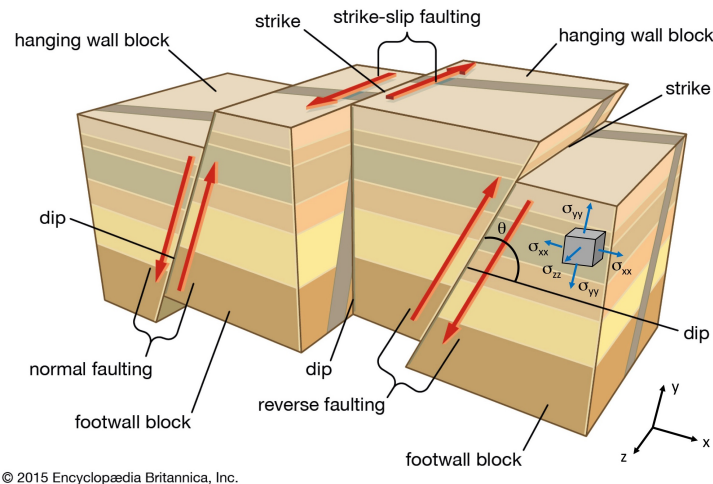
The development of equation 2.38 gives:

$$
\begin{aligned}
\sigma_{x'x'} &= \sigma_{xx}\cos^2\theta + 2\sigma_{xy}\sin\theta\cos\theta + \sigma_{yy}\sin^2\theta & (2.40)\\
\sigma_{y'y'} &= \sigma_{xx}\sin^2\theta - 2\sigma_{xy}\sin\theta\cos\theta + \sigma_{yy}\cos^2\theta \\
\sigma_{z'z'} &= \sigma_{zz} \\
\sigma_{x'y'} &= (\sigma_{yy} - \sigma_{xx})\sin\theta\cos\theta + \sigma_{xy}\left(\cos^2\theta - \sin^2\theta\right) \\
\sigma_{y'z'} &= \sigma_{yz} \\
\sigma_{x'z'} &= \sigma_{xz}
\end{aligned}
$$

Using trigonometry rules, the equations above can be rewritten as:

$$
\begin{aligned}
\sigma_{x'x'} &= \frac{\sigma_{xx}+\sigma_{yy}}{2} + \frac{\sigma_{xx}-\sigma_{yy}}{2}\cos 2\theta + \sigma_{xy}\sin 2\theta & (2.41)\\
\sigma_{y'y'} &= \frac{\sigma_{xx}+\sigma_{yy}}{2} - \frac{\sigma_{xx}-\sigma_{yy}}{2}\cos 2\theta - \sigma_{xy}\sin 2\theta \\
\sigma_{z'z'} &= \sigma_{zz} \\
\sigma_{x'y'} &= \frac{\sigma_{yy}-\sigma_{xx}}{2}\sin 2\theta + \sigma_{xy}\cos 2\theta \\
\sigma_{y'z'} &= \sigma_{yz} \\
\sigma_{x'z'} &= \sigma_{xz}
\end{aligned}
$$

Rotations about other axes are obtained in the same way, using compositions of rotations, as explained in Subsection 1.2.1.5.
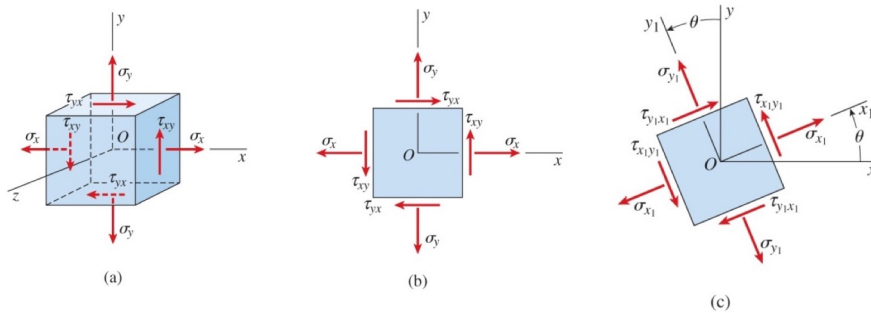
© 2015 Encyclopædia Britannica, Inc.

Figure 2.3   An example where a rotation of stress is needed: here the stress is known at every point in the rock mass, but only for material points oriented with faces orthogonal to the unit vectors of the Cartesian base. The components σ_{xx}, σ_{yy}, σ_{zz}, σ_{xy}, σ_{xz} and σ_{yz} are thus known (note that for clarity, only σ_{xx}, σ_{yy} and σ_{zz} were represented in the sketch). But typically, what is needed is the stress on a face oriented parallel to a fault, at an angle θ to the horizontal. Knowing the shear stress on the fault plan could help understanding whether that fault slips or not, for instance.

The same result can be obtained from equilibrium equations. For simplicity, let us restrict ourselves to plane stress (i.e., to a state of stress in which there is a direction e_i such that all components of stress in that direction are zero, i.e, $\boldsymbol{\sigma} \cdot e_i = 0$). The reasoning is the same in 3D. Let us thus assume that a material point is subjected to a state of plane stress in the plane (x,y), that is, the stress can be represented by the following 2 x 2 matrix:

$$[\boldsymbol{\sigma}]_{e_x, e_y,} = \begin{pmatrix} \sigma_{xx} & \sigma_{xy} \\ \sigma_{xy} & \sigma_{yy} \end{pmatrix} \tag{2.42}$$

We seek to express the state of stress at the same material point, on a plane of normal e_{x1} oriented by an angle θ compared to the x-axis, as shown in Figure 2.4. We note $\boldsymbol{\sigma}_1$ the state of stress in the coordinate system (e_{x1}, e_{x2}). To calculate the components of $\boldsymbol{\sigma}_1$, we consider the free body diagram of a wedge that is part of the material point, as shown in Figure 2.5. Forces that apply on a face of normal e_{x1} are balanced by forces that are applied on faces of normal e_x and e_y.

(a)   (b)   (c)

Figure 2.4 The material point in plane stress. (a) In 3D. (b) In 2D, before rotation. (c) In 2D, after rotation. Image taken from [9].

Noting A_0 the area of the face of the wedge that is normal e_x, the force balance equations in directions e_{x1} and e_{y1} are obtained as follows:
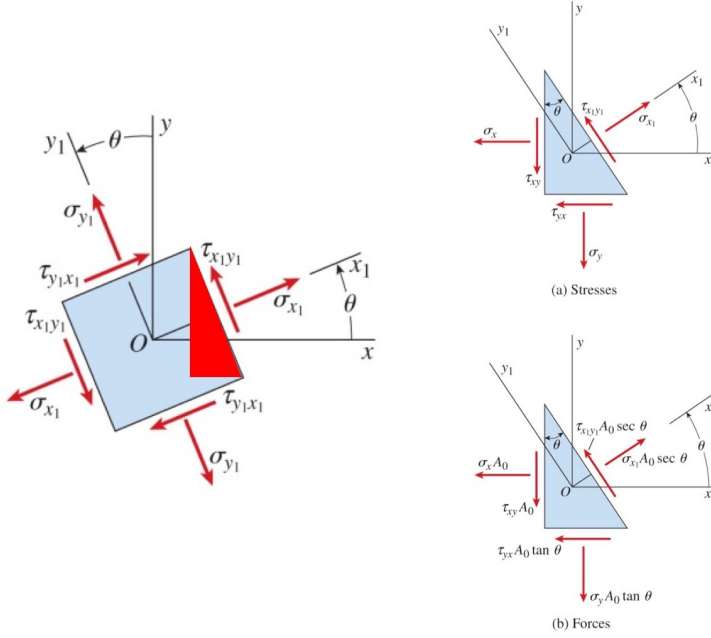
$$\frac{A_0}{\cos \theta} \sigma_{x1x1} = A_0 \sigma_{xx} \cos \theta + A_0 \sigma_{xy} \sin \theta + A_0 \tan \theta \sigma_{xy} \cos \theta + A_0 \tan \theta \sigma_{yy} \sin \theta \tag{2.43}$$

$$\frac{A_0}{\cos \theta} \sigma_{x1y1} = -A_0 \sigma_{xx} \sin \theta + A_0 \sigma_{xy} \cos \theta - A_0 \tan \theta \sigma_{xy} \sin \theta + A_0 \tan \theta \sigma_{yy} \cos \theta$$

from which we get:

$$\sigma_{x1x1} = \sigma_{xx} \cos^2 \theta + \sigma_{xy} \sin \theta \cos \theta + \sigma_{xy} \sin \theta \cos \theta + \sigma_{yy} \sin^2 \theta \tag{2.44}$$

$$\sigma_{x1y1} = -\sigma_{xx} \sin \theta \cos \theta + \sigma_{xy} \cos^2 \theta - \sigma_{xy} \sin^2 \theta + \sigma_{yy} \sin \theta \cos \theta$$

which can also be written as:

$$\sigma_{x1x1} = \sigma_{xx} \cos^2 \theta + \sigma_{yy} \sin^2 \theta + 2\sigma_{xy} \sin \theta \cos \theta \tag{2.45}$$

$$\sigma_{x1y1} = -(\sigma_{xx} - \sigma_{yy}) \sin \theta \cos \theta + \sigma_{xy} \left(\cos^2 \theta - \sin^2 \theta \right)$$

(a) Stresses

(b) Forces

Figure 2.5 Free body diagram of the wedge within the material point. Image taken from [9].

and finally transformed into:

$$\sigma_{x1x1} = \frac{\sigma_{xx} + \sigma_{yy}}{2} + \frac{\sigma_{xx} - \sigma_{yy}}{2}\cos 2\theta + \sigma_{xy}\sin 2\theta \qquad (2.46)$$

$$\sigma_{x1y1} = \frac{\sigma_{yy} - \sigma_{xx}}{2}\sin 2\theta + \sigma_{xy}\cos 2\theta$$

We check that the result above is the same as that found by using the rotation matrices, in Equation 2.41. Note that σ_{y1y1} is calculated according to the same formula as σ_{x1x1}, in which θ is replaced by $\theta + \pi/2$ (rotation by θ plus a right angle compared to the x-axis). The variations of the normal stress (σ_{x1x1} or σ_{y1y1}) and of the shear stress (σ_{x1y1}) with the angle θ are shown in Figure 2.6. The normal stress reaches an extremum when $\sigma_{x1y1} = 0$, which was expected since, from Equation 2.46, σ_{x1y1} is the derivative of σ_{x1x1} in reference to θ. That means that when the normal stress reaches an extremum, the normal stress is a principal stress.

Figure 2.6   Variations of the normal and shear stress components with the rotation angle θ. Image taken from [9].

2.2.6   Mohr's circle representation

To start, let us continue our stress analysis in plane stress. From Equation 2.46, we have:

$$\left(\sigma_{x1x1} - \frac{\sigma_{xx} + \sigma_{yy}}{2}\right)^2 + (\sigma_{x1y1})^2 \;=\; \left(\frac{\sigma_{xx} - \sigma_{yy}}{2}\right)^2 \left(\cos^2 2\theta + \sin^2 2\theta\right) \tag{2.47}$$

$$+ \;\; \sigma_{xy}^2 \left(\sin^2 2\theta + \cos^2 2\theta\right) + \left(\sigma_{xx} - \sigma_{yy}\right) \sigma_{xy} \sin 2\theta \cos 2\theta$$

$$+ \;\; \left(\sigma_{yy} - \sigma_{xx}\right) \sigma_{xy} \cos 2\theta \sin 2\theta$$

After simplification:

$$\left(\sigma_{x1x1} - \frac{\sigma_{xx} + \sigma_{yy}}{2}\right)^2 + (\sigma_{x1y1})^2 \;=\; \left(\frac{\sigma_{xx} - \sigma_{yy}}{2}\right)^2 + \sigma_{xy}^2 \tag{2.48}$$

Noting:
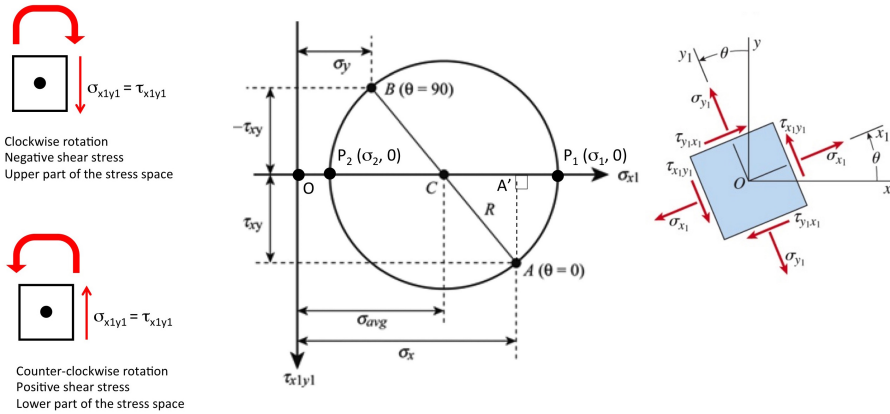
$$\sigma_{avg} = \frac{\sigma_{xx} + \sigma_{yy}}{2}, \quad R = \sqrt{\left(\frac{\sigma_{xx} - \sigma_{yy}}{2}\right)^2 + \sigma_{xy}^2} \tag{2.49}$$

Equation 2.48 becomes:

$$\left(\sigma_{x1x1} - \sigma_{avg}\right)^2 + (\sigma_{x1y1})^2 \;=\; R^2 \tag{2.50}$$

Equation 2.50 is the equation of a circle of center $(\sigma_{avg}, 0)$ and of radius R in the space (σ, τ), where σ stands for a normal stress and τ stands for a shear stress. What this equation means is that: (i) At a given material point, the state of stress at a face, given by the two stress components ($\sigma = \sigma_{x1x1}$, $\tau = \sigma_{x1y1}$) is a point in the (σ, τ) space; (ii) That point takes different coordinates for different values of the inclination angle θ; (iii) If the points marking the state of stress are plotted for all the possible values of θ, then a circle is obtained in the plane (σ, τ). In other words, the point that marks the state of

stress in the (σ, τ) plane travel on the circle when the material point rotates. The circle representing all the possible values of the stress components at a material point is called Mohr's circle. Figure 2.7 provides a graphical representation of the Mohr circle. Note that by convention, a shear stress that tends to rotate the material element counterclockwise is positive, but plotted in the bottom half of the (σ, τ) space. That is why in Figure 2.7, the τ axis is pointing downwards. Points P_1 and P_2 are the points that mark principal states of stress, where the shear stress is zero. Point A represents the state of stress $(\sigma_{xx}, \sigma_{xy})$ and B represents the state of stress $(\sigma_{yy}, -\sigma_{xy})$ and B. We will see later why A and B are diametrically opposite.

Figure 2.7   Mohr circle in plane stress. Image adapted from *chegg.com*.

Now the question is: How to relate the physical rotation by an angle θ to the rotation of the point that marks the stress state around the center of Mohr's circle? To answer that question, let us first calculate the angle of the rotation θ_p needed to go from the state of stress A $(\sigma_{xx}, \sigma_{xy})$ to the principal state of stress P_1 $(\sigma_1, 0)$. A principal stress is reached when the shear stress is zero. According to Equation 2.46, the shear stress is zero when:

$$\tan 2\theta_p = \frac{2\sigma_{xy}}{\sigma_{xx} - \sigma_{yy}} \tag{2.51}$$

Now let us calculate the angle $\widehat{ACP_1}$ in Figure 2.7:

$$\tan\left(\widehat{ACP_1}\right) = \frac{AA'}{CA'} = \frac{AA'}{OA - OC'} = \frac{\sigma_{x1y1}}{\sigma_{xx} - \sigma_{avg}} = \frac{2\sigma_{x1y1}}{\sigma_{xx} - \sigma_{yy}} = 2\tan 2\theta_p \tag{2.52}$$

in which A' is the projection of A on the horizontal axis and O is the origin of the coordinate system. Since both θ_p and $\widehat{ACP_1}$ are sought in an interval $\left[-\frac{\pi}{2}, +\frac{\pi}{2}\right]$ deduce from Equation 2.52 that:

$$\widehat{ACP_1} = 2\theta_p \tag{2.53}$$

We just showed that whenever the principal stress state is reached on a face that has a normal oriented by an angle $+\theta_p$ to the physical horizontal axis e_x, then a rotation by $+2\theta_p$ is needed on Mohr's circle to travel from the stress state at A (face that has a normal equal to e_x) to the stress state at P_1 (principal stress). Now, let us examine the rotation

needed on Mohr's circle to travel from the state of stress at A to the state of stress at D, where D represents the state of stress on a face with a normal oriented by an angle θ to the horizontal. Figure 2.8 provides a graphical representation of the problem. Let us note θ_{p1} the angle of the rotation needed in the physical space to go from the state of stress at D to the principal stress state. Following the same reasoning as above, we have:

$$\widehat{DCP_1} = 2\theta_{p1} \tag{2.54}$$

Therefore:

$$\widehat{ACD} = \widehat{ACP_1} - \widehat{DCP_1} = 2(\theta_p - \theta_{p1}) \tag{2.55}$$

Now, looking at the rotation needed to go from stress state A to stress state D in the physical space (Figure 2.8), we have:
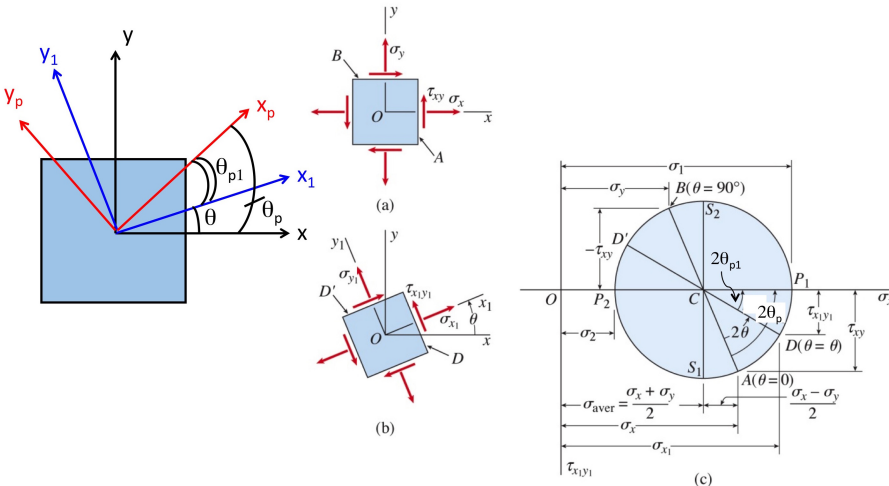
$$\theta = \theta_p - \theta_{p1} \tag{2.56}$$

As a result, we have:

$$\widehat{ACD} = 2\theta \tag{2.57}$$
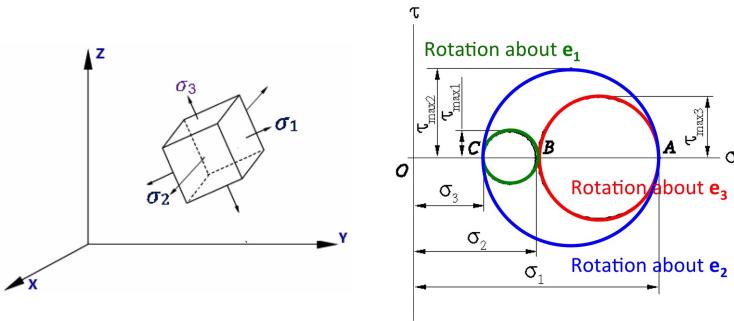
which shows that a rotation by an angle θ in the physical space is equivalent to a rotation by an angle 2θ in the stress space, on Mohr's circle. This is a general and important result. We now understand why A and B are diametrically opposite: the face of normal e_y where the state of stress B is applied is oriented by angle $\pi/2$ compared to the face of normal e_x where the state of stress A is applied, which means that a rotation by an angle π is needed in the stress space to travel from A to B. Lastly, one ca see from Mohr's circle that the maximum shear stress at the material point is reached at the top of the circle, where the normal stress is equal to σ_{avg}, and we have:

$$\tau_{max} = R = \sqrt{\left(\frac{\sigma_{xx} - \sigma_{yy}}{2}\right)^2 + (\sigma_{x1y1})^2} \tag{2.58}$$


Figure 2.8 Rotation of a material element and corresponding rotation in the stress space. Image adapted from [9].

Now, what happens if the state of stress in not plane, in other words, what is the graphical representation of the state of stress for a three-dimensional stress state? First think of a state of triaxial stress, i.e. a 3D state of stress without any shear stress, see Figure 2.9. If $\sigma_3 = 0$, the material point is in plane stress in the plane (e_1, e_2) and the state of stress is described by a Mohr circle of center $((\sigma_1 + \sigma_2)/2, 0)$ and of radius $(\sigma_1 - \sigma_2)/2$. Similarly, if $\sigma_2 = 0$, the material point is in plane stress in the plane (e_1, e_3) and the state of stress is described by a Mohr circle of center $((\sigma_1 + \sigma_3)/2, 0)$ and of radius $(\sigma_3 - \sigma_2)/2$. Finally, if $\sigma_1 = 0$, the material point is in plane stress in the plane (e_2, e_3) and the state of stress is described by a Mohr circle of center $((\sigma_2 + \sigma_3)/2, 0)$ and of radius $(\sigma_2 - \sigma_3)/2$. If the element is in a 3D principal stress state, the state of stress is represented by the three points A, B and C in Figure 2.9. If now σ_3 is maintained constant and the element is rotated about the axis e_3, the shear stresses exerted on the faces normal to the e_3 axis remain equal to zero, and the normal stress σ_3 remains perpendicular to the plane spanned by e_1 and e_2 in which the transformation takes place and thus, does not affect this transformation. As a result, the state of stress is represented by three points: point C and two diametrically opposite points on the red circle, which describes the state of plane stress in the plane (e_1, e_2). A similar situation occurs if a rotation of the element is operated about the axis e_2: after rotation, the state of stress is described by point B, and by two diametrically opposite points on the blue circle, which describes the state of plane stress in the plane (e_1, e_3). And finally, if a rotation of the element is operated about the axis e_1: after rotation, the state of stress is described by point A, and by two diametrically opposite points on the green circle, which describes the state of plane stress in the plane (e_2, e_3).

Figure 2.9 Mohr circles for a material point subjected to a 3D triaxial stress state, with rotations about the principal axes. Image adapted from *learnengineering.com*.

Now, the question is: What happens if element shown in Figure 2.9 is not rotated about one of the principal axes, so that some shear stress is produced one more than two opposite faces? First, let us show that the state of stress is represented by points that are all within the zone enclosed by the three Mohr's circles [22]. This is the yellow zone in Figure 2.10. The normal and shear components of the stress vector $\mathbf{T^{(n)}}$, for a given plane with unit vector $\mathbf{n}$, satisfy the following equations:

$$\left(T^{(n)} \right)^2 = \sigma_{ij}\sigma_{ik}n_j n_k \qquad (2.59)$$
$$\sigma_n^2 + \tau_n^2 = \sigma_1^2 n_1^2 + \sigma_2^2 n_2^2 + \sigma_3^2 n_3^2$$
$$\sigma_n = \sigma_1 n_1^2 + \sigma_2 n_2^2 + \sigma_3 n_3^2$$

Knowing that $n_i n_i = n_1^2 + n_2^2 + n_3^2 = 1$, we can solve for n_1^2, n_2^2, n_3^2. Using the Gauss elimination method which yields:

$$n_1^2 = \frac{\tau_n^2 + (\sigma_n - \sigma_2)(\sigma_n - \sigma_3)}{(\sigma_1 - \sigma_2)(\sigma_1 - \sigma_3)} \geq 0 \qquad (2.60)$$

$$n_2^2 = \frac{\tau_n^2 + (\sigma_n - \sigma_3)(\sigma_n - \sigma_1)}{(\sigma_2 - \sigma_3)(\sigma_2 - \sigma_1)} \geq 0$$

$$n_3^2 = \frac{\tau_n^2 + (\sigma_n - \sigma_1)(\sigma_n - \sigma_2)}{(\sigma_3 - \sigma_1)(\sigma_3 - \sigma_2)} \geq 0$$

Since $\sigma_1 > \sigma_2 > \sigma_3$, and $(n_i)^2$ is non-negative, the numerators from these equations satisfy

$$\tau_n^2 + (\sigma_n - \sigma_2)(\sigma_n - \sigma_3) \geq 0 \text{ because } \sigma_1 - \sigma_2 > 0, \quad \sigma_1 - \sigma_3 > 0 \quad (2.61)$$

$$\tau_n^2 + (\sigma_n - \sigma_3)(\sigma_n - \sigma_1) \leq 0 \text{ because } \sigma_2 - \sigma_3 > 0, \quad \sigma_2 - \sigma_1 < 0$$

$$\tau_n^2 + (\sigma_n - \sigma_1)(\sigma_n - \sigma_2) \geq 0 \text{ because } \sigma_3 - \sigma_1 < 0, \quad \sigma_3 - \sigma_2 < 0$$

These expressions can be rewritten as

$$\tau_n^2 + \left[\sigma_n - \tfrac{1}{2}(\sigma_2 + \sigma_3)\right]^2 \geq \left(\tfrac{1}{2}(\sigma_2 - \sigma_3)\right)^2 \qquad (2.62)$$

$$\tau_n^2 + \left[\sigma_n - \tfrac{1}{2}(\sigma_1 + \sigma_3)\right]^2 \leq \left(\tfrac{1}{2}(\sigma_1 - \sigma_3)\right)^2$$

$$\tau_n^2 + \left[\sigma_n - \tfrac{1}{2}(\sigma_1 + \sigma_2)\right]^2 \geq \left(\tfrac{1}{2}(\sigma_1 - \sigma_2)\right)^2$$
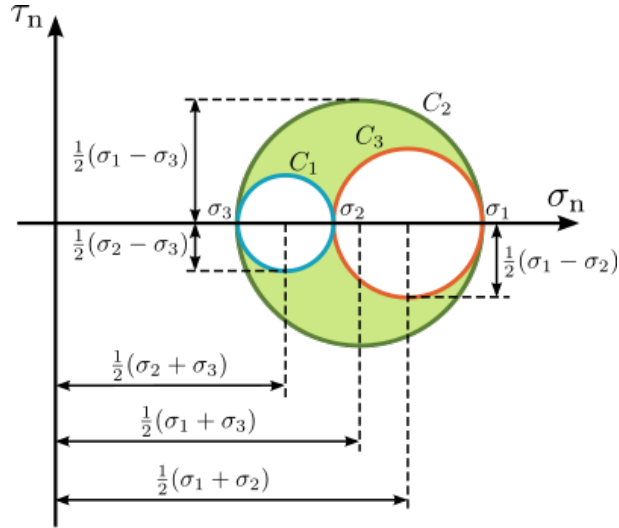
which are the equations of the three Mohr's circles for stress C_1, C_2, and C_3, with radii $R_1 = \tfrac{1}{2}(\sigma_2 - \sigma_3)$, $R_2 = \tfrac{1}{2}(\sigma_1 - \sigma_3)$, and $R_3 = \tfrac{1}{2}(\sigma_1 - \sigma_2)$, and their centers with coordinates $\left[\tfrac{1}{2}(\sigma_2 + \sigma_3), 0\right]$, $\left[\tfrac{1}{2}(\sigma_1 + \sigma_3), 0\right]$, $\left[\tfrac{1}{2}(\sigma_1 + \sigma_2), 0\right]$, respectively. These equations for the Mohr circles show that all admissible stress points (σ_n, τ_n) lie on these circles or within the shaded area enclosed by them (see Figure 2.10). Stress points (σ_n, τ_n) satisfying the equation for circle C_1 lie on, or outside circle C_1. Stress points (σ_n, τ_n) satisfying the equation for circle C_2 lie on, or inside circle C_2. And finally, stress points (σ_n, τ_n) satisfying the equation for circle C_3 lie on, or outside circle C_3.

So one may wonder how a stress point travels in the stress space when the 3D material point is rotated about an arbitrary axis. Let us denote the components of the unit normal vector of an arbitrary plane, relative to the principal coordinate system, by (l, m, n). We denote the three principal directions (i.e. the directions of the vectors normal to the planes that are subjected to a principal stress), by (x, y, z). It can be shown [13] that the normal and shear tractions acting on this plane are:

$$\sigma = l^2 \sigma_1 + m^2 \sigma_2 + n^2 \sigma_3 \qquad (2.63)$$

$$\tau^2 = l^2 \sigma_1 + m^2 \sigma_2 + n^2 \sigma_3 - \sigma^2$$

where:

$$l^2 + m^2 + n^2 = 1 \qquad (2.64)$$

Figure 2.10   The zone of 3D admissible states of stress with the Mohr circle representation. Image taken from [22].

Solving these equations yields:

$$l^2 = \frac{(\sigma_2 - \sigma)(\sigma_3 - \sigma) + \tau^2}{(\sigma_2 - \sigma_1)(\sigma_3 - \sigma_1)} \qquad (2.65)$$

$$m^2 = \frac{(\sigma_3 - \sigma)(\sigma_1 - \sigma) + \tau^2}{(\sigma_3 - \sigma_2)(\sigma_1 - \sigma_2)}$$

$$n^2 = \frac{(\sigma_1 - \sigma)(\sigma_2 - \sigma) + \tau^2}{(\sigma_1 - \sigma_3)(\sigma_2 - \sigma_3)}$$

Suppose that the direction n is fixed, so that the normal vector makes a fixed angle $\theta = arcos(n)$ with the z-axis, as shown in Figure 2.11. The intersection of the normal vector with the unit sphere will lie on the small circle F'E'D'. Equation 2.65 can be rearranged to yield:

$$\tau^2 + \left[\sigma - \frac{1}{2}(\sigma_1 + \sigma_2)\right]^2 = \frac{1}{4}(\sigma_1 - \sigma_2)^2 + n^2(\sigma_1 - \sigma_3)(\sigma_2 - \sigma_3) \qquad (2.66)$$

which is the equation of a circle in the (σ, τ) plane. The center of this circle, A, is located at:

$$\sigma = \frac{1}{2}(\sigma_1 + \sigma_2), \quad \tau = 0 \qquad (2.67)$$

and the radius of the circle is:

$$r = \left[\frac{1}{4}(\sigma_1 - \sigma_2)^2 + n^2(\sigma_1 - \sigma_3)(\sigma_2 - \sigma_3)\right]^{1/2} \qquad (2.68)$$

As n varies from 0 to 1, the radius varies from AQ$=(\sigma_1 - \sigma_2)/2$ to AR$=[(\sigma_1 + \sigma_2)/2] - \sigma_3$. A typical circle for an intermediate value of n is shown in Figure 2.11 as DEF. In the same
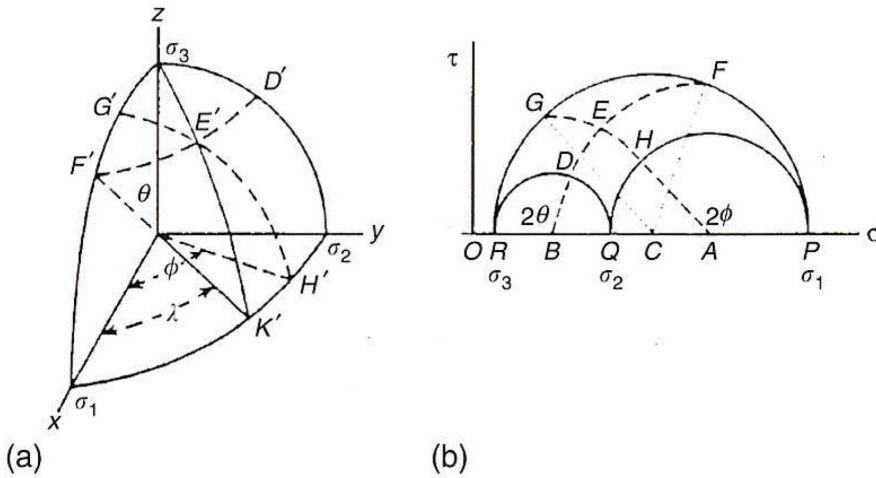
manner, holding l constant in Equation 2.65 gives the family of circles:

$$\tau^2 + \left[\sigma - \frac{1}{2}(\sigma_2 + \sigma_3)\right]^2 = \frac{1}{4}(\sigma_2 - \sigma_3)^2 + l^2(\sigma_2 - \sigma_1)(\sigma_3 - \sigma_1) \qquad (2.69)$$

The centers of these circles are at B, located at $\sigma = (\sigma_2 + \sigma_3)/2$, $\tau = 0$. The radii vary from BQ=$(\sigma_2 - \sigma_3)/2$ when $l = 0$, to BP=$\sigma_1 - [(\sigma_2 + \sigma_3)/2]$, when $l = 1$. A typical circle for intermediate values of l is GEH. In Figure 2.11, planes for which l is a constant lie on a cone that make an angle $\phi = arcos(l)$ with the x-axis, and which intersects the unit sphere at G'E'H'. Finally, holding m constant in Equation 2.65 gives the family of circles:

$$\tau^2 + \left[\sigma - \frac{1}{2}(\sigma_1 + \sigma_3)\right]^2 = \frac{1}{4}(\sigma_1 - \sigma_3)^2 + m^2(\sigma_3 - \sigma_2)(\sigma_1 - \sigma_2) \qquad (2.70)$$

The centers of these circles are at C, located at $\sigma = (\sigma_1 + \sigma_3)/2$, $\tau = 0$. The radii vary from CR=$(\sigma_1 - \sigma_2)/2$ when $m = 0$, to CQ=$[(\sigma_1 + \sigma_3)/2] - \sigma_2$, when $m = 1$. Note that these circles are no shown in Figure 2.11. The last question to answer is what is the relationship between an angle of rotation in the 3D physical space and the 3D stress space illustrated in Figure 2.11. We will not perform such operations in this course, so the reader is referred to [13] for the details of that procedure.

Figure 2.11   Mohr's circles in three dimensions. Image taken from [13].

2.2.7   Deviatoric plane representation and Lode angle

In the principal stress space, the hydrostatic axis (or space diagonal) is the line that makes equal angles with all three axes. The unit vector along the hydrostatic axis has components:

$$n = \left\{\frac{1}{\sqrt{3}}, \frac{1}{\sqrt{3}}, \frac{1}{\sqrt{3}}\right\} \qquad (2.71)$$

Any plane perpendicular to the hydrostatic axis is called deviatoric plane. The deviatoric plane that passes through the origin is called the p-plane. Any given stress state plots

as a point P with coordinates $(\sigma_1, \sigma_2, \sigma_3)$, as shown in Figure 2.12. The vector $\mathbf{OP}= \{\sigma_1, \sigma_2, \sigma_3\}$ is referred to as the stress vector. The stress vector may be decomposed into two components, $\mathbf{OP}=\mathbf{ON}+\mathbf{NP}$ where $\mathbf{ON}$ is carried by the space diagonal and $\mathbf{NP}$ is contained in the deviatoric stress plane passing through N and P. We have:
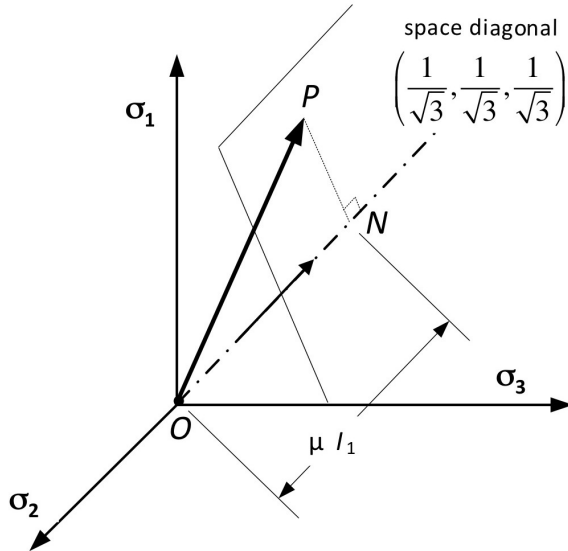
$$|\mathbf{ON}| = \mathbf{OP} \cdot \mathbf{n} = \frac{1}{\sqrt{3}}(\sigma_1 + \sigma_2 + \sigma_3) = \frac{1}{\sqrt{3}} I_1 \qquad (2.72)$$

The vector $\mathbf{ON}$ has components $\{p, p, p\}$ along the three reference axes, and the vector $\mathbf{NP}$ has components:

$$\mathbf{NP} = \mathbf{OP} - \mathbf{ON} = \{s_1, s_2, s_3\} \qquad (2.73)$$

in which $s_1 = \sigma_1 - p$, $s_2 = \sigma_2 - p$ and $s_3 = \sigma_3 - p$ are the principal stresses of the deviatoric stress tensor associated with $\boldsymbol{\sigma}$. The length of the vector $\mathbf{NP}$ is:
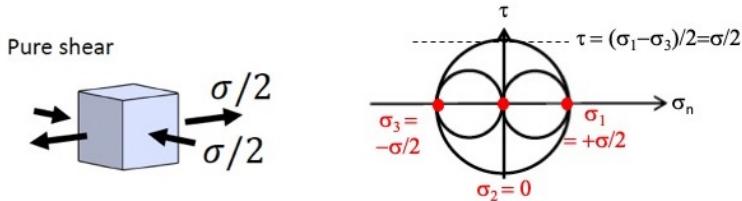
$$|\mathbf{NP}| = \left(s_1^2 + s_2^2 + s_3^2\right)^{1/2} = Tr\left(\mathbf{s}^2\right) = \sqrt{2\,J_2} \qquad (2.74)$$

Figure 2.12   Stress vector decomposition in the principal stress space. Image taken from [2].

The state of pure shear is defined as a state of stress in which a face is subhected to a tension $-\sigma/2$ on one face while being subjected to a compression $+\sigma/2$ on a face orthogonal to the face in tension (note the soil mechanics sign convention adopted here). In the state of pure shear, the minor principal stress is $\sigma_3 = -\sigma/2$, the major principal stress is $\sigma_1 = +\sigma/2$ and the intermediate principal stress is $\sigma_2 = 0$, as shown in Figure 2.13. Using Mohr's circles (see Subsection 2.2.6), it can be found that the shear stress that is applied on the faces of normal $\mathbf{e}_2$ is $\tau = (\sigma_1 - \sigma_3)/2 = (s_1 - s_3)/2 = \sigma/2$. Moreover, $\sigma_2 = (\sigma_1 + \sigma_3)/2$, which yields $s_2 = (s_1 + s_3)/2$. Correspondingly, in the deviatoric plane, the pure shear axis is defined by the equation: $s_2 = (s_1 + s_3)/2$.

Figure 2.14 shows a view at right angle to the deviatoric plane through N, so that the three principal stress axes appear at angles of $2\pi/3$ to each other. Let θ be the polar angle

Figure 2.13   State of pure shear. Image adapted from [16].
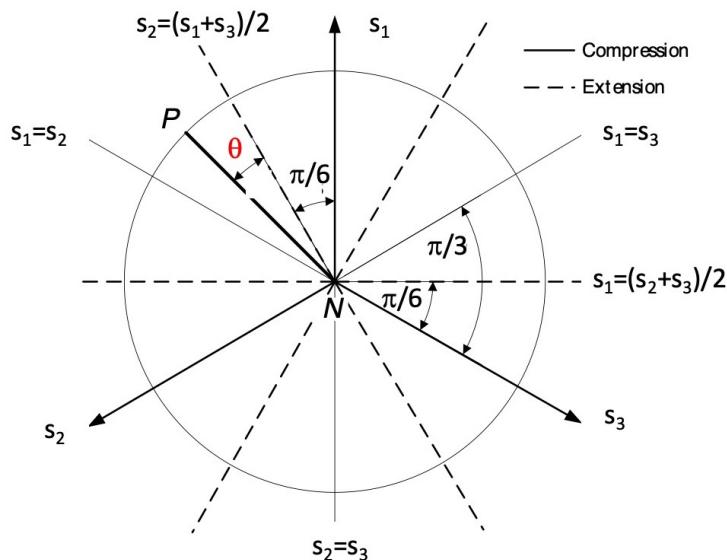
measured from pure shear axis. From Figure 2.14, it can be shown that:

$$sin\theta = \frac{\sqrt{3}s_2}{2\sqrt{J_2}} = \sqrt{\frac{3}{2}}\frac{s_2}{\sqrt{2\,J_2}} = \sqrt{\frac{3}{2}}\frac{s_2}{|\boldsymbol{NP}|}, \quad -\frac{\pi}{6} \le \theta \le +\frac{\pi}{6} \qquad (2.75)$$

Using the trigonometric identity $sin(3\theta) = 3sin\theta - 4sin^3\theta$ and performing the algebraic manipulations:

$$sin3\theta = \frac{3\sqrt{3}J_3}{2J_2^{3/2}}, \quad J_3 = \det(\boldsymbol{s}) = Tr\left(\frac{\boldsymbol{s}^3}{3}\right) \qquad (2.76)$$

The angle θ is called the Lode angle.
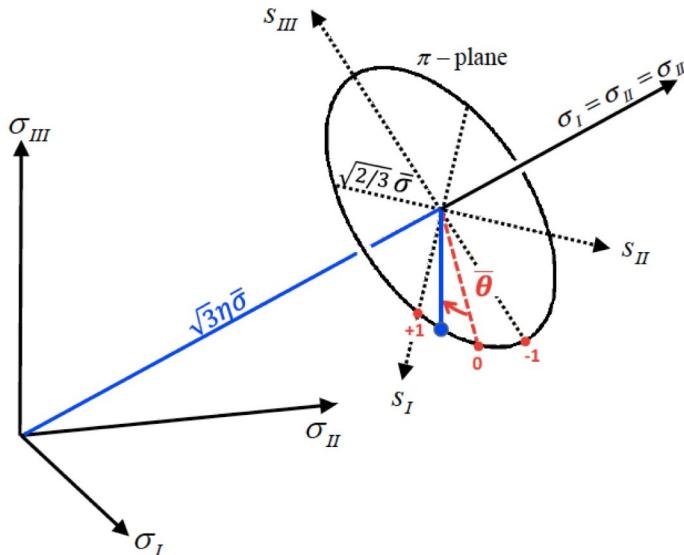
Figure 2.14   The deviatoric stress space. Image taken from [2].

The three principal stresses are explicitly given by the three roots of the characteristic equation (Equation 2.29):

$$\left.\begin{array}{rcl}
\sigma_1 &=& p + \frac{2}{\sqrt{3}}\sqrt{J_2}\sin\left(\theta + \frac{2\pi}{3}\right) \\[2mm]
\sigma_2 &=& p + \frac{2}{\sqrt{3}}\sqrt{J_2}\sin\theta \\[2mm]
\sigma_3 &=& p + \frac{2}{\sqrt{3}}\sqrt{J_2}\sin\left(\theta - \frac{2\pi}{3}\right)
\end{array}\right\} \quad \sigma_1 \geq \sigma_2 \geq \sigma_3 \qquad (2.77)$$

Note that while J_2 is proportional to the magnitude of the shearing stress, J_3 relates to the direction of shearing by means of the Lode angle. Figure 2.15 provides another representation of the Lode angle, in 3D.

Figure 2.15   Representation of the Lode angle (noted $\bar{\theta}$ in this sketch) in the principal stress space. Image taken from [16].

Finally, a path in stress space indicates successive states stressing in a material specimen, and is called a stress path. If the path lies entirely within the plane passing through the s_1 axis and making equal angles of 45° with both the s_2 and s_3 axes, it is called an axial stress path.

2.2.8   Octahedral stress

When the directions of the three principal stresses are taken as coordinates, planes that have outward normal forming equal angles with these three axes must have the mean normal stress p acting on them as the normal stress. There are eight such planes as can be seen Figure 2.16, and the mean normal stress and resultant shear stress on these planes are
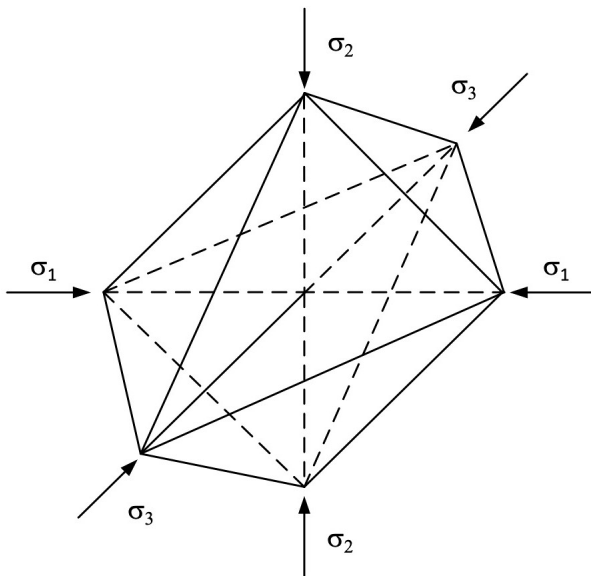
referred to as octahedral normal and octahedral shear stress respectively:

$$s_{11}^* = s_{oct} = \frac{1}{3}(s_1 + s_2 + s_3) \tag{2.78}$$

$$s_{12}^* = \frac{1}{\sqrt{6}}(s_2 - s_1)$$

$$s_{13}^* = \frac{1}{3\sqrt{2}}(2s_3 - s_1 - s_2)$$

$$t_{oct}^2 = (s_{12}^*)^2 + (s_{13}^*)^2 = \frac{1}{9}\left[(s_1 - s_2)^2 + (s_2 - s_3)^2 + (s_3 - s_1)^2\right]$$
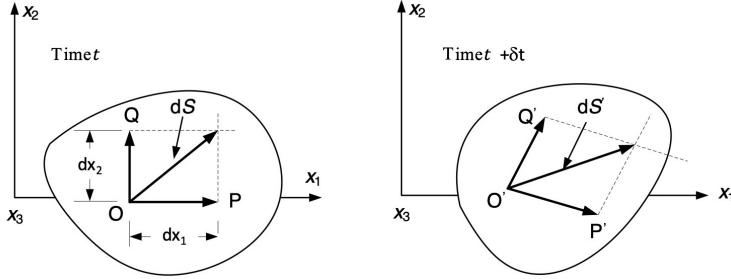
Figure 2.16   The eight planes subjected to the mean normal stress p. Image taken from [16].

2.3 Concept of deformation

2.3.1 Geometric transformation and Green-Lagrange deformation tensor

2.3.1.1 Deformed and undeformed configurations

The configuration of a solid body is described by a continuous mathematical model, whose geometric points are identified with particles of the body. For example, consider the configuration shown in Figure 2.17. At time t, the solid body illustrated on the left is undeformed, and at time $t + \delta t$ it has deformed given the externally applied loads and boundary conditions at time t. The so-called concept of kinematics in solid mechanics refers to the description of deformations that are associated with the differences in the deformed and undeformed configurations. Any change that introduces new boundary surfaces shall be regarded as an extraordinary circumstance and will not be considered in the context of this course (e.g. fractures that introduce new surface by means of cracks).

Figure 2.17   Illustration of deformed and undeformed configurations. Image taken from [2].

2.3.1.2 Jacobian

We note $\underline{X}$ the position vector in the initial configuration (at time t) and $\underline{x}$ the position vector in the current configuration (at time $t + \delta t$). The coordinate change between a space derivative at t and a space derivative at $t + \delta t$ can be operated by the Jacobian matrix, which is defined as follows in the Cartesian coordinate system:

$$[J] = \begin{bmatrix} \frac{\partial x_1}{\partial X_1} & \frac{\partial x_2}{\partial X_1} & \frac{\partial x_3}{\partial X_1} \\ \frac{\partial x_1}{\partial X_2} & \frac{\partial x_2}{\partial X_2} & \frac{\partial x_3}{\partial X_2} \\ \frac{\partial x_1}{\partial X_3} & \frac{\partial x_2}{\partial X_3} & \frac{\partial x_3}{\partial X_3} \end{bmatrix} \tag{2.79}$$

The determinant of $[J]$ is noted J and is called the Jacobian. The Jacobian satisfies the following property:

$$\Omega_{t+\delta t} = \int_{\Omega_t} J \, d\Omega \tag{2.80}$$

in which Ω_t and $\Omega_{t+\delta t}$ are the volume of the body at time t and $t + \delta t$, respectively. In incremental version:

$$d\Omega_{t+\delta t} = J \, d\Omega_t \tag{2.81}$$

Equation 2.81 is very useful whenever a coordinate change is needed in space integrals. The condition for integration is that $J > 0$. The Jacobian represents the volumetric dilation of the volume between the initial and current configurations.
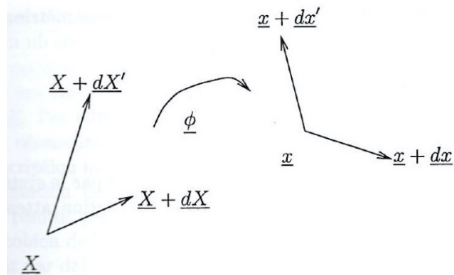
2.3.1.3 Green-Lagrange deformation tensor and small deformation assumption

Consider two vectors $d\underline{X}$ and $d\underline{X}'$ of origin the position $\underline{X}$ in the initial configuration. Suppose that these two vectors are transformed into the vectors $d\underline{x}$ and $d\underline{x}'$ of origin the position $\underline{x}$ in the current configuration, as shown in Figure 2.18. The transport of vector $\underline{X}$ into $\underline{x}$ is operated by the transport function $\underline{\Phi}$: $\underline{x} = \underline{\Phi}(\underline{X}, t)$, and we have:

$$d\underline{x} = \underline{\Phi}(\underline{X} + d\underline{X}, t) - \underline{\Phi}(\underline{X}, t) = \underline{\underline{F}}(\underline{X}, t) \cdot d\underline{X}, \quad \underline{\underline{F}}(\underline{X}, t) = \underline{\nabla}(\underline{\Phi}) \tag{2.82}$$

Deformation implies a change in length and or/angles, i.e. a deformation is the opposite of an isometry. A fundamental property of an isometry is to conserve the scalar product. Let us calculate the difference between the scalar product of the two vectors $d\underline{x}$ and $d\underline{x}'$ in the current configuration and the scalar product of the two vectors $d\underline{X}$ and $d\underline{X}'$ in the initial configuration:

$$d\underline{x} \cdot d\underline{x}' - d\underline{X} \cdot d\underline{X}' = d\underline{X} \cdot \left({}^T\underline{\underline{F}} \cdot \underline{\underline{F}} - \underline{\underline{I}}\right) \cdot d\underline{X}' = 2 \, d\underline{X} \cdot \underline{\underline{e}} \cdot d\underline{X}' \tag{2.83}$$

Figure 2.18   Transport of material vectors from the initial to the current configuration. Image taken from [6].

in which:

$$\underline{\underline{e}} = \frac{1}{2} \left({}^T\underline{\underline{F}} \cdot \underline{\underline{F}} - \underline{\underline{I}} \right) \tag{2.84}$$

$\underline{\underline{e}}$ is called the Green-Lagrange deformation tensor. It is zero if and only if $\underline{\underline{F}} \cdot \underline{\underline{F}} = \underline{\underline{I}}$, i.e., when $\underline{\underline{F}}$ is a rotation or the identity. As a result, the transformation from the initial configuration to the current configuration is an isometry if, and only if, the transformation is a rigid body motion. If the transformation is not an isometry, there is a deformation between the initial and current configurations, and this deformation is quantified by the tensor $\underline{\underline{e}}$. We define the displacement field $\underline{u}$ as follows:

$$\underline{u}\left(\underline{X},\, t\right) = \underline{\Phi}\left(\underline{X}, t\right) - \underline{X} = \underline{x} - \underline{X} \tag{2.85}$$

From Equations 2.82 and 2.85, we have:

$$\underline{\underline{F}}\left(\underline{X}\, t\right) = \underline{\underline{I}} + \underline{\nabla}\left(\underline{u}\left(\underline{X},\, t\right)\right) \tag{2.86}$$

The combination of Equations 2.84 and 2.86 gives the expression of the Green-Lagrange tensor deformation as a function of the displacement field, as follows:

$$\underline{\underline{e}} = \frac{1}{2}\left(\underline{\nabla}\left(\underline{u}\right) + {}^T\underline{\nabla}\left(\underline{u}\right) + \underline{\nabla}\left(\underline{u}\right) \cdot {}^T\underline{\nabla}\left(\underline{u}\right)\right) \tag{2.87}$$

Under the assumtion that:

$$\left|\underline{\nabla}\left(\underline{u}\right)\right| << 1 \tag{2.88}$$

we can neglecct the terms $\underline{\nabla}\left(\underline{u}\right)$ or order two in Equation 2.87. The resulting tensor is called the linearized deformation tensor and is noted $\underline{\underline{\epsilon}}$:

$$\underline{\underline{\epsilon}} = \frac{1}{2}\left(\underline{\nabla}\left(\underline{u}\right) + {}^T\underline{\nabla}\left(\underline{u}\right)\right) \tag{2.89}$$

The statement in Equation 2.88 is called the small deformation assumption. One can calculate deformation with the linearized deformation tensor defined in Equation 2.89 only if the small deformation assumption holds. The properties of the linearized deformation tensor are similar to those of the Cauchy's stress tensor, in particular, $\underline{\underline{\epsilon}}$ is symmetric, and possesses invariants defined in the same as in Equations 2.30 and 2.32. Lastly, we define the volumetric deformation as follows:

$$\epsilon_v = Tr\left(\underline{\underline{\epsilon}}\right) = \sum_i \epsilon_{ii} \tag{2.90}$$

2.3.2 Kinetic admissibility

The compatibility equations are derived from kinematic considerations which relate the components of a strain field ϵ_{ij} to the components of the displacement field u_i. It may also be necessary to impose the condition of compatibility of strains or displacements in order to ensure that these strain-displacement relations are integrable for a prescribed strain field. A set of displacements and strains that satisfies these geometry conditions in addition to the imposed displacement boundary conditions is called *kinematically admissible set*, or *simply compatible set.* The kinematic considerations lead to the following conditions for small deformations:

- Strain-displacement relations:

$$\epsilon_{ij} = \frac{1}{2}\left(\frac{\partial u_i}{\partial x_j} + \frac{\partial u_j}{\partial x_i}\right) \tag{2.91}$$

- Compatibility conditions:

$$\frac{\partial^2 \epsilon_{ij}}{\partial x_k \partial x_l} + \frac{\partial^2 \epsilon_{kl}}{\partial x_i \partial x_j} - \frac{\partial^2 \epsilon_{ik}}{\partial x_j \partial x_l} - \frac{\partial^2 \epsilon_{jl}}{\partial x_i \partial x_k} = 0 \tag{2.92}$$
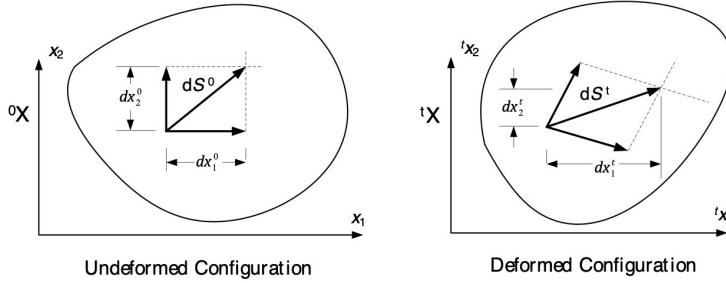
The compatibility conditions are the geometrical relationship that strain tensor ϵ_{ij} at each material point must satisfy in order to ensure a continuous deformation for the continuum. These conditions comprise 81 equations, however only six equations are independent to each other, given that the symmetry of the strain tensor is accounted for, i.e. $\epsilon_{ij} = \epsilon_{ji}$. Therefore, a compatible set of displacements u_i and strains ϵ_{ij} must satisfy Equations **??** and along with the displacement boundary conditions. In most practical problems, the displacements are taken explicitly as the unknowns in the formulation. Then, the compatibility conditions in Equation 2.3.2 are not needed, and only Equation 2.91 is required to derive strains from the displacements. In such cases, there are nine independent unknowns (namely, six stress components σ_{ij} plus three displacement components u_i, while strains are expressed in terms of the displacements). On the other hand, for static problems, only three equations of motion are available, thus the six additional equations needed to complete the formulation of the problem are furnished by the constitutive (stress-strain) relations of the material.

2.3.3 Large deformation

There are problems in soil mechanics where geometrical nonlinearities, which refer to nonlinear phenomena occurring due to the effects of deformation on the overall geometry change of the configuration, cannot be described by means of small-stain theory. In this case, namely when the displacement-gradient components are not small compared to unity, the problem of characterizing the strain from the initial state is more cumbersome than in the small-strain case, and implies that the concept of finite strains needs to be introduced. Phenomena described by this concept include the progressive failure response of a soft ground to footing load, 1D consolidation of very compressible soils (e.g. slurry consolidation), liquefaction and landslides. We shall here present an overview of the two most commonly used solution procedures for the analysis of large-strain and large-displacement continuum problems. The finite strain definitions associated with these procedures, can be categorized as follows:

1. Definitions in terms of the undeformed configuration (referred to as Lagrangian), and

2. Definitions in terms of the deformed configuration (referred to as Eulerian).

When coordinates are introduced, the first class uses material coordinates in the undeformed configuration, while the second class uses spatial coordinates in the deformed configuration, as illustrated in Figure 2.19.

Undeformed Configuration   Deformed Configuration

Figure 2.19   Coordinate systems in the underformed (initial) configuration and in the deformed (current) configuration. Image taken from [2].

In the undeformed configuration shown in Figure 2.19, we have:

$$\left(dS^0\right)^2 = \delta_{ij}\, dx_i^0\, dx_j^0 \tag{2.93}$$

In the deformed configuration shown in Figure 2.19, we have:

$$\left(dS^t\right)^2 = \delta_{ij}\, dx_i^t\, dx_j^t \tag{2.94}$$

We shall now write the position vector in the current $^t x$ coordinate frame, in terms of the initial $^0 x$ frame:

$$d^t x_i = \left(\frac{\partial^t x_i}{\partial^0 x_j}\right) d^0 x_j = \left[\frac{\partial}{\partial^0 x_j}\left(^0 x_i +^t u_i\right)\right] d^0 x_j \tag{2.95}$$

Note that we use the displacement definition: $^t x_i =^0 x_i +^t u_i$, where $^t u_i$ is the displacement vector. Therefore, Equation 2.95 can be rewritten as:

$$d^t x_i = \left[\frac{\partial\left(^0 x_i +^t u_i\right)}{\partial^0 x_j}\right] d^0 x_j = \left[\delta_{ij} + \frac{\partial^t u_i}{\partial^0 x_j}\right] d^0 x_j \tag{2.96}$$

The strain tensors are defined so that they give the change in the square length of the material vector $d\underline{S}$. Therefore, the formulation of the strain tensor in the two alterative reference configurations is:

- Lagrangian strain definition:

$$\left[\left(dS^t\right)^2 - \left(dS^0\right)^2\right] = 2L_{ij}dx_i^0 dx_j^0 \tag{2.97}$$

- Eulerian strain definition:

$$\left[\left(dS^t\right)^2 - \left(dS^0\right)^2\right] = 2E_{ij}dx_i^t dx_j^t \tag{2.98}$$

The tensors $\underline{L}$ and $\underline{E}$ are defined as:

$$L_{ij} = \frac{1}{2} \left[\frac{\partial^t u_i}{\partial^0 x_j} + \frac{\partial^t u_j}{\partial^0 x_i} + \frac{\partial^t u_k}{\partial^0 x_i} \frac{\partial^t u_k}{\partial^0 x_j} \right] \tag{2.99}$$

$$E_{ij} = \frac{1}{2} \left[\frac{\partial^t u_i}{\partial^t x_j} + \frac{\partial^t u_j}{\partial^t x_i} - \frac{\partial^t u_k}{\partial^t x_i} \frac{\partial^t u_k}{\partial^t x_j} \right] \tag{2.100}$$

2.4   Linear elastic constitutive relationships

2.4.1   Linear elastic stiffness tensor

Having derived the mathematical descriptions of stress, strain and rate of deformation, we here consider equations characterizing the individual materials and their reactions to applied loads; such equations are called constitutive equations, since they describe the macroscopic behavior resulting from the internal constitution of the material. Nonetheless, solid materials behave in a very complex way when the entire range of possible temperatures and deformations is considered, that is not feasible to derive equations which describe accurately a real material over its entire range of behavior. Instead, we formulate separately equations that describe various categories of ideal material behavior, each one of which is a mathematical formulation designed to approximate physical observations of a real material?s response over a suitably restricted (practical) range of interest. In soil mechanics, the simplest constitutive relation that can be formulated is the one that describes the stress-stain behavior of ideal elastic materials.

The linear elastic solid (or Hookean solid) is the ideal material most commonly assumed for stress analysis in continuum mechanics theory. It is assumed to obey Hooke?s law, which in a uniaxial stress situation takes the form $\sigma = E\epsilon$, expressing a linear relation between the axial stress and strain, where E is the modulus of elasticity. The basic relations between stress and strain, upon which many of the others are based, are those of linear elasticity. Since there are 9 independent components of stress and 9 of strain, 81 coefficients are needed to relate them linearly in the most general way, i.e. $\sigma_{ij} = C_{ijkl}\epsilon_{lk}$. Therefore, the matrix $\boldsymbol{C}$, called the stiffness matrix, is a fourth order tensor that contains 81 linear coefficients. The stress-strain relation can also be expressed in the inverse form, i.e. $\epsilon_{ij} = C_{ijkl}^{-1}\sigma_{lk} = D_{ijkl}\sigma_{lk}$. The matrix $\boldsymbol{D}$ that relates strains to stresses is referred to as the compliance matrix. We have illustrated above, however, that the stress and strain tensors are symmetric, namely that they contain 6 independent components instead of 9. That means that only 36 coefficients are needed to relate the stress and strain tensors linearly in the most general way, namely:

$$\left. \begin{array}{l} \sigma_{ij} = \sigma_{ji} \Rightarrow C_{ijkl} = C_{jikl} \\[2mm] \epsilon_{kl} = \epsilon_{lk} \Rightarrow C_{ijkl} = C_{ijlk} \end{array} \right\} \Rightarrow C_{ijkl} \text{ contains 36 components.} \tag{2.101}$$

However, by considering the energy stored in a strained linear elastic body, one can show that the coefficients must form a symmetric array. The term relating, say, σ_{ij} to ϵ_{kl}, must be the same as the one relating σ_{kl} to ϵ_{ij}, through $C_{ijkl} = C_{klij}$. This symmetry of the stress-strain relation reduces the number of independent terms to 21 coefficients.

For most numerical purposes, it is most useful to use Voigt notation for the stress and strain tensors, i.e., to write the stresses and strains as vectors:

$$\{\boldsymbol{\sigma}\}^T = \{\sigma_{11}, \sigma_{22}, \sigma_{33}, \sigma_{12}, \sigma_{23}, \sigma_{31}\} \tag{2.102}$$

$$\{\boldsymbol{\epsilon}\}^T = \{\epsilon_{11}, \ \epsilon_{22}, \ \epsilon_{33}, \ \epsilon_{12}, \ \epsilon_{23}, \ \epsilon_{31}\} \tag{2.103}$$

With Voigt notation, the linear elastic stress-strain relationship is written as:

$$\begin{Bmatrix} \sigma_{11} \\ \sigma_{22} \\ \sigma_{33} \\ \sigma_{12} \\ \sigma_{23} \\ \sigma_{31} \end{Bmatrix} = \begin{bmatrix} C_{11}^* & C_{12}^* & C_{13}^* & C_{14}^* & C_{15}^* & C_{16}^* \\ \dots & C_{22}^* & C_{23}^* & C_{24}^* & C_{25}^* & C_{26}^* \\ \dots & \dots & C_{33}^* & C_{34}^* & C_{35}^* & C_{36}^* \\ \dots & \dots & \dots & C_{44}^* & C_{45}^* & C_{46}^* \\ \dots & \dots & \dots & \dots & C_{55}^* & C_{56}^* \\ \dots & \dots & \dots & \dots & \dots & C_{66}^* \end{bmatrix} \begin{Bmatrix} \epsilon_{11} \\ \epsilon_{22} \\ \epsilon_{33} \\ \epsilon_{12} \\ \epsilon_{23} \\ \epsilon_{31} \end{Bmatrix} \tag{2.104}$$

in which we only wrote the terms of the Voigt stiffness matrix above the diagonal, since the matrix is symmetric. Note that the relation between the Voigt matrix and the actual matrix is as follows: $C_{1111} = C_{11}^*$, $C_{1112} = C_{12}^*$, etc. The number of independent terms can be further reduced by considering the planes or axes of isotropy in the material. In geotechnical engineering, the three most commonly used types are (with decreasing level of complexity) orthotropy, cross-anisotropy (also called transverse isotropy) and complete isotropy. Note that these symmetries are a directional property and not a positional property. Even when the material has a certain elastic symmetry at each point, the properties may vary from point to point irrespective of the symmetry of the shape of the body.

2.4.2   Orthotropic symmetry
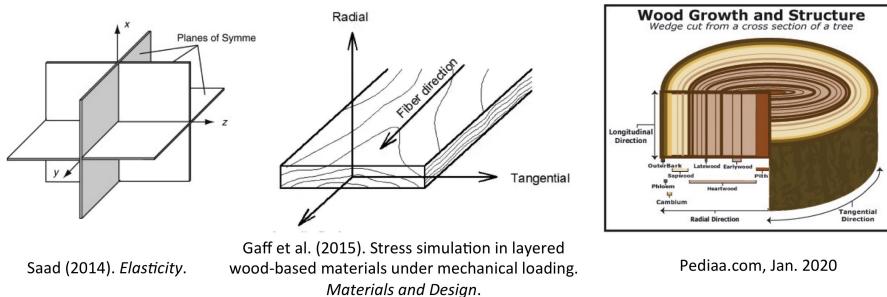
An orthotropic material has 3 orthogonal planes of symmetry, as shown in Figure 2.20. The coefficient matrix for orthotropic symmetry with respect to the coordinate planes has 9 independent coefficients, namely:

$$[C^*] = \begin{bmatrix} C_{11}^* & C_{12}^* & C_{13}^* & 0 & 0 & 0 \\ \dots & C_{22}^* & C_{23}^* & 0 & 0 & 0 \\ \dots & \dots & C_{33}^* & 0 & 0 & 0 \\ \dots & \dots & \dots & C_{44}^* & 0 & 0 \\ \dots & \dots & \dots & \dots & C_{55}^* & 0 \\ \dots & \dots & \dots & \dots & \dots & C_{66}^* \end{bmatrix} \tag{2.105}$$

Note that in an orthotropic material, the normal stresses are decoupled from the shear stresses, however, the limitations of applying this formulation to represent geomaterials can be readily seen when we consider phenomena such as dilation or contraction during shear, namely phenomena where shear strain introduces volume changes.

2.4.3   Transverse isotropy
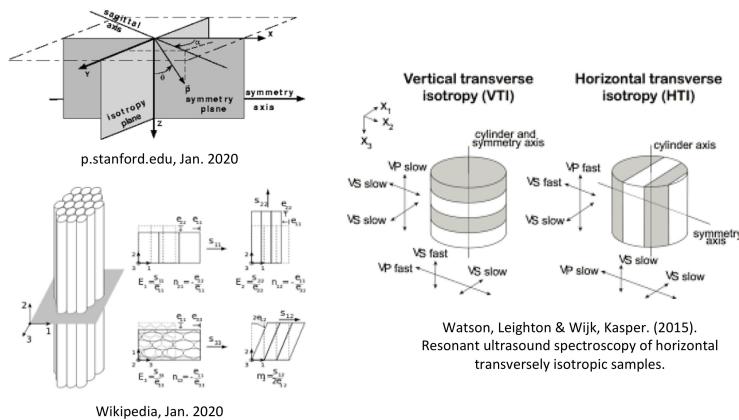
Cross-anisotropic symmetry, also called transverse isotropy, applies when there is some plane (usually horizontal) in which all stress-strain relations are isotropic; i.e., it makes no difference how the axes are chosen within the plane: the elastic constants are the same. The elastic constants for stresses and strains outside the plane are different. Figure 2.21 illustrates what cross-anisotropy is. The resulting matrix $[C^*]$ has 5 independent constants.

Saad (2014). *Elasticity*.

Gaff et al. (2015). Stress simulation in layered wood-based materials under mechanical loading. *Materials and Design*.

Pediaa.com, Jan. 2020

Figure 2.20 Definition of orthotropy and examples of orthotropic materials.

For example, if the x_3 axis is normal to the plane of isotropy, the matrix becomes:

$$[C^*] = \begin{bmatrix} C_{11}^* & C_{12}^* & C_{13}^* & 0 & 0 & 0 \\ \dots & C_{11}^* & C_{13}^* & 0 & 0 & 0 \\ \dots & \dots & C_{33}^* & 0 & 0 & 0 \\ \dots & \dots & \dots & 2\left(C_{11}^* - C_{12}^*\right) & 0 & 0 \\ \dots & \dots & \dots & \dots & C_{55}^* & 0 \\ \dots & \dots & \dots & \dots & \dots & C_{55}^* \end{bmatrix} \tag{2.106}$$

p.stanford.edu, Jan. 2020

Watson, Leighton & Wijk, Kasper. (2015). Resonant ultrasound spectroscopy of horizontal transversely isotropic samples.

Wikipedia, Jan. 2020

Figure 2.21 Definition of cross-anisotropy and examples of transverse isotropic materials.

2.4.4   Elastic coefficients in isotropic materials

In an isotropic material, the elastic constants are independent of the orientation of the coordinate axes, which implies that there are only 2 independent elastic constants, namely:

$$\left. \begin{array}{l} C_{11}^* = C_{22}^* = C_{33}^* \\ C_{12}^* = C_{13}^* \end{array} \right\} \;\Rightarrow\; 2 \text{ independent coefficients} \tag{2.107}$$

The constants can be expressed in terms of several different parameters. The most common ones are as follows:

- Young's modulus E, which relates axial stress to axial strain in a simple tension or compression test:

$$\sigma_{11} = E\epsilon_{11}, \quad \text{all other stresses are zero} \tag{2.108}$$

- Poisson's ratio ν, which relates axial strains in a simple tension or compression test:

$$\epsilon_{22} = \epsilon_{33} = -\nu\epsilon_{11}, \quad \text{all other stresses are zero except } \sigma_{11} \text{ are zero} \tag{2.109}$$

- Shear modulus G, which relates shear stress to shear strain:

$$\sigma_{12} = 2G\epsilon_{12} \tag{2.110}$$

- Bulk modulus K, which relates volumetric strain to average or octahedral stress:

$$\sigma_{oct} = K\epsilon_v \tag{2.111}$$

- Lamé constants, λ and $\mu = G$, which relate the stresses and strains as follows:

$$\sigma_{ij} = \lambda\epsilon_{kk}\delta_{ij} + 2\mu\epsilon_{ij} \tag{2.112}$$

- Constrained modulus M, which relates axial strain to axial stress when the other two axial strains are held to zero, namely:

$$\sigma_{11} = M\epsilon_{11}, \quad \text{all other strains are zero} \tag{2.113}$$

The following relations exist between these constants:

$$
\begin{aligned}
G &= \mu = \frac{E}{2(1+\nu)}, \quad K = \frac{E}{3(1-2\nu)} = \lambda + \frac{2}{3}\mu \\
\lambda &= \frac{\nu E}{(1+\nu)(1-2\nu)}, \quad M = \frac{E(1-\nu)}{(1+\nu)(1-2\nu)}
\end{aligned}
\tag{2.114}
$$

In terms of the Young's modulus and the Poisson's ratio, the matrix $[C^*]$ is (expressions in terms of the other coefficients can be deduced from the Equation 2.114):

$$[C^*] = \frac{E}{(1+\nu)(1-2\nu)}
\begin{bmatrix}
1-\nu & \nu & \nu & 0 & 0 & 0 \\
\nu & 1-\nu & \nu & 0 & 0 & 0 \\
\nu & \nu & 1-\nu & 0 & 0 & 0 \\
\dots & \dots & \dots & \frac{1-2\nu}{2} & 0 & 0 \\
\dots & \dots & \dots & \dots & \frac{1-2\nu}{2} & 0 \\
\dots & \dots & \dots & \dots & \dots & \frac{1-2\nu}{2}
\end{bmatrix}
\tag{2.115}$$

2.5   Elastic potential (strain energy function)

2.5.1   Conservation of energy

The energy equation is an additional field equation, formulated on the basis of the energy-balance postulate of the first law of thermodynamics. The energy equation involves an additional unknown quantity, the so called internal energy, thus makes a useful addition to the equations of continuum mechanics only when it is possible to relate the internal energy to the other state variables. In continuum mechanics, the thermodynamic system is usually be chosen as a given collection of continuous matter, i.e. the system is a closed system not interchanging matter with it?s surroundings; the bounding surface of the system in general moves with the flow of the matter (an alternative approach is to used a fixed control surface in space and account for the flux of the matter through it). The first law of thermodynamics relates the work done on the system and the heat transfer into the system to the change in energy of the system:

$$\delta W + \delta Q = \delta U + \delta K \tag{2.116}$$

in which δW is the increment of mechanical work, δQ is the rate of incremental heat input, δU is the incremental internal energy, and δK is the increment of kinetic energy. A typical assumption in continuum mechanics is that the only energy transfers to the system are by mechanical work done on the system by surface tractions and body forces, by heat transfer through the boundary, and possibly by distributed internal heat sources. In particular, for linear elasticity, heat transfer is considered insignificant, and all of the input work is assumed converted into internal energy in the form of recoverable stored elastic strain energy, which can be recovered as work when the body is unloaded. In general, however, the major part of the input work into a deforming material is not recoverably stored, but dissipated by the deformation process, causing an increase in the body?s temperature and eventually being conducted away as heat.

2.5.2   Statically and kinetically admissible fields

2.5.2.1   *Statically admissible stress*

When external body and surface forces are prescribed as acting on a deformable body, a statically admissible stress distribution is defined as one satisfying the equilibrium partial differential equations:

$$\frac{\partial \sigma_{ij}}{\partial x_j} + f_i = 0 \tag{2.117}$$

in the interior of the body, and boundary conditions:

$$t_i = \sigma_{ij} n_j \tag{2.118}$$

whenever any boundary tractions t_i are prescribed. It is important to remember that the proposed equilibrium stress distribution used in connection with the principle need not to be the actual stress distribution in the deformed body. Even when all the boundary conditions are in terms of stress, the stress distribution is not completely determined by the equilibrium conditions and the boundary conditions, but depends in general upon material properties. Usually, many different possible statically admissible stress distributions exist, all satisfying equilibrium requirements. Any one of them may be the distribution referred to in the principle of virtual displacements. In the ensuing, we shall restrict the formulation to the non-polar case, namely the case where the Cauchy stress tensor is symmetric ($\sigma_{ij} = \sigma_{ji}$).

2.5.2.2 Kinetically admissible displacement

A kinematically admissible displacement distribution is one satisfying any prescribed displacement boundary conditions and possessing continuous first derivatives in the interior of the body.

2.5.3 Principle of Virtual Work

Variational methods have played a prominent role in continuum mechanics. The fundamental variational principle is the principle of virtual displacements, referred to as principle of virtual work. Although it takes a form similar to equation **??**, this is not an energy principle because the work computed is a fictitious work computed with a set of statically admissible forces and stresses assumed to remain constant while they do work on a set of infinitesimal, kinematically admissible displacements. In other words, the stresses need not to be the actual stresses occurring in the real physical material, and the displacements need not to be the actual displacements. Since the virtual displacements to be considered are additional displacements from the equilibrium configuration, a virtual displacement component must actually be zero wherever the actual displacement is prescribed by the boundary conditions. In the statics of particles and rigid bodies, the principle of virtual displacements is an alternative way of expressing the equilibrium conditions, and we shall see that the same holds for the equilibrium of a deformable medium.

   Suppose that a body is in a certain equilibrium configuration, and that each point of the body is given an infinitesimal virtual displacement δu_i from the equilibrium configuration. Each component of the displacement is a function of position of the body. We suppose that the three functions δu_i have continuous first partial derivatives with respect to x_1, x_2 and x_3, and that $\delta u_i = 0$ on those parts of the boundary surface where the actual displacement u_i is prescribed. Thus, the virtual displacements satisfy displacement boundary conditions where prescribed means that no additional virtual displacement is permitted where the boundary condition fixes the value of displacements which would occur under the given loads, but merely hypothetical, kinematically possible displacements.

   At each boundary point, we choose a local Cartesian axis system (usually with one axis along the normal) and require:

$$
\begin{aligned}
\text{either} \quad & \overline{\sigma}_{1j}\overline{n}_j = \overline{t}_1 \quad && \text{or } \delta\overline{u}_1 \text{ but not both} && (2.119)\\
\text{either} \quad & \overline{\sigma}_{2j}\overline{n}_j = \overline{t}_2 \quad && \text{or } \delta\overline{u}_2 \text{ but not both} &&\\
\text{either} \quad & \overline{\sigma}_{3j}\overline{n}_j = \overline{t}_3 \quad && \text{or } \delta\overline{u}_3 \text{ but not both} &&
\end{aligned}
$$

In the equation above, the barred symbols $\overline{t}_i$ are given functions of position on those parts of the boundary where the traction components are prescribed. The traction vector components t_i in a fixed system x_i can be then expressed in terms of $\overline{t}_i$ and $t_i\,\delta u_i\,dS = \overline{t}_i\,\delta\overline{u}_i\,dS$ represents the virtual work of the traction forces on dS.

   If the forces are assumed to be unchanged during the virtual displacement, the virtual work δW of the external surface tractions t_i and body forces b_i is:

$$
\delta W = \int_S t_i\,\delta u_i\,dS + \int_V \rho\,b_i\,\delta u_i dV \qquad (2.120)
$$

where δu_i denotes the change in the displacement field. Since $t_i = \sigma_{ij} n_j$ on the surface S, the surface integral can be transformed into a volume integral, as follows:

$$\delta W = \int_S \sigma_{ij} n_j \, \delta u_i \, dS + \int_V \rho \, b_i \, \delta u_i dV \tag{2.121}$$

$$= \int_V \frac{\partial (\delta u_i \, \sigma_{ij})}{\partial x_j} \, dV + \int_V \rho \, b_i \, \delta u_i dV$$

$$= \int_V \frac{\partial \sigma_{ij}}{\partial x_j} \delta u_i \, dV + \int_V \frac{\partial (\delta u_j)}{\partial x_j} \sigma_{ij} \, dV + \int_V \rho \, b_i \, \delta u_i \, dV$$

$$= \int_V \left(\frac{\partial \sigma_{ij}}{\partial x_j} + \rho \, b_i \right) \delta u_i \, dV + \int_V \frac{\partial (\delta u_j)}{\partial x_j} \sigma_{ij} \, dV$$

The equation of equilibrium imposes $\frac{\partial \sigma_{ij}}{\partial x_j} + \rho \, b_i = 0$ and therefore:

$$\delta W = \int_V \frac{\partial (\delta u_j)}{\partial x_j} \sigma_{ij} \, dV \tag{2.122}$$

By definition, the linearized deformation tensor is the symmetric part of the gradient of the displacement field, so that:

$$\delta \epsilon_{ij} = \frac{1}{2} \left(\frac{\partial (\delta u_j)}{\partial x_j} + \frac{\partial (\delta u_i)}{\partial x_i} \right) \tag{2.123}$$

Let us note ω_{ij} the skew part of the gradient of the displacement field, and we have:

$$\delta \omega_{ij} = \frac{1}{2} \left(\frac{\partial (\delta u_j)}{\partial x_j} - \frac{\partial (\delta u_i)}{\partial x_i} \right) \tag{2.124}$$

Equation 2.122 now writes:

$$\delta W = \int_V (\delta \epsilon_{ij} + \delta \omega_{ij}) \, \sigma_{ij} \, dV \tag{2.125}$$

Since Cauchy stress tensor is symmetric, we can easily show that $\omega_{ij} \sigma_{ij} = 0$, so that Equation 2.125 becomes:

$$\delta W = \int_V \sigma_{ij} \, \delta \epsilon_{ij} \, dV \tag{2.126}$$

Restraining consideration to adiabatic situations with no appreciable change in kinetic energy, the first law of thermodynamics (Equation 2.116) reduces to:

$$\delta W = \int_V \sigma_{ij} \, \delta \epsilon_{ij} \, dV = \delta U \tag{2.127}$$

Equation 2.127 shows that if the stress is statically admissible, the total virtual work of the external forces on any kinematically admissible virtual displacement field is equal to $\int_V \sigma_{ij} \, \delta \epsilon_{ij} \, dV$. This concept and its converse, together, are the principle of virtual displacements for a deformable body. The converse proposition states that if the virtual work of the prescribed external forces is equal to $\int_V \sigma_{ij} \, \delta \epsilon_{ij} \, dV$ for a certain assumed stress field σ_{ij} for every kinematically admissible virtual displacement field, then the stress field

is statically admissible, i.e. it satisfies: (i) Equilibrium equations in the interior; and (ii) Traction boundary conditions wherever traction boundary conditions are prescribed on the surface.
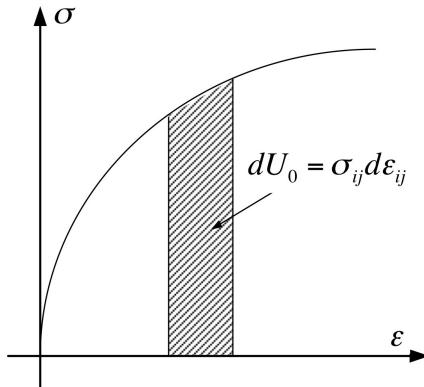
Within the context of solid mechanics, the internal energy U is usually called the strain energy. Assume the existence of a strain energy density function U_0 depending only on the strains and perhaps the temperature, such that:

$$\delta U = \int_V \delta U_0 dV \tag{2.128}$$

from which it follows that $dU_0 = \sigma_{ij} d\epsilon_{ij}$. Note that this development also contains the result that $dU_0 = -dW_i$, stating that the the change in internal strain energy is negative the work done by internal forces. In fact, U_0 is the area under the stress strain curve for the material in question, shown in Figure 2.22. In other words, we have:

$$U_0 = \int \sigma_{ij} \delta\epsilon_{ij} = \int (C_{ijkl}\epsilon_{lk}) \, \delta\epsilon_{ij} = \frac{1}{2}C_{ijkl}\epsilon_{ij}\epsilon_{kl} \tag{2.129}$$

in which we made use of the symmetry of the linearized deformation tensor in the indicial notations.

Figure 2.22   The concept of strain energy. Picture taken from [2].

PROBLEMS

2.1   We consider the 2D domain $0 < x_1 < L$, $-c < x_2 < c$ (in Cartesian coordinates). We define: $I = 4c^3/3$. The state of stress in the domain is given as follows:

$$\sigma_{11} = \frac{p}{I}\left(x_1^2 x_2 - \frac{2}{3}x_2^3\right), \quad \sigma_{22} = \frac{p}{I}\left(\frac{1}{3}x_2^3 - c^2 x_2 + \frac{2}{3}c^3\right), \quad \sigma_{12} = \frac{p}{I}\left((c^2 - x_2^2)x_1\right)$$

a. Show that the state of stress is in equilibrium, i.e., $\underline{div}\left(\underline{\sigma}\right) = \underline{0}$.
b. Calculate the state of stress on each of the four sides of the domain.
c. Calculate the resulting force that is applied on the face $x_1 = x_{10}$ by the part of the domain $x_1 \geq x_{10}$. Calculate the resulting moment at the point $(x_{10}, 0)$.
d. Suppose that $c << L$. Give a loading boundary condition that approximates the stress

field given in the equation above.

e. Numerical application: consider a plane wing (shaped as a parallelepiped) that is 20m long (i.e., L=20m), and that has a half width c=1 cm. The wing is subjected to a uniformly distributed lifting surface force $p = C_z \rho_a V^2/2$. We give: C_z=0.8; V=200 m/s; ρ_a=1 kg/m^3. Calculate σ_{11}^{max}.

2.2 By considering the initial state of stress σ_{ij} at a point and a general increment of stress $\Delta\sigma_{ij}$, determine which of the stress invariants I allows superposition such that: $I_{\text{final}} = I_{\text{initial}} + I_{\text{incremental}}$.

2.3 The stress state at a point is given as:

$$[\sigma] = \begin{bmatrix} 4 & 3 & 2 \\ 3 & 5 & 1 \\ 2 & 1 & 6 \end{bmatrix} \quad \text{[kPa]}$$

a. Determine the stress invariants I_1, I_2 and I_3 at the point.
b. Determine the invariants J_1, J_2 and J_3 of the deviatoric stress tensor s_{ij}.
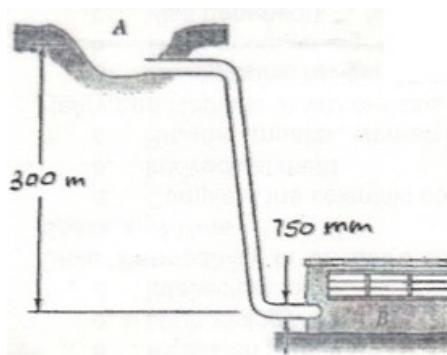
2.4 Consider a point in plane stress, at which the state of stress is given by: $\sigma_{xx} = 2$ MPa, $\sigma_{yy} = -1$ MPa and $\sigma_{xy} = 0.5$ MPa. For the given state of stress:
a. Draw Mohr's circle.
b. Determine the orientation of the principal planes and the corresponding principal stresses.
c. Determine the state of stress after the element has been rotated through and angle of 30° *clockwise*.
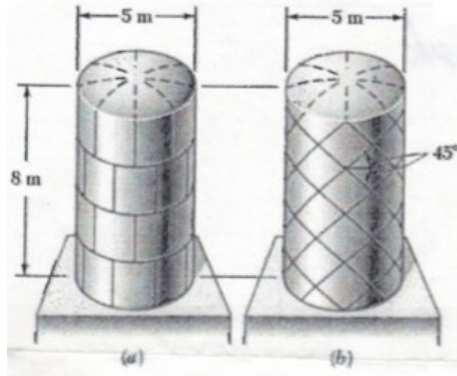
2.5 A steel penstock has a 750-mm outer diameter, a 12-mm wall thickness and connects a reservoir at A with a generating station at B, as shown in Figure 2.23. Knowing that the density of water is 1000kg/m^3, determine the maximum normal stress and the maximum shearing stress in the penstock under static conditions. *Hint: in a cylindrical pressurized vessel (i.e., in a cylindrical container that has a radius that is large compared to the thickness of the shell, and in which the pressure inside is larger than the pressure outside), the hoop stress is equal to pr/t and the longitudinal stress is equal to $pr/2t$, in which p is the pressure of the fluid inside the vessel, r is the inner radius of the vessel and t is the thickness of the shell.*


Figure 2.23   Penstock studied in Problem 2.5.

2.6   Square plates, each of 16-mm thickness, can be bent and welded together in either of the two ways shown to form the cylindrical portion of a compressed air tank, as shown in Figure Figure 2.24. Knowing that the allowable normal stress perpendicular to the weld is 65MPa, determine the largest allowable gage pressure in each case. *Use the same hint as in Problem 2.5.*

Figure 2.24   Compressed air tanks studied in Problem 2.6.

2.7   Show which of the following strain states satisfies the compatibility condition:

$$u_3 = 0, \quad \epsilon_{11} = \frac{\left(x_1^2 + x_2^2\right)}{a^2}, \quad \epsilon_{22} = \frac{x_2^2}{a^2}, \quad \epsilon_{12} = \frac{x_1 x_2}{a^2} \tag{2.130}$$

$$u_3 = 0, \quad \epsilon_{11} = \frac{x_3\left(x_1^2 + x_2^2\right)}{a^3}, \quad \epsilon_{22} = \frac{x_2^2 x_3}{a^3}, \quad \epsilon_{12} = \frac{x_1 x_2 x_3}{a^3} \tag{2.131}$$

2.8   Let us consider a vertical beam of length L = 2m and half-width h=0.2 m, as shown in Figure 4.29.a. The position vector is given as $\boldsymbol{OP} = X\boldsymbol{e}_X + Y\boldsymbol{e}_Y$ in the Cartesian coordinate system, with $-h \leq X \leq +h$ and $0 \leq Y \leq L$. Consider the deformed configuration shown in Figure 4.29.b. such that the new position vector is given as:

$$\boldsymbol{OP} = \boldsymbol{x}_0(Y,t) + X\boldsymbol{e}_r\left(\theta(Y,t)\right), \quad \boldsymbol{e}_r = \cos\theta\boldsymbol{e}_X + \sin\theta\boldsymbol{e}_Y, \quad \boldsymbol{e}_\theta(\theta) = -\sin\theta\boldsymbol{e}_X + \cos\theta\boldsymbol{e}_Y$$

in which $\boldsymbol{x}_0(Y,t)$ and $\theta(Y,t)$ will be defined later.
a. Calculate the Green-Lagrange deformation tensor e as a function of $\boldsymbol{x}_0(Y,t)$ and $\theta(Y,t)$.
b. Calculate the elongation in the $\boldsymbol{e}_X$-direction.
c. Calculate the elongation in the $\boldsymbol{e}_Y$-direction, on the vertical axis $(X = 0)$ and on the lateral sides $(X = \pm h)$.
d. Calculate the distortion in the direction $(\boldsymbol{e}_X, \boldsymbol{e}_Y)$ as a function of Y.
e. Now we pose:
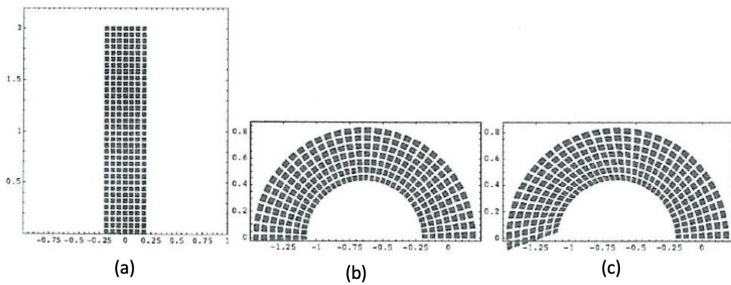
$$\boldsymbol{x}_0(Y,t) = \frac{L}{\pi}\left(-\boldsymbol{e}_X + \boldsymbol{e}_r\left(\theta(Y,t)\right)\right), \quad \theta(Y,t) = \frac{\pi Y}{L}$$

Repeat questions a.-d. above.
f. Now suppose that the deformed configuration is that shown in Figure 4.29.c, in which:

$$\boldsymbol{OP} = \boldsymbol{x}_0(Y,t) + X\boldsymbol{e}_r\left(1.1\theta(Y,t)\right)$$
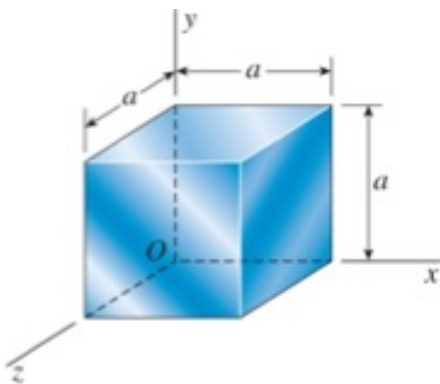
Figure 2.25   Beam problem studied in Problem 2.8.

Explain the difference between Figure 4.29.b and Figure 4.29.c.

2.9   A cube of granite with sides of length a = 89 mm (see Figure 2.26) is tested in a laboratory under triaxial stress. Assume E = 80 GPa, ν = 0.25. Gages mounted on the testing machine show that the compressive strains in the material are ϵ_{xx} = -138 x 10^{-5} and $\epsilon_{yy} = \epsilon_{zz}$ = -510 x 10^{-6}. Determine the following quantities:
a. The normal stresses σ_{xx}, σ_{yy}, and σ_{zz} acting on the x, y, and z faces of the cube;
b. The maximum shear stress τ_{max} in the material;
c. The change ΔV in the volume of the cube;
d. The maximum value of σ_{xx} when the change in volume must be limited to -0.11%.

Figure 2.26   Granite sample studied in Problem 2.9.

2.10   Consider a parallelepidic specimen of length L, with a square section of edge length a. The square section of the specimen lies on the plane $(0, x_1, x_2)$. The parallelepiped can slide on the plane but cannot loose contact with the plane. The specimen is loaded at $x_3 = L$ by a uniform compression $-F$ in the e_3 direction. The material that makes the specimen is isotropic and linear elastic, with a Young's modulus E and a Poisson's ratio ν. We assume that deformations are very small, and we neglect the gravity and inertia forces. We give: L=20 cm, a=1 cm, E=200 GPa, ν=0.3, F=100 N.
a. Calculate the displacement field at $x_3 = L$ if the lateral faces of the specimen are free of stress.
b. Calculate the displacement field at $x_3 = L$ if the specimen is encased in a very rigid

support, within which it can slide. c. Calculate the displacement field at $x_3 = L$ if the the faces $x_1 \pm a/2$ are fixed and if the other two lateral faces are free of stress.

d. Now suppose that the specimen is encased in a very rigid support and that there is an initial misfit of 0.01 mm between the lateral faces. What is the required value of the compression force F for which the lateral faces of the specimen get in contact with the rigid support?

CHAPTER 3

ANALYTICAL SOLUTIONS OF BOUNDARY VALUE PROBLEMS IN LINEAR ELASTICITY

3.1 Fundamental principles

3.1.1 Superposition principle

The solution of a problem of a given elastic solid with given surface and body forces requires us to determine stress components or displacements that satisfy the spatial-domain (and time-domain) differential equations and the boundary conditions. In the case that the problem is formulated on the basis of stress components, the solution needs to satisfy:

- the equations of equilibrium:

$$\frac{\partial \sigma_{ij}}{\partial x_j} + b_i = 0 \qquad (3.1)$$

- the compatibility equations:

$$\frac{\partial^2 \epsilon_{ij}}{\partial x_k \partial x_l} + \frac{\partial^2 \epsilon_{kl}}{\partial x_i \partial x_j} - \frac{\partial^2 \epsilon_{ik}}{\partial x_j \partial x_l} - \frac{\partial^2 \epsilon_{jl}}{\partial x_i \partial x_k} = 0 \qquad (3.2)$$
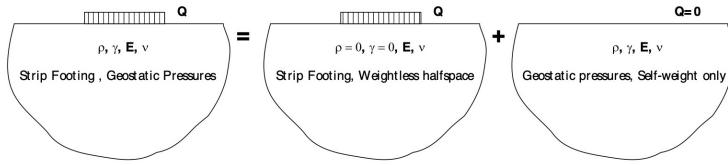
- the boundary conditions.

Let σ_{ij} be the normal and shear stresses that have been determined, developed due to the presence of surface tractions t_i and body forces b_i. Let also σ_{ij}^* be the normal and shear stresses that have been determined, developed due to the presence of surface tractions t_i^* and body forces b_i^*. Then the stress components $\sigma_{ij} + \sigma_{ij}^*$ will represent the stress

developed due to the presence of surface tractions $t_i + t_i^*$ and body forces $b_i + b_i^*$. This holds because all the differential equations and boundary conditions are linear. As a result, the equilibrium equation becomes:

$$\frac{\partial \sigma_{ij}}{\partial x_j} + b_i = 0 \quad \frac{\partial \sigma_{ij}^*}{\partial x_j} + b_i^* = 0 \left.\right\} \Rightarrow \frac{\partial}{\partial x_j} \left(\sigma_{ij} + \sigma_{ij}^* \right) \rho \left(b_i + b_i^* \right) = 0 \qquad (3.3)$$

The compatibility equations can be combined in the same way. The complete set of equations shows that $\sigma_{ij} + \sigma_{ij}^*$ satisfies the complete set of equations and conditions determining the stress due to forces $t_i + t_i^*$ and $b_i + b_i^*$. This is an instance of the principle of superposition, and it can be extended to other types of boundary conditions such as prescribed displacements. Figure 3.1 provides an example.

Figure 3.1   An example of application of the principle of superposition in elatostatics. Picture taken from [2].

Note that in deriving the equations of equilibrium and boundary conditions, we made no distinction between the position and form of the element before loading, and its position and form after loading. As a consequence, our equations and the conclusions drawn from them are valid only so long as the small displacements in the deformation do not affect substantially the action of the external forces. Nonetheless, there are cases where the deformation must be taken into account and the justification of the principle of superposition fails (large displacements).
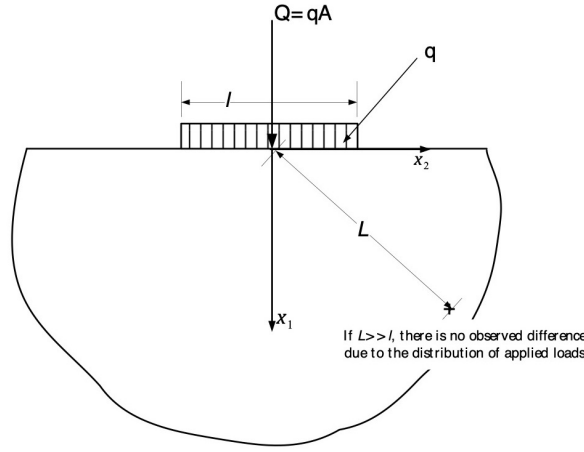
3.1.2   Saint-Venant's principle

St. Venant's principle can be stated as follows:

In elastostatics, if the boundary tractions on a part S_1 of the boundary S are replaced by a statically equivalent traction distribution, the effects on the stress distribution in the body are negligible at points whose distance from S_1 is large compared to the maximum distance between points on S_1.

This principle is of great importance in applied elasticity, where it is frequently invoked to justify solutions in long structural members, where the end traction boundary conditions are satisfied only in an average sense, so that the correct stress resultants act on the ends. In such solutions, the actual stress distribution near the ends may differ considerably from the calculated stress distribution. There are two reasons for using such approximate solutions in applied elasticity: (i) it is not usually known in detail how the loads applied at the end of a structural member will be distributed, and (ii) simple solutions, obtained by inverse methods, can sometimes be applied if not all the boundary conditions are exactly

satisfied, while the exact solutions may require elaborate calculations. Figure 3.2 provides an example.

Figure 3.2   Illustration of Saint-Venant's principle. Picture taken from [2].

3.2   Elastostatics equations

3.2.1   Equations of equilibrium in Cartesian, cylindrical and spherical coordinates

In vector notation, the equation of equilibrium established in Section 5.1.2 is:

$$\boldsymbol{div\sigma} + \boldsymbol{f} = \boldsymbol{0} \tag{3.4}$$

in which $\boldsymbol{f}$ is a body force.
In Cartesian coordinates:

$$\begin{cases} \frac{\partial \sigma_{xx}}{\partial x} + \frac{\partial \sigma_{yx}}{\partial y} + \frac{\partial \sigma_{zx}}{\partial z} + f_x = 0 \\[2mm] \frac{\partial \sigma_{xy}}{\partial x} + \frac{\partial \sigma_{yy}}{\partial y} + \frac{\partial \sigma_{zy}}{\partial z} + f_y = 0 \\[2mm] \frac{\partial \sigma_{xz}}{\partial x} + \frac{\partial \sigma_{yz}}{\partial y} + \frac{\partial \sigma_{zz}}{\partial z} + f_z = 0 \end{cases} \tag{3.5}$$

In cylindrical coordinates (see Figure 3.3):

$$\begin{cases} \frac{\partial \sigma_{rr}}{\partial r} + \frac{1}{r} \frac{\partial \sigma_{\theta r}}{\partial \theta} + \frac{\partial \sigma_{zr}}{\partial z} + \frac{\sigma_{rr} - \sigma_{\theta\theta}}{r} + \rho f_r = 0 \\[2mm] \frac{\partial \sigma_{r\theta}}{\partial r} + \frac{1}{r} \frac{\partial \sigma_{\theta\theta}}{\partial \theta} + \frac{\partial \sigma_{z\theta}}{\partial z} + \frac{2\sigma_{r\theta}}{r} + \rho f_\theta = 0 \\[2mm] \frac{\partial \sigma_{rz}}{\partial r} + \frac{1}{r} \frac{\partial \sigma_{\theta z}}{\partial \theta} + \frac{\partial \sigma_{zz}}{\partial z} + \frac{\sigma_{rz}}{r} + \rho f_z = 0 \end{cases} \tag{3.6}$$

In spherical coordinates (see Figure 3.3), we have:

$$x = r \sin \phi \cos \theta, \quad y = r \sin \phi \sin \theta, \quad z = r \cos \phi \tag{3.7}$$

The general form of the elasticity equations in spherical coordinates was established by Sokolnikoff (1956) and Goodier (1970). The most common and important special case is that of radial symmetry, in which case the only non-zero displacement component will be the radial component, $u(r)$. The only non-zero strains will be the three normal strains, which are related to the radial displacements by:

$$\epsilon_{rr} = \frac{\partial u}{\partial r}, \quad \epsilon_{\theta\theta} = \epsilon_{\phi\phi} = \frac{u}{r} \tag{3.8}$$

Using the linear elasticity constitutive equations, we get:
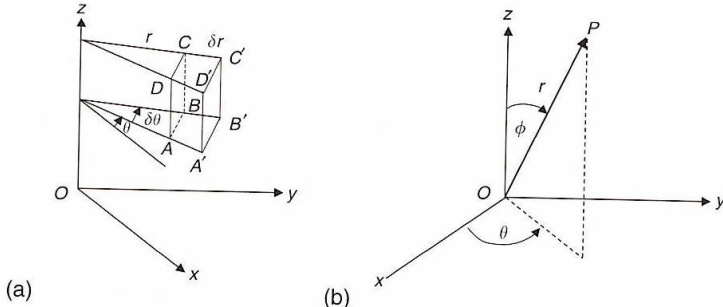
$$\begin{cases} \sigma_{rr} = (\lambda + 2G)\epsilon_{rr} + \lambda(\epsilon_{\theta\theta} + \epsilon_{\phi\phi}) \\[2mm] \sigma_{\theta\theta} = (\lambda + 2G)\epsilon_{\theta\theta} + \lambda(\epsilon_{rr} + \epsilon_{\phi\phi}) \\[2mm] \sigma_{\phi\phi} = (\lambda + 2G)\epsilon_{\phi\phi} + \lambda(\epsilon_{rr} + \epsilon_{\theta\theta}) \end{cases} \tag{3.9}$$

where $\sigma_{\theta\theta}$ and $\sigma_{\phi\phi}$ anre the normal stresses in the two directions perpendicular to r. From the above equations, we get the stress-displacement equations for spherically symmetric deformations:

$$\sigma_{rr} = (\lambda + 2G)\frac{\partial u}{\partial r} + 2\lambda\frac{u}{r}, \quad \sigma_{\theta\theta} = \sigma_{\phi\phi} = \lambda\frac{\partial u}{\partial r} + 2(\lambda + G)\frac{u}{r} \tag{3.10}$$

The only non-trivial equation of stress equilibrium is:

$$\frac{\partial \sigma_{rr}}{\partial r} + \frac{2(\sigma_{rr} - \sigma_{\theta\theta})}{r} = 0 \tag{3.11}$$

Figure 3.3   Spherical (a) and cylincrical (b) coordinate systems. Picture taken from [13].

3.2.2 Navier's displacement equations of motion

When combining the equations of equilibrium, the stress-strain equations and the strain-displacement equations, we obtain the so-called Navier's displacement equations of motion. For example, in a Cartesian coordinate system (noting u, v and w the components of displacement in the x, y and z directions respectively):

$$\lambda\left(\frac{\partial^2 u}{\partial x^2} + \frac{\partial^2 v}{\partial x \partial y} + \frac{\partial^2 w}{\partial x \partial z}\right) + G\left(\frac{\partial^2 u}{\partial x^2} + \frac{\partial^2 v}{\partial x \partial y} + \frac{\partial^2 w}{\partial x \partial z} + \frac{\partial^2 u}{\partial x^2} + \frac{\partial^2 u}{\partial y^2} + \frac{\partial^2 u}{\partial z^2}\right) + \rho f_x = 0 \tag{3.12}$$

$$\lambda \left(\frac{\partial^2 u}{\partial x \partial y} + \frac{\partial^2 v}{\partial y^2} + \frac{\partial^2 w}{\partial y \partial z} \right) + G \left(\frac{\partial^2 u}{\partial x \partial y} + \frac{\partial^2 v}{\partial y^2} + \frac{\partial^2 w}{\partial y \partial z} + \frac{\partial^2 v}{\partial x^2} + \frac{\partial^2 v}{\partial y^2} + \frac{\partial^2 v}{\partial z^2} \right) + \rho f_y = 0 \tag{3.13}$$

$$\lambda \left(\frac{\partial^2 u}{\partial x \partial z} + \frac{\partial^2 v}{\partial y \partial z} + \frac{\partial^2 w}{\partial z^2} \right) + G \left(\frac{\partial^2 u}{\partial z \partial y} + \frac{\partial^2 v}{\partial y \partial z} + \frac{\partial^2 w}{\partial z^2} + \frac{\partial^2 w}{\partial x^2} + \frac{\partial^2 w}{\partial y^2} + \frac{\partial^2 w}{\partial z^2} \right) + \rho f_z = 0 \tag{3.14}$$

In tensorial notation:

$$(\lambda + G) \frac{\partial}{\partial x} (\boldsymbol{\nabla} \cdot \boldsymbol{u}) + G \boldsymbol{\nabla}^2 u + \rho f_x = 0 \tag{3.15}$$

$$(\lambda + G) \frac{\partial}{\partial y} (\boldsymbol{\nabla} \cdot \boldsymbol{u}) + G \boldsymbol{\nabla}^2 v + \rho f_y = 0 \tag{3.16}$$

$$(\lambda + G) \frac{\partial}{\partial z} (\boldsymbol{\nabla} \cdot \boldsymbol{u}) + G \boldsymbol{\nabla}^2 w + \rho f_z = 0 \tag{3.17}$$

And finally:

$$(\lambda + G) \boldsymbol{\nabla} (\boldsymbol{\nabla} \cdot \boldsymbol{u}) + G \boldsymbol{\nabla}^2 \boldsymbol{u} + \rho \boldsymbol{f} = 0 \tag{3.18}$$

According to Equation 3.11, the Navier's equation of motion for spherically symmetric deformations is:

$$\frac{\partial^2 u}{\partial r^2} + \frac{2}{r} \frac{\partial u}{\partial r} - \frac{2u}{r} = 0 \tag{3.19}$$

3.2.3 Beltrami-Michell's compatibility equations - stress equations

When the displacements do not explicitly appear as dependent field variables, the compatibility equations must be satisfied to ensure the existence of a displacement field. The compatibility equations can be expressed as:

$$\frac{\partial^2 \epsilon_{ij}}{\partial x_k \partial x_l} + \frac{\partial^2 \epsilon_{kl}}{\partial x_i \partial x_j} - \frac{\partial^2 \epsilon_{ik}}{\partial x_j \partial x_l} - \frac{\partial^2 \epsilon_{jl}}{\partial x_i \partial x_k} = 0 \tag{3.20}$$

which represents only six linearly independent equations (in fact, only three functionally independent conditions). Also, Hooke's law in equation can be expressed as follows:

$$\epsilon_{ij} = \frac{1 + \nu}{E} \sigma_{ij} - \frac{\nu}{E} \sigma_{kk} \delta_{ij} \tag{3.21}$$

Combining the two equations above, we get:

$$\frac{\partial^2 \sigma_{ij}}{\partial x_k \partial x_m} + \frac{\partial^2 \sigma_{km}}{\partial x_i \partial x_j} - \frac{\partial^2 \sigma_{ik}}{\partial x_j \partial x_m} - \frac{\partial^2 \sigma_{jm}}{\partial x_i \partial x_k} = \tag{3.22}$$

$$\frac{\nu}{1 + \nu} \left[\delta_{ij} \frac{\partial^2 \sigma_{pp}}{\partial x_k \partial x_m} + \delta_{km} \frac{\partial^2 \sigma_{pp}}{\partial x_i \partial x_j} - \delta_{ik} \frac{\partial^2 \sigma_{pp}}{\partial x_j \partial x_m} - \delta_{jm} \frac{\partial^2 \sigma_{pp}}{\partial x_i \partial x_k} \right]$$

Since only six of these 81 equations are linearly independent, they are equivalent to the six linearly independent equations obtained by putting k=m and summing to obtain:

$$\frac{\partial^2 \sigma_{ij}}{\partial x_k \partial x_k} + \frac{\partial^2 \sigma_{kk}}{\partial x_i \partial x_j} - \frac{\partial^2 \sigma_{ik}}{\partial x_j \partial x_k} - \frac{\partial^2 \sigma_{jk}}{\partial x_i \partial x_k} = \tag{3.23}$$

$$\frac{\nu}{1 + \nu} \left[\delta_{ij} \frac{\partial^2 \sigma_{pp}}{\partial x_k \partial x_k} + \delta_{kk} \frac{\partial^2 \sigma_{pp}}{\partial x_i \partial x_j} - \delta_{ik} \frac{\partial^2 \sigma_{pp}}{\partial x_j \partial x_k} - \delta_{jk} \frac{\partial^2 \sigma_{pp}}{\partial x_i \partial x_k} \right]$$

which is a set of nine equations, but only six distinct equations, because of the symmetry in the free indices i, j. These equations can be simplified by using the equations of equilibrium as follows:

$$-\frac{\partial^2 \sigma_{ik}}{\partial x_k \partial x_j} = \frac{\partial f_i}{\partial x_j}, \quad -\frac{\partial^2 \sigma_{jk}}{\partial x_k \partial x_i} = \frac{\partial f_j}{\partial x_i} \tag{3.24}$$

so that we have:

$$\nabla^2 \sigma_{ij} + \frac{1}{1+\nu}\frac{\partial^2 \sigma_{pp}}{\partial x_i \partial x_j} - \frac{\nu}{1+\nu}\delta_{ij}\nabla^2 \sigma_{pp} = -\frac{\partial f_i}{\partial x_j} - \frac{\partial f_j}{\partial x_i} \tag{3.25}$$

Now substituting k=i and m=j in Equation 3.25 and combining the resulting expressions with the equation above, we get:

$$\frac{\partial^2 \sigma_{ij}}{\partial x_i \partial x_j} = \frac{1-\nu}{1+\nu}\nabla^2 \sigma_{pp} \tag{3.26}$$

From the equations of equilibrium, we have:

$$\frac{\partial^2 \sigma_{ij}}{\partial x_i \partial x_j} = -\frac{\partial f_i}{\partial x_i} \tag{3.27}$$

and so we have:

$$\nabla^2 \sigma_{pp} = -\frac{1+\nu}{1-\nu}\frac{\partial f_i}{\partial x_i} \tag{3.28}$$

As a result, Equation 3.25 takes the following form:

$$\nabla^2 \sigma_{ij} + \frac{1}{1+\nu}\frac{\partial^2 \sigma_{pp}}{\partial x_i \partial x_j} = -\frac{\nu}{1-\nu}\delta_{ij}\frac{\partial f_i}{\partial x_i} - \frac{\partial f_i}{\partial x_j} - \frac{\partial f_j}{\partial x_i} \tag{3.29}$$

Equations 3.29 are nine distinct equations but provide three linearly independent equations to solve for six stress components. To solve a boundary value problem in linear elasticity, one needs to add the three equations of equilibrium and solve nine equations for six stress components. It is not convenient to solve nine equations for only six unknowns, and very few solutions of the full three-dimensional boundary-value problem have been attempted. A more convenient formulation in terms of stress functions is possible in certain special cases.

3.2.4   Airy's stress functions

Elasticity problems can be approached by using the three Navier equations, in which the dependent variables are the three components of displacement. Alternatively, one can use the six Beltrami-Michell equations, in which the stresses are the dependent variables. The Navier equations may seem to be simpler to use, since they form a system of three coupled equations instead of six. When displacements are imposed at the boundaries, Navier equations are convenient to use. However, in most practical problems, tractions, rather than displacements, are known at the boundary. For these problems, it is more convenient to use a stress-based formulation. A stress-based method of solving the elasticity equations becomes particularly simple for plane stress or plane strain problems, in which case, the governing equations reduce to a single differential equation. It is not easy to see that the

Beltrami-Michell equations reduce to a single equation in this case; rather, it is easier to start with the single strain-compatibility equation for two dimensional problems:

$$\frac{\partial^2 \epsilon_{xx}}{\partial y^2} + \frac{\partial^2 \epsilon_{yy}}{\partial x^2} = 2\frac{\partial^2 \epsilon_{xy}}{\partial x \partial y} \tag{3.30}$$

Substituting the stress-strain relationships in the equation above, one gets:

$$(\chi + 1)\left[\frac{\partial^2 \sigma_{xx}}{\partial y^2} + \frac{\partial^2 \sigma_{yy}}{\partial x^2}\right] + (\chi - 3)\left[\frac{\partial^2 \sigma_{xx}}{\partial x^2} + \frac{\partial^2 \sigma_{yy}}{\partial y^2}\right] = 8\frac{\partial^2 \sigma_{xy}}{\partial x \partial y} \tag{3.31}$$

where $\chi = 3 - 4\nu$ for plane strain and $\chi = (3 - \nu)/(1 + \nu)$ for plane stress. Next, differentiation of the two equilibrium equations yields [13]:

$$\frac{\partial^2 \sigma_{xy}}{\partial x \partial y} = -\frac{\partial^2 \sigma_{xx}}{\partial x^2} - \rho\frac{\partial f_x}{\partial x} = -\frac{\partial^2 \sigma_{yy}}{\partial y^2} - \rho\frac{\partial f_y}{\partial y} \tag{3.32}$$

which is to say:

$$-8\frac{\partial^2 \sigma_{xy}}{\partial x \partial y} = 4\left[\frac{\partial^2 \sigma_{xx}}{\partial x^2} + \frac{\partial^2 \sigma_{yy}}{\partial y^2}\right] + 4\rho\left[\frac{\partial f_x}{\partial x} + \frac{\partial f_y}{\partial y}\right] \tag{3.33}$$

Substituting Equation 3.33 in Equation 3.31, one gets:

$$\left(\frac{\partial^2}{\partial y^2} + \frac{\partial^2}{\partial x^2}\right)[\sigma_{xx} + \sigma_{yy}] = \frac{-4\rho}{(\chi + 1)}\left(\frac{\partial f_x}{\partial x} + \frac{\partial f_y}{\partial y}\right) \tag{3.34}$$

which can also be written as:

$$\nabla^2 (\sigma_{xx} + \sigma_{yy}) = \frac{-4\rho}{(\chi + 1)}\left(\frac{\partial f_x}{\partial x} + \frac{\partial f_y}{\partial y}\right) \tag{3.35}$$

It is often the case that the body force can be expressed as the gradient of a potential function, V, that satisfies Laplace's equation: $\nabla^2 V = \nabla \cdot (\nabla V) = 0$. A common example is the body force due to gravity, for which $v = -g\,z$. In these situations, we have $\boldsymbol{F} = -\nabla V$, that is:

$$f_x = -\frac{\partial V}{\partial x}, \quad f_y = -\frac{\partial V}{\partial y} \tag{3.36}$$

And then the right-hand side of Equation 3.35 vanishes, because $\nabla \cdot \boldsymbol{F} = -\nabla \cdot (\nabla V) = 0$, that is:

$$\frac{\partial f_x}{\partial x} + \frac{\partial f_y}{\partial y} = -\frac{\partial}{\partial x}\left(\frac{\partial V}{\partial x}\right) - \frac{\partial}{\partial y}\left(\frac{\partial V}{\partial y}\right) = -\left(\frac{\partial^2 V}{\partial x^2} + \frac{\partial^2 V}{\partial y^2}\right) = 0 \tag{3.37}$$

Then, Equation 3.35 reduces to the Laplace equation:

$$\nabla^2 (\sigma_{xx} + \sigma_{yy}) = 0$$

Note that for a linear elastic material, the governing equation does not depend on the constitutive parameters E and ν. We note that the stress equilibrium equations will automatically be satisfied if we define the three independent stress components in terms of some function U, as follows:

$$\sigma_{xx} = \frac{\partial^2 U(x,y)}{\partial y^2} + \rho\,V, \quad \sigma_{yy} = \frac{\partial^2 U(x,y)}{\partial x^2} + \rho\,V, \quad \sigma_{xy} = -\frac{\partial^2 U(x,y)}{\partial x \partial y}$$

Now inserting Equation 3.2.4 in Equation 3.2.4, we have:

$$0 = \nabla^2\left(\sigma_{xx} + \sigma_{yy}\right) = \frac{1}{2}\nabla^2\left[\frac{\partial^2 U(x,y)}{\partial x^2} + \frac{\partial^2 U(x,y)}{\partial y^2} + 2\rho\,V\right] = \frac{1}{2}\nabla^2\left(\nabla^2 U\right) + \rho\nabla^2 V$$

But $\nabla^2 V = 0$ so we see that the function U must satisfy the following so-called *biharmonic equation*:

$$\nabla^2\left(\nabla^2 U(x,y)\right) = \nabla^4\,U(x,y) = 0 \tag{3.38}$$

The biharmonic function U is called *Airy stress function*. If the Airy stress function satisfies the biharmonic equation, then the stresses that are derived from U via Equation 3.2.4 will automatically satisfy the two-dimensional elasticity equations (including Hooke's law, compatibility equations and equilibrium equations). The advantage of the biharmonic equation is that it has to be solved for one unknown only. The approach is convenient if the boundary conditions are all given in terms of tractions, rather than displacements. Otherwise, a displacement-based formulation must be used.

In Cartesian coordinates, the biharmonic equation takes the form:

$$\frac{\partial^4 U}{\partial x^4} + \frac{\partial^4 U}{\partial y^4} + \frac{\partial^4 U}{\partial x^2 \partial y^2} = 0 \tag{3.39}$$

In cylindrical coordinates:

$$\sigma_{rr} = \frac{1}{r}\frac{\partial U}{\partial r} + \frac{1}{r^2}\frac{\partial^2 U}{\partial \theta^2}, \quad \sigma_{\theta\theta} = \frac{\partial^2 U}{\partial r^2}, \quad \sigma_{r\theta} = -\frac{\partial}{\partial r}\left(\frac{1}{r}\frac{\partial U}{\partial \theta}\right) \tag{3.40}$$

and so:

$$\left(\frac{\partial^2}{\partial r^2} + \frac{1}{r}\frac{\partial}{\partial r} + \frac{1}{r^2}\frac{\partial^2}{\partial \theta^2}\right)\left(\frac{\partial^2 U}{\partial r^2} + \frac{1}{r}\frac{\partial U}{\partial r} + \frac{1}{r^2}\frac{\partial^2 U}{\partial \theta^2}\right) = 0 \tag{3.41}$$

3.3   Complex variable method for 2D elasticity problems

Two-dimensional problems in elasticity can be solved by the complex variable method developed by Kolosov (1909) and Muskhelishvili (1963). In this method, the displacements and stresses are represented in terms of two analytic functions of a complex variable, i.e., in terms of two functions of a complex variable that are locally given by a convergent power series. General solutions are readily generated, as any pair of analytic functions automatically leads to displacements and stresses that satisfy the equations of stress equilibrium and Hooke's law. The only non-trivial aspect of the solution procedure is in satisfying the boundary conditions of the specific problem at hand. A brief introduction to those aspects of the theory that are needed for solving elasticity problems is given in [13] and reported here.

3.3.1   Complex-valued functions

A complex-valued function of a complex variable $z = x + iy$ can be represented by $\zeta(z)$, where the dependent variable is a complex number that can be written as:

$$\zeta = \xi + i\eta \tag{3.42}$$

Both ξ and η are real-valued functions ot the two real variables x and y. The function $\zeta(z)$ is said to be analytic in a certain region of the complex plane if it is coninuous throughout

that region and has a derivative at every point in the region. The derivative, noted $d\zeta/dz = \zeta'(z)$, is also a complex number and so can temporarily be written as $\zeta'(z) = a + ib$. The differential of ζ can therefore be expressed as:

$$d\zeta = \zeta'(z)dz = (a + ib)(dx + idy) = (adx - bdy) + i(bdx + ady) \tag{3.43}$$

and can also be written as:

$$d\zeta = d\xi + id\eta = \left(\frac{\partial \xi}{\partial x} dx + \frac{\partial \xi}{\partial y} dy \right) + i \left(\frac{\partial \eta}{\partial x} dx + \frac{\partial \eta}{\partial y} dy \right) \tag{3.44}$$

The comparison of Equations 3.43 and 3.44 reveals that the two functions ξ and η must satisfy the so-called Cauchy-Riemann equations, expressed as:

$$\frac{\partial \xi}{\partial x} = \frac{\partial \eta}{\partial y}, \quad \frac{\partial \xi}{\partial y} = -\frac{\partial \eta}{\partial x} \tag{3.45}$$

Hence, $\zeta'(z)$ can be written in any of the following four equivalent forms:

$$\zeta'(z) = \frac{\partial \xi}{\partial x} - i\frac{\partial \xi}{\partial y} = \frac{\partial \eta}{\partial y} + i\frac{\partial \eta}{\partial x} = \frac{\partial \xi}{\partial x} + i\frac{\partial \eta}{\partial x} = \frac{\partial \eta}{\partial y} - i\frac{\partial \xi}{\partial y} \tag{3.46}$$

If ζ is analytic, it follows from Equation 3.45 that both the real and imaginary parts of ζ satisfy Laplace's equation:

$$\nabla^2 \xi(x, y) = 0, \quad \nabla^2 \eta(x, y) = 0 \tag{3.47}$$

Functions that satisfy Laplace's equation are called harmonic functions, and two harmonic functions that are related through the Cauchy-Riemann equations are called conjugate harmonic functions. It can be proven that if ξ is any harmonic function, Equation 3.45 can always be integrated to find its harmonic conjugate function, η, and vice versa. Moreover, the resulting function $\zeta = \xi + i\eta$ will be an analytic function of z.

3.3.2 Complex potentials

It was shown in Subsection 3.2.4 that two dimensional elasticity problems can be solved in terms of an Airy stress function U, which satisfies the biharmonic equation (Equation 3.38). We now demonstrate that the Airy stress function for a particular problem can always be expressed in terms of two analytic functions of a complex variable. First, let

$$P = \sigma_{xx} + \sigma_{yy} = \nabla^2 U \tag{3.48}$$

so that P is a harmonic function. Then, as remarked before, its harmonic conjugate, Q, can in principle be found, and the function:

$$f(z) = P + iQ \tag{3.49}$$

will be analytic. The function found by integrating $f(z)$ along any contour that lies within a region in which $f(z)$ is analytic will itself be analytic, so we can define another analytic function, $\phi(z)$, by:

$$\phi(z) = \frac{1}{4} \int f(z)dz = p + iq \tag{3.50}$$

where p and q are the real and imaginary parts of $\phi(z)$. It follows from Equation 3.46 that:

$$\phi'(z) = \frac{\partial p}{\partial x} + i\frac{\partial q}{\partial x} = \frac{1}{4}f(z) = \frac{1}{4}(P + iQ) \tag{3.51}$$

Equating the real and imaginary parts of the expression above, and making use of Equation 3.45, we have:

$$\frac{1}{4}P = \frac{\partial p}{\partial x} = \frac{\partial q}{\partial y}, \quad \frac{1}{4}Q = \frac{\partial q}{\partial x} = -\frac{\partial p}{\partial y} \tag{3.52}$$

Next, we note that the function $p_1 = U - px - qy$ is harmonic since:

$$\nabla^2(p_1 = U - px - qy) = \nabla^2 U - x\nabla^2 p - 2\frac{\partial p}{\partial x} - y\nabla^2 q - 2\frac{\partial q}{\partial y} = 0 \tag{3.53}$$

It follows that p_1 is the real part of an analytic function, which we will call $\chi(z)$. Noting that the real part of $\bar{z}\phi(z)$ is:

$$\mathcal{R}\{\bar{z}\phi(z)\} = \mathcal{R}\{(x - iy)(p + iq)\} = px + qy \tag{3.54}$$

it follows that:

$$U = p_1 + px + qy = \mathcal{R}\{\chi(z)\} + \mathcal{R}\{\bar{z}\phi(z)\} = \frac{1}{2}\left[\bar{z}\phi(z) + z\overline{\phi(z)} + \chi(z) + \overline{\chi(z)}\right] \tag{3.55}$$

where $\overline{\phi(z)} = p - iq$, etc. Therefore, we have shown that the Airy stress function U can always be expressed in terms of two analytic functions $\phi(z)$ and $\chi(z)$, which are called complex potentials in the following.

3.3.3   Solution procedure with the complex potentials

By differentiating Equation 3.55, we find:

$$2\frac{\partial U}{\partial x} = \phi(z) + \bar{z}\phi'(z) + \overline{\phi(z)} + z\overline{\phi'(z)} + \chi'(z) + \overline{\chi'(z)} \tag{3.56}$$

$$2\frac{\partial U}{\partial y} = -i\phi(z) + i\bar{z}\phi'(z) + i\overline{\phi(z)} - iz\overline{\phi'(z)} + i\chi'(z) - i\overline{\chi'(z)}$$

$$2\frac{\partial^2 U}{\partial x^2} = 2\phi'(z) + \bar{z}\phi''(z) + 2\overline{\phi'(z)} + z\overline{\phi''(z)} + \chi''(z) + \overline{\chi''(z)}$$

$$2\frac{\partial^2 U}{\partial y^2} = 2\phi'(z) - \bar{z}\phi''(z) + 2\overline{\phi'(z)} - z\overline{\phi''(z)} - \chi''(z) - \overline{\chi''(z)}$$

$$2\frac{\partial^2 U}{\partial x\partial y} = i\bar{z}\phi''(z) - iz\overline{\phi''(z)} + i\chi''(z) - i\overline{\chi''(z)}$$

Let us define a new function:

$$\psi(z) = \chi'(z) \tag{3.57}$$

FromEquations 3.56 and 3.57, we can express the stress solution as a function of the complex potentials $\phi(z)$ and $\psi(z)$, as follows:

$$\sigma_{xx} + \sigma_{yy} = \frac{\partial^2 U}{\partial x^2} + \frac{\partial^2 U}{\partial y^2} = 2\left[\phi'(z) + \overline{\phi'(z)}\right] = 2\mathcal{R}\left[\phi'(z)\right] \tag{3.58}$$

$$\sigma_{yy} - \sigma_{xx} + 2i\sigma_{xy} = \frac{\partial^2 U}{\partial x^2} - \frac{\partial^2 U}{\partial y^2} - 2i\frac{\partial^2 U}{\partial x \partial y} = 2\left[\bar{z}\phi''(z) + \psi'(z)\right]$$

Let us note the following useful relationship:

$$\frac{\partial U}{\partial x} + i\frac{\partial U}{\partial y} = \phi(z) + z\overline{\phi'(z)} + \overline{\psi(z)} \tag{3.59}$$

To get the solution in displacements, it is necessary to introduce the constitutive relationships. In linear elasticity, the strain components are related to the components of stress according to [13]:

$$8G\epsilon_{xx} = (\kappa + 1)\sigma_{xx} + (\kappa - 3)\sigma_{yy} \tag{3.60}$$
$$8G\epsilon_{yy} = (\kappa + 1)\sigma_{yy} + (\kappa - 3)\sigma_{xx}$$

in which $\kappa = 3 - 4\nu$ in plane strain and $\kappa = (3 - \nu)/(1 + \nu)$ for plane stress. These relations can also be written as [13]:

$$2G\frac{\partial u}{\partial x} = -\sigma_{yy} + \frac{1}{4}(\kappa + 1)(\sigma_{xx} + \sigma_{yy}) \tag{3.61}$$

$$2G\frac{\partial v}{\partial y} = -\sigma_{xx} + \frac{1}{4}(\kappa + 1)(\sigma_{xx} + \sigma_{yy})$$

Using the real and imaginary parts of the complex potential, the equation above can be rewritten as [13]:

$$2G\frac{\partial u}{\partial x} = -\frac{\partial^2 U}{\partial x^2} + (\kappa + 1)\frac{\partial p}{\partial x} \tag{3.62}$$

$$2G\frac{\partial v}{\partial y} = -\frac{\partial^2 U}{\partial y^2} + (\kappa + 1)\frac{\partial q}{\partial y}$$

Integrating the first and second equations above with respect to x and y, respectively, we get:

$$2G\,u = -\frac{\partial U}{\partial x} + (\kappa + 1)p + g(y) \tag{3.63}$$

$$2G\,v = -\frac{\partial U}{\partial y} + (\kappa + 1)q + h(x)$$

where g and h are yet-unknown functions of y and x, respectively. To study these two functions, recall that $2G\epsilon_{xy} = \sigma_{xy}$, in which case, in the absence of body force, Equation

3.2.4 gives:

$$2G\left(\frac{\partial u}{\partial y} + \frac{\partial v}{\partial x}\right) = -2\frac{\partial^2 U}{\partial x \partial y} \tag{3.64}$$

But differentiation of Equation 3.57 gives:

$$2G\left(\frac{\partial u}{\partial y} + \frac{\partial v}{\partial x}\right) = -2\frac{\partial^2 U}{\partial x \partial y} + g'(y) + h'(x) \tag{3.65}$$

from which we deduce that:

$$g'(y) + h'(x) = 0 \tag{3.66}$$

The general solution of the equation above is:

$$g(y) = \omega\, y + a, \quad h(y) = -\omega\, x + b \tag{3.67}$$

where ω, a and b are constants. The portion of the displacement vector that is represented by g and h therfore corresponds to a rigid-body motion and has no stresses associated with it. Ignoring this rigid-body motion, the displacement vector can be written as a complex number. Using the equations above, one gets:

$$2G(u + iv) = -\left(\frac{\partial U}{\partial x} + i\frac{\partial U}{\partial y}\right) + (\kappa + 1)(p + iq) = \kappa\phi(z) - z\overline{\phi'(z)} - \overline{\chi'(z)} \tag{3.68}$$

3.4 Analytical solutions of cavity expansion

When the boundary conditions are given in terms of tractions, it is convenient to use the biharmonic equation (Equation 3.38) to solve for the stress components. In other cases, a displacement-based formulation is preferred. In the previous section, solutions to elasticity problems were presented in terms of arbitrary analytic functions of the complex variable z. Many important problems can be solved by taking the complex potentials to be polynomials in either z or $1/z$. In the following, we will explain fundamental solutions of underground stress obtained by solving the biharmonic equation or by using the complex potentials.

3.4.1 Uniform state of stress

A uniform state of stress abd strain can be found by taking the two potentials to be linear functions of z:

$$\phi(z) = c\, z, \quad \psi(z) = d\, z \tag{3.69}$$

where c and d are constants that may be complex. From Equation 3.156, we have:

$$\begin{aligned}
\sigma_{xx} - \sigma_{yy} &= 4\mathcal{R}(c) \tag{3.70}\\
\sigma_{xx} - \sigma_{yy} + 2i\sigma_{xy} &= 2\left[\overline{z}\phi''(z) + \psi'(z)\right] = 2d
\end{aligned}$$

As the imaginary part of c does not affect the stresses, we may take c to be purely real. The imaginary part of d, however, determines the shear component σ_{xy}, and cannot be ignored. As c and d are constants, the two equations above show that Equation 3.69 represents a

uniform state of stress. If the principal stresses are denoted σ_1 and σ_2, with the rotation of σ_1 rotated by an angle β from the x-axis, then we have [13]:

$$\sigma_1 - \sigma_2 = 4c \tag{3.71}$$
$$\sigma_2 - \sigma_1 = (\sigma_{xx} - \sigma_{yy} + 2i\sigma_{xy})\,e^{2i\beta} = 2d\,e^{2i\beta}$$

These relations can be inverted to yield:

$$c = \frac{1}{4}\,(\sigma_1 + \sigma_2), \quad d = \frac{1}{2}\,(\sigma_2 - \sigma_1)\,e^{-2i\beta} \tag{3.72}$$

In other words, the uniform stress state consisiting of principal stresses σ_1 rotated by an angle β from the x-axis and principal stress σ_2 rotated by an angle β from the y-axis is represented by the complex potentials:

$$\phi(z) = \frac{1}{4}\,(\sigma_1 + \sigma_2)\,z, \quad \psi(z) = \frac{1}{2}\,(\sigma_2 - \sigma_1)\,z\,e^{-2i\beta} \tag{3.73}$$

and following Equation 3.63, the displacement field is determined by the following equation:

$$2G(u + iv) = \frac{1}{4}(\kappa - 1)\,(\sigma_1 + \sigma_2)\,z - \frac{1}{2}\,(\sigma_2 - \sigma_1)\,\overline{z}\,e^{2i\beta} \tag{3.74}$$

3.4.2   Pressurized circular cavity subjected to uniform stress in the far field

We focus on a 2D elasticity problem (plane strain or plane stress). We consider a pressurized circular cavity of radius a subjected to a uniform state of stress at a distance b from the center, as shown in Figure 3.17. We will show how to find the state of stress around the cavity, between a and b, using two methods: (i) the compex potentials method; (ii) the resolution of the biharmonic equation.

3.4.2.1   Complex potentials
We take the complex potentials as follows:

$$\phi(z) = c\,z, \quad \psi(z) = \frac{d}{z} \tag{3.75}$$

in which c and d are constants. The imaginary components of c and d would lead to shear stresses and rotations, so for the present problem, which presents radial symmetry, we can take c and d to be real. The displacement vector follows from Equation 3.63:
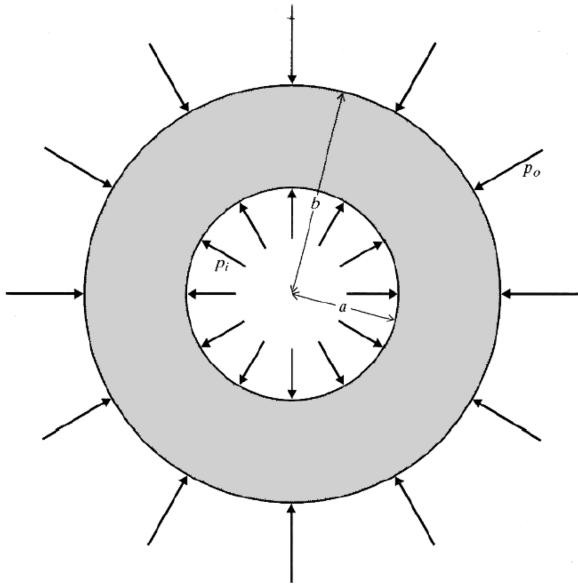
$$2G(u_x + iv_y) = (\kappa - 1)c\,z - \frac{d}{\overline{z}} \tag{3.76}$$

In polar coordinates, we have $z = r\,e^{i\theta}$ and therefore:

$$2G(u_x + iv_y) = (\kappa - 1)c\,r\,e^{i\theta} - \frac{d\,e^{i\theta}}{r} \tag{3.77}$$

So we have:

$$2G(u_r + iv_\theta) = 2G(u_x + iv_y)\,e^{-i\theta} = (\kappa - 1)\,c\,r - \frac{d}{r} \tag{3.78}$$

Figure 3.4   Circular pressurized cavity subject to isotropic stress in the far field. Picture taken from [4].

Since c and d are real:

$$2G\,u_r = (\kappa - 1)\,c\,r - \frac{d}{r}, \quad 2G\,u_\theta = 0 \tag{3.79}$$

The stresses are found from Equations 3.156:

$$\sigma_{rr} + \sigma_{\theta\theta} = \sigma_{xx} + \sigma_{yy} = 4\mathcal{R}\left(\phi'(z)\right) = 4\,c \tag{3.80}$$

$$\sigma_{yy} - \sigma_{xx} + 2i\sigma_{xy} = 2\left[\bar{z}\phi''(z) + \psi'(z)\right] = \frac{-2d}{z^2} = \frac{-2d}{r^2}e^{-2i\theta}$$

And we have:

$$\sigma_{\theta\theta} - \sigma_{rr} + 2i\sigma_{r\theta} = \left(\sigma_{yy} - \sigma_{xx} + 2i\sigma_{xy}\right)e^{2i\theta} = \frac{-2d}{r^2} \tag{3.81}$$

Separating out the real and imaginary parts, we get:

$$\sigma_{\theta\theta} - \sigma_{rr} = \frac{-2d}{r^2}, \quad \sigma_{r\theta} = 0 \tag{3.82}$$

The boundary conditions impose (Figure 3.17):

$$\sigma_{rr}(a) = p_i, \quad \sigma_{rr} = p_0 \tag{3.83}$$

Therefore, we have:

$$c = \frac{b^2 p_0 - a^2 p_i}{2(b^2 - a^2)}, \quad d = \frac{a^2 b^2 (p_i - p_0)}{(b^2 - a^2)} \tag{3.84}$$

The full solution is then:

$$\sigma_{rr} = \frac{(b^2 p_0 - a^2 p_i)}{(b^2 - a^2)} + \frac{a^2 b^2 (p_i - p_0)}{(b^2 - a^2)\, r^2} \tag{3.85}$$

$$\sigma_{\theta\theta} = \frac{(b^2 p_0 - a^2 p_i)}{(b^2 - a^2)} - \frac{a^2 b^2 (p_i - p_0)}{(b^2 - a^2)\, r^2}$$

$$2G\, u_r = (\kappa - 1)\frac{(b^2 p_0 - a^2 p_i)\, r}{2(b^2 - a^2)} - \frac{a^2 b^2 (p_i - p_0)}{(b^2 - a^2)\, r}$$

When the uniform stress p_0 is applied at infinity, i.e., when $b >> a$, then:

$$\sigma_{rr} = p_0 + \frac{a^2}{r^2}(p_i - p_0) \tag{3.86}$$

$$\sigma_{\theta\theta} = p_0 - \frac{a^2}{r^2}(p_i - p_0)$$

$$2G\, u_r = (\kappa - 1)\frac{p_0\, r}{2} - \frac{a^2(p_i - p_0)}{r}$$

If a borehole in an infinite rock mass is loaded by a hydrostatic pressure P, the resulting displacement of the borehole wall will be $u_r(a) = -Pa/2G$. This equation is useful is estimating the shear modulus G from borehole measurements.

3.4.2.2 Biharmonic equation

In axis-symmetric conditions, the biharmonic Equation 3.41 becomes:

$$\frac{d^4}{dr^4}U(r) + \frac{2}{r}\frac{d^3}{dr^3}U(r) - \frac{1}{r^2}\frac{d^2}{dr^2}U(r) + \frac{1}{r^3}\frac{d}{dr}U(r) = 0 \tag{3.87}$$

The general solution was established by Timoshenko & Goodier (1970):

$$U(r) = A\, ln(r) + B\, r^2\, ln(r) + C\, r^2 + D \tag{3.88}$$

Another solution was then given by Barber (2010):

$$U(r\theta) = A\, ln(r) + C\, r^2 + E\, \theta \tag{3.89}$$

The expression of stress is found by using the following derivation formulae in polar coordinates (Barber, 2010):

$$\sigma_{rr} = \frac{1}{r}\frac{\partial U}{\partial r} + \frac{1}{r^2}\frac{\partial^2 U}{\partial \theta^2}$$

$$\sigma_{\theta\theta} = \frac{\partial^2 U}{\partial r^2}$$

$$\sigma_{r\theta} = \frac{1}{r^2}\frac{\partial U}{\partial \theta} - \frac{1}{r}\frac{\partial^2 U}{\partial r \partial \theta} \tag{3.90}$$

The problem is axis-symmetric, therefore:

$$\sigma_{rr} = \frac{1}{r}\frac{\partial U}{\partial r}, \quad \sigma_{\theta\theta} = \frac{\partial^2 U}{\partial r^2}, \quad \sigma_{r\theta} = 0 \tag{3.91}$$

For a pressurized circular cavity subject to isotropic stress in the far-field (see Figure 3.17), the solution by Timoshenko & Goodier is:

$$\sigma_{rr} = \frac{A}{r^2} + 2C + B(1 + 2\ln(r))$$

$$\sigma_{\theta\theta} = -\frac{A}{r^2} + 2C + B(3 + 2\ln(r))$$

$$\sigma_{r\theta} = 0 \tag{3.92}$$

and the olution by Barber is:

$$\sigma_{rr} = \frac{A}{r^2} + 2C$$

$$\sigma_{\theta\theta} = -\frac{A}{r^2} + 2C$$

$$\sigma_{r\theta} = 0 \tag{3.93}$$

For the boundary conditions considered: $\sigma_{rr}(r = a) = p_i$, $\sigma_{r\theta}(r = a) = 0$, $\sigma_{rr}(r = b) = p_0$, $\sigma_{r\theta}(r = b) = 0$, both analytical solutions lead to:

$$\sigma_{rr} = \frac{A}{r^2} + 2C$$

$$\sigma_{\theta\theta} = -\frac{A}{r^2} + 2C$$

$$\sigma_{r\theta} = 0$$

$$A = \frac{(p_i - p_0)a^2b^2}{b^2 - a^2} \qquad 2C = \frac{p_0b^2 - p_ia^2}{b^2 - a^2}$$

$$\tag{3.94}$$

3.4.3   Free circular cavity subjected to horizontal stress
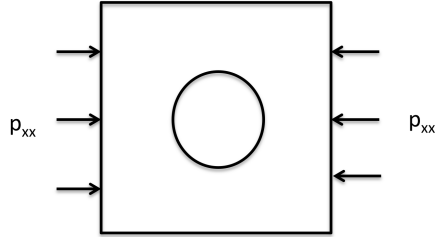
We consider the free circular cavity subjected to a uniform horizontal stress in the far field, as illustrated in Figure 3.5. In the absence of the hole, the complex potentials associated with a uniaxial stress state p_{xx} aligned with the x-axis would be $\phi(z) = p_{xx}\, z/4$, $\psi(z) = -p_{xx}\, z/2$, as found for the case of a uniform state of stress. Although this solution gives the correct far-field stress, it will give incorrect, non-zero tractions at the borehole wall. We must therefore find additional terms in the potentials that will cancel out these unwanted tractions, but not give any additional stresses at infinity. The only such terms which may be of use and which will lead to stresses that vary as functions of 2θ, are the following:

$$\phi(z) = \frac{1}{4}p_{xx}\left(z + \frac{A}{z}\right), \quad \psi(z) = -\frac{1}{2}p_{xx}\left(z + \frac{B}{z} + \frac{C}{z^2}\right) \tag{3.95}$$

where A, B and C are real constants.

The derivatives that will be needed for subsequent calculation of displacements and stresses are:

$$\phi'(z) = \frac{1}{4}p_{xx}\left(1 - \frac{A}{z^2}\right), \quad \phi''(z) = \frac{p_{xx}A}{2z^3}, \quad \psi'(z) = -\frac{1}{2}p_{xx}\left(1 - \frac{B}{z^2} - \frac{3C}{z^4}\right)$$

$$\tag{3.96}$$

Figure 3.5   Free circular cavity subjected to a horizontal stress p_{xx} in the far field

Working in polar coordinates, we have:

$$\sigma_{rr} + \sigma_{\theta\theta} = 4\mathcal{R}\left[\phi'(z)\right] = p_{xx}\mathcal{R}\left[1 - Ar^{-2}e^{-2i\theta}\right] = p_{xx}\left(1 - Ar^{-2}\cos(2\theta)\right) \quad (3.97)$$

Next, we have:

$$\begin{aligned}
\sigma_{yy} - \sigma_{xx} + 2i\sigma_{xy} &= 2\left[\bar{z}\phi''(z) + \psi'(z)\right] = \frac{Ap_{xx}\bar{z}}{z^3} - p_{xx}\left(1 - \frac{B}{z^2} - \frac{3C}{z^4}\right) \\
&= Ap_{xx}r^{-2}e^{-4i\theta} - p_{xx}\left(1 - Br^{-2}e^{-2i\theta} - 3Cr^{-4}e^{-4i\theta}\right)
\end{aligned} \quad (3.98)$$

Then we find:

$$\begin{aligned}
\sigma_{\theta\theta} - \sigma_{rr} + 2i\sigma_{r\theta} &= \left(\sigma_{yy} - \sigma_{xx} + 2i\sigma_{xy}\right)e^{2i\theta} \\
&= p_{xx}\left[Br^{-2} - e^{2i\theta} + (Ar^{-2} + 3Cr^{-4})e^{-2i\theta}\right]
\end{aligned} \quad (3.99)$$

The real part gives:

$$\sigma_{\theta\theta} - \sigma_{rr} = p_{xx}\left[Br^{-2} - e^{2i\theta} - (1Ar^{-2} - 3Cr^{-4})\cos(2\theta)\right] \quad (3.100)$$

Then, Equations 3.97 and 3.100 can be solved to give:

$$\sigma_{rr} = \frac{1}{2}p_{xx}\left[1 - Br^{-2} + (1 - 2Ar^{-2} - 3Cr^{-4})\cos(2\theta)\right] \quad (3.101)$$

$$\sigma_{\theta\theta} = \frac{1}{2}p_{xx}\left[1 + Br^{-2} + (3Cr^{-4} - 1)\cos(2\theta)\right]$$

The imaginary part of Equation 3.99 gives:

$$\sigma_{r\theta} = -\frac{1}{2}p_{xx}\left[(1 + Ar^{-2} + 3Cr^{-4})\sin(2\theta)\right] \quad (3.102)$$

In order for the hole boundary to be traction-free, both Equations 3.101 and 3.102 must vanish at $r = a$. This requires A, B and C to satisfy the following equations:

$$1 - Ba^{-2} = 0, \quad 1 - 2Aa^{-2} - 3Ca^{-4} = 0, \quad 1 + Aa^{-2} + 3Ca^{-4} = 0 \quad (3.103)$$

The solution is:

$$A = 2a^2, \quad B = a^2, \quad C = -a^4 \quad (3.104)$$

The full expression of the stresses follows:

$$
\sigma_{rr} = \frac{1}{2}p_{xx}\left(1 - \frac{a^2}{r^2}\right) + \frac{1}{2}p_{xx}\left(1 - 4\frac{a^2}{r^2} + 3\frac{a^4}{r^4}\right)\cos(2\theta)
$$

$$
\sigma_{\theta\theta} = \frac{1}{2}p_{xx}\left(1 + \frac{a^2}{r^2}\right) - \frac{1}{2}p_{xx}\left(1 + 3\frac{a^4}{r^4}\right)\cos(2\theta)
$$

$$
\sigma_{r\theta} = -\frac{1}{2}p_{xx}\left(1 + 2\frac{a^2}{r^2} - 3\frac{a^4}{r^4}\right)\sin(2\theta)
$$

The displacement field are found by solving the following equation:

$$
\frac{8G\left(u + iv\right)}{p_{xx}} = \kappa\left(re^{i\theta} + Ar^{-1}e^{-i\theta}\right) - \left(re^{i\theta} - Ar^{-1}e^{3i\theta}\right) + \left(re^{-i\theta} + Br^{-1}e^{i\theta} + Cr^{-3}e^{3i\theta}\right)
$$

$$(3.105)$$

Multiplying by $e^{-i\theta}$ and using the values of A, B and C and separating out the real and imaginary parts, we get the components of the displacement field, as follows:

$$
\frac{8Gu_r}{ap_{xx}} = \left[(\kappa - 1)\left(\frac{r}{a}\right) + 2\left(\frac{a}{r}\right)\right] \tag{3.106}
$$

$$
+ \; 2\left[\left(\frac{r}{a}\right) + (\kappa + 1)\left(\frac{a}{r}\right) - \left(\frac{a}{r}\right)^3\right]\cos(2\theta)
$$

$$
\frac{8Gu_\theta}{ap_{xx}} = -2\left[\left(\frac{r}{a}\right) + (\kappa - 1)\left(\frac{a}{r}\right) + \left(\frac{a}{r}\right)^3\right]\sin(2\theta)
$$

where $\kappa = 3 - 4\nu$ for plane strain and $\kappa = (3 - \nu)/(1 + \nu)$ for plane stress.

3.4.4 Kirsch equations
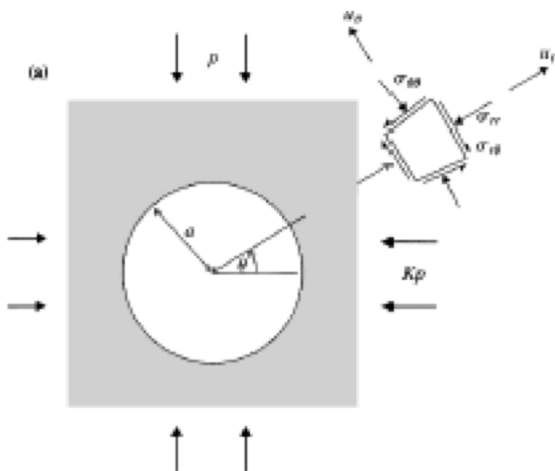
Kirsch equations provide the stress solution for a free circular cavity subjected to a biaxial state of stress in the far field (Figure 3.6).

Kirsch equations can be obtained by superposition. The first option is to superpose the case of a pressurized circular cavity under uniform stress in the far field (Figure 3.7):

$$
\sigma_{rr} = p\left(1 - \frac{a^2}{r^2}\right)
$$

$$
\sigma_{\theta\theta} = p\left(1 + \frac{a^2}{r^2}\right) \tag{3.107}
$$

$$
\sigma_{r\theta} = 0
$$
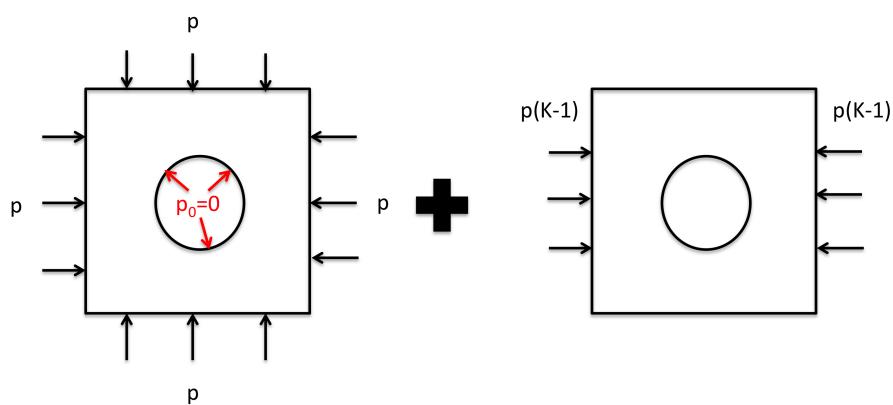
with the case of a free circular cavity subjected to a horizontal state of stress in the far field:

$$
\sigma_{rr} = p\left(1 - \frac{a^2}{r^2}\right) + \frac{1}{2}(Kp - p)\left(1 - 4\frac{a^2}{r^2} + 3\frac{a^4}{r^4}\right)\cos(2\theta)
$$

$$
\sigma_{\theta\theta} = p\left(1 + \frac{a^2}{r^2}\right) - \frac{1}{2}(Kp - p)\left(1 + 3\frac{a^4}{r^4}\right)\cos(2\theta) \tag{3.108}
$$

$$
\sigma_{r\theta} = -\frac{1}{2}(Kp - p)\left(1 + 2\frac{a^2}{r^2} - 3\frac{a^4}{r^4}\right)\sin(2\theta)
$$
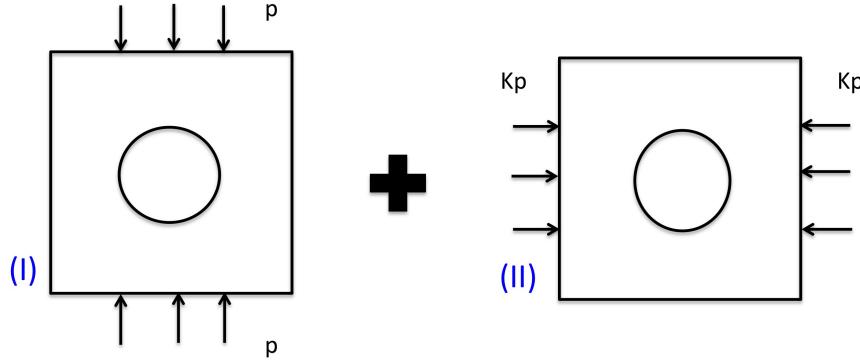
Figure 3.6   Free circular cavity subjected to a biaxial stress in the far field. Picture taken from [4].

Figure 3.7   First superposition option to establish Kirsch equations

The second option is to superpose the case of a free circular cavity under vertical stress in the far field to the case of a free circular cavity under horizontal stress in the far field (Figure 3.8):

$$\sigma_{rr}^{(I)} = \tfrac{1}{2}p\left(1 - \tfrac{a^2}{r^2}\right) - \tfrac{1}{2}p\left(1 - 4\tfrac{a^2}{r^2} + 3\tfrac{a^4}{r^4}\right)cos(2\theta)$$

$$\sigma_{rr}^{(II)} = \tfrac{1}{2}Kp\left(1 - \tfrac{a^2}{r^2}\right) + \tfrac{1}{2}Kp\left(1 - 4\tfrac{a^2}{r^2} + 3\tfrac{a^4}{r^4}\right)cos(2\theta)$$

$$\sigma_{\theta\theta}^{(I)} = \tfrac{1}{2}p\left(1 + \tfrac{a^2}{r^2}\right) + \tfrac{1}{2}p\left(1 + 3\tfrac{a^4}{r^4}\right)cos(2\theta)$$

$$\sigma_{\theta\theta}^{(II)} = \tfrac{1}{2}Kp\left(1 + \tfrac{a^2}{r^2}\right) - \tfrac{1}{2}Kp\left(1 + 3\tfrac{a^4}{r^4}\right)cos(2\theta) \qquad (3.109)$$

$$\sigma_{r\theta}^{(I)} = -\tfrac{1}{2}p\left(1 + 2\tfrac{a^2}{r^2} - 3\tfrac{a^4}{r^4}\right)sin(2\theta)$$

$$\sigma_{r\theta}^{(II)} = \tfrac{1}{2}Kp\left(1 + 2\tfrac{a^2}{r^2} - 3\tfrac{a^4}{r^4}\right)sin(2\theta)$$

Figure 3.8   Second superposition option to establish Kirsch equations

For both cases, the following equations are obtained to solve for the stress field:
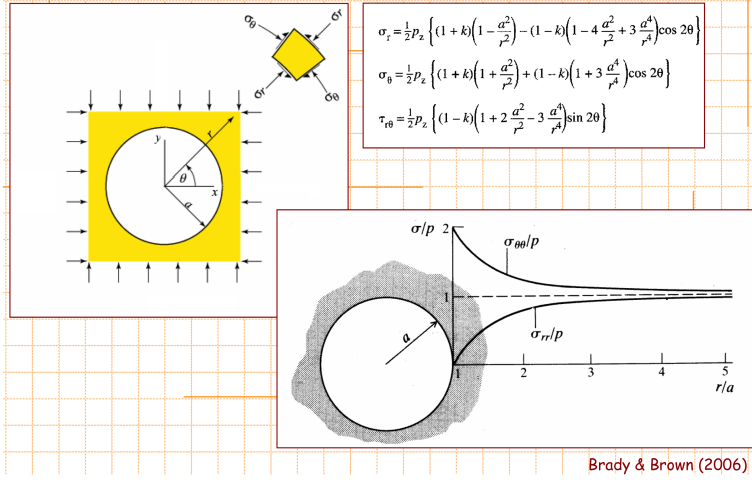
$$\sigma_{rr} = \tfrac{1}{2}p(1 + K)\left(1 - \tfrac{a^2}{r^2}\right) - \tfrac{1}{2}p(1 - K)\left(1 - 4\tfrac{a^2}{r^2} + 3\tfrac{a^4}{r^4}\right)cos(2\theta)$$

$$\sigma_{\theta\theta} = \tfrac{1}{2}p(1 + K)\left(1 + \tfrac{a^2}{r^2}\right) + \tfrac{1}{2}p(1 - K)\left(1 + 3\tfrac{a^4}{r^4}\right)cos(2\theta) \qquad (3.110)$$

$$\sigma_{r\theta} = \tfrac{1}{2}p(1 - K)\left(1 + 2\tfrac{a^2}{r^2} - 3\tfrac{a^4}{r^4}\right)sin(2\theta)$$

The above equations are called the Kirsch equations. The trends of the stress field predicted by the Kirsch equations are shown in Figure 3.9.
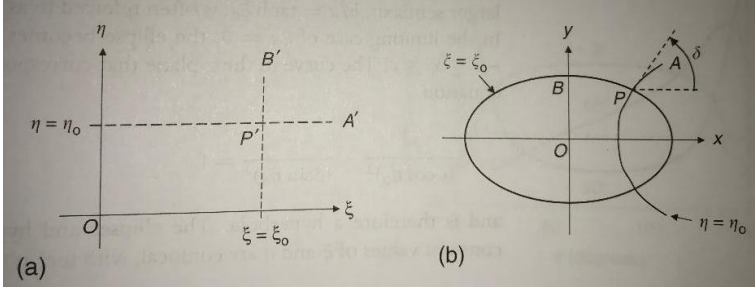
3.4.5   Elliptical cavities Introduction to conformal mapping

Consider two complex planes, $z = x + iy$ and $\zeta = \xi + i\eta$ (see Figure 3.10). The transformation from the ζ-plane to the z-plane is defined by an analytic function ω: $z = \omega(\zeta)$. We note:

$$dz = dx + idy = \omega'(\zeta)d\zeta = Mexp(i\delta)\left[d\xi + id\eta\right] \qquad (3.111)$$

Figure 3.9   Stress field predicted by the Kirsch equations

Figure 3.10   Principle of conformal mapping. Image taken from [13].

We have [13]:

$$\frac{\omega'(\zeta)}{\overline{\omega'(\zeta)}} = exp(2i\delta), \quad \left(\frac{dy}{dx}\right)_{\eta=\eta_0} = tan\delta, \quad \left(\frac{dx}{dy}\right)_{\xi=\xi_0} = -\frac{1}{tan\delta} \tag{3.112}$$
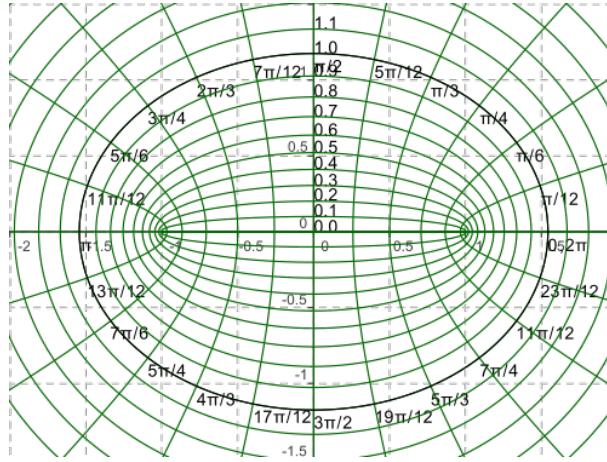
The curves of equations $\xi = \xi_0$ and $\eta = \eta_0$ are orthogonal lines in the ζ-plane and they are orthogonal curves in the z-plane. Moreover, δ is the angle between the x axis and the tangent to the curve of equation $\eta = \eta_0$ in the z-plane.

We have:

$$\phi'(z) = \frac{d\phi}{dz} = \frac{d\phi(\zeta)}{d\zeta}\frac{d\zeta}{dz} = \frac{1}{\omega'(\zeta)}\frac{d\phi(\zeta)}{d\xi} \tag{3.113}$$

and similar relationships hold for ϕ'' and χ''. It is thus possible to express the stress field in the ζ-plane. After some calculations:

$$\sigma_{\xi\xi} + \sigma_{\eta\eta} = 2\left[\phi'(z)\right] \tag{3.114}$$

$$\sigma_{\eta\eta} - \sigma_{\xi\xi} + 2i\sigma_{\xi\eta} = 2\left[\overline{z}\phi''(z) + \chi''(z)\right]\frac{\omega'(\zeta)}{\overline{\omega'(\zeta)}}$$

$$= 2\left[\overline{z}\phi''(z) + \chi''(z)\right]exp(2i\delta)$$

Figure 3.11   Use of elliptical coordinates for conformal mapping.Image taken from *Wikipedia, 2014*.

When the cavity is elliptical, axis-symmetry does not hold and the balance equation in the physical space becomes complicated, which makes it challenging to find an analytical solution for the fields of stress and displacements. Hence the idea of using conformal mapping. An ellipse can be represented by the equation $\xi = \xi_0$, see Figure 3.11. Lines perpendicular to the ellipse are iso-η values. Each point of the ellipse is located at an angle δ from the major axis.

The specific mapping transformation is the following:

$$z = x + iy = c\,cosh\zeta = c\,cosh(\xi + i\eta) \tag{3.115}$$

where:

$$cosh(x) = \frac{e^x + e^{-x}}{2}, \quad sinh(x) = \frac{e^x - e^{-x}}{2} \tag{3.116}$$

We thus have:

$$x = c\,cosh\xi\,cos\eta, \quad y = c\,sinh\xi\,sin\eta \tag{3.117}$$

The equation of the ellipse is $\xi = \xi_0$, which can also be written as:

$$\frac{x^2}{(c\,cosh\xi_0)^2} + \frac{y^2}{(c\,sinh\xi_0)^2} = 1 \tag{3.118}$$

The major axis a_0 and the minor axis b_0 of the initial ellipse are:

$$a_0 = c\,cosh\xi_0, \quad b_0 = c\,sinh\xi_0 \tag{3.119}$$

We have:

$$dx + idy = Me^{i\delta}d\xi \tag{3.120}$$

Using the complex variable method, the elastic stress distribution around an ellipse in the ζ-plane is given by:

$$
\begin{aligned}
\sigma_{\xi\xi} + \sigma_{\eta\eta} &= 2\left[\phi'(z) + \overline{\phi'(z)}\right] \\
\sigma_{\xi\xi} - \sigma_{\eta\eta} + 2i\tau_{\xi\eta} &= 2\left[\bar{z}\phi''(z) + \chi''(z)\right]e^{2i\delta}
\end{aligned}
\tag{3.121}
$$

For a traction-free elliptical hole subjected to a far field stress σ_1^∞ in a direction rotated from the major axis of the ellipse by an angle β, the potentials are:

$$4\phi(z) = \sigma_1^\infty c \left[e^{2(\xi_0 + i\beta)} \cosh\zeta + (1 - e^{2\xi_0 + i\beta}) \sinh\zeta \right] \tag{3.122}$$

$$4\chi'(z) = -\sigma_1^\infty c \left[\cosh 2\xi_0 - \cos 2\beta + e^{2\xi_0} \sinh 2(\zeta - \xi_0 - i\beta) \right] / \sinh\zeta$$

For a traction-free cavity, $\sigma_{\xi\xi} = 0$ and:

$$\sigma_{\eta\eta} = 2\left[\phi'(z) + \overline{\phi'(z)} \right] \tag{3.123}$$

$$\sigma_{\xi\eta} = -i\left[\phi'(z) + \overline{\phi'(z)} \right] - i\left[\bar{z}\phi''(z) + \chi''(z) \right] e^{2i\delta}$$

For a traction-free elliptical hole subjected to a far field stress σ_1^∞ in a direction rotated from the major axis of the ellipse by an angle β:

$$\sigma_{\eta\eta} = \frac{2ab + (a^2 - b^2)\cos(2\beta) - (a^2 + b^2)\cos(2(\beta - \eta))}{(a^2 + b^2 - (a^2 - b^2)\cos(2\eta)} \tag{3.124}$$

The conform plane is the (ρ, θ)-plane in which the ellipse of the ζ-plane becomes a circle of unit radius:

$$z = x + iy = R\left(\zeta_2 + \frac{m}{\zeta_2} \right) = \omega(\zeta_2), \quad \zeta_2 = \xi_2 + i\eta_2 = \rho e^{i\theta} \tag{3.125}$$

$$R = \frac{a_0 + b_0}{2}, \quad m = \frac{a_0 - b_0}{a_0 + b_0} \tag{3.126}$$

θ is the angle between the ρ- and ξ_2- axes:

$$\rho = \frac{a + b}{a_0 + b_0} = e^{\xi - \xi_0}, \quad \theta = \eta \tag{3.127}$$
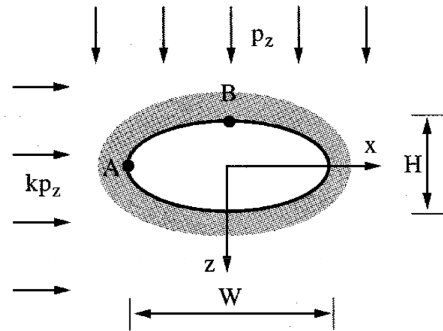
$$(\sigma_{\rho\rho}, \sigma_{\theta\theta})(\rho, \theta) = (\sigma_{\xi\xi}, \sigma_{\eta\eta})(\rho, \theta) = (\sigma_{\xi\xi}, \sigma_{\eta\eta})(e^{\xi - \xi_0}, \eta) \tag{3.128}$$

The stress components in the conform phase plane $(\sigma_{\rho\rho}, \sigma_{\theta\theta})$ can be obtained from the stress components in the phase plane $(\sigma_{\xi\xi}, \sigma_{\eta\eta})$ by substituting ξ by $\ln\rho + \xi_0$. Once the stress components in the conform phase plane are known, it is possible to obtain the stress components in the physical plane by using a transformation of stress. Considering α the direct angle between the ρ- and the x- axes, we have:

$$\begin{cases} \sigma_{xx} = \frac{\sigma_{\rho\rho} + \sigma_{\theta\theta}}{2} + \frac{\sigma_{\rho\rho} - \sigma_{\theta\theta}}{2} \cos(2\alpha) + \sigma_{\rho\theta} \sin(2\alpha) \\[2mm] \sigma_{yy} = \frac{\sigma_{\rho\rho} + \sigma_{\theta\theta}}{2} - \frac{\sigma_{\rho\rho} - \sigma_{\theta\theta}}{2} \cos(2\alpha) - \sigma_{\rho\theta} \sin(2\alpha) \\[2mm] \sigma_{xy} = -\frac{\sigma_{\rho\rho} - \sigma_{\theta\theta}}{2} \sin(2\alpha) + \sigma_{\rho\theta} \cos(2\alpha) \end{cases} \tag{3.129}$$

Taking the notations of Figure 3.12, we have in particular:

$$\sigma_A = p\left(1 - K + 2\frac{W}{H} \right) \tag{3.130}$$

$$\sigma_B = p\left(K - 1 + 2K\frac{H}{W} \right)$$
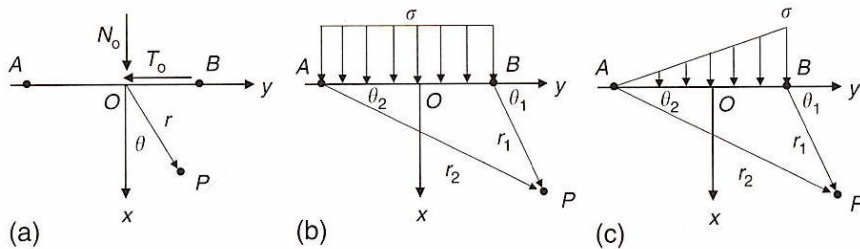
Figure 3.12   Problem of finding the stress around a free elliptical cavity subjected to a biaxial stress in the far field. Image taken from *Eberhardt, ISRM lecture 8, 2014.*

3.5   Fundamental analytical solutions for point loads and line loads

In elastostatics, the fundamental solutions are derived using the principle of superposition and St. Venant's principle, on the basis of a small number of fundamental problems. We have covered a few problems of cavity expansion. We will now study basic problems of point loads and line loads.

3.5.1   Point and line loads in 2D

The complex variable method for solving two-dimensonal elasticity problems can be used to investigate the stresses and displacements in an elastic half-space under the action of surface loads. In order to maintain the standard practice of letting x and y be real variables that represent the two coordinates, and taking $z = x + iy$ to be a complex variable, in this subsection, we let x be the vertical coordinate normal to the surface of the half-space $x \geq 0$, as shown in Figure 3.13.

Figure 3.13   Surface loads applied to a half-space: (a) normal and tangential line laods; (b) uniform normal traction applied over a strip; (c) linearly increasing normal traction applied over a strip. Image taken from [13].

The normal load applied to the surface between points A and B, per unit length in the direction normal to the plane (x,y), can be calculated as [13]:

$$\int_A^B (N + iT)dy = \int_A^B \left[\frac{\partial^2 U}{\partial y^2} - i\frac{\partial^2 U}{\partial x \partial y} \right] dy \tag{3.131}$$

$$= -i \left[\frac{\partial U}{\partial x} + i\frac{\partial U}{\partial y} \right]_A^B = -i \left[\phi(z) + z\overline{\phi'(z)} + \overline{\psi(z)} \right]_A^B$$

where we used Equations 3.56.

Now consider the functions:

$$\phi(z) = C \, ln(z), \quad \psi(z) = D \, ln(z) \tag{3.132}$$

which have singularities at the origin and so may be expected to correspond to point loads applied there. We now write point A as $a \, e^{-i\pi/2}$ and point B as $a \, e^{i\pi/2}$. Using equation 3.131, the total loads represented by the functions given in Equation 3.132 are found to be:

$$\int_A^B (N + iT)dy = -i \left[C \, ln\left(\frac{b}{a}\right) + i\pi C + \overline{D}ln\left(\frac{b}{a}\right) i\pi\overline{D} \right] \tag{3.133}$$

For this to correspond to a point load having components (N_0, T_0), the complex constants C and D must be chosen so that:

$$-i \left[C \, ln\left(\frac{b}{a}\right) + i\pi C + \overline{D}ln\left(\frac{b}{a}\right) i\pi\overline{D} \right] = N_0 + iT_0 \tag{3.134}$$

This is achieved by choosing:

$$C = \frac{(N_0 + iT_0)}{2\pi}, \quad D = -\frac{(N_0 - iT_0)}{2\pi} \tag{3.135}$$

We see that:

$$\phi(z) = \frac{(N_0 + iT_0)}{2\pi} \, ln(z), \quad \psi(z) = -\frac{(N_0 - iT_0)}{2\pi} \, ln(z) \tag{3.136}$$

are the complex stress potentials that correspond to a concentrated load (N_0, T_0) per unit length in the third direction, applied to the surface of the half space at the origin. As the load acts along the entire line corresponding to $(x = 0, y = 0)$, that is, the entire z-axis, the solutions represent *line loads*.

The normal line load is found by taking $T_0 = 0$. Then we have:

$$\sigma_{rr} + \sigma_{\theta\theta} = 4\mathcal{R}\left(\phi'(z)\right) = \frac{2N_0}{\pi}\mathcal{R}\left(\frac{1}{z}\right) = \frac{2N_0 \cos\theta}{\pi r} \tag{3.137}$$

$$\sigma_{\theta\theta} - \sigma_{rr} + 2i\sigma_{r\theta} = 2\left[\bar{z}\phi''(z) + \psi'(z)\right] e^{2i\theta} = -\frac{N_0}{\pi}\left[\frac{\bar{z}}{z^2} + \frac{1}{z}\right] e^{2i\theta} = -\frac{2N_0 \cos\theta}{\pi r}$$

from which the stresses follow as:

$$\sigma_{rr} = \frac{2N_0 \cos\theta}{\pi r}, \quad \sigma_{\theta\theta} = \sigma_{r\theta} = 0 \tag{3.138}$$

In Cartesian coordinates, it can be shown that [13]:

$$\sigma_{xx} = \frac{2N_0 x^3}{\pi r^4}, \quad \sigma_{yy} = \frac{2N_0 xy^2}{\pi r^4}, \quad \sigma_{xy} = \sigma_{xx} = \frac{2N_0 x^2 y}{\pi r^4} \tag{3.139}$$

The displacement is:

$$2G(u + iv) = \frac{N_0}{2\pi} \left[4(1 - \nu)ln(r) - \cos(2\theta) + i\left(2(1 - 2\nu)\theta - \sin(2\theta)\right) \right] \tag{3.140}$$

so that along the upper loaded surface ($x = 0$), the normal displacement is:

$$u(x = 0) = \frac{(1 - \nu)N_0}{G\pi} ln(y) \tag{3.141}$$

The tangential line load is found by taking $N_0 = 0$. Proceeding the same way as above, we then have:

$$\sigma_{xx} = \frac{2T_0 x^2 y}{\pi r^4}, \quad \sigma_{yy} = \frac{2T_0 y^3}{\pi r^4}, \quad \sigma_{xy} = \frac{2T_0 xy^2}{\pi r^4} \tag{3.142}$$

$$2G(u + iv) = \frac{T_0}{2\pi} \left[-2(1 - 2\nu)\theta - \sin(2\theta) + i\left(4(1 - \nu)ln(r) + \cos(2\theta)\right) \right] \tag{3.143}$$

3.5.2 Tractions applied over a strip in 2D

Consider the loading case illustrated in Figure 3.13.b. The vertical line load which corresponds to a force N_0 per unit of length in the z direction is now distributed over an infinitesimal strip of width dy. The compressive normal traction σ under this load will then be N_0/dy, which shows that the loading should be represented by $N_0 = \sigma\,dy$. Using superposition, the resultant stresses and displacements are found by integrating Equations 3.139 and 3.140 over the entire loaded region, noting that in the integrand, y must represent the horizontal distance between the point of application of the load and the observation point. For a uniform normal stress applied over the strip $-a \leq y \leq a$, we have:

$$\begin{aligned}
\sigma_{xx} &= \frac{2\sigma x^3}{\pi} \int_{-a}^{+a} \frac{dy'}{[x^2 + (y - y')^2]^2} \tag{3.144}\\[2mm]
&= \frac{\sigma}{\pi} \left[(\theta_1 - \theta_2) - \frac{x(y - a)}{r_1^2} + \frac{x(y + a)}{r_2^2} \right] \\[2mm]
&= \frac{\sigma}{\pi} \left[(\theta_1 - \theta_2) - \sin(\theta_1 - \theta_2)\cos(\theta_1 + \theta_2) \right]
\end{aligned}$$

where the angles and radii are defined in Figure 3.13.b. Similarly, the other components of stress are given by:

$$\begin{aligned}
\sigma_{yy} &= \frac{\sigma}{\pi} \left[(\theta_1 - \theta_2) + \frac{x(y - a)}{r_1^2} - \frac{x(y + a)}{r_2^2} \right] \tag{3.145}\\[2mm]
&= \frac{\sigma}{\pi} \left[(\theta_1 - \theta_2) + \sin(\theta_1 - \theta_2)\cos(\theta_1 + \theta_2) \right]
\end{aligned}$$

$$\sigma_{xy} = \frac{\sigma x^2 (r_2^2 - r_1^2)}{\pi r_1^2 r_2^2} = \frac{\sigma}{\pi} \left[\sin(\theta_1 - \theta_2)\sin(\theta_1 + \theta_2) \right] \tag{3.146}$$

The normal displacement of the surface is, except for an additive constant:

$$u(x = 0) = \frac{(1 - \nu)N_0}{G\pi} \left[2a + (y - a)ln|y - a| - (y + a)ln|y + a| \right] \qquad (3.147)$$

Now consider the loading case illustrated in Figure 3.13.c. The normal surface traction increases linearly from 0 at A to σ at B. In this case, the results are [13]:

$$
\begin{aligned}
\sigma_{xx} &= \frac{\sigma}{2\pi} \left[\left(1 + \frac{y}{a} \right) (\theta_1 - \theta_2) - \sin(2\theta_1) \right] && (3.148) \\
\sigma_{yy} &= \frac{\sigma}{2\pi} \left[\left(1 + \frac{y}{a} \right) (\theta_1 - \theta_2) + \sin(2\theta_1) - \frac{2x}{a}ln \left(\frac{r_2}{r_1} \right) \right] \\
\sigma_{xy} &= \frac{\sigma}{2\pi} \left[\left(1 - \frac{x}{a} \right) (\theta_1 - \theta_2) + \cos(2\theta_1) \right]
\end{aligned}
$$

This solution was used to estimate the stresses in the crust beneath mountain ranges. In such models, the weight of the mountain is assumed to provide a vertical normal traction that acts on the surface of a flat half-space. The subsurface stresses thus calculated are then added to the $\rho g x$ term that is due to the weight of the material below the nominal $x = 0$ surface. The overall effect is that the subsurface vertical stress will, in general, not be equal to that which would be calculated from the lithostatic gradient using the depth below the actual ground surface.

3.5.3 Fundamental solutions for point loads in 3D

Like in 2D, it is possible to obtain solutions for line loads or surface loads in 3D by integrating solutions for point loads. The derivation of these fundamental solutions for point loads in 3D is not straightforward. So in the following, we will only list the solutions for a few basic cases, so that the reader can reconstruct more complex 3D cases by superposition. We adopt the formalism of Poulos and Davis, who provide an exhaustive catalog of solutions in [17].

3.5.3.1 *Kelvin's solution for a vertical point load acting within an infinite elastic mass*
This solution is in cylindrical coordinates (r, θ, z). For $\theta = 0$, we note $R^2 = r^2 + z^2$. The point load P is applied at the origin of the coordinate system and it is parallel to the z-axis.

The solution for the stresses is:

$$\sigma_{rr} = \frac{P}{8\pi(1-\nu)} \frac{r}{R^3} \left[\frac{3r^2}{R^2} - (1-2\nu) \right] \tag{3.149}$$

$$\sigma_{\theta\theta} = -\frac{P(1-2\nu)}{8\pi(1-\nu)} \frac{z}{R^3}$$

$$\sigma_{zz} = \frac{P}{8\pi(1-\nu)} \left[\frac{3z^3}{R^5} + \frac{(1-2\nu)z}{R^3} \right]$$

$$\sigma_{rz} = \frac{P}{8\pi(1-\nu)} \frac{r}{R^3} \left[\frac{3z^2}{R^2} + (1-2\nu) \right]$$

$$\sigma_{r\theta} = 0$$

$$\sigma_{z\theta} = 0$$

The solution for the displacements is:

$$u_r = -\frac{P(1+\nu)}{8\pi(1-\nu)E} \frac{r\,z}{R^3} \tag{3.150}$$

$$\theta = \frac{P}{8\pi(1-\nu)E} \frac{2(1+\nu)z}{R^3}$$

$$u_z = -\frac{P(1+\nu)}{8\pi(1-\nu)ER} \left(3 - 4\nu + \frac{r^2}{R^2} \right)$$

$$\tag{3.151}$$

3.5.3.2 *Boussinesq's solution for a vertical point load acting on the surface of a semi-infinite mass*

This solution is in cylindrical coordinates (r, θ, z). For $\theta = 0$, we note $R^2 = r^2 + z^2$. The point load P is applied at the origin of the coordinate system and it is parallel to the z-axis. The solution for the stresses is:

$$\sigma_{rr} = -\frac{P}{2\pi R^2} \left[-\frac{3r^2 z}{R^3} + \frac{(1-2\nu)R}{R+z} \right] \tag{3.152}$$

$$\sigma_{\theta\theta} = -\frac{(1-2\nu)P}{2\pi R^2} \left[\frac{r}{R} - \frac{R}{R+z} \right]$$

$$\sigma_{zz} = \frac{3Pz^3}{2\pi R^5}$$

$$\sigma_{rz} = \frac{3Prz^2}{2\pi R^5}$$

$$\sigma_{r\theta} = 0$$

$$\sigma_{z\theta} = 0$$

The solution for the displacements is:

$$u_r = \frac{P(1+\nu)}{2\pi ER}\left[\frac{rz}{R^2} - \frac{(1-2\nu)r}{R+z}\right] \tag{3.153}$$

$$\theta = \frac{(1+\nu)Pz}{\pi R^3}$$

$$u_z = \frac{P(1+\nu)}{2\pi ER}\left[2(1-\nu) + \frac{z^2}{R^2}\right]$$

3.5.3.3 Cerutti's solution for a horizontal point load acting along the surface of a semi-infinite mass

This solution is in Cartesian coordinates. The point load P is applied at the origin of the coordinate system and it is parallel to the x-axis. We note $R^2 = x^2 + y^2 + z^2$. The solution for the stresses is:
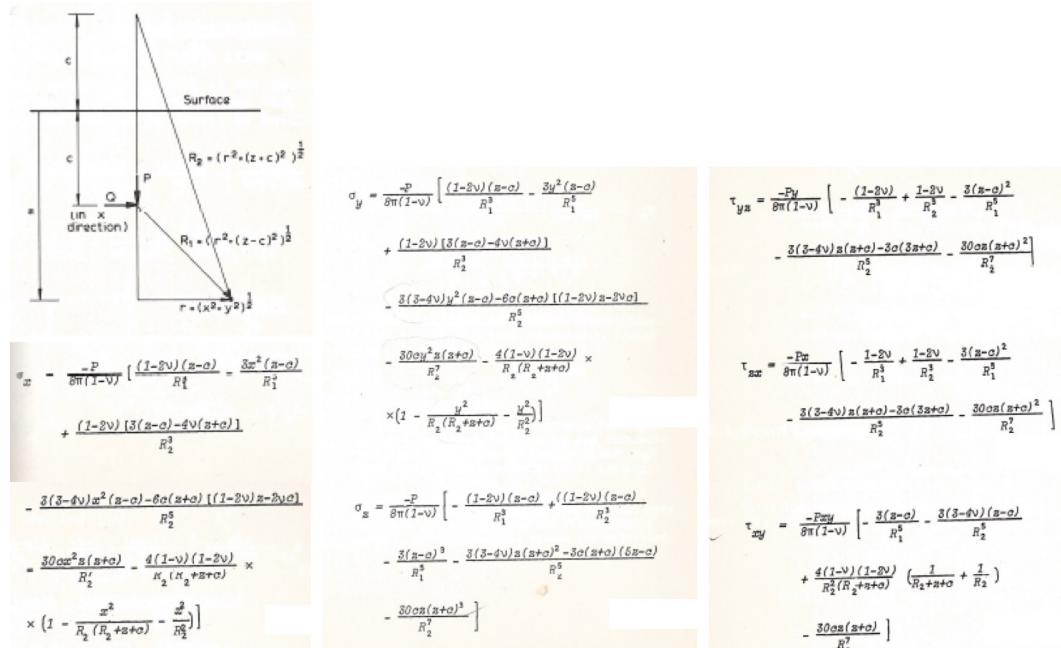
$$\sigma_{xx} = -\frac{Px}{2\pi R^3}\left[-\frac{3x^2}{R^2} + \frac{(1-2\nu)}{(R+z)^2}\left(R^2 - y^2 - \frac{2Ry^2}{R+z}\right)\right] \tag{3.154}$$

$$\sigma_{yy} = -\frac{Px}{2\pi R^3}\left[-\frac{3y^2}{R^2} + \frac{(1-2\nu)}{(R+z)^2}\left(3R^2 - x^2 - \frac{2Rx^2}{R+z}\right)\right]$$

$$\sigma_{zz} = \frac{3Pxz^2}{2\pi R^5}$$

$$\sigma_{xy} = -\frac{Py}{2\pi R^3}\left[-\frac{3x^2}{R^2} + \frac{(1-2\nu)}{(R+z)^2}\left(-R^2 + x^2 + \frac{2Rx^2}{R+z}\right)\right]$$

$$\sigma_{xz} = \frac{3Px^2z}{2\pi R^5}$$

$$\sigma_{yz} = \frac{3Pxyz}{2\pi R^5}$$

The solution for the displacements is:
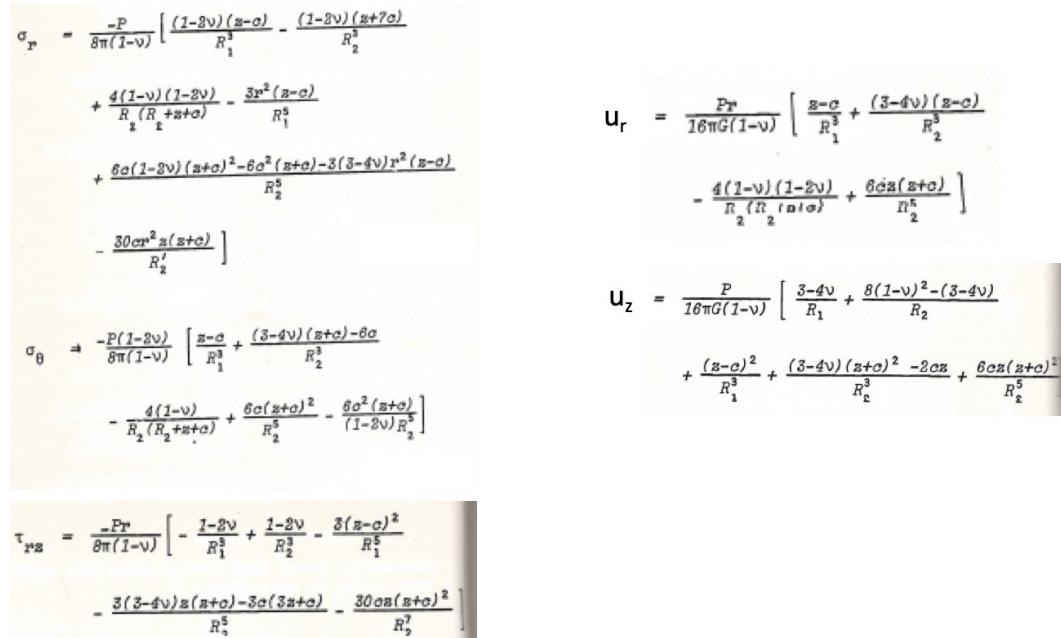
$$u_x = \frac{P(1+\nu)}{2\pi ER}\left[1 + \frac{x^2}{R^2} + (1-2\nu)\left(\frac{R}{R+z} - \frac{x^2}{(R+z)^2}\right)\right] \tag{3.155}$$

$$u_y = \frac{P(1+\nu)}{2\pi ER}\left[\frac{xy}{R^2} - \frac{(1-2\nu)xy}{(R+z)^2}\right]$$

$$u_z = \frac{P(1+\nu)}{2\pi ER}\left[\frac{xy}{R^2} + \frac{(1-2\nu)x}{(R+z)}\right]$$

3.5.3.4 Mindlin's solution for a vertical point load acting beneath the surface of a semi-infinite mass

The solution to this problem is shown in Figure 3.14 in Cartesian coordinates and in Figure 3.15 in cylindrical coordinates.

$$\sigma_y = \frac{-P}{8\pi(1-\nu)}\left[\frac{(1-2\nu)(z-c)}{R_1^3} - \frac{3y^2(z-c)}{R_1^5}\right.$$
$$+ \frac{(1-2\nu)[3(z-c)-4\nu(z+c)]}{R_2^3}$$
$$- \frac{3(3-4\nu)y^2(z-c)-6c(z+c)[(1-2\nu)z-2\nu c]}{R_2^5}$$
$$- \frac{30cy^2 z(z+c)}{R_2^7} - \frac{4(1-\nu)(1-2\nu)}{R_2(R_2+z+c)} \times$$
$$\times \left(1 - \frac{y^2}{R_2(R_2+z+c)} - \frac{y^2}{R_2^2}\right)\bigg]$$

$$\sigma_x = \frac{-P}{8\pi(1-\nu)}\left[\frac{(1-2\nu)(z-c)}{R_1^3} - \frac{3x^2(z-c)}{R_1^5}\right.$$
$$+ \frac{(1-2\nu)[3(z-c)-4\nu(z+c)]}{R_2^3}$$
$$- \frac{3(3-4\nu)x^2(z-c)-6c(z+c)[(1-2\nu)z-2\nu c]}{R_2^5}$$
$$- \frac{30cx^2 z(z+c)}{R_2^7} - \frac{4(1-\nu)(1-2\nu)}{R_2(R_2+z+c)} \times$$
$$\times \left(1 - \frac{x^2}{R_2(R_2+z+c)} - \frac{x^2}{R_2^2}\right)\bigg]$$

$$\sigma_z = \frac{-P}{8\pi(1-\nu)}\left[-\frac{(1-2\nu)(z-c)}{R_1^3} + \frac{((1-2\nu)(z-c)}{R_2^3}\right.$$
$$- \frac{3(z-c)^3}{R_1^5} - \frac{3(3-4\nu)z(z+c)^2-3c(z+c)(5z-c)}{R_2^5}$$
$$- \frac{30cz(z+c)^3}{R_2^7}\bigg]$$

$$\tau_{yz} = \frac{-Py}{8\pi(1-\nu)}\left[-\frac{(1-2\nu)}{R_1^3} + \frac{1-2\nu}{R_2^3} - \frac{3(z-c)^2}{R_1^5}\right.$$
$$- \frac{3(3-4\nu)z(z+c)-3c(3z+c)}{R_2^5} - \frac{30cz(z+c)^2}{R_2^7}\bigg]$$

$$\tau_{zx} = \frac{-Px}{8\pi(1-\nu)}\left[-\frac{1-2\nu}{R_1^3} + \frac{1-2\nu}{R_2^3} - \frac{3(z-c)^2}{R_1^5}\right.$$
$$- \frac{3(3-4\nu)z(z+c)-3c(3z+c)}{R_2^5} - \frac{30cz(z+c)^2}{R_2^7}\bigg]$$

$$\tau_{xy} = \frac{-Pxy}{8\pi(1-\nu)}\left[-\frac{3(z-c)}{R_1^5} - \frac{3(3-4\nu)(z-c)}{R_2^5}\right.$$
$$+ \frac{4(1-\nu)(1-2\nu)}{R_2^2(R_2+z+c)}\left(\frac{1}{R_2+z+c}+\frac{1}{R_2}\right)$$
$$- \frac{30cz(z+c)}{R_2^7}\bigg]$$

Figure 3.14   Mindlin's solution for a vertical point load acting beneath the surface of a semi-infinite mass. Cartesian coordinates. Image taken from [17].

$$\sigma_r = \frac{-P}{8\pi(1-\nu)}\left[\frac{(1-2\nu)(z-c)}{R_1^3} - \frac{(1-2\nu)(z+7c)}{R_2^3}\right.$$
$$+ \frac{4(1-\nu)(1-2\nu)}{R_2(R_2+z+c)} - \frac{3r^2(z-c)}{R_1^5}$$
$$+ \frac{6c(1-2\nu)(z+c)^2-6c^2(z+c)-3(3-4\nu)r^2(z-c)}{R_2^5}$$
$$- \frac{30cr^2 z(z+c)}{R_2^7}\bigg]$$

$$\sigma_\theta = \frac{-P(1-2\nu)}{8\pi(1-\nu)}\left[\frac{z-c}{R_1^3} + \frac{(3-4\nu)(z+c)-6c}{R_2^3}\right.$$
$$- \frac{4(1-\nu)}{R_2(R_2+z+c)} + \frac{6c(z+c)^2}{R_2^5} - \frac{6c^2(z+c)}{(1-2\nu)R_2^5}\bigg]$$

$$\tau_{rz} = \frac{-Pr}{8\pi(1-\nu)}\left[-\frac{1-2\nu}{R_1^3} + \frac{1-2\nu}{R_2^3} - \frac{3(z-c)^2}{R_1^5}\right.$$
$$- \frac{3(3-4\nu)z(z+c)-3c(3z+c)}{R_2^5} - \frac{30cz(z+c)^2}{R_2^7}\bigg]$$

$$u_r = \frac{Pr}{16\pi G(1-\nu)}\left[\frac{z-c}{R_1^3} + \frac{(3-4\nu)(z-c)}{R_2^3}\right.$$
$$- \frac{4(1-\nu)(1-2\nu)}{R_2(R_2+z+c)} + \frac{6cz(z+c)}{R_2^5}\bigg]$$

$$u_z = \frac{P}{16\pi G(1-\nu)}\left[\frac{3-4\nu}{R_1} + \frac{8(1-\nu)^2-(3-4\nu)}{R_2}\right.$$
$$+ \frac{(z-c)^2}{R_1^3} + \frac{(3-4\nu)(z+c)^2-2cz}{R_2^3} + \frac{6cz(z+c)^2}{R_2^5}\bigg]$$

Figure 3.15   Mindlin's solution for a vertical point load acting beneath the surface of a semi-infinite mass. Cylindrical coordinates. Image taken from [17].

3.5.3.5 Mindlin's solution for a horizontal point load acting beneath the surface of a semi-infinite mass

The solution to this problem is shown in Figure 3.16 in Cartesian coordinates.

$$\sigma_{xx} = \frac{-Qx}{8\pi(1-\nu)}\left[-\frac{(1-2\nu)}{R_1^3} + \frac{(1-2\nu)(5-4\nu)}{R_2^3} - \frac{3x^2}{R_1^5}\right.$$
$$-\frac{3(3-4\nu)x^2}{R_2^5} - \frac{4(1-\nu)(1-2\nu)}{R_2(R_2+z+c)^2} \times$$
$$\times\left(3 - \frac{x^2(3R_2+z+c)}{R_2^2(R_2+z+c)}\right)$$
$$\left. + \frac{6c}{R_2^5}\left(3c - (3-2\nu)(z+c) + \frac{5x^2z}{R_2^2}\right)\right]$$

$$\sigma_{yy} = \frac{-Qx}{8\pi(1-\nu)}\left[\frac{(1-2\nu)}{R_1^3} + \frac{(1-2\nu)(3-4\nu)}{R_2^3} - \frac{3y^2}{R_1^5}\right.$$
$$-\frac{3(3-4\nu)y^2}{R_2^5} - \frac{4(1-\nu)(1-2\nu)}{R_2(R_2+z+c)^2} \times$$
$$\times\left(1 - \frac{y^2(3R_2+z+c)}{R_2^2(R_2+z+c)}\right)$$
$$\left. + \frac{6c}{R_2^5}\left(c - (1-2\nu)(z+c) + \frac{5y^2z}{R_2^2}\right)\right]$$

$$\sigma_{zz} = \frac{-Qx}{8\pi(1-\nu)}\left[\frac{(1-2\nu)}{R_1^3} - \frac{(1-2\nu)}{R_2^3} - \frac{3(z-c)^2}{R_1^5}\right.$$
$$-\frac{3(3-4\nu)(z+c)^2}{R_2^5}$$
$$\left. + \frac{6c}{R_2^5}\left(c + (1-2\nu)(z+c) + \frac{5z(z+c)^2}{R_2^2}\right)\right]$$

$$\sigma_{yz} = \frac{-Qxy}{8\pi(1-\nu)}\left[-\frac{3(z-c)}{R_1^5} - \frac{3(3-4\nu)(z+c)}{R_2^5}\right.$$
$$\left. + \frac{6c}{R_2^5}\left(1 - 2\nu + \frac{5z(z+c)}{R_2^2}\right)\right]$$

$$\sigma_{zx} = \frac{-Q}{8\pi(1-\nu)}\left[-\frac{(1-2\nu)(z-c)}{R_1^3} + \frac{(1-2\nu)(z-c)}{R_2^3}\right.$$
$$-\frac{3x^2(z-c)}{R_1^5} - \frac{3(3-4\nu)x^2(z+c)}{R_2^5}$$
$$\left. - \frac{6c}{R_2^5}\left(z(z+c)-(1-2\nu)x^2 - \frac{5x^2z(z+c)}{R_2^2}\right)\right]$$

$$\sigma_{xy} = \frac{-Qy}{8\pi(1-\nu)}\left[-\frac{(1-2\nu)}{R_1^3} + \frac{(1-2\nu)}{R_2^3} - \frac{3x^2}{R_1^5}\right.$$
$$-\frac{3(3-4\nu)x^2}{R_2^5} - \frac{4(1-\nu)(1-2\nu)}{R_2(R_2+z+c)^2} \times$$
$$\times\left(1 - \frac{x^2(3R_2+z+c)}{R_2^2(R_2+z+c)}\right) - \frac{6cz}{R_2^5}\left(1 - \frac{5x^2}{R_2^2}\right)\right]$$

$$u_x = \frac{Q}{16\pi G(1-\nu)}\left[\frac{(3-4\nu)}{R_1} + \frac{1}{R_2} + \frac{x^2}{R_1^3} + \frac{(3-4\nu)x^2}{R_2^3}\right.$$
$$+ \frac{2cz}{R_2^3}\left(1 - \frac{3x^2}{R_2^2}\right) + \frac{4(1-\nu)(1-2\nu)}{R_2+z+c} \times$$
$$\left. \times\left(1 - \frac{x^2}{R_2(R_2+z+c)}\right)\right]$$

$$u_y = \frac{Qxy}{16\pi G(1-\nu)}\left[\frac{1}{R_1^3} + \frac{(3-4\nu)}{R_2^3} - \frac{6cz}{R_2^5}\right.$$
$$\left. - \frac{4(1-\nu)(1-2\nu)}{R_2(R_2+z+c)^2}\right]$$

$$u_z = \frac{Qx}{16\pi G(1-\nu)}\left[\frac{z-c}{R_1^3} + \frac{(3-4\nu)(z-c)}{R_2^3}\right.$$
$$\left. - \frac{6cz(z+c)}{R_2^5} + \frac{4(1-\nu)(1-2\nu)}{R_2(R_2+z+c)}\right]$$

Figure 3.16   Mindlin's solution for a horizontal point load acting beneath the surface of a semi-infinite mass. Cartesian coordinates. Image taken from [17].

PROBLEMS
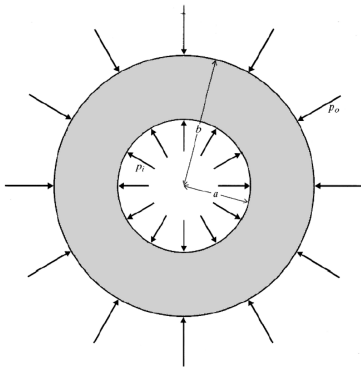
3.1   Prove the Navier's equations of motion in Cartesian coordinates:

$$\lambda\left(\frac{\partial^2 u}{\partial x^2} + \frac{\partial^2 v}{\partial x\partial y} + \frac{\partial^2 w}{\partial x\partial z}\right) + G\left(\frac{\partial^2 u}{\partial x^2} + \frac{\partial^2 v}{\partial x\partial y} + \frac{\partial^2 w}{\partial x\partial z} + \frac{\partial^2 u}{\partial x^2} + \frac{\partial^2 u}{\partial y^2} + \frac{\partial^2 u}{\partial z^2}\right) + \rho f_x = 0$$

$$\lambda\left(\frac{\partial^2 u}{\partial x\partial y} + \frac{\partial^2 v}{\partial y^2} + \frac{\partial^2 w}{\partial y\partial z}\right) + G\left(\frac{\partial^2 u}{\partial x\partial y} + \frac{\partial^2 v}{\partial y^2} + \frac{\partial^2 w}{\partial y\partial z} + \frac{\partial^2 v}{\partial x^2} + \frac{\partial^2 v}{\partial y^2} + \frac{\partial^2 v}{\partial z^2}\right) + \rho f_y = 0$$

$$\lambda\left(\frac{\partial^2 u}{\partial x\partial z} + \frac{\partial^2 v}{\partial y\partial z} + \frac{\partial^2 w}{\partial z^2}\right) + G\left(\frac{\partial^2 u}{\partial z\partial y} + \frac{\partial^2 v}{\partial y\partial z} + \frac{\partial^2 w}{\partial z^2} + \frac{\partial^2 w}{\partial x^2} + \frac{\partial^2 w}{\partial y^2} + \frac{\partial^2 w}{\partial z^2}\right) + \rho f_z = 0$$

3.2   We consider a pressurized circular cavity of radius a subjected to a uniform state of stress at a distance b from the center, as shown in Figure 3.17. We focus on a 2D elasticity problem (plane strain or plane stress). Find the state of stress around the cavity, between a and b, by solving the biharmonic equation.

Figure 3.17 Circular pressurized cavity subject to isotropic stress in the far field. Picture taken from [4].

3.3 Show that in Cartesian coordinates, the stress solution can be expressed in terms of two complex potentials $\phi(z)$ and $\psi(z) = \chi'(z)$, as follows:

$$\sigma_{xx} + \sigma_{yy} = \frac{\partial^2 U}{\partial x^2} + \frac{\partial^2 U}{\partial y^2} = 2\left[\phi'(z) + \overline{\phi'(z)}\right] = 2\mathcal{R}\left[\phi'(z)\right]$$

$$\sigma_{yy} - \sigma_{xx} + 2i\sigma_{xy} = \frac{\partial^2 U}{\partial x^2} - \frac{\partial^2 U}{\partial y^2} - 2i\frac{\partial^2 U}{\partial x \partial y} = 2\left[\bar{z}\phi''(z) + \psi'(z)\right]$$

3.4 At a depth of 750 m, a 10-m diameter circular tunnel is driven in rock having a unit weight of 26 kN/m³ and uniaxial compressive and tensile strengths of 80 MPa and 3 MPa, respectively. Will the strength of the rock on the tunnel boundary be exceeded if: (i) K=0.3? (ii) K=2?
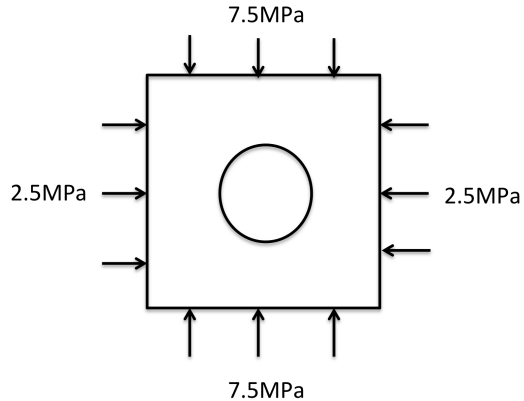
3.5 A gold-bearing quartz vein, 2 m thick and dipping 90°, is to be exploited by a small-cut-and-fill stoping operation. The mining is to take place at a depth of 800 m, and the average unit weight of the granite host rock above this level is 29 kN/m³. The strike of the vein is parallel to the intermediate stress, and the major principal stress is horizontal with a magnitude of 37 MPa. The uniaxial compressive strength of the vein material is 218 MPa (in absolute value), and the tensile strength of the host rock is 5 MPa (in absolute value). What is the maximum permissible stope height before failure occurs?

3.6 In Figure 3.18, the uniaxial rock compressive strength is 50 MPa and the corresponding crack initiation stress is $\sigma_c = 16$ MPa. Calculate the extent of the failure zone in tension and compression.
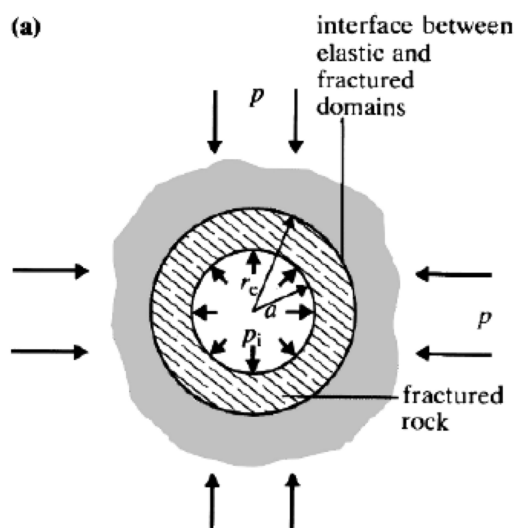
3.7 Provided the boundary conditions in Figure 3.19, and knowing that the following purely frictional strength criterion holds: $\sigma_1 = d\,\sigma_3 + C_0$, $C_0 = 0$, calculate: (i) the extent of the damaged zone (r_e), (ii) the pressure in the damaged zone (p_1).

3.8 In Figure 3.20: Does the plane of weakness affect the elastic stress distribution? Under which conditions does the rock mass slip along the plane of weakness?
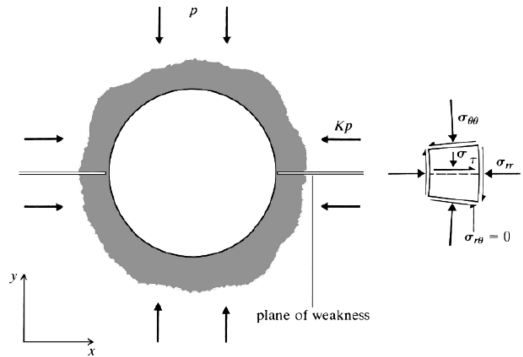
3.9 In Figure 3.21: Does the plane of weakness affect the elastic stress distribution? Under which conditions does the rock mass slip along the plane of weakness?
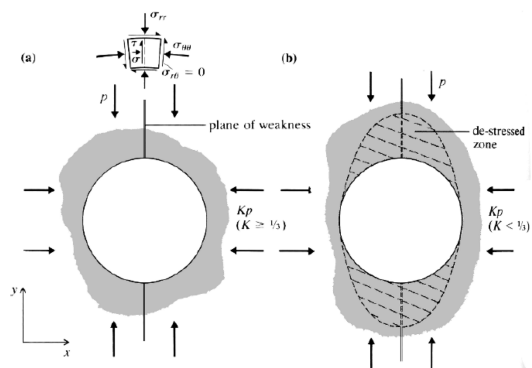
**Figure 3.18**   Cavity studied in Problem 3.6.

**Figure 3.19**   Cavity studied in Problem 3.7. [4]
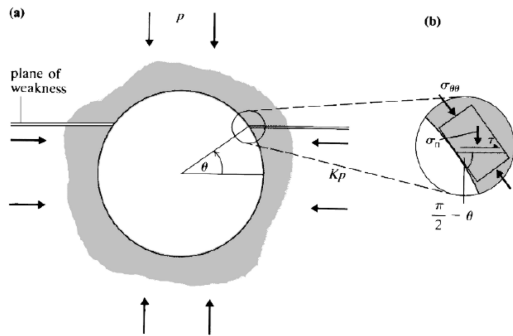
**Figure 3.20**   Cavity studied in Problem 3.8. [4]
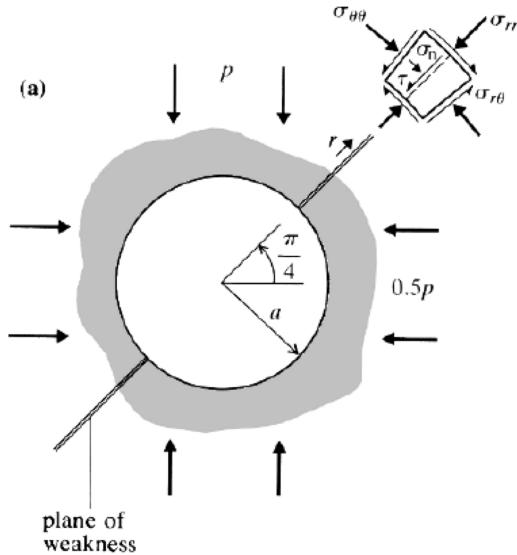
Figure 3.21   Cavity studied in Problem 3.9. [4]

3.10   In Figure 3.22: Does the plane of weakness affect the elastic stress distribution? Under which conditions does the rock mass slip along the plane of weakness?

Figure 3.22   Cavity studied in Problem 3.10. [4]

3.11   In Figure 3.23: Does the plane of weakness affect the elastic stress distribution? Under which conditions does the rock mass slip along the plane of weakness?
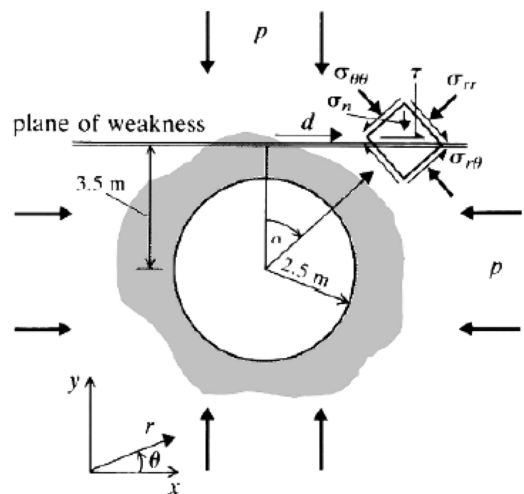
Figure 3.23   Cavity studied in Problem 3.11. [4]

3.12   In Figure 3.24: Does the plane of weakness affect the elastic stress distribution? Under which conditions does the rock mass slip along the plane of weakness?
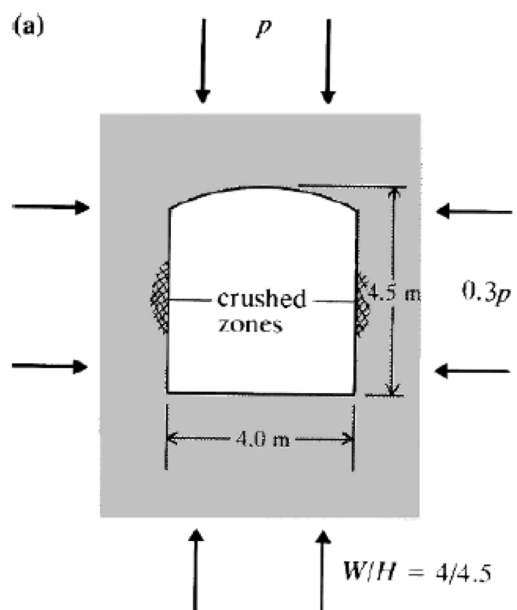
3.13   Considering Figure 3.25: How can we improve the design in order to avoid compressive failure at the sidewalls?

3.14   Considering Figure 3.26: What are the stresses at the sidewall and at the crown?
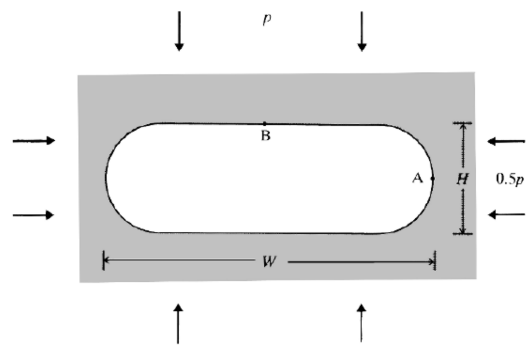
**3.15**   Considering Figure 3.27: What are is the stress at edge A?
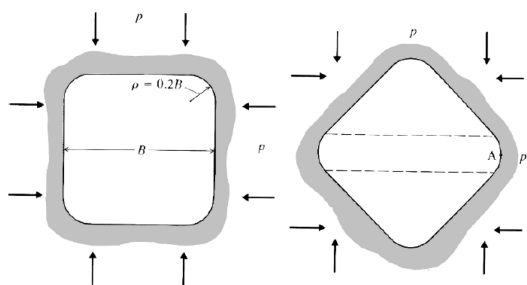
Figure 3.24   Cavity studied in Problem 3.12. [4]


**Figure 3.25**   Cavity studied in Problem 3.13. [4]
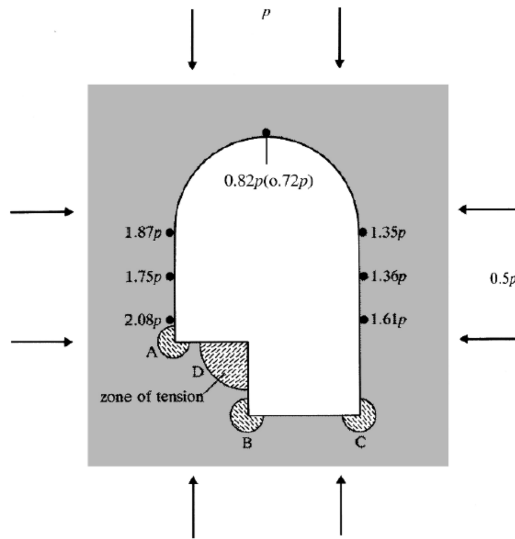
**Figure 3.26** Cavity studied in Problem 3.14. [4]

Figure 3.27 Cavity studied in Problem 3.15. [4]

3.16 Considering Figure 3.28: Comment on the boundary stresses at the crown, at the sidewall, and at edges A, B, C and D.


Figure 3.28 Cavity studied in Problem 3.16. [4]

3.17 Consider Figure 3.29. We give:
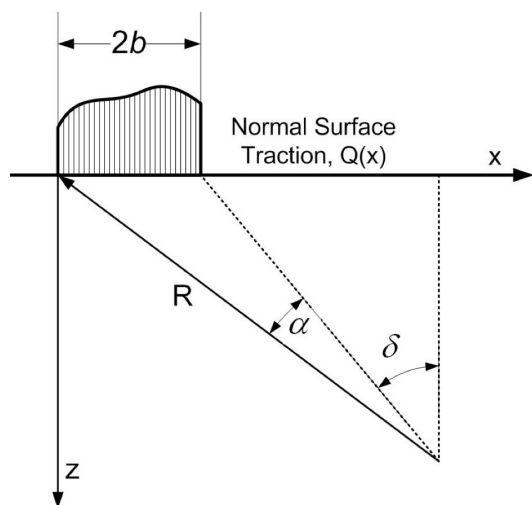
▪ Solution for the line load:

$$\sigma_{xx} = \frac{2P}{\pi} \frac{x^2 z}{R^4}, \quad \sigma_{zz} = \frac{2P}{\pi} \frac{z^3}{R^4}, \quad \sigma_{xz} = \frac{2P}{\pi} \frac{z^2 x}{R^4}$$

▪ Solution for the footing:

$$\sigma_{zz} = \frac{Q}{\pi} \left(a + \sin a \cos(a + 2\delta) \right)$$

1. Using the solution for the stresses (σ_{xx}, σ_{zz}, σ_{xz}) under a line load of intensity P (force/unit length) acting normal to the surface, obtain the stresses due to a strip footing of width $2a$ with an applied surface traction $Q(x)$. Write specific solutions for the case when $Q = Q_0$ (i.e. for surface constant loading).

2. Show that the loci of points with σ_1 = constant (or σ_3 = constant) describe a circle.

3. What is the locus of $q = 0.5(\sigma_1 - \sigma_3)$=constant? The value of q represents the maximum shear stress acting at a point. Show that $q_{max} = Q/\pi$.

**Figure 3.29**   Distributed load studied in Problem 3.17. [2]

CHAPTER 4

FINITE ELEMENT METHOD IN LINEAR ELASTICITY

4.1 Variational formulation for 1 variable in 1D

4.1.1 Typical governing equation for 1 variable in 1D

In the following, we will explain the principle of the variational method by considering a 1D problem that needs to be solved for only one dependent variable, the function $u(x)$. Many 1D problems of engineering are governed by this differential equation:

$$-\frac{d}{dx}\left[a\frac{du}{dx}\right] = q, \qquad 0 < x < L \tag{4.1}$$

For example, the axial deformation of a bar subjected to an axial load is determined by the following governing equation:

$$-\frac{d}{dx}\left(EA\frac{du}{dx}\right) = f_{ext} \tag{4.2}$$

The differential equation that describe the buckling of a double-pin ended column is:

$$EI_z\frac{d^2y}{dx^2} + P = 0 \tag{4.3}$$

The governing equation for a 1D Newtonian fluid flow is:

$$\mu_w\frac{d^2v_{wx}}{dy^2} = \frac{dp_w}{dx}, \quad \mu_w\frac{d^2v_{wx}}{dy^2} = f(y) \tag{4.4}$$

For conductive heat transfer, in 2D, the governing equations are:

$$\begin{cases} q_x(x,y) = -k_T \frac{\partial^2 T}{\partial x^2} \\[3mm] q_y(x,y) = -k_T \frac{\partial^2 T}{\partial y^2} \end{cases} \tag{4.5}$$

4.1.2   Principle of the variational formulation

The strong formulation of a problem is given by a governing equation and boundary conditions. The variational formulation is a "weak formulation" of the problem, obtained by: (i) Writing the weighted integral statement; (ii) Performing an integration by parts; (iii) Applying the boundary conditions. For the typical governign equation given in Equation 4.1, the weighted integral statement is:

$$\forall w \sim \delta u, \quad \int_0^L w(x) \left[-\frac{d}{dx}\left[a\frac{du}{dx}\right] - q \right] dx = 0 \tag{4.6}$$

in which w is a so-called weight function, which has the smae physical dimension as a small variation of u. An integration by parts is then performed to balance the orders of the derivtives between w and u. For example, if a is constant:

$$\forall w \sim \delta u, \quad -\int_0^L \frac{d}{dx}\left(w(x)\left[a\frac{du}{dx}\right]\right) dx + \int_0^L \frac{dw}{dx}\left[a\frac{du}{dx}\right] dx + \int_0^L w(x)q(x)dx = 0 \tag{4.7}$$

and the we obtain:

$$\int_0^L \frac{dw}{dx}\left[a\frac{du}{dx}\right] dx + \int_0^L w(x)q(x)dx - \left(w(x)\left[a\frac{du}{dx}\right]\right)_{x=L} + \left(w(x)\left[a\frac{du}{dx}\right]\right)_{x=0} = 0 \tag{4.8}$$

Assume that the boundary condition at the origin is $u(0) = \bar{u}$. Then $\delta u(0) = 0$ since $u(0)$ is fixed. Then, $w(0) = 0$. It follows that the essential boundary conditions are automatically satisfied in the variational formulation. In the example case studied here, the variational formulation becomes:

$$\forall w \sim \delta u, \quad \int_0^L \frac{dw}{dx}\left[a\frac{du}{dx}\right] dx + \int_0^L w(x)q(x)dx - \left(w(x)\left[a\frac{du}{dx}\right]\right)_{x=L} = 0 \tag{4.9}$$

If the dependent variable u is not known at the other end of the domain (at $x = L$), then that means that a natural boundary condition is applied at L. In that case, $w(L) \neq 0$ and the value of $\left[a\frac{du}{dx}\right]$ is known at L. The variable $\left[a\frac{du}{dx}\right]$ is often noted Q and it is called secondary variable (as opposed to the dependent variable, which is called primary variable). The primary and secondary variables are work-conjugate. For example, if u is a displacement, Q is a force. If u is a temperature, Q is a heat flux.

4.2   Building a FEM model for 1 variable in 1D

4.2.1   Space discretization

The first step in building a FEM model is to discretize the domain of study into subdomains called elements (in the previous example, that would mean to divide the domain $[0, L]$

in small segments). Space discretization makes it easier to compute the integrals of the variational formulation, because integrating over a small elementary domain of regular shape can be done with simple calculations that can be parallelized. For elements of same shape, the formulas to calcualte the integrals are the same, which accelerates even more the computations. The choice of the number of elements in different parts of the domain depends on the number of objects to mode, the number of constitutive materials in the domain, the load type and the boundary conditinos. The discretized domain is called a mesh. The mesh can be refied by increasing the number of elements or by calculating the approximate solution of the problem on each element with interpolation functions of higher order (we will come back to the concept of interpolation later).

4.2.2 Elementary equations: Ritz method

The Finite Element Method is an approximation based on the interpolation of nodal degrees of freedom:

$$U_N(x) = \sum_{j=1}^{M} c_j \Phi_j(x) + \sum_{i=1}^{K} u_i \Psi_i(x), \quad u_i = u(x_i) \tag{4.10}$$

The FEM can be based on the Weighted Integral Statement (e.g., Galerkin Method) or on the Weak Formulation (e.g., Ritz Method). In this course, we will use the Ritz Method, in which the approximation is sought in the form:

$$U_N(x) = \sum_{j=1}^{N} u_i \Psi_j(x), \quad u_i = u(x_j) \tag{4.11}$$

Most often the Ψ_i functions will be polynomials. If the maximal order of the derivative of the dependent variable is n:

$$E^n(u, \mathbf{x}) = f(\mathbf{x}) \tag{4.12}$$

then, p integrations by parts on the Weighted Integral Statement lead to ($p < n$):

$\forall w \sim \delta u,$

$$(-1)^p \int_\Omega \frac{\partial^p w(\mathbf{x})}{\partial \mathbf{x}^p} E^{n-p}(u, \mathbf{x}) d\Omega \tag{4.13}$$

$$= \int_\Omega w(\mathbf{x}) f(\mathbf{x}) d\Omega - \Sigma_{k=1}^p (-1)^k \int_\Gamma \frac{\partial^{k-1} w(\mathbf{x})}{\partial \mathbf{x}^{k-1}} \widehat{Q}_{n-k} ds$$

Ritz method is an approximation method, in which in each element, the solution $u(x)$ is sought in the form:

$$u(\mathbf{x}) \simeq U_N(\mathbf{x}) = \sum_{j=1}^{N} u_i \Psi_j(\mathbf{x}) \tag{4.14}$$

...applied on the weak formulation of the problem...

$\forall w \sim \delta u,$

$$(-1)^p \int_\Omega \frac{\partial^p w(\mathbf{x})}{\partial \mathbf{x}^p} E^{n-p}(U_N, \mathbf{x}) d\Omega \tag{4.15}$$

$$= \int_\Omega w(\mathbf{x}) f(\mathbf{x}) d\Omega - \Sigma_{k=1}^p (-1)^k \int_\Gamma \frac{\partial^{k-1} w(\mathbf{x})}{\partial \mathbf{x}^{k-1}} \widehat{Q}_{n-k} ds$$

instead of the Weighted Integral Statement:

$$\forall i = 1..N,$$

$$\int_\Omega w_i(\mathbf{x}) E^n(U_N, \mathbf{x}) d\Omega \;=\; \int_\Omega w_i(\mathbf{x}) f(\mathbf{x}) d\Omega \tag{4.16}$$

In each element, there are N unknowns (N nodal values u_j). To solve for these unknowns, one needs N independent equations. We can obtain N linearly independent equations by writing the variational formulation with N linearly independent weight functions. We note that:

$$w(\mathbf{x}) \sim \delta u(\mathbf{x}) \simeq \delta U_N(\mathbf{x}) = \Sigma_{j=1}^N \delta u_j\, \Psi_j(\mathbf{x}) \tag{4.17}$$

A simple set of N weight functions w_i is thus:

$$\forall i = 1..N, \quad w_i(\mathbf{x}) \;=\; \Psi_i(\mathbf{x}) \tag{4.18}$$

In Ritz method, the family of weight functions is the same as the family of interpolation functions. For an operator E that is linear in u:

$$\forall i = 1..N,$$

$$\Sigma_{j=1}^N \left[(-1)^p \int_\Omega \frac{\partial^p \Psi_i(\mathbf{x})}{\partial \mathbf{x}^p} E^{n-p}(\Psi_j, \mathbf{x}) d\Omega \right] u_j \tag{4.19}$$

$$= \int_\Omega \Psi_i(\mathbf{x}) f(\mathbf{x}) d\Omega \;-\; \Sigma_{k=1}^p (-1)^k \int_\Gamma \frac{\partial^{k-1} \Psi_i(\mathbf{x})}{\partial \mathbf{x}^{k-1}} \widehat{Q}_{n-k} ds$$

In a matrix form:

$$[A]\{c\} \;=\; \{F\} \tag{4.20}$$

with:

$$A_{ij} \;=\; \left[(-1)^p \int_\Omega \frac{\partial^p \Psi_i(\mathbf{x})}{\partial \mathbf{x}^p} E^{n-p}(\Psi_j, \mathbf{x}) d\Omega \right] \tag{4.21}$$

$$F_i \;=\; \int_\Omega \Psi_i(\mathbf{x}) f(\mathbf{x}) d\Omega - \Sigma_{k=1}^p (-1)^k \int_\Gamma \frac{\partial^{k-1} \Psi_i(\mathbf{x})}{\partial \mathbf{x}^{k-1}} \widehat{Q}_{n-k} ds$$

If $E^n \;=\; cst\, \frac{\partial^n}{\partial \mathbf{x}^n}$, then $[A]$ is symmetric if p=n-p, which requires n=2p (even number), i.e. "self-adjoint" equations.

Let us take the example of the following (typical) 1D differential equation, which we want to solve for $u(x)$:

$$-\frac{d}{dx}\left[a\frac{du}{dx} \right] + cu(x) \;=\; f(x) \tag{4.22}$$

The weighted integral statement on an element $[x_a,\, x_b]$ is:

$$\forall w = \delta u, \quad \int_{x_a}^{x_b} w(x)\left[-\frac{d}{dx}\left[a\frac{du}{dx} \right] + cu(x) - f(x) \right] dx \;=\; 0 \tag{4.23}$$

The integration by parts gives:

$$\int_{x_a}^{x_b} a\frac{dw(x)}{dx}\frac{du}{dx}dx + \int_{x_a}^{x_b} cw(x)u(x)dx \tag{4.24}$$

$$-\int_{x_a}^{x_b} w(x)f(x)dx \;-\; w(x_b)\left[a\frac{du}{dx} \right]_{x=x_b} + w(x_a)\left[a\frac{du}{dx} \right]_{x=x_a} \;=\; 0$$

We now apply the boundary conditions:

- If x_a (respectively x_b) is a boundary, replace $w(x_a)$ or $Q(x_a) = \left[a\frac{du}{dx}\right]_{x=x_a}$ (respectively $w(x_b)$ or $Q(x_b)$) by its value.

- If x_a (respectively x_b) is not a boundary, use the continuity conditions:

  (i) $u(x_a^+) = u(x_a^-)$ (respectively $u(x_b^+) = u(x_b^-)$), i.e. the dependent variable at a node shared by several elements has the same value on all elements at that node;

  (ii) $Q(x_a^+) = Q(x_a^-)$ (respectively $Q(x_b^+) = Q(x_b^-)$), i.e. fluxes at a node cancel out.

4.2.3 Interpolation functions

Next, we seek the FEM interpolation functions in the form of (independent) polynomials, so that the approximation of the problem can be expressed as:

$$U_N(x) = c_0 + c_1 x + c_2 x^2 + ... + c_{N-1} x^{N-1} \tag{4.25}$$

Therefore we must ensure that:

$$U_N(x) = \sum_{j=1}^{N} u_j \Psi_j(x) = c_0 + c_1 x + c_2 x^2 + ... + c_{N-1} x^{N-1}, \quad u(x_j) = u_j \tag{4.26}$$

We can find a set of interpolation functions Ψ_j by solving the following system of equations:

$$\forall i = 1..N, \quad u_i = U_N(x_i) = \sum_{j=1}^{N} u_i \Psi_j(x_i) = c_0 + c_1 x_i + c_2 (x_i)^2 + ... + c_{N-1}(x_i)^{N-1} \tag{4.27}$$

In a matrix form:

$$\begin{bmatrix} 1 & x_1 & & (x_1)^{N-1} \\ 1 & x_2 & \cdots & (x_2)^{N-1} \\ \cdots & \cdots & \cdots \cdots & \cdots \\ 1 & x_N & \cdots & (x_N)^{N-1} \end{bmatrix} \begin{Bmatrix} c_0 \\ c_1 \\ \cdots \\ c_{N-1} \end{Bmatrix} = \begin{Bmatrix} u_1 \\ u_2 \\ \cdots \\ u_N \end{Bmatrix} \tag{4.28}$$

The equation:

$$\forall i = 1..N, \quad u_i = U_N(x_i) = \sum_{j=1}^{N} u_i \Psi_j(x_i) = c_0 + c_1 x_i + c_2 (x_i)^2 + ... + c_{N-1}(x_i)^{N-1} \tag{4.29}$$

should hold for any set of values $(u_i)_{i=1..N}$, in particular for (1,0,0, ...,0); (0,1,0,...,0); ... ; (0,0,...,0,1). We deduce from there the interpolation property:

$$\forall i, j = 1..N, \quad \Psi_j(x_i) = \delta_{ij} \tag{4.30}$$

For a constant function $u(x) = U_N(x) = \alpha$, we have: $\alpha = \sum_{j=1}^{N} \alpha \Psi_j(x) = \alpha \sum_{j=1}^{N} \Psi_j(x)$, from which we deduce the partition of unity:

$$\forall x, \quad \sum_{j=1}^{N} \Psi_j(x) = 1 \tag{4.31}$$

For all node located at x_i, $U_N(x_i) = u(x_i)$. In particular true for nodes on the boundary. The approximate solution thus automatically satisfies the boundary conditions. The FEM approximation is designed so that the elementary approximation matches the exact solution $u_i^e = U_N^e(x_i) = U_N(x_i) = u(x_i)$. But in case of approximation errors: $u_i^e = U_N^e(x_i) = U_N(x_i) \simeq u(x_i)$. **Lagrange interpolation functions** are derived from the knowledge of **nodal values of the dependent variables**. For example, for an element $[x_1, x_2]$ with two end nodes at x_1 and x_2, the linear Lagrange polynomials are given by: $N = 2$, $\Psi_1(x_1) = 1$, $\Psi_1(x_2) = 0$, $\Psi_2(x_1) = 0$ and $\Psi_2(x_2) = 1$, which provides:

$$\Psi_1(x) = \frac{x - x_2}{x_1 - x_2}, \quad \Psi_2(x) = \frac{x - x_1}{x_2 - x_1} \tag{4.32}$$

Quadratic Lagrange polynomials allow interpolating between three nodes over the element. The expression of these polynomials are found by solving $\Psi_i(x_j) = \delta_{ij}$ for i,j=1,2,3. When interpolation functions are derived from **nodal values of the dependent variable as well as its derivatives**, **Hermite interpolation functions** are obtained. For example, for an element with two end nodes at x_1 and x_2, cubic Hermite polynomials are given by:

$$\Psi_1(x_1) = 1, \quad \Psi_1'(x_1) = 0, \quad \Psi_1(x_2) = 0, \quad \Psi_1'(x_2) = 0 \tag{4.33}$$

$$\Psi_2(x_1) = 0, \quad \Psi_2'(x_1) = 1, \quad \Psi_2(x_2) = 0, \quad \Psi_2'(x_2) = 0$$

$$\Psi_3(x_1) = 0, \quad \Psi_3'(x_1) = 0, \quad \Psi_3(x_2) = 1, \quad \Psi_3'(x_2) = 0$$

$$\Psi_4(x_1) = 0, \quad \Psi_4'(x_1) = 0, \quad \Psi_4(x_2) = 0, \quad \Psi_4'(x_2) = 1$$

Going back to the previous example:

$$-\frac{d}{dx}\left[a\frac{du}{dx}\right] + cu(x) = f(x) \tag{4.34}$$

$$\int_{x_a}^{x_b} a\frac{dw(x)}{dx}\frac{du}{dx}dx + \int_{x_a}^{x_b} cw(x)u(x)dx = \tag{4.35}$$

$$\int_{x_a}^{x_b} w(x)f(x)dx + w(x_b)\left[a\frac{du}{dx}\right]_{x_b} - w(x_a)\left[a\frac{du}{dx}\right]_{x_a}$$

$$\forall x \in]x_a, x_b[, \quad u_N(x) = \sum_j u_j\Psi_j(x) \tag{4.36}$$

$$\forall i = 1..N, \quad \sum_{j=1}^{N}\left[\int_{x_a}^{x_b} a\frac{d\Psi_i(x)}{dx}\frac{d\Psi_j(x)}{dx}dx + \int_{x_a}^{x_b} c\Psi_i(x)\Psi_j(x)dx\right]u_j \tag{4.37}$$

$$= \int_{x_a}^{x_b} \Psi_i(x)f(x)dx + \Psi_i(x_b)\left[a\frac{du}{dx}\right]_{x_b} - \Psi_i(x_a)\left[a\frac{du}{dx}\right]_{x_a}$$

$$[A]\{u\} = \{F\} + \{Q\} \tag{4.38}$$

$$A_{ij} = \left[\int_{x_a}^{x_b} a \frac{d\Psi_i(x)}{dx} \frac{d\Psi_j(x)}{dx} dx + \int_{x_a}^{x_b} c\Psi_i(x)\Psi_j(x)dx \right]$$

$$F_i = \int_{x_a}^{x_b} \Psi_i(x)f(x)dx \qquad (4.39)$$

$$Q_i = \Psi_i(x_b) \left[a\frac{du}{dx} \right]_{x_b} - \Psi_i(x_a) \left[a\frac{du}{dx} \right]_{x_a}$$

A more general formulation is as follows:

$$E^n(u, x) = f(x) \qquad (4.40)$$

For each element: $[K^e]\{u^e\} = \{F^e\} + \{Q^e\}$, in which $[K^e]\{u^e\}$ is the elementary stiffness matrix, and $\{F^e\} + \{Q^e\}$ are vectors that contain the values of the secondary variable, e.g. the values of forces.

$$K_{ij}^e = \left[(-1)^p \int_\Omega \frac{\partial^p \Psi_i(\mathbf{x})}{\partial \mathbf{x}^p} E^{n-p}(\Psi_j, \mathbf{x})d\Omega \right]$$

$$F_i^e = \int_\Omega \Psi_i(\mathbf{x})f(\mathbf{x})d\Omega \qquad (4.41)$$

$$Q_i^e = -\Sigma_{k=1}^p (-1)^k \int_\Gamma \frac{\partial^{k-1}\Psi_i(\mathbf{x})}{\partial \mathbf{x}^{k-1}} \widehat{Q}_{n-k}^e ds$$

For one element delimited by N_{nd} nodes, assuming that operator E is linear in u:

$$\forall i = 1..N_{nd},$$

$$\Sigma_{j=1}^{N_{nd}} \left[(-1)^p \int_\Omega \frac{\partial^p \Psi_i(\mathbf{x})}{\partial \mathbf{x}^p} E^{n-p}(\Psi_j, \mathbf{x})d\Omega \right] u_j^e$$

$$= \int_\Omega \Psi_i(\mathbf{x})f(\mathbf{x})d\Omega \qquad (4.42)$$

$$-\Sigma_{k=1}^p (-1)^k \int_\Gamma \frac{\partial^{k-1}\Psi_i(\mathbf{x})}{\partial \mathbf{x}^{k-1}} \widehat{Q}_{n-k}^e ds$$

4.2.4 Assembling the elementary equations

The boundary value problem requires solving all the elementary equations $[A]\{u\} = \{F\} + \{Q\}$. These elementary conditions are coupled because of:

- Primary Variables are continuous, i.e. a node may belong to several adjacent elements but the value of the primary variable at that node is the same in all the elements that this node belongs to. The corresponding continuity condition is expressed as:

$$u_I = u_i^{elt\,k} = u_j^{elt\,k+1} = u_n^{elt\,k+2} = u_p^{elt\,k+3} \qquad (4.43)$$

- Secondary Variables satisfy equilibrium at the nodes, i.e. the sum of forces of flux that converge to a node is equal to zero. The corresponding balance condition is expressed as:
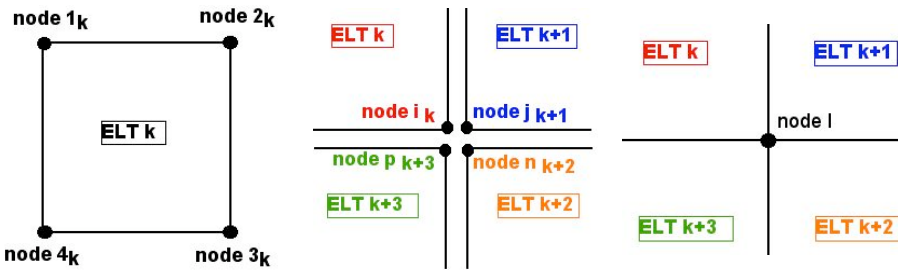
$$Q_I = Q_i^{elt\,k} + Q_j^{elt\,k+1} + Q_n^{elt\,k+2} + Q_p^{elt\,k+3} \qquad (4.44)$$

Table 4.1 Principle of a connectivity table

elt	loc. node 1	loc. node 2	...	loc. node N_{nd}
1	I_1	I_2	...	$I_{N_{nd}}$
2	J_1	J_2	...	$J_{N_{nd}}$
...				
N_e	N_1	N_2	...	$N_{N_{nd}}$

Note that if no external loading is imposed on node I, the secondary variable equilibrium equation is $Q_I = 0$ by default.

In order to satisfy the continuity and balance requirements above, the elementary equations are assembled into a unique system of equations that is solved at the scale of the entire domain. The assembling process requires double-numbering the nodes, which possess a local number in the element and a global number in the domain (Figure 4.1). The connectivity table relates local and global node numbers (Table 4.1).


Figure 4.1 Local and global node numbers.

Elements of the same interpolation order and same geometry are governed by the same elementary equations. A coordinate change can be done to adapt the elementary equations of elements of same interpolation order but different geometries. In practice, elementary equations are calculated only once for each type of Finite Element - called the **master**

elements. In most 1D cases, for element $n^o k$:

$$K_{ij}^k = cst_1 \int_{x_a}^{x_b} \frac{d\Psi_i(x)}{dx} \frac{d\Psi_j(x)}{dx} dx + cst_0 \int_{x_a}^{x_b} \Psi_i(x)\Psi_j(x)dx \tag{4.45}$$

Coordinate change: $\overline{x} = x - x_a$, $l_e = x_b - x_a$, $dx = d\overline{x}$:

$$K_{ij}^k = cst_1 \int_0^{l_e} \frac{d\Psi_i(\overline{x} + x_a)}{d\overline{x}} \frac{d\Psi_j(\overline{x} + x_a)}{d\overline{x}} d\overline{x} + cst_0 \int_0^{l_e} \Psi_i(\overline{x} + x_a)\Psi_j(\overline{x} + x_a)d\overline{x} \tag{4.46}$$

By construction, $\Psi_i(\overline{x} + x_a)$ only depends on $\overline{x}$ and l_e. For all elements of length l_e:

$$K_{ij}^e = cst_1 \int_0^{l_e} \frac{d\Psi_i(\overline{x})}{d\overline{x}} \frac{d\Psi_j(\overline{x})}{d\overline{x}} d\overline{x} + cst_0 \int_0^{l_e} \Psi_i(\overline{x})\Psi_j(\overline{x})d\overline{x} \tag{4.47}$$

The elementary stiffness matrix is then the same for for all elements (of length l_e).

In most cases, for element $n^o k$:

$$F_i^k = \int_{x_a}^{x_b} \Psi_i(x)f(x)dx \tag{4.48}$$

Coordinate change: $\overline{x} = x - x_a$, $l_e = x_b - x_a$, $dx = d\overline{x}$:

$$F_i^k = \int_0^{l_e} \Psi_i(\overline{x} + x_a)f(\overline{x} + x_a)d\overline{x} \tag{4.49}$$

By construction, $\Psi_i(\overline{x} + x_a)$ only depends on $\overline{x}$ and l_e.

$$F_i^k = \int_0^{l_e} \Psi_i(\overline{x})f(\overline{x} + x_a)d\overline{x} \tag{4.50}$$

Generally, f depends on x_a and the integral depends on the element, so that the F_i coefficients must generally be computed for each element.

We call "number of degrees of freedom" the number of dependent variables (u, u'...) that one needs to solve for, multiplied by the number of nodes. After assembling the elementary equations, we obtain N_{dof} global equations to solve for $2\,N_{dof}$ unknowns

$$\begin{bmatrix} K_{11} & ... & K_{1\,N_{dof}} \\ ... & ... & ... \\ K_{1N_{dof}\,1} & ... & K_{N_{dof}\,N_{dof}} \end{bmatrix} \begin{Bmatrix} u_1 \\ ... \\ u_{N_{dof}} \end{Bmatrix} = \begin{Bmatrix} F_1 \\ ... \\ F_{N_{dof}} \end{Bmatrix} + \begin{Bmatrix} Q_1 \\ ... \\ Q_{N_{dof}} \end{Bmatrix}$$

We have 1 additional equation per degree of freedom:

- either a boundary condition ($\widehat{u}$ or $\widehat{Q}$)

- or a connectivity requirement ($\Sigma_{i=I}Q_i^e = 0$ if nothing imposed)

As a result, we dispose of $N_{dof} + N_{dof}$ equations for $2\,N_{dof}$ unknowns, so in principle, it is possible to solve the problem.

4.2.5 Resolution and post-processing

For each degree of freedom, the boundary conditions, continuity conditions and balance conditions impose the value of either the primary variable ($u = \widehat{u}$) or the secondary variable ($Q = \widehat{Q}$). Noting (I) the conditions on primary variables and (II) the conditions on the secondary variables, we can write the global FEM equation with block matrices, as follows:

$$
\begin{bmatrix} [K_{I,I}] & [K_{I,II}] \\ \\ [K_{II,I}] & [K_{II,II}] \end{bmatrix} \left\{ \begin{array}{c} \{\widehat{u_I}\} \\ \{u_{II}\} \end{array} \right\} = \left\{ \begin{array}{c} \{F_I\} \\ \{F_{II}\} \end{array} \right\} + \left\{ \begin{array}{c} \{Q_I\} \\ \{\widehat{Q_{II}}\} \end{array} \right\} \tag{4.51}
$$

We first solve for the unknown primary variables stored in the vector $\{u_{II}\}$ ("resolution"):

$$
\{u_{II}\} = [K_{II,II}]^{-1} \left(\{F_{II}\} + \{\widehat{Q_{II}}\} - [K_{I,II}]\{\widehat{u_I}\} \right) \tag{4.52}
$$

We then solve for the unknown secondary variables stored in the vector $\{Q_I\}$ ("post-processing"):

$$
\{Q_I\} = [K_{I,I}]\{\widehat{u_I}\} + [K_{I,II}]\{u_{II}\} - \{F_I\} \tag{4.53}
$$

It is possible to use a so-called "condensation technique" to reduce the number of equations to solve for the primary variable in the first step, by getting rid of the rows of the system of equations for which the primary variable is known. The process is illustrated below, in the case when the primary variable is known to be equal to $\widehat{u}_p$ at the pth node. Initially, the system of equation, is written as:

$$
\begin{bmatrix}
K_{11} & \dots & \dots & K_{1p} & \dots & \dots & K_{1\,N_{dof}} \\
\dots & \dots & \dots & \dots & \dots & \dots & \dots \\
\dots & \dots & \dots & \dots & \dots & \dots & \dots \\
K_{p1} & \dots & \dots & K_{pp} & \dots & \dots & K_{p\,N_{dof}} \\
\dots & \dots & \dots & \dots & \dots & \dots & \dots \\
\dots & \dots & \dots & \dots & \dots & \dots & \dots \\
K_{1\,N_{dof}} & \dots & \dots & K_{N_{dof}\,p} & \dots & \dots & K_{N_{dof}\,N_{dof}}
\end{bmatrix}
\left\{ \begin{array}{c}
u_1 \\
\dots \\
u_{p-1} \\
\widehat{u_p} \\
u_{p+1} \\
\dots \\
u_{N_{dof}}
\end{array} \right\}
=
\left\{ \begin{array}{c}
F_1 + Q_1 \\
\dots \\
F_{p-1} + Q_{p-1} \\
F_p + Q_p \\
F_{p+1} + Q_{p+1} \\
\dots \\
F_{N_{dof}} + Q_{N_{dof}}
\end{array} \right\}
\tag{4.54}
$$

We then replace the pth row and the pth column of the stiffness matrix by zeros and ones, as follows:

$$\begin{bmatrix} K_{11} & ... & ... & 0 & ... & ... & K_{1\,N_{dof}} \\ ... & ... & ... & ... & ... & ... & ... \\ ... & ... & ... & 0 & ... & ... & ... \\ 0 & ... & 0 & 1 & 0 & ... & 0 \\ ... & ... & ... & ... & ... & ... & ... \\ ... & ... & ... & ... & ... & ... & ... \\ K_{1\,N_{dof}} & ... & ... & 0 & ... & ... & K_{N_{dof}\,N_{dof}} \end{bmatrix} \begin{Bmatrix} u_1 \\ ... \\ u_{p-1} \\ 0 \\ u_{p+1} \\ ... \\ u_{N_{dof}} \end{Bmatrix} + \begin{Bmatrix} K_{1\,p} \\ ... \\ K_{p-1\,p} \\ 1 \\ K_{p+1\,p} \\ ... \\ K_{N_{dof}\,p} \end{Bmatrix} \widehat{u_p} = \begin{Bmatrix} F_1 + Q_1 \\ ... \\ F_{p_1} + Q_{p-1} \\ \widehat{u_p} \\ F_{p+1} + Q_{p+1} \\ ... \\ F_{N_{dof}} + Q_{N_{dof}} \end{Bmatrix}$$

(4.55)

We then put the second term on the left hand-side to the rirght-hand side:

$$\begin{bmatrix} K_{11} & ... & ... & 0 & ... & ... & K_{1\,N_{dof}} \\ ... & ... & ... & ... & ... & ... & ... \\ ... & ... & ... & 0 & ... & ... & ... \\ 0 & ... & 0 & 1 & 0 & ... & 0 \\ ... & ... & ... & ... & ... & ... & ... \\ ... & ... & ... & ... & ... & ... & ... \\ K_{1\,N_{dof}} & ... & ... & 0 & ... & ... & K_{N_{dof}\,N_{dof}} \end{bmatrix} \begin{Bmatrix} u_1 \\ ... \\ u_{p-1} \\ 0 \\ u_{p+1} \\ ... \\ u_{N_{dof}} \end{Bmatrix} = \begin{Bmatrix} F_1 + Q_1 - K_{1\,p}\,\widehat{u_p} \\ ... \\ F_{p_1} + Q_{p-1} - K_{p-1\,p}\,\widehat{u_p} \\ 0 \\ F_{p+1} + Q_{p+1} - K_{p+1\,p}\,\widehat{u_p} \\ ... \\ F_{N_{dof}} + Q_{N_{dof}} - K_{N_{dof}\,p}\,\widehat{u_p} \end{Bmatrix}$$

(4.56)

We notice that one equation is "0=0", so we can rid of it to obtain the following reduced system of equations:

$$
\begin{bmatrix}
K_{11} & \dots & \dots & \dots & \dots & K_{1\,N_{dof}} \\
\dots & \dots & \dots & \dots & \dots & \dots \\
\dots & \dots & \dots & \dots & \dots & \dots \\
\dots & \dots & \dots & \dots & \dots & \dots \\
\dots & \dots & \dots & \dots & \dots & \dots \\
K_{1\,N_{dof}} & \dots & \dots & \dots & \dots & K_{N_{dof}\,N_{dof}}
\end{bmatrix}
\begin{Bmatrix}
u_1 \\
\dots \\
u_{p-1} \\
u_{p+1} \\
\dots \\
u_{N_{dof}}
\end{Bmatrix}
=
\begin{Bmatrix}
F_1 + Q_1 - K_{1\,p}\,\widehat{u_p} \\
\dots \\
F_{p_1} + Q_{p-1} - K_{p-1\,p}\,\widehat{u_p} \\
F_{p+1} + Q_{p+1} - K_{p+1\,p}\,\widehat{u_p} \\
\dots \\
F_{N_{dof}} + Q_{N_{dof}} - K_{N_{dof}\,p}\,\widehat{u_p}
\end{Bmatrix}
\tag{4.57}
$$

After solving for the primary variables, there are two ways to calcualte the secondary variables:

- From the condensed equations:

$$\{Q\} = [K]\{u\} - \{F\} \tag{4.58}$$

- From the elementary contributions:

$$Q_I = \Sigma_{i=I}Q_i^e \tag{4.59}$$
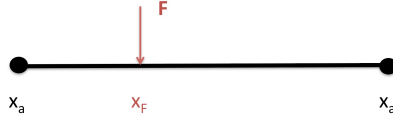
If u is the primary variable and $a\frac{du}{dx}$ is the secondary variable:

$$Q_I = \Sigma_{i=I}a\frac{du_I}{dx} \tag{4.60}$$
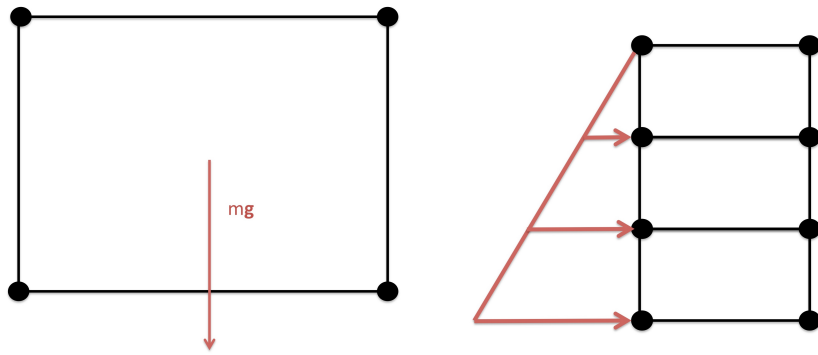
Using the elementary contributions may lead to an accumulation of approximation errors made on the nodal values of the dependent variable, and is thus less accurate than using condensed equations. However, using the elementary contributions is less computationally expensive, because it does not require using any matrix product. It also requires less memory, since calculating the seconday variables from the elementary contributions does not require using the values of the coefficients of the stiffness matrix, which are sometimes modified and destroyed during the stiffness inversion process. As a result, unknown nodal values of the seconday variables are most often calculated from the elementary contributions - a process called post-processing.

When the secondary variable (e.g., force) is not applied at the location of a node of an element, one can use an interpolation to express the imposed secondary variable as a function of different forces applied at the neighboring nodes (Figure 4.2). Using the coordinate of the application point x_F: A simple solution is:

$$
\begin{cases}
\widehat{Q_a} = F\left(1 - \frac{x_F - x_a}{x_b - x_a}\right) \\
\\
\widehat{Q_b} = F\frac{x_F - x_a}{x_b - x_a}
\end{cases}
\tag{4.61}
$$

Figure 4.2   An example where a force is not applied at a node of the mesh.


Figure 4.3   Forces applied outside ot the nodes of a 2D mesh.

so that $Q(x_a) = F$ if $x_F = x_a$, $Q(x_b) = F$ if $x_F = x_b$, and $Q(x_a) + Q(x_b) = F$ in all cases (F applied on the element). In more than 1D, an interpolation is needed on each face of the element (Figure 4.3).

4.3   Applications of the FEM for 1 variable in 1D

4.3.1   Heat and mass transfer

Heat transfer
The balance of heat fluxes is expressed as:

$$-kA\frac{\partial T}{\partial x} + \beta A(T - T_\infty) = Q_0 \tag{4.62}$$

in which Q_0 represents a heat source, $-kA\frac{\partial T}{\partial x}$ represents conductive flow and $\beta A(T - T_\infty)$ represents convective flow. The conservation of energy is expressed as:

$$divQ = \rho C_p \frac{\partial T}{\partial t} \tag{4.63}$$

so that:
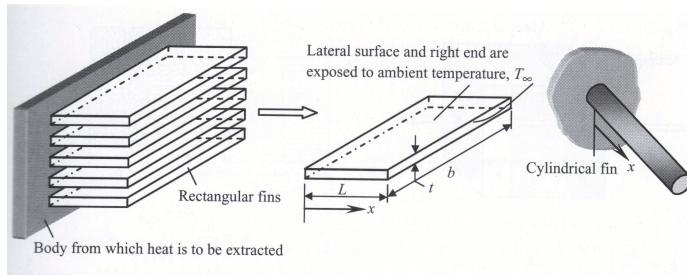
$$-\frac{\partial}{\partial x}\left(kA\frac{\partial T}{\partial x}\right) + \beta P(T - T_\infty) - Aq_0 = \rho C_p \frac{\partial T}{\partial t} \tag{4.64}$$

In steady state:

$$-\frac{\partial}{\partial x}\left(kA\frac{\partial T}{\partial x}\right) + \beta P(T - T_\infty) = Aq_0 \tag{4.65}$$

If there is convection on the whole surface of the element (Figure 4.4):

$$-\frac{\partial}{\partial x}\left(kA\frac{\partial T}{\partial x}\right) + \beta P(T - T_\infty) = Aq_0 \qquad (4.66)$$
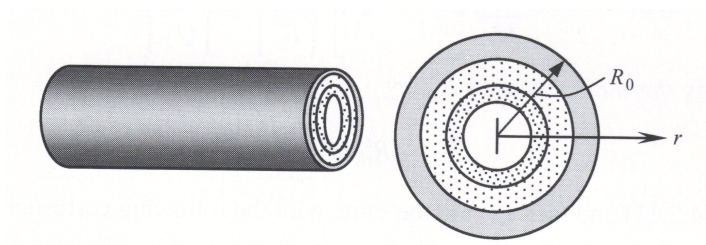

Figure 4.4   Examples of bodies subjected to convection heat transfer. Image taken from [18]

For bodies that present axis-symmetry, like in Figure 4.5:

- The transfer equation written for an elementary surface of the section;

- There is no convection at the element perimeter;

- Convection happens only at the outer boundaries of the system.

In cylindrical coordinates:

$$\int_r\int_\theta\int_z f(r)dV = \int_0^R\int_0^{2\Pi}\int_0^1 f(r)dr\,rd\theta\,dz = 2\pi\int_0^R f(r)rdr \qquad (4.67)$$

Figure 4.5   Heat transfer through a cylindrical composite. Image taken from [18]

The governing equation is:

$$-\frac{1}{r}\frac{d}{dr}\left(kr\frac{dT}{dr}\right) = q_0(r) \tag{4.68}$$

In spherical coordinates:

$$\int_r\int_\theta\int_\phi f(r)dV = \int_0^R\int_0^{2\Pi}\int_0^\Pi f(r)dr\,rd\theta\,rsin\phi d\phi = 4\Pi\int_0^R f(r)r^2dr \tag{4.69}$$

The governing equation is:

$$-\frac{1}{r^2}\frac{d}{dr}\left(kr^2\frac{dT}{dr}\right) = q_0(r) \tag{4.70}$$

Fluid Transfer

For fluid transfer (Figure 4.6), we start by expressing the water mass conservation equation:

$$\frac{\partial(\rho_w)}{\partial t} + div\,(\rho_w\,\mathbf{v}_w) = 0 \tag{4.71}$$

For an incompressible fluid:

$$div\,(\mathbf{v}_w) = 0 \tag{4.72}$$

The water balance of momentum is written as follows:

$$\mathbf{div}\,(p_w\boldsymbol{\delta}) + \mathbf{f_w} = \mathbf{a_w}(\mathbf{x}, t) \tag{4.73}$$

For a Newtonian fluid, the resulting force that resists the flow due to the fluid's viscosity is:

$$\mathbf{f_w} = -\mu_w\nabla^2\mathbf{v_w} \tag{4.74}$$

Thus, in static conditions:
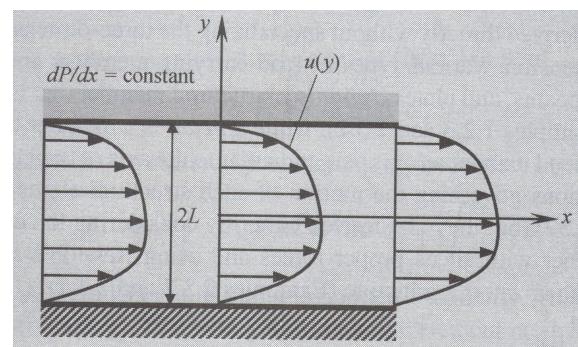
$$\nabla p_w - \mu_w\nabla^2\mathbf{v_w} = \mathbf{0} \tag{4.75}$$

Thus, the governing equation in 1D is:

$$\mu_w\frac{d^2v_{wx}}{dy^2} = \frac{dp_w}{dx}, \quad \mu_w\frac{d^2v_{wx}}{dy^2} = f(y) \tag{4.76}$$

Using Ritz Method:

$$\forall = 1..N, \quad \left[\int_{y_1}^{y_2}\mu\frac{d\Psi_i}{dy}\frac{d\Psi_j}{dy}dy\right]v_{xj} = -\int_{y_1}^{y_2}\Psi_i(y)f(y)dy + Q_i \tag{4.77}$$

Figure 4.6   1D Newtonian fluid flow in a pipe. Image taken from [18]

4.3.2 Bars and beams

Bar elements

Beam elements are subject to deflection and undergo deflection. By contrast, a bar element is only loaded axially. The dependent variable in a bar element is an axial displacement. The governing equation is:

$$-\frac{d}{dx}\left(EA\frac{du}{dx}\right) = f(x) \tag{4.78}$$

The weak formulation is:

$$\forall w \simeq \delta u,$$

$$\int_{x_a}^{x_b} EA\frac{dw}{dx}\frac{du}{dx}dx - \int_{x_a}^{x_b} w(x)f(x)dx - [w(x)EA\frac{du}{dx}]_{x_a}^{x_b} = 0 \tag{4.79}$$

in which the secondary variable has the physical dimension of a traction force, and is expressed as:

$$Q = EA\frac{du}{dx} \tag{4.80}$$

After introducing the approximation $u(x) \simeq \sum_{i=1}^{N} u_i \Psi_i(x)$, one gets the following elementary equations:

$$\forall i = 1, 2, \quad \left[\int_{x_a}^{x_b} EA\frac{d\Psi_i}{dx}\frac{d\Psi_j}{dx}dx\right] u_j^e = \int_{x_a}^{x_b} \Psi_i(x)f(x)dx + [Q_i(x)]_{x_a}^{x_b} \tag{4.81}$$

In a matrix form:

$$[K^e]\{u^e\} = \{F^e\} + \{Q^e\} \tag{4.82}$$

in which the force vector is:

$$\{F^e\} = \int_{x_a}^{x_b} \{N^e\}f(x)dx \tag{4.83}$$

and the stiffness matrix is:

$$[K^e] = \int_{x_a}^{x_b} AE\{B^e\} \otimes \{B^e\}dx \tag{4.84}$$

where we used the following notation:

$$u_N^e(x) = \{N^e(x)\}\cdot\{u^e\} = \begin{Bmatrix} \Psi_1(x) \\ \Psi_2(x) \\ ... \\ \Psi_N(x) \end{Bmatrix} \cdot \begin{Bmatrix} u_1^e \\ u_2^e \\ ... \\ u_N^e \end{Bmatrix} \tag{4.85}$$

$$\epsilon_N^e(x) = \frac{du_N^e(x)}{dx} = \{\frac{dN^e(x)}{dx}\}\cdot\{u^e\}$$

$$= \{B^e(x)\}\cdot\{u^e\} = \begin{Bmatrix} d\Psi_1(x)/dx \\ d\Psi_2(x)/dx \\ ... \\ d\Psi_N(x)/dx \end{Bmatrix} \cdot \begin{Bmatrix} u_1^e \\ u_2^e \\ ... \\ u_N^e \end{Bmatrix} \tag{4.86}$$

For a **linear** bar element of length l_e that is made of a homogeneous material of Young's modulus E and that has a cross-section of uniform area A_e:

$$K_{ij}^e = \int_{x_a}^{x_b} EA \frac{d\Psi_i}{dx} \frac{d\Psi_j}{dx} dx \qquad (4.87)$$
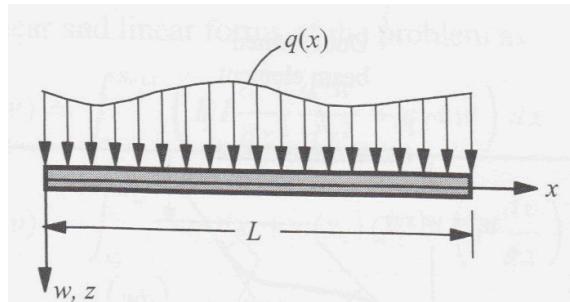
$$[K^e] = \frac{EA_e}{l_e} \begin{bmatrix} 1 & -1 \\ -1 & 1 \end{bmatrix} \qquad (4.88)$$

Euler-Bernouilli beam elements

In a beam deflection problem (Figure 4.7, the goal is to find the deflection $w(x)$, and the deflection angle, noted $\Psi(x)$ in the following. The governing equations are:

$$\begin{cases} -\frac{d}{dx}\left[GAK_s\left(\psi + \frac{dw}{dx}\right)\right] + c_f\, w(x) = q(x) \\[2mm] -\frac{d}{dx}\left(EI\frac{d\psi}{dx}\right) + GAK_s\left(\psi + \frac{dw}{dx}\right) = 0 \end{cases} \qquad (4.89)$$

In Euler-Bernouilli's beam model (Figure 4.8), it is assumed that the cross section remains
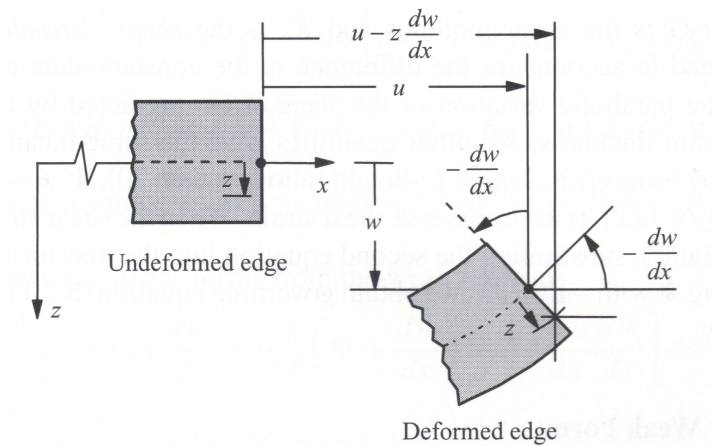
Figure 4.7   Beam deflection problem. Image taken from [18]

perpendicular to the beam axis, so that $\psi = \frac{dw}{dx}$. In other words, the problem has to be

solved for only 1 dependent variable, the deflection w. The governing equation is:

$$\frac{d^2}{dx^2}\left(EI\frac{d^2w}{dx^2}\right) + c_f\, w(x) = q(x), \qquad 0 < x < L \qquad (4.90)$$

Two integration by parts are needed for the two primary variables w and dw/dx. The

Figure 4.8   Euler-Bernouilli's assumptions. Image taken from [18]

two primary variables are related by a differential operator. As a result, Hermite interpolation polynomials will be needed. The maximum order of the differential operator in the integral equations of the variational method is 2, so it is necessary to choose interpolation polynomials of order 2 at least. However, the minumum number of degrees of freedom per element is 4 (two degrees of freedom for a minimum of two nodes), so the interpolation polynomials should be of order 3 at least (a cubic polynomial has four independent coefficients). The interpolation functions for the two-noded Euler-Bernouilli element are of the form:

$$\Psi_j^e(x) = a_3x^3 + a_2x^2 + a_1x + a_0 \qquad (4.91)$$

with:

$$\frac{d\Psi_j^e(x)}{dx} = 3a_3x^2 + 2a_2x + a_1 \tag{4.92}$$

Noting x_e and x_{e+1} the coordinates of the two nodes of the element, the coeffiicents of the interpolation polynomilals can be found by solving the following system of equations:

$$\begin{Bmatrix} w(x_e) \\ [dw/dx](x_e) \\ w(x_{e+1}) \\ [dw/dx](x_{e+1}) \end{Bmatrix} = \begin{bmatrix} 1 & x_e & x_e{}^2 & x_e{}^3 \\ 0 & 1 & 2x_e & 3x_e{}^2 \\ 1 & x_{e+1} & x_{e+1}{}^2 & x_{e+1}{}^3 \\ 0 & 1 & 2x_{e+1} & 3x_{e+1}{}^2 \end{bmatrix} \begin{Bmatrix} a_0 \\ a_1 \\ a_3 \\ a_4 \end{Bmatrix} \tag{4.93}$$

And we obtain:

$$\begin{cases} \Psi_1^e(x) = 1 - 3\left(\frac{x-x_e}{l_e}\right)^2 + 2\left(\frac{x-x_e}{l_e}\right)^3 \\[2ex] \Psi_2^e(x) = -(x-x_e)\left(1 - \frac{x-x_e}{l_e}\right)^2 \\[2ex] \Psi_3^e(x) = 3\left(\frac{x-x_e}{l_e}\right)^2 - 2\left(\frac{x-x_e}{l_e}\right)^3 \\[2ex] \Psi_4^e(x) = -(x-x_e)\left[\left(\frac{x-x_e}{l_e}\right)^2 - \frac{x-x_e}{l_e}\right] \end{cases} \tag{4.94}$$

The variational formulation is obtained as follows:

$$\frac{d^2}{dx^2}\left(EI\frac{d^2w}{dx^2}\right) + c_f\,w(x) = q(x), \qquad 0 < x < L \tag{4.95}$$

After two integration by parts:

$$\forall f \simeq \delta w,$$

$$\int_{x_e}^{x_{e+1}} \left(EI\frac{d^2f}{dx^2}\frac{d^2w}{dx^2} + c_f f(x)w(x) - f(x)q(x)\right)dx \tag{4.96}$$

$$-f(x_e)Q_1^e - \left(\frac{df}{dx}\right)(x_e)Q_2^e - f(x_{e+1})Q_3^e - \left(\frac{df}{dx}\right)(x_{e+1})Q_4^e$$

with:

$$Q_1^e = \left[\frac{d}{dx}\left(EI\frac{d^2w}{dx^2}\right)\right](x_e) = -V(x_e), \qquad Q_3^e = -\left[\frac{d}{dx}\left(EI\frac{d^2w}{dx^2}\right)\right](x_{e+1}) = V(x_{e+1}) \tag{4.97}$$

$$Q_2^e = \left[-EI\frac{d^2w}{dx^2}\right](x_e) = M(x_e), \qquad Q_4^e = \left[\frac{d}{dx}\left(-EI\frac{d^2w}{dx^2}\right)\right](x_{e+1}) = -M(x_{e+1}) \tag{4.98}$$

The general form of the matrix equation over one element is as follows:

$$
[K]
\left\{
\begin{array}{l}
U_1 = w(x_e) \\[6pt]
U_2 = dw/dx(x_e) \\[6pt]
U_3 = w(x_{e+1}) \\[6pt]
U_4 = dw/dx(x_{e+1})
\end{array}
\right\}
=
\left\{
\begin{array}{l}
F_1 + Q_1 \\[6pt]
F_2 + Q_2 \\[6pt]
F_3 + Q_3 \\[6pt]
F_4 + Q_4
\end{array}
\right\}
\tag{4.99}
$$

With a Finite Element Method based on Ritz Method:

$$
K_{ij}^e = \int_{x_e}^{x_{e+1}} \left(EI \frac{d^2 \Psi_i^e}{dx^2} \frac{d^2 \Psi_j^e}{dx^2} + c_f \Psi_i^e(x)\Psi_j^e \right) dx
\tag{4.100}
$$

If E, I and c_f are constant over the element:

$$
[K^e] = \frac{2EI}{(l_e)^3}
\begin{bmatrix}
6 & -3l_e & -6 & -3l_e \\[4pt]
-3l_e & 2(l_e)^2 & 3l_e & (l_e)^2 \\[4pt]
-6 & 3l_e & 6 & 3l_e \\[4pt]
-3l_e & (l_e)^2 & 3l_e & 2(l_e)^2
\end{bmatrix}
+ \frac{c_f l_e}{420}
\begin{bmatrix}
156 & -22l_e & 54 & 13l_e \\[4pt]
-22l_e & 4(l_e)^2 & -13l_e & -3(l_e)^2 \\[4pt]
54 & -13l_e & 156 & 22l_e \\[4pt]
13l_e & -3(l_e)^2 & 22l_e & 4(l_e)^2
\end{bmatrix}
\tag{4.101}
$$

$$
F_i^e + Q_i^e = \int_{x_e}^{x_{e+1}} \Psi_i^e(x)q(x)dx + Q_i^e
\tag{4.102}
$$

If the load q is constant $(=q_0)$ over the element:
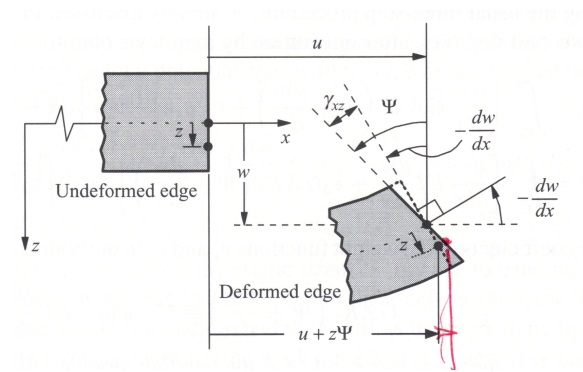
$$
\{F^e + Q^e\} = \frac{q_0 l_e}{12}
\left\{
\begin{array}{c}
6 \\[6pt]
-l_e \\[6pt]
6 \\[6pt]
l_e
\end{array}
\right\}
+
\left\{
\begin{array}{c}
Q_1 \\[6pt]
Q_2 \\[6pt]
Q_3 \\[6pt]
Q_4
\end{array}
\right\}
\tag{4.103}
$$

Timoshenko beam elements

In Timoshenko's beam model (Figure 4.9), the orientation of the cross section of the beam is not known, i.e. $\psi \neq dw/dx$. The deflection problem has to be solved for two independent variables, $w(x)$ and $\psi(x)$. The formulation of the problem is based on the two following governing equations, for $0 \leq x \leq L$:

$$
\begin{cases}
-\frac{d}{dx}\left[GAK_s \left(\psi + \frac{dw}{dx} \right) \right] + c_f\, w(x) = q(x) \\[10pt]
-\frac{d}{dx}\left(EI \frac{d\psi}{dx} \right) + GAK_s \left(\psi + \frac{dw}{dx} \right) = 0
\end{cases}
\tag{4.104}
$$

The variational formulation of Timoshenko's beam deflection problem is the following:

Figure 4.9   Assumptions made in Timoshenko beam's model.

$$\begin{cases} \forall f \simeq \delta w, \\ \int_{x_e}^{x_{e+1}} \left(\frac{df}{dx} GAK_s \left(\psi + \frac{dw}{dx} \right) + c_f f(x) w(x) - f(x) q(x) \right) dx \\ - \left[f(x) GAK_s \left(\psi + \frac{dw}{dx} \right) \right]_{x_e}^{x_{e+1}} = 0 \\ \\ \forall g \simeq \delta \psi, \\ \int_{x_e}^{x_{e+1}} \left(\frac{dg}{dx} EI \frac{d\psi}{dx} + g(x) GAK_s \left(\psi + \frac{dw}{dx} \right) \right) dx \\ - \left[g(x) EI \frac{d\psi}{dx} \right]_{x_e}^{x_{e+1}} = 0 \end{cases} \qquad (4.105)$$

The secondary variables are the shear force (conjugate to w) and the bending moment (conjugate to ψ). Since the problem needs to be solved for two independent degrees of freedom, two families of Lagrange interpolation functions are needed:

$$w^e(x) = \Sigma_{j=1}^N w_j^e f_j^e(x), \qquad \psi^e(x) = \Sigma_{j=1}^M \psi_j^e g_j^e(x) \qquad (4.106)$$

In general, the interpolation orders N and M are different. After introducing the expressions of the interpolation functions in the variational formulation, one obtaines to coupled

integral equations, which can be expressed in the form of a matrix equation of the form:

$$
\begin{bmatrix} [K^{11}] & [K^{12}] \\ \\ [K^{21}] & [K^{22}] \end{bmatrix} \left\{ \begin{array}{c} \{w\} \\ \\ \{\psi\} \end{array} \right\} = \left\{ \begin{array}{c} \{F^1 + Q^1\} \\ \\ \{F^2 + Q^2\} \end{array} \right\}
\tag{4.107}
$$

The first block row is related to the first equation of deflection:

$$
\begin{aligned}
&\forall f \simeq \delta w, \\
&\int_{x_e}^{x_{e+1}} \left(\frac{df}{dx} GAK_s \left(\psi + \frac{dw}{dx} \right) + c_f f(x) w(x) - f(x) q(x) \right) dx \\
&- \left[f(x) GAK_s \left(\psi + \frac{dw}{dx} \right) \right]_{x_e}^{x_{e+1}} = 0
\end{aligned}
\tag{4.108}
$$

With Ritz Method:

$$
\begin{aligned}
&\forall i = 1..N, \\
&\left[\int_{x_e}^{x_{e+1}} \left(\frac{df_i^e}{dx} GAK_s \frac{df_j^e}{dx} + c_f f_i(x) f_j(x) \right) dx \right] w_j + \left[\int_{x_e}^{x_{e+1}} \left(\frac{df_i^e}{dx} GAK_s g_{j'}^e \right) dx \right] \psi_{j'} \\
\\
&= \int_{x_e}^{x_{e+1}} f_i(x) q(x) dx + \left[f_i(x) GAK_s \left(\psi + \frac{dw}{dx} \right) \right]_{x_e}^{x_{e+1}}
\end{aligned}
\tag{4.109}
$$

$$
K_{ij}^{11} = \int_{x_e}^{x_{e+1}} \left(\frac{df_i^e}{dx} GAK_s \frac{df_j^e}{dx} + c_f f_i(x) f_j(x) \right) dx
$$

$$
K_{ij}^{12} = \int_{x_e}^{x_{e+1}} \left(\frac{df_i^e}{dx} GAK_s g_j^e \right) dx
$$

$$
F_i^1 = \int_{x_e}^{x_{e+1}} f_i(x) q(x) dx
\tag{4.110}
$$

$$
Q_i^1 = \left[f_i(x) GAK_s \left(\psi + \frac{dw}{dx} \right) \right]_{x_e}^{x_{e+1}}
$$

The second block fow is related to the second equation of deflection:

$$
\begin{aligned}
&\forall g \simeq \delta \psi, \\
&\int_{x_e}^{x_{e+1}} \left(\frac{dg}{dx} EI \frac{d\psi}{dx} + g(x) GAK_s \left(\psi + \frac{dw}{dx} \right) \right) dx - \left[g(x) EI \frac{d\psi}{dx} \right]_{x_e}^{x_{e+1}} = 0
\end{aligned}
\tag{4.111}
$$

With Ritz Method:

$$
\begin{aligned}
&\forall i = 1..M, \\
&\left[\int_{x_e}^{x_{e+1}} \left(\frac{dg_i^e}{dx} EI \frac{dg_j^e}{dx} + GAK_s g_i(x) g_j(x) \right) dx \right] \psi_j + \left[\int_{x_e}^{x_{e+1}} \left(g_i^e GAK_s \frac{df_{j'}^e}{dx} \right) dx \right] w_{j'} \\
\\
&= \left[g_i(x) EI \frac{d\psi}{dx} \right]_{x_e}^{x_{e+1}}
\end{aligned}
\tag{4.112}
$$

$$K_{ij}^{22} = \int_{x_e}^{x_{e+1}} \left(\frac{dg_i^e}{dx} EI \frac{dg_j^e}{dx} + GAK_s g_i(x) g_j(x) \right) dx$$

$$K_{ij}^{21} = \int_{x_e}^{x_{e+1}} \left(g_i^e GAK_s \frac{df_j^e}{dx} \right) dx$$

$$F_i^2 = 0 \tag{4.113}$$

$$Q_i^2 = \left[g_i(x) EI \frac{d\psi}{dx} \right]_{x_e}^{x_{e+1}}$$

Each dependent variable is differentiated only once in the integral equations. There is a minimum of two nodal values to match for each beam element (minimum two nodes per element). So the minimum order possible for the interpolation polynomials is 1 (linear interpolation functions). That said, the angle of deflection ψ has the *physical dimension* of the derivative of the deflection w. So the order of interpolation of w should exceed that of ψ by one. So since the minimum order of the interpolation polynomials for ψ is 1 (linear functions), the minimum order of the interpolation polynomials for w should be 2 (quadratic functions). A consistency node is added in the middle of the element, just for the deflection degree of freedom. The other two nodes at the ends of the beam element both have two d.o.f. (deflection and deflection angle). For a quadratic interpolation of the deflection and a linear interpolation of the deflection angle, and for EI, GAK_s and c_f constant over the element:

$$[K^{11}] = \frac{GAK_s}{3l_e} \begin{bmatrix} 7 & -8 & 1 \\ -8 & 16 & -8 \\ 1 & -8 & 7 \end{bmatrix} + \frac{c_f l_e}{30} \begin{bmatrix} 4 & 2 & -1 \\ 2 & 16 & 2 \\ -1 & 2 & 4 \end{bmatrix} \tag{4.114}$$

$$[K^{12}] = [K^{21}]^T = \frac{GAK_s}{6} \begin{bmatrix} -5 & -1 \\ 4 & -4 \\ 1 & 5 \end{bmatrix} \tag{4.115}$$

$$[K^{22}] = \frac{EI}{l_e} \begin{bmatrix} 1 & -1 \\ -1 & 1 \end{bmatrix} + \frac{GAK_s l_e}{6} \begin{bmatrix} 2 & 1 \\ 1 & 2 \end{bmatrix} \tag{4.116}$$

The general form of the elementary equation is:

$$
\begin{bmatrix} & & & & \\ & & & & \\ & & K^e(5x5) & & \\ & & & & \\ & & & & \end{bmatrix}
\begin{Bmatrix} w_1 \\ w_c \\ w_2 \\ \psi_1 \\ \psi_2 \end{Bmatrix}
=
\begin{Bmatrix} F_1^1 + Q_1^1 \\ F_c^1 + Q_c^1 \\ F_2^1 + Q_2^1 \\ F_1^2 + Q_1^2 \\ F_2^2 + Q_2^2 \end{Bmatrix}
\tag{4.117}
$$

The equation related to the additional consistency node:

$$
K_{22}^e w_c = F_c^1 + Q_c^1 - K_{21}^e w_1 - K_{23}^e w_2 - K_{24}^e \psi_1 - K_{25}^e \psi_2
\tag{4.118}
$$

is used as a boundary condition on w_c to get condensed equations of the form:

$$
\begin{bmatrix} & & & \\ & & & \\ & \widehat{K}^e(4x4) & & \\ & & & \\ & & & \end{bmatrix}
\begin{Bmatrix} w_1 \\ w_2 \\ \psi_1 \\ \psi_2 \end{Bmatrix}
=
\begin{Bmatrix} \widehat{F}_1^1 + Q_1^1 \\ \widehat{F}_2^1 + Q_2^1 \\ \widehat{F}_1^2 + Q_1^2 \\ \widehat{F}_2^2 + Q_2^2 \end{Bmatrix}
\tag{4.119}
$$

To avoid adding consistency nodes, the same order of interpolation can be used for both the deflection and the deflection angle. If a linear interplation is used for both w and ψ, then dw/dx is constant over the beam element while ψ varies linearly over that element. We note that the shear energy stored in one element is:

$$
E_{shear} = \int_{x_e}^{x_{e+1}} \frac{GAK_s}{2} \left(\frac{dw}{dx} + \psi \right)^2 dx
\tag{4.120}
$$

If the shear energy has to be computed by a numerical integration, one integration term is sufficient to evaluate the terms in dw/dx (up to order 1 only, in $\psi \frac{dw}{dx}$), but one integration term is not sufficient to integrate exactly the bending energy in ψ^2 (order 2). That is why Timoshenk beam elements with the same interpolation order for the deflection and the deflection angle are called "reduced integration elements". For a linear interpolation in both w and ψ, and for EI and GAK_s constant over the element, with $c_f = 0$:

$$
[K^{11}] = \frac{GAK_s}{l_e} \begin{bmatrix} 1 & -1 \\ -1 & 1 \end{bmatrix}
\tag{4.121}
$$

$$
[K^{12}] = [K^{21}] = \frac{GAK_s}{2} \begin{bmatrix} -1 & 1 \\ 1 & -1 \end{bmatrix}
\tag{4.122}
$$

$$[K^{22}] = \frac{EI}{l_e} \begin{bmatrix} 1 & -1 \\ -1 & 1 \end{bmatrix} + \frac{GAK_s l_e}{4} \begin{bmatrix} 1 & 1 \\ 1 & 1 \end{bmatrix} \quad (4.123)$$

4.4 2D Finite Elements

4.4.1 Variational formulation in 2D

To explain the principle of the FEM in 2D for 1 dependent variable, we take the example of the following typical second-order partial differential equation:

$$-\frac{\partial}{\partial x} \left(a_{11} \frac{\partial u}{\partial x} + a_{12} \frac{\partial u}{\partial y} \right) - \frac{\partial}{\partial y} \left(a_{21} \frac{\partial u}{\partial x} + a_{22} \frac{\partial u}{\partial y} \right) + a_{00} u(x,y) = f(x,y) \quad (4.124)$$

We start with the variational formulation of the problem. The Weighted integral statement is written as:

$$\forall w \sim \delta u,$$

$$0 = \int_\Omega w(x,y) \left[-\frac{\partial}{\partial x} \left(F_1(x,y) \right) - \frac{\partial}{\partial y} \left(F_2(x,y) \right) + a_{00} u(x,y) - f(x,y) \right] dxdy \tag{4.125}$$

with:

$$\begin{cases} F_1(x,y) = a_{11} \frac{\partial u}{\partial x} + a_{12} \frac{\partial u}{\partial y} \\[2mm] F_2(x,y) = a_{21} \frac{\partial u}{\partial x} + a_{22} \frac{\partial u}{\partial y} \end{cases} \tag{4.126}$$

So that we have:

$$0 = \int_\Omega w(x,y) \left[-\frac{\partial}{\partial x} \left(F_1(x,y) \right) - \frac{\partial}{\partial y} \left(F_2(x,y) \right) + a_{00} u(x,y) - f(x,y) \right] dxdy \tag{4.127}$$

The integration by parts is performed as follows:

$$\begin{cases} -w(x,y) \frac{\partial F_1(x,y)}{\partial x} = \frac{\partial w(x,y)}{\partial x} F_1(x,y) - \frac{\partial}{\partial x} \left(w(x,y) F_1(x,y) \right) \\[2mm] -w(x,y) \frac{\partial F_2(x,y)}{\partial y} = \frac{\partial w(x,y)}{\partial y} F_2(x,y) - \frac{\partial}{\partial y} \left(w(x,y) F_2(x,y) \right) \end{cases} \tag{4.128}$$

According to the divergence theorem:

$$\begin{cases} \int_\Omega \frac{\partial}{\partial x} \left(w(x,y) F_1(x,y) \right) dxdy = \oint_\Gamma w(x,y) F_1(x,y) n_x ds \\[2mm] \int_\Omega \frac{\partial}{\partial y} \left(w(x,y) F_2(x,y) \right) dxdy = \oint_\Gamma w(x,y) F_2(x,y) n_y ds \end{cases} \tag{4.129}$$

where **n** is the unit vector normal to the surface of the domain:

$$\mathbf{n} = n_x \mathbf{e_x} + n_y \mathbf{e_y} \tag{4.130}$$

The weak formulation is obtained as follows:

$\forall w \sim \delta u,$

$$\int_\Omega \frac{\partial w(x,y)}{\partial x} \left(a_{11} \frac{\partial u}{\partial x} + a_{12} \frac{\partial u}{\partial y} \right) dxdy + \int_\Omega \frac{\partial w(x,y)}{\partial y} \left(a_{21} \frac{\partial u}{\partial x} + a_{22} \frac{\partial u}{\partial y} \right) dxdy$$

$$+ \int_\Omega [a_{00} w(x,y) u(x,y) - w(x,y) f(x,y)] \, dxdy$$

$$- \oint_\Gamma w(x,y) \left[n_x \left(a_{11} \frac{\partial u}{\partial x} + a_{12} \frac{\partial u}{\partial y} \right) + n_y \left(a_{21} \frac{\partial u}{\partial x} + a_{22} \frac{\partial u}{\partial y} \right) \right] ds = 0 \tag{4.131}$$

The primary variable is:

$$u(x,y) \tag{4.132}$$

The secondary variable is:

$$q_n = n_x \left(a_{11} \frac{\partial u}{\partial x} + a_{12} \frac{\partial u}{\partial y} \right) + n_y \left(a_{21} \frac{\partial u}{\partial x} + a_{22} \frac{\partial u}{\partial y} \right) \tag{4.133}$$

The Finite Element Method provides an approximate solution of the problem over each element of the mesh:

$$u(x,y) \simeq u^e(x,y) = \Sigma_{j=1}^N u_j^e \Psi_j^e(x,y) \tag{4.134}$$

In 2D, the interpolation property is written as follows:

$$\Psi_i^e(x_j, y_j) = \delta_{ij} \tag{4.135}$$

In Ritz Method, the weight functions used in the variational formulation are assumed to be equal to the interpolation functions:

$$\forall i = 1..N, \qquad w_i(x,y) = \Psi_i^e(x,y) \tag{4.136}$$

Using Ritz method, the variational formulation can thus be written as:

$\forall w \sim \delta u,$

$$\int_\Omega \frac{\partial w(x,y)}{\partial x} \left(a_{11} \frac{\partial u}{\partial x} + a_{12} \frac{\partial u}{\partial y} \right) dxdy + \int_\Omega \frac{\partial w(x,y)}{\partial y} \left(a_{21} \frac{\partial u}{\partial x} + a_{22} \frac{\partial u}{\partial y} \right) dxdy$$

$$+ \int_\Omega [a_{00} w(x,y) u(x,y) - w(x,y) f(x,y)] \, dxdy$$

$$- \oint_\Gamma w(x,y) \left[n_x \left(a_{11} \frac{\partial u}{\partial x} + a_{12} \frac{\partial u}{\partial y} \right) + n_y \left(a_{21} \frac{\partial u}{\partial x} + a_{22} \frac{\partial u}{\partial y} \right) \right] ds = 0 \tag{4.137}$$

$$\forall i = 1..N,$$

$$\Sigma_{j=1}^N \left[\int_{\Omega^e} \frac{\partial \Psi_i(x,y)}{\partial x} \left(a_{11} \frac{\partial \Psi_j}{\partial x} + a_{12} \frac{\partial \Psi_j}{\partial y} \right) dxdy \right] u_j^e$$

$$+ \Sigma_{j=1}^N \left[\int_{\Omega^e} \frac{\partial \Psi_i(x,y)}{\partial y} \left(a_{21} \frac{\partial \Psi_j}{\partial x} + a_{22} \frac{\partial \Psi_j}{\partial y} \right) dxdy \right] u_j^e$$

$$+ \Sigma_{j=1}^N \left[\int_{\Omega^e} [a_{00} \Psi_i(x,y) \Psi_j(x,y)] \, dxdy \right] u_j^e$$

$$= \int_{\Omega^e} \Psi_i(x,y) f(x,y) dxdy + \oint_{\Gamma^e} \Psi_i(x,y) q_n(s) ds \tag{4.138}$$

The elementary matrix equations are typically of the following form:

$$[K^e]\{u^e\} = \{F^e\} + \{Q^e\} \tag{4.139}$$

$$K_{ij}^e = \int_{\Omega^e} \frac{\partial \Psi_i(x,y)}{\partial x} \left(a_{11} \frac{\partial \Psi_j}{\partial x} + a_{12} \frac{\partial \Psi_j}{\partial y} \right) dxdy$$
$$+ \int_{\Omega^e} \frac{\partial \Psi_i(x,y)}{\partial y} \left(a_{21} \frac{\partial \Psi_j}{\partial x} + a_{22} \frac{\partial \Psi_j}{\partial y} \right) dxdy + \int_{\Omega^e} [a_{00} \Psi_i(x,y) \Psi_j(x,y)] dxdy$$

$$\tag{4.140}$$

$$F_i^e = \int_{\Omega^e} \Psi_i(x,y) f(x,y) dxdy$$

$$Q_i^e = \oint_{\Gamma^e} \Psi_i(x,y) q_n(s) ds$$

4.4.2 Linear 2D Finite Elements

Like in 1D, it is convenient in 2D to work with master elements, because master elements of same shape and same interpolation order will yield the same elementary stiffness matrix. The integration required to calculate the coefficients of the elementary stiffness matrix needs to be done only once per type of master element used in the mesh. Often times, the elementary stiffness matrix coefficients are pre-calculated for a catalog of basic master elements. In this course, we will limit our study to triangular and rectangular elements. In this subsection, we derive the interpolation functions of the linear triangular and rectangular elements.

Consider a **linear triangular element** $A_1 A_2 A_3$ with $A_k(x_k, y_k)$. The approximation is:

$$u^e(x,y) = c_1 + c_2 x + c_3 y \tag{4.141}$$

Interpolation functions are linear in x and y, so:

$$\Psi_i(x,y) = b_1 + b_2 x + b_3 y \tag{4.142}$$

According to the 2D interpolation property:

$$\begin{Bmatrix} u_1^e \\ u_2^e \\ u_3^e \end{Bmatrix} = \begin{bmatrix} 1 & x_1 & y_1 \\ 1 & x_2 & y_2 \\ 1 & x_3 & y_3 \end{bmatrix} \begin{Bmatrix} c_1 \\ c_2 \\ c_3 \end{Bmatrix} \Rightarrow \begin{cases} 2A_e\, c_1 = \alpha_1^e u_1^e + \alpha_2^e u_2^e + \alpha_3^e u_3^e \\ 2A_e\, c_2 = \beta_1^e u_1^e + \beta_2^e u_2^e + \beta_3^e u_3^e \\ 2A_e\, c_3 = \gamma_1^e u_1^e + \gamma_2^e u_2^e + \gamma_3^e u_3^e \end{cases} \tag{4.143}$$

With A_e the area of the triangular element and, for $i \neq j$, $j \neq k$ and $k \neq i$:

$$\begin{cases} \alpha_i^e = x_j y_k - x_k y_j \\ \beta_i^e = y_j - y_k \\ \gamma_i^e = -(x_j - x_k) \end{cases} \tag{4.144}$$

The resulting linear interpolation functions are:
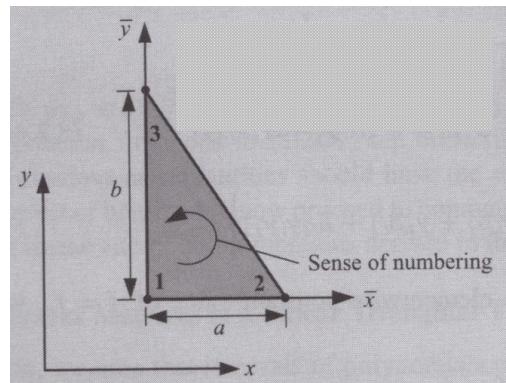
$$\Psi_i^e(x,y) = \frac{1}{2A_e} \left(\alpha_i^e + \beta_i^e x + \gamma_i^e y \right) \tag{4.145}$$

$$\begin{cases} \alpha_i^e = x_j y_k - x_k y_j \\ \beta_i^e = y_j - y_k \\ \gamma_i^e = -(x_j - x_k) \end{cases} \tag{4.146}$$

In a local coordinate system (Figure 4.10):

$$\begin{aligned} \Psi_1(\overline{x}, \overline{y}) &= 1 - \frac{\overline{x}}{a} - \frac{\overline{y}}{b} \\ \Psi_2(\overline{x}, \overline{y}) &= \frac{\overline{x}}{a} \\ \Psi_3(\overline{x}, \overline{y}) &= \frac{\overline{y}}{b} \end{aligned} \tag{4.147}$$

For the following governing equation:

Figure 4.10   Local coordinate system of a linear triangular element. Image taken from [18]

$$-\frac{\partial}{\partial x}\left(a_{11}\frac{\partial u}{\partial x} + a_{12}\frac{\partial u}{\partial y}\right) - \frac{\partial}{\partial y}\left(a_{21}\frac{\partial u}{\partial x} + a_{22}\frac{\partial u}{\partial y}\right) \tag{4.148}$$
$$+a_{00}u(x,y) = f(x,y)$$

If $a_{00} = a_{12} = a_{21} = 0$, with $a_{11} = a_{22} = k^e$:

$$[K^e] = \frac{k^e}{2ab} \begin{bmatrix} a^2 + b^2 & -b^2 & -a^2 \\ -b^2 & b^2 & 0 \\ -a^2 & 0 & a^2 \end{bmatrix} \tag{4.149}$$

If $f(x, y) = f^e$ (constant):

$$\{F^e\} = \frac{f^e \, ab}{6} \begin{Bmatrix} 1 \\ 1 \\ 1 \end{Bmatrix}$$

For the **linear rectangular element**, interpolation functions have a linear term in x, a linear term in y, and one bilinear term:

$$\Psi_i(x, y) = b_1 + b_2 \, x + b_3 \, y + b_4 \, xy \tag{4.150}$$

In a local coordinate system (Figure 4.11):
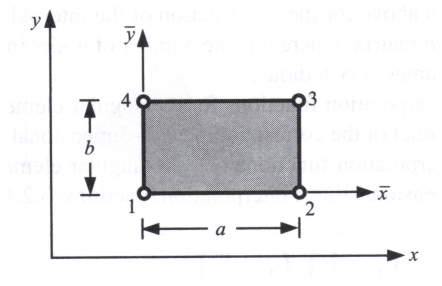
$$\begin{aligned} \Psi_1(\overline{x}, \overline{y}) &= \left(1 - \frac{\overline{x}}{a}\right)\left(1 - \frac{\overline{y}}{b}\right) \\ \Psi_2(\overline{x}, \overline{y}) &= \frac{\overline{x}}{a}\left(1 - \frac{\overline{y}}{b}\right) \\ \Psi_3(\overline{x}, \overline{y}) &= \frac{\overline{x}}{a}\frac{\overline{y}}{b} \\ \Psi_4(\overline{x}, \overline{y}) &= \left(1 - \frac{\overline{x}}{a}\right)\frac{\overline{y}}{b} \end{aligned} \tag{4.151}$$

For the governing equation:

$$\begin{aligned} -\frac{\partial}{\partial x}\left(a_{11}\frac{\partial u}{\partial x} + a_{12}\frac{\partial u}{\partial y}\right) - \frac{\partial}{\partial y}\left(a_{21}\frac{\partial u}{\partial x} + a_{22}\frac{\partial u}{\partial y}\right) \\ + a_{00}u(x, y) = f(x, y) \end{aligned} \tag{4.152}$$

If $f(x, y) = f^e$ (constant):

$$\{F^e\} = \frac{f^e \, ab}{4} \begin{Bmatrix} 1 \\ 1 \\ 1 \\ 1 \end{Bmatrix} \tag{4.153}$$

Figure 4.11   Local coordinate system of a linear reactnagular element. Image taken from [18]

If $a_{00} = a_{12} = a_{21} = 0$, with $a_{11} = a_{22} = k^e$:

$$[K^e] = \frac{k^e}{6ab} \begin{bmatrix} 2\left(a^2 + b^2\right) & a^2 - 2b^2 & -\left(a^2 + b^2\right) & b^2 - 2a^2 \\ a^2 - 2b^2 & 2\left(a^2 + b^2\right) & b^2 - 2a^2 & -\left(a^2 + b^2\right) \\ -\left(a^2 + b^2\right) & b^2 - 2a^2 & 2\left(a^2 + b^2\right) & a^2 - 2b^2 \\ b^2 - 2a^2 & -\left(a^2 + b^2\right) & a^2 - 2b^2 & 2\left(a^2 + b^2\right) \end{bmatrix} \tag{4.154}$$

The assembling process in 2D is similar to that in 1D. Figure 4.12 gives an overview of the procedure for a mesh with different types of 2D elements.

The boundary integrals $\{Q\}$ are computed on the external boundaries of the domain only (the other boundary integrals balance each other due to connectivity conditions):
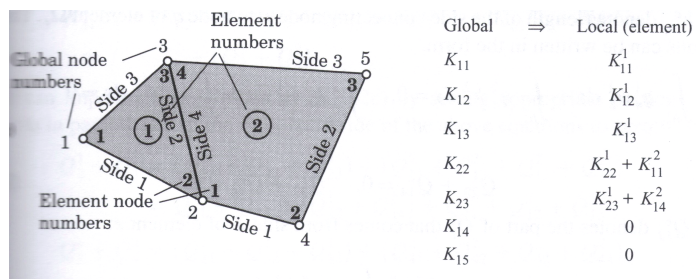
$$Q_i^e = \oint_{\Gamma^e} \Psi_i^e(x, y) q_n(s) ds \tag{4.155}$$

We perform a coordinate change to get x(s), y(s):

$$Q_i^e = \oint_{\Gamma^e} \Psi_i^e(s) q_n(s) ds \tag{4.156}$$

The boundary integral is the sum of 1D integrals defined on the sides of the 2D element. If the linear element has P sides, each of which being delimited by nodes P_1 and P_2:

$$Q_i^e = \sum_{k=1}^{P} \int_{\text{side k, node } P_1}^{\text{side k, node } P_2} \Psi_i^e(s) q_n(s) ds \tag{4.157}$$

Figure 4.12   Assembming elements of different types in 2D.

Ψ_i is zero except at the $i - th$ node so the 1D integrals on the sides of the element that do not contain the $i - th$ node vanish. Example on a triangular element:

$$Q_1^e = \int_{1-2} \Psi_1^e(s) q_{n_{1-2}}(s) ds + \int_{3-1} \Psi_1^e(s) q_{n_{3-1}}(s) ds \qquad (4.158)$$

4.4.3 Higher-order 2D Finite Elements

In 1D, we established a methodology to calculate sets of independent interpolation functions. The idea is to solve for the coefficients of polynomials of a given order. For example, if the element has N degrees of freedom, interpolation functions are sought in the form:

$$\Psi_j^e(x) = \sum_{i=1}^{N} c_i^e x^{i-1} \qquad (4.159)$$

Since the dependent variable is approximated as:

$$u^e(x) \simeq \sum_{j=1}^{N} u_j^e \Psi_j^e(x) \qquad (4.160)$$

and since in the FEM, the approximate solution is designed to be exact at the nodes, we have:

$$\begin{Bmatrix} u_1^e \\ ... \\ u_N^e \end{Bmatrix} = \begin{bmatrix} 1 & x_1 & ... & x_1^N \\ ... & ... & ... & ... \\ 1 & x_N & ... & x_N^N \end{bmatrix} \begin{Bmatrix} c_1^e \\ ... \\ c_N^e \end{Bmatrix} \qquad (4.161)$$

which is a system of equations that can be solved for the unknown coefficients c_i^e. The coefficients c_i^e determine the expression of the interpolation functions.

A similar procedure can be adopted in 2D to find the expressions of the interpolation functions of master elements of higher order. Having a library of interpolation functions of higher order is useful, because it allows computing elementary integrals over standardized master elements and using a geometric transform to get back to the current element, with redundant elementary computations. We start with **quadratic elements** (Figure 4.13). The general form of the interpolation functions of the quadratic triangular element is:

$$\Psi_i(x, y) = b_1 + b_2 x + b_3 y + b_4 xy + b_5 x^2 + b_6 y^2 \qquad (4.162)$$
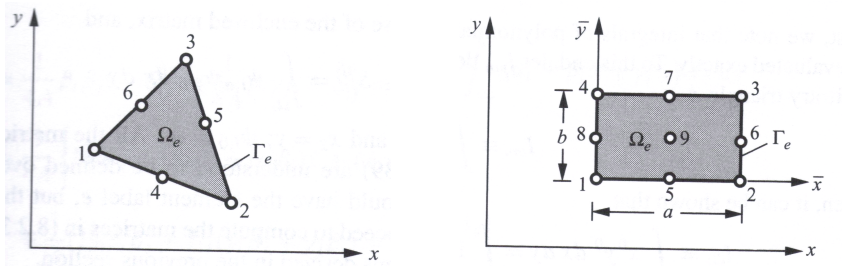
The general form of the interpolation functions of the 9-node quadratic rectangular element is:

$$\Psi_i(x, y) = b_1 + b_2 x + b_3 y + b_4 xy + b_5 x^2 + b_6 y^2 + b_7 xy^2 + b_8 x^2 y + b_9 x^2 y^2 \qquad (4.163)$$
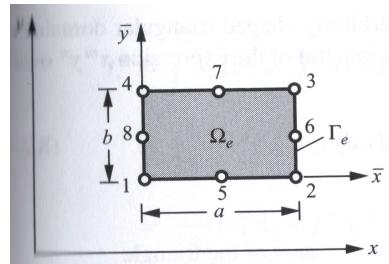
The so-called "serendipity element" is an 8-node rectangular element, similar to the 9-node rectangular element, but without internal node (Figure 4.14). The serendipity element has one less degree of freedom than the regular quadratic element so calculations made with serendipity elements are faster. Besides, the degree of freedom in the center of the element

is not subjected to continuity conditions, so removing the central node of a rectangular element does not significantly decrease the accuracy of the FEM solution. The general form of the interpolation functions of the 8-node quadratic rectangular element is:

$$\Psi_i(x, y) = b_1 + b_2\, x + b_3\, y + b_4\, xy + b_5\, x^2 + b_6\, y^2 + b_7\, xy^2 + b_8\, x^2 y \qquad (4.164)$$


Figure 4.13   Quadratic triangular and rectangular elements. Image taken from [18]


Figure 4.14   Serendipity element. Image taken from [18]

It is not straightforward to calculate the b_i coefficients using the same method as in 1D, because it that method requires inverting a large matrix. Here, we present more efficient

techniques that can be used to find the interpolation functions of quadratic elements and **elements of higher order**. For triangular elements, we define area coordinates as follows:

$$L_i = \frac{A_i}{A} = \frac{s}{h}, \qquad i = 1, 2, 3 \tag{4.165}$$

We verify the interpolation property for a linear element:

$$L_i(x_j, y_j) = L_i(s_j) = \delta_{ij}, \qquad i, j = 1, 2, 3 \tag{4.166}$$

Area coordinates can be viewed as linear interpolation functions (Figure 4.15).

If a triangular element has k nodes per side (Figure 4.16, the number of nodes per element is:

$$N = k + (k - 1) + \dots + 1 = \sum_{i=0}^{k-1}(k - i) \tag{4.167}$$

$$N = \frac{k^2}{2} + \frac{k}{2} = \frac{1}{2}k(k + 1) \tag{4.168}$$

There are k unknown coefficients per polynomial interpolation function, so the degree of the interpolation polynomials is k-1. So, p^{th}-order Lagrange elements are interpolated on each side by p^{th}-order interpolation polynomials expressed with the boundary coordinate s. For the pth node on a side that has k equally spaced nodes, we define:

$$s_p = \frac{p}{k - 1} \sim \frac{s}{h} \tag{4.169}$$

The positions of the nodes are distributed on Pascal's triangle:

$$1$$
$$x \qquad y$$
$$x^2 \qquad xy \qquad y^2$$
$$x^3 \qquad x^2y \qquad xy^2 \qquad y^3$$

At the vertices of the triangle:

$$\Psi_I(s) = 1 \quad on \quad s_{k-1}, \qquad \Psi_I(s) = 0 \quad on \quad s_0, s_1, \dots, s_{k-2} \tag{4.170}$$

with:

$$L_I(s) = \frac{s}{h} = s_p \quad \text{for equally spaced nodes} \tag{4.171}$$
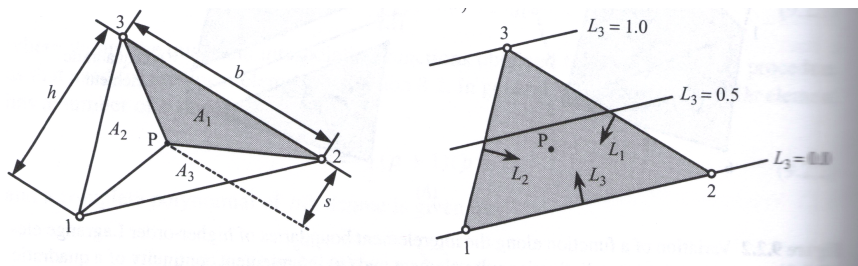
A $(k-1)^{th}$ order polynomial allows solving for k-1 roots while satisfying 1 normalization condition:

$$\Psi_I(s) = \frac{L_I(s) - s_0}{s_{k-1} - s_0} \frac{L_I(s) - s_1}{s_{k-1} - s_1} \dots \frac{L_I(s) - s_{k-2}}{s_{k-1} - s_{k-2}} = \Pi_{p=1}^{k-2}\left(\frac{L_I(s) - s_p}{s_{k-1} - s_p}\right) \tag{4.172}$$
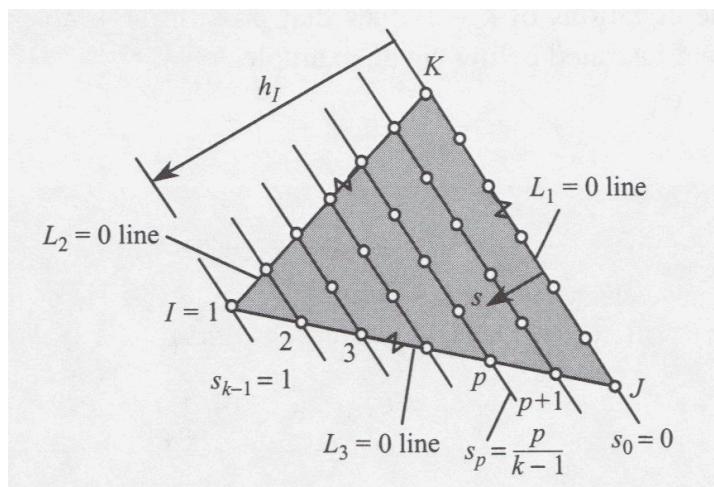
Out of the vertices of the triangle:

$$\Psi_i(s) = \Pi_{j=1}^{k-1}\left(\frac{f_j}{f_j^i}\right) \tag{4.173}$$

$f_j^i = f_j(x_i, y_i)$, with f_j a function of L_1, L_2 and L_3.

**Figure 4.15**   Area coordinates and linear interpolation on a triangular element. Image taken from [18]

Figure 4.16   Triangular element of higher order. Image taken from [18]

Linear $(p=1)$

$$\begin{bmatrix} \psi_1 & \psi_3 \\ \psi_2 & \psi_4 \end{bmatrix} = \begin{Bmatrix} 1 - \dfrac{x}{a} \\[2mm] \dfrac{x}{a} \end{Bmatrix} \begin{Bmatrix} 1 - \dfrac{y}{b} & \dfrac{y}{b} \end{Bmatrix}$$

$$= \begin{bmatrix} \left(1 - \dfrac{x}{a}\right)\left(1 - \dfrac{y}{b}\right) & \left(1 - \dfrac{x}{a}\right)\dfrac{y}{b} \\[3mm] \dfrac{x}{a}\left(1 - \dfrac{y}{b}\right) & \dfrac{x}{a}\dfrac{y}{b} \end{bmatrix}$$

Quadratic $(p=2)$
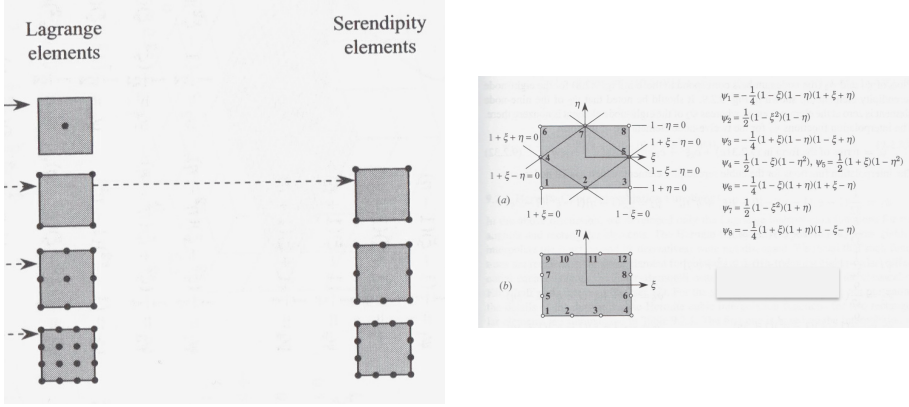
$$\begin{bmatrix} \psi_1 & \psi_4 & \psi_7 \\ \psi_2 & \psi_5 & \psi_8 \\ \psi_3 & \psi_6 & \psi_9 \end{bmatrix} = \begin{Bmatrix} \dfrac{\left(x - \frac{1}{2}a\right)(x - a)}{\left(-\frac{1}{2}a\right)(-a)} \\[3mm] \dfrac{x(x - a)}{\frac{1}{2}a\left(\frac{1}{2}a - a\right)} \\[3mm] \dfrac{x\left(x - \frac{1}{2}a\right)}{a\left(\frac{1}{2}a\right)} \end{Bmatrix} \begin{Bmatrix} \dfrac{\left(y - \frac{1}{2}b\right)(y - b)}{\frac{1}{2}b^2} \\[3mm] \dfrac{y(y - b)}{-\frac{1}{4}b^2} \\[3mm] \dfrac{y(y - b/2)}{\frac{1}{2}b^2} \end{Bmatrix}^T$$

Figure 4.17 Interpolation functions of rectangular elements by convolution of 1D interpolation functions. Image taken from [18]

Interpolation polynomials of higher-order rectangular elements can be found by doing a convolution of 1D interpolation functions:

$$[\Psi_i(x,y)] = \{\Psi_i(x)\}^T\{\Psi_i(y)\}$$

Figure 4.17 illustrates the process. However, the convolution technique does not work for serendipity elements, which do not have internal nodes (Figure 4.18).


Figure 4.18   Construction of rectangular serendipity elements and derivation of their interpolation functions. Image taken from [18]

We note that if polynomials of pth order are used to interpolate on a rectangular element, that element must have $N = (p+1)^2$ nodes (unless it is a serendipity element). The $N = (p+1)^2$ independent monomials that are involved in the expression of the interpolation polynomials of pth order can be found by using Pascal's triangle technique, as explained in Figure 4.19. PAscal's triangle can also be used to find the monomials involved in the serendipity elements of higher-order, see Figure 4.20.

4.5   Master elements and numerical integration
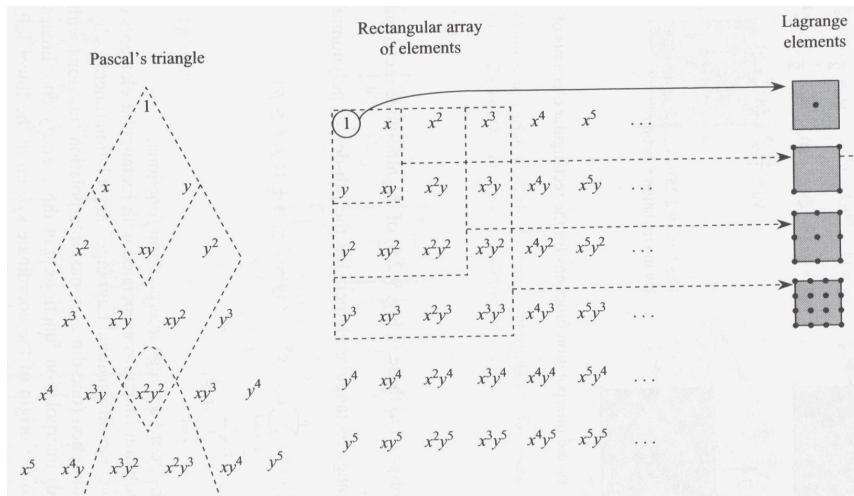
4.5.1   Coordinate transformation

In 2D dimensions, the boundaries of the domain are typically irregular. The mesh usually approximates the shape of the domain, which yields a geometric interpolation. In the same was as the dependent variable $u(x,y)$ is interpolated:
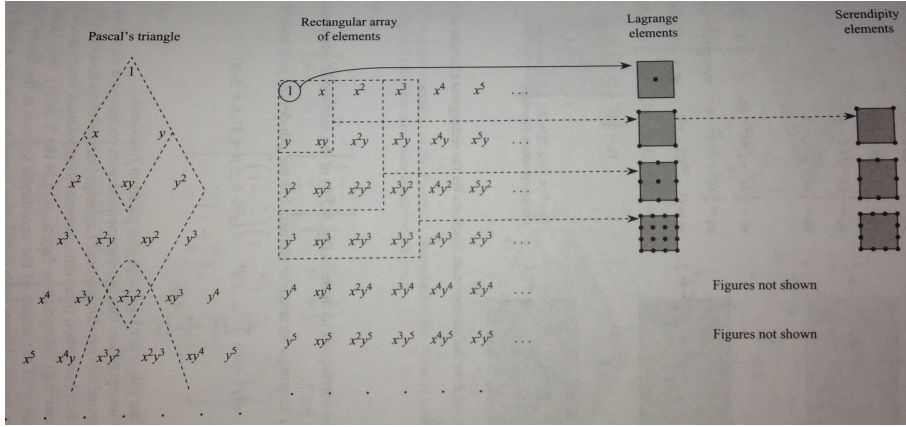
$$u^e(x,y) \simeq \Sigma_{j=1}^{N} u_j^e \Psi_j^e(x,y) \tag{4.174}$$

the geometry is also interpolated, i.e. the coordinates of the points inside an element are interpolated between the coordinates of the nodes of that element:

$$x \simeq \Sigma_{j=1}^{M} x_j^e \widehat{\Psi}_j^e(\xi,\eta), \qquad y \simeq \Sigma_{j=1}^{M} y_j^e \widehat{\Psi}_j^e(\xi,\eta) \tag{4.175}$$

Figure 4.19 Pascal's triangle used to find the monomials involved in the interpolation functions of a higher-order rectangular elements. Image taken from [18]

Figure 4.20   Pascal's triangle used to find the monomials involved in the interpolation functions of a higher-order rectangular **serendipity** elements. Image taken from [18]

Three types of elements exist:
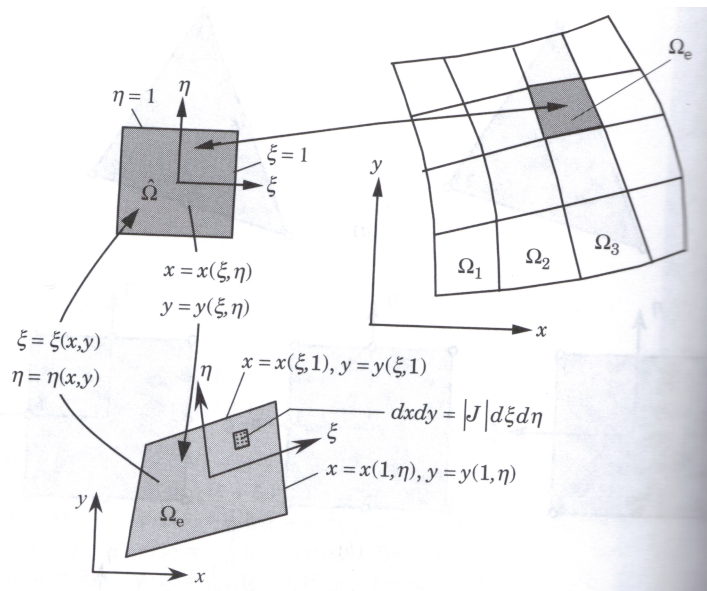
- If the order of the geometric interpolation is equal to the order of the interpolation of the dependent variable (M=N), the element is isoparametric (most common);

- If the order of the geometric interpolation is less than the order of interpolation of the dependent variable (M¡N), the element is subparametric (eg, deflection of an Euler-Bernouilli beam);

- If the order of the geometric interpolation is greater than the order of interpolation of the dependent variable (M¿N), the element is superparametric (scarce).

Interpolation functions are expressed in the local coordinate system of master elements, and the elementary stiffness of all master elements of the same type are equal. However in an actual mesh, not all elements have the shape of a master element. For instance, a mesh may contain distorted quadrilaterals instead of 2x2 square master elements. So in order to take advantage of redundant formulas over master elements, a coordinate transform is needed, from the coordinate system of the actual element (x,y) to that of the master element (ξ, η), and vice versa (Figure 4.21).

The coordinate change is performed by means of the Jacobian matrix $[J]$, as follows:

$$x \simeq \Sigma_{j=1}^{M} x_j^e \widehat{\Psi}_j^e(\xi, \eta), \qquad y \simeq \Sigma_{j=1}^{M} y_j^e \widehat{\Psi}_j^e(\xi, \eta) \tag{4.176}$$

$$[J] = \begin{bmatrix} \frac{\partial x}{\partial \xi} & \frac{\partial y}{\partial \xi} \\ \\ \frac{\partial x}{\partial \eta} & \frac{\partial y}{\partial \eta} \end{bmatrix} = \begin{bmatrix} \Sigma_{j=1}^{M} x_j \frac{\partial \widehat{\Psi}_j}{\partial \xi} & \Sigma_{j=1}^{M} y_j \frac{\partial \widehat{\Psi}_j}{\partial \xi} \\ \\ \Sigma_{j=1}^{M} x_j \frac{\partial \widehat{\Psi}_j}{\partial \eta} & \Sigma_{j=1}^{M} y_j \frac{\partial \widehat{\Psi}_j}{\partial \eta} \end{bmatrix} \tag{4.177}$$

Figure 4.21   Principle of the coordinate transform. Image taken from [18]

$$
[J] \;=\; \begin{bmatrix} \frac{\partial \widehat{\Psi}_1}{\partial \xi} & \frac{\partial \widehat{\Psi}_2}{\partial \xi} & \cdots & \frac{\partial \widehat{\Psi}_M}{\partial \xi} \\[2mm] \frac{\partial \widehat{\Psi}_1}{\partial \eta} & \frac{\partial \widehat{\Psi}_2}{\partial \eta} & \cdots & \frac{\partial \widehat{\Psi}_M}{\partial \eta} \end{bmatrix} \begin{bmatrix} x_1 & y_1 \\[1mm] x_2 & y_2 \\[1mm] \cdots & \cdots \\[1mm] x_M & y_M \end{bmatrix} \tag{4.178}
$$

Computing the stiffness matrix requires computing:

$$
\left\{ \begin{array}{c} \frac{\partial \Psi_i^e}{\partial x} \\[2mm] \frac{\partial \Psi_i^e}{\partial y} \end{array} \right\} = \begin{bmatrix} \frac{\partial \xi}{\partial x} & \frac{\partial \eta}{\partial x} \\[2mm] \frac{\partial \xi}{\partial y} & \frac{\partial \eta}{\partial y} \end{bmatrix} \left\{ \begin{array}{c} \frac{\partial \Psi_i^e}{\partial \xi} \\[2mm] \frac{\partial \Psi_i^e}{\partial \eta} \end{array} \right\} = [J]^{-1} \left\{ \begin{array}{c} \frac{\partial \Psi_i^e}{\partial \xi} \\[2mm] \frac{\partial \Psi_i^e}{\partial \eta} \end{array} \right\} \tag{4.179}
$$

so that the Jacobian matrix must be inversible:

$$
J \;=\; det[J] \;=\; \frac{\partial x}{\partial \xi}\frac{\partial y}{\partial \eta} - \frac{\partial x}{\partial \eta}\frac{\partial y}{\partial \xi} \;\neq\; 0 \tag{4.180}
$$

If nodes are numbered in the same sequence (e.g., counter clockwise) in the current and master elements:

$$
J \;=\; det[J] \;=\; \frac{\partial x}{\partial \xi}\frac{\partial y}{\partial \eta} - \frac{\partial x}{\partial \eta}\frac{\partial y}{\partial \xi} \;>\; 0 \tag{4.181}
$$

Also note this useful formula:

$$
dA \;=\; dx\,dy \;=\; J\,d\xi\,d\eta \tag{4.182}
$$

4.5.2 Numerical integration

The calculation of the stiffness matrix of higher-order elements can be quite involved, because of the complex functions to be integrate d(especially for higher-order interpolation), and/or because of the complex shape of the elements. For this reason, it is necessary to expedite some of the calculations by using approximation methods. In the following, we explain the principle of numerical integration, which allows approximating complex integral expressions.

In 1D, the Newton-Cotes quadrature consists in approximating a function by doing a linear interpolation between values of that functions reached at equally spaced points (Figure 4.22):

$$
\forall r > 1, \quad \int_a^b F(x)dx \;\simeq\; (b-a)\sum_{I=1}^{r} w_I \widehat{F}\left(\frac{I-1}{r-1}(b-a) + a \right) \tag{4.183}
$$

A Newton-Cotes quadrature of order r depends on r weight coefficients w_I.

- $r = 1$: the numerical approximation provides the exact integral if F is a polynomial of order $r - 1 = 0$, i.e. if $F=1$:
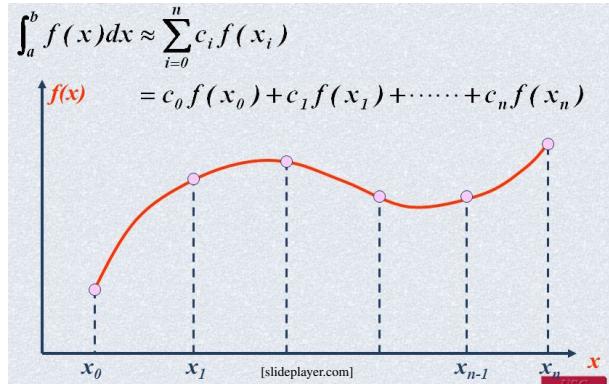
$$
\int_a^b 1dx \;=\; (b-a)\,w_1 \;\Rightarrow\; w_1 = 1
$$

- $r = 2$: the numerical approximation provides the exact integral if F is a polynomial of order $r - 1 = 1$, i.e. if $F=1$ or $F=x$:

$$\begin{cases} (b-a) = \int_a^b 1dx = (b-a)(w_1 + w_2) \\ \frac{b^2-a^2}{2} \int_a^b xdx = (b-a)(w_1\,a + w_2\,b) \end{cases} \Rightarrow w_1 = w_2 = 0.5$$

- $r = 3$: the numerical approximation provides the exact integral if F is a polynomial of order $r - 1 = 2$, i.e. if $F=1$ or $F=x$ or $F=x^2$. We get: $w_1 = w_3 = 1/6;\ w_2 = 4/6$.

Newton-cotes quadrature is exact for polynomials F of order r when r is odd, and for polynomials F or order $r - 1$ when r is even.

Figure 4.22   Principle of Newton-Cotes quadrature.

In 1D, the Gauss-Legenre quadrature is written:

$$\int_a^b F(x)dx = \int_{-1}^{+1} \widehat{F}(\xi)d\xi \simeq \Sigma_{I=1}^r \widehat{F}(\xi_I)w_I \tag{4.184}$$

in which $\widehat{F}(\xi)$ is the integrand, expressed on the master element. The Gauss-Legenre quadrature of order r depends on r weight coefficients w_I and r integration points ξ_I. The numerical approximation provides the exact integral for polynomials of order p if $r \geq int\left[\frac{p+1}{2}\right]$.

- $r = 1$: $\widehat{F} = 1$ or $\widehat{F} = x$:

$$2 = \int_{-1}^{+1} 1dx = w_1 \times 1 \Rightarrow w_1 = 2, \qquad 0 = \int_{-1}^{+1} xdx = w_1 \times \xi_1 \Rightarrow \xi_1 = 0$$

- $r = 2$: $\widehat{F} = 1$ or $\widehat{F} = x$ or $\widehat{F} = x^2$ or $\widehat{F} = x^3$:

$$2 = \int_{-1}^{+1} 1dx = w_1 + w_2, \qquad 0 = \int_{-1}^{+1} xdx = w_1\xi_1 + w_2\xi_2$$

$$\frac{2}{3} = \int_{-1}^{+1} x^2 dx = w_1(\xi_1)^2 + w_2(\xi_2)^2, \qquad 0 = \int_{-1}^{+1} x^3 dx = w_1(\xi_1)^3 + w_2(\xi_2)^3$$

$$\Rightarrow w_1 = w_2 = 1, \quad \xi_1 = -\frac{1}{\sqrt{3}}, \quad \xi_2 = \frac{1}{\sqrt{3}}$$

In 2D, the Gauss-Legendre quadrature allows approximating an elementary integral defined on the rectangular domain Ω^e into an integral defined on the rectangular master element $\widehat{\Omega}^e = [(-1,1);(1,1);(1,-1);(-1,-1)]$:

$$\int_{\Omega^e} F(x,y)dxdy = \int_{\widehat{\Omega}^e} \widehat{F}(\xi,\eta)Jd\xi d\eta = \int_{-1}^{+1}\left[\int_{-1}^{+1} J\widehat{F}(\xi,\eta)d\eta\right]d\xi \tag{4.185}$$
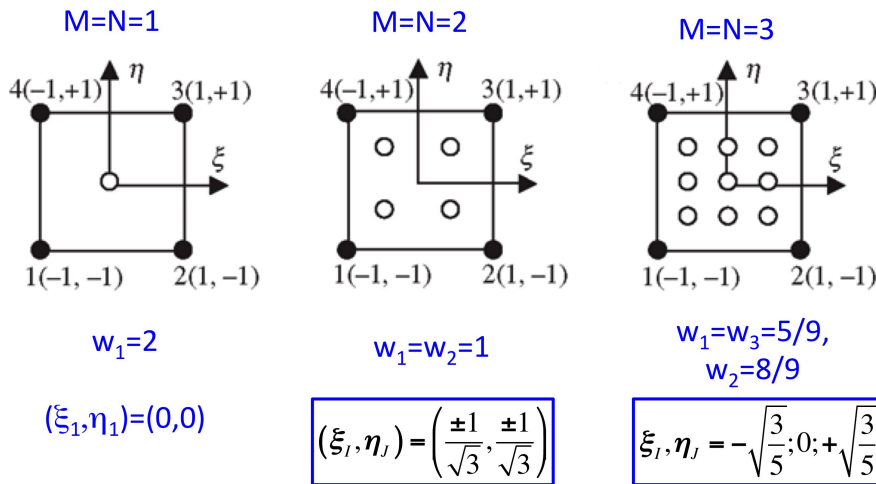
First approximation:

$$\int_{-1}^{+1}\left[\int_{-1}^{+1} J\widehat{F}(\xi,\eta)d\eta\right]d\xi \simeq \int_{-1}^{+1}\left[\Sigma_{J=1}^{R_2} J\widehat{F}(\xi,\eta_J)W_J\right]d\xi \tag{4.186}$$

Second approximation:

$$\int_{-1}^{+1}\left[\Sigma_{J=1}^{R_2} J\widehat{F}(\xi,\eta_J)W_J\right]d\xi \simeq \Sigma_{I=1}^{R_1}\Sigma_{J=1}^{R_2} J\widehat{F}(\xi_I,\eta_J)W_I W_J \tag{4.187}$$

The weights and the coordinates of the integration points in 2D, (w_I, ξ_I) and (w_J, η_J), can be deduced from those in 1D, as explained in Figure 4.23.


Figure 4.23   Link between the 1D and 2D Gauss-Legendre quadratures. Image taken from [18].

For a linear triangular element, for $i, j = 1, 2, 3$:

$$\Psi_i(x_j, y_j) = L_i = \frac{A_i}{A}, \quad \Psi_i(x_j, y_j) = \delta_{ij}, \quad \Sigma_{i=1}^3 \Psi_i(x_j) = 1 \tag{4.188}$$

The linear interpolation of the geometry imposes:

$$\int_{\Omega^e} F(x,y)dxdy = \int_{\widehat{\Omega}^e} \widehat{F}(\xi,\eta)Jd\xi d\eta = \int_{\widehat{\Omega}^e} \widetilde{F}(L_1,L_2,L_3)dL_1 dL_2$$

Then, for or R integration points, we have:

$$\int_{\widehat{\Omega}^e} \widetilde{F}(L_1,L_2,L_3)dL_1 dL_2 \simeq \frac{1}{2}\Sigma_{I=1}^R W_I \widetilde{F}(S_I)$$

S_I depends on L_1, L_2, L_3, which gives the coordinates of the integration points.

4.6   FEM for Plane Elasticity

4.6.1   Weak formulation in plane elasticity

In linear elasticity, the constitutive equation is:

$$\epsilon_{ij} = \frac{1+\nu}{E}\sigma_{ij} - \frac{\nu}{E}\sigma_{kk}\delta_{ij} \tag{4.189}$$

The balance equations in 2D are:

$$\begin{cases} \frac{\partial \sigma_{xx}}{\partial x} + \frac{\partial \sigma_{xy}}{\partial y} + f_x = \rho\frac{\partial^2 u_x}{\partial t^2} \\[2mm] \frac{\partial \sigma_{yx}}{\partial x} + \frac{\partial \sigma_{yy}}{\partial y} + f_y = \rho\frac{\partial^2 u_y}{\partial t^2} \end{cases} \tag{4.190}$$

The boundary conditions are written:

$$\begin{cases} u_i = \widehat{u}_i \quad on \quad \Gamma_u \\[2mm] \sigma_{ij}n_j = \widehat{t}_i \quad on \quad \Gamma_\sigma \end{cases} \tag{4.191}$$

$$\Gamma_u \cup \Gamma_\sigma = \Gamma, \qquad \Gamma_u \cap \Gamma_\sigma = \emptyset \tag{4.192}$$

The relationship between displacement and strains is noted in a matrix form, as follows:

$$\begin{Bmatrix} \epsilon_{xx} \\ \epsilon_{yy} \\ 2\epsilon_{xy} \end{Bmatrix} = \begin{bmatrix} \partial/\partial x & 0 \\ 0 & \partial/\partial y \\ \partial/\partial y & \partial/\partial x \end{bmatrix} \begin{Bmatrix} u_x \\ u_y \end{Bmatrix} = [B]\begin{Bmatrix} u_x \\ u_y \end{Bmatrix} \tag{4.193}$$

In plane elasticity, the constitutive model takes the following matrix form:

$$\begin{Bmatrix} \sigma_{xx} \\ \sigma_{yy} \\ \sigma_{xy} \end{Bmatrix} = \begin{bmatrix} c_{11} & c_{12} & 0 \\ c_{12} & c_{22} & 0 \\ 0 & 0 & c_{66} \end{bmatrix} \begin{Bmatrix} \epsilon_{xx} \\ \epsilon_{yy} \\ 2\epsilon_{xy} \end{Bmatrix} = [D_e]\begin{Bmatrix} \epsilon_{xx} \\ \epsilon_{yy} \\ 2\epsilon_{xy} \end{Bmatrix} \tag{4.194}$$

in which the coefficients c_{11}, c_{12}, c_{22} and c_{66} depend on whether the problem is in plane stress or plane strain. The weak formulation comprises two equations. From the balance

equation in the x-direction: $\forall w_1(x,y) \sim \delta u_x(x,y)$:

$$\int_{\Omega_e} \left[h_e \left[\frac{\partial w_1}{\partial x} \left(c_{11} \frac{\partial u_x}{\partial x} + c_{12} \frac{\partial u_y}{\partial y} \right) + c_{66} \frac{\partial w_1}{\partial y} \left(\frac{\partial u_x}{\partial y} + \frac{\partial u_y}{\partial x} \right) \right] + \rho w_1 \ddot{u}_x \right] dxdy$$

$$= \int_{\Omega_e} h_e w_1 f_x dxdy + \oint_{\Gamma_e} h_e w_1 \widehat{t_x} ds$$

(4.195)

From the balance equation in the y-direction: $\forall w_2(x,y) \sim \delta u_y(x,y)$:

$$\int_{\Omega_e} \left[h_e \left[\frac{\partial w_2}{\partial y} \left(c_{12} \frac{\partial u_x}{\partial x} + c_{22} \frac{\partial u_y}{\partial y} \right) + c_{66} \frac{\partial w_2}{\partial x} \left(\frac{\partial u_x}{\partial y} + \frac{\partial u_y}{\partial x} \right) \right] + \rho w_2 \ddot{u}_y \right] dxdy$$

$$= \int_{\Omega_e} h_e w_2 f_y dxdy + \oint_{\Gamma_e} h_e w_2 \widehat{t_y} ds$$

(4.196)

in which h_e is the thickness of the element, with $d\Omega_e = h_e dxdy$. There are now two dependent variables (the displacements in the x- and y- directions). It is convenient to sort all the displacement degrees of freedom by node as opposed to direction. We note $\{\Delta\}$ the global vector of degrees of freedom (d.o.f.), with u_x and u_y d.o.f. at each node, and for N nodes on the mesh:

$$\{\Delta\} = \begin{Bmatrix} u_x^1 \\ u_y^1 \\ u_x^2 \\ u_y^2 \\ ... \\ u_x^N \\ u_y^N \end{Bmatrix}$$

(4.197)

We define the interpolation matrix as follows:

$$[\Psi] = \begin{bmatrix} \Psi_1 & 0 & \Psi_2 & 0 & ... & \Psi_N & 0 \\ 0 & \Psi_1 & 0 & \Psi_2 & ... & 0 & \Psi_N \end{bmatrix}$$

(4.198)

The elementary matrix equations are:

$$\left(\int_{\Omega_e} [\Psi]^T [B]^T [D_e] [B][\Psi]dV \right) \{\Delta\} + \left(\int_{\Omega_e} \rho[\Psi]^T [\Psi]dV \right) \{\ddot{\Delta}\}$$

(4.199)

$$= \int_{\Omega_e} [\Psi]^T \{f\}dV + \oint_{\Gamma_e} [\Psi]^T \{\widehat{t}\}dS$$

For assembling purposes, we reorganize the equation in $\begin{Bmatrix} \{u_x\} \\ \{u_y\} \end{Bmatrix}$ instead of $\{\Delta\}$:

$$\begin{bmatrix} [M] & [0] \\ [0] & [M] \end{bmatrix} \begin{Bmatrix} \{\ddot{u}_x\} \\ \{\ddot{u}_y\} \end{Bmatrix} + \begin{bmatrix} [K_{11}] & [K_{12}] \\ [K_{12}]^T & [K_{22}] \end{bmatrix} \begin{Bmatrix} \{u_x\} \\ \{u_y\} \end{Bmatrix} = \begin{Bmatrix} \{F_x^{tot}\} \\ \{F_y^{tot}\} \end{Bmatrix}$$

(4.200)

4.6.2 Numerical integration in plane elasticity

We have independent d.o.f. u_x, u_y, so the interpolation will onl depend on nodal values of the dependent functions, i.e. we will need Lagrange interpolation functions for both

dependent variables $u_x(x, y)$ and $u_y(x, y)$. The two dependent variables have the same physical dimension (displacements), so we will use the same order of interpolation for both u_x and u_y:

$$u_x^e(x, y) \simeq \sum_{j=1}^{N} u_{xj}^e \Psi_j(x, y), \qquad u_y^e(x, y) \simeq \sum_{j=1}^{N} u_{yj}^e \Psi_j(x, y) \tag{4.201}$$

The simplest elements are the linear triangular element and the linear rectangular element, with 2 d.o.f. per node (N nodes, 2N d.o.f.). Even for linear elements, stiffness and mass matrices are often computed by a numerical integration. Sometimes, it is possible to calculate [K] analytically for triangular elements (with constant elasticity parameters). For the vector of external distributed loads $\{F\}$, it is usually possible to get analytical solutions, especially for constant external loads (f_0). For boundary integrals, a nuerical integration is almost always needed:

$$\{Q^e\} = \oint_{\Gamma_e} h_e [\Psi]^T \{\hat{t}\} ds \tag{4.202}$$

In the global coordinate system:

$$\{Q^e\} = \oint_{\Gamma_e} h_e [\Psi]^T \begin{Bmatrix} \hat{t}_x \\ \\ \hat{t}_y \end{Bmatrix} ds \tag{4.203}$$

For the sake of simplicity, $\{Q^e\}$ is often computed in a local coordinate system, related to the normal and tangential vectors characterizing the boundary Γ_e:

$$\{Q^e_{loc}\} = \oint_{\Gamma_e} h_e [\Psi]^T \begin{Bmatrix} \hat{t}_n \\ \\ \hat{t}_t \end{Bmatrix} ds \tag{4.204}$$

So we need a coordinate change:

$$\{Q^e\} = [R]^T \{Q^e_{loc}\} \tag{4.205}$$

$$[R] = \begin{bmatrix} cos\alpha & sin\alpha & 0 & 0 & ... \\ -sin\alpha & cos\alpha & 0 & 0 & ... \\ 0 & 0 & cos\alpha & sin\alpha & ... \\ 0 & 0 & -sin\alpha & cos\alpha & ... \\ ... & ... & ... & ... & ... \end{bmatrix} \tag{4.206}$$

with α the inclination angle of the element surface.
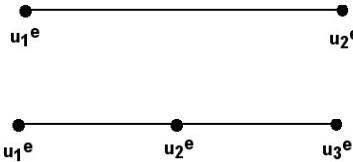
PROBLEMS

4.1   Write the variational formulation of the following problem:

$$\frac{d^2}{dx^2} \left[EI \frac{d^2 u(x)}{dx^2} \right] - q_0 = 0, \quad 0 < x < L$$

$$u(0) = \left[\frac{du(x)}{dx} \right]_{x=0} = 0, \quad EI \left[\frac{d^2 u(x)}{dx^2} \right]_{x=L} = -M_0, \quad EI \left[\frac{d^3 u(x)}{dx^3} \right]_{x=L} = F_0$$

4.2   Find the expression of the interpolation functions of order 1 is by using the interpolation property. Consider elements with 2 and 3 nodes.

Figure 4.24   Problem 4.2.

4.3   Consider the following boundary value problem:

$$-\frac{d^2 u(x)}{dx^2} - u(x) + x^2 = 0, \quad 0 < x < 1$$

$$u(0) = u(1) = 0$$
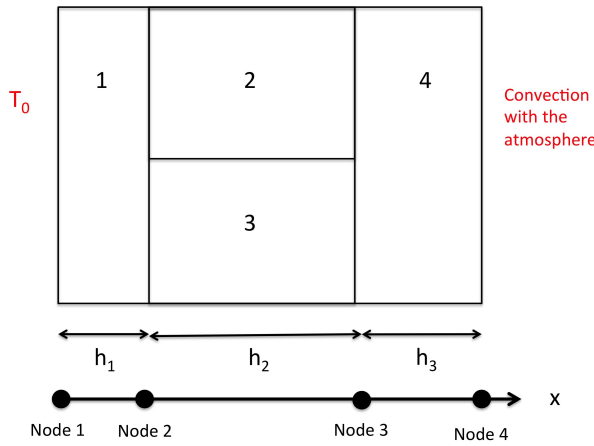
Provide the FEM equations to solve for the unknown primary and secondary variables when the domain is discretized with: (a) four linear elements; (b) two quadratic elements (Figure 4.25).

Figure 4.25   Meshes considered in Problem 4.3.

4.4   Solve the problem of heat transfer through the composite wall shown in Figure 4.26 by using Ritz method, with four linear elements.
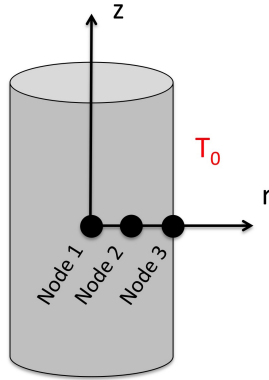
$$-\frac{\partial}{\partial x}\left(kA\frac{\partial T}{\partial x}\right) + \beta P(T - T_\infty) = Aq_0$$

Figure 4.26   Heat transfer through a composite wall.

4.5   Solve the problem of heat transfer through the cylindrical canister shown in Figure 4.27 by using Ritz method, with two linear elements.

$$-\frac{1}{r}\frac{d}{dr}\left(kr\frac{dT}{dr}\right) = q_0(r)$$
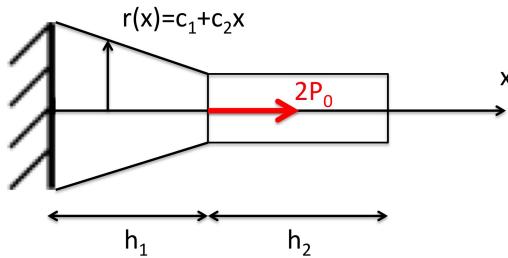
Figure 4.27   Heat transfer through a cylindrical canister.

4.6   Solve the 1D Newtonian fluid flow problem (Figure 4.6) with Ritz method (Equation 4.77), by using two linear elements, and for the two following sets of boundary conditions: (a) $v_x(-L) = v_x(L) = 0$; (b) $v_x(-L) = 0$, $v_x(L) = v_0$.
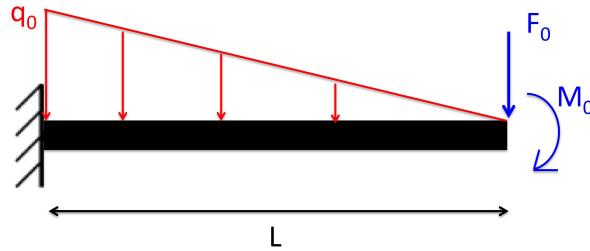
4.7   Solve the problem of bar elongation shown in Figure 4.28 by using Ritz method, with two linear elements.

$$-\frac{d}{dx}\left(EA\frac{du}{dx}\right) = f(x) \tag{4.207}$$

Figure 4.28   Bar element with a non-uniform cross section.

4.8   Solve the problem of beam deflection shown in Figure 4.29 by using two Euler-Bernouilli elements.

Figure 4.29   fig/C04/Deflection problem with Euler-Bernouilli beam elements.

4.9   Calculate the coefficients of the elementary stiffness matrix and force vector of a linear trianular element, if the numbering convention in Figure 4.10 is changed such that: node 1 is (a,0); node 2 is (0,b); node 3 is (0,0).

4.10   Calculate the three boundary integrals Q_1, Q_2 and Q_3 for the linear triangular element shown in Figure 4.30.

4.11   Consider a problem described by the Poisson's equation:
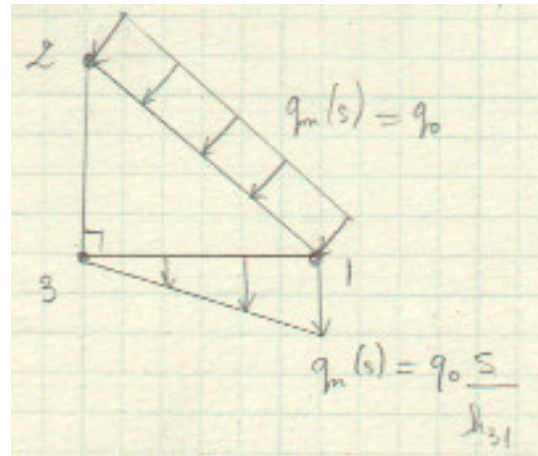
$$-\nabla^2 u = -\left(\frac{\partial^2 u}{\partial x^2} + \frac{\partial^2 u}{\partial y^2}\right) = f_0 \quad \text{in} \quad \Omega$$

in the square region shown in Figure 4.31. The boundary conditions are:
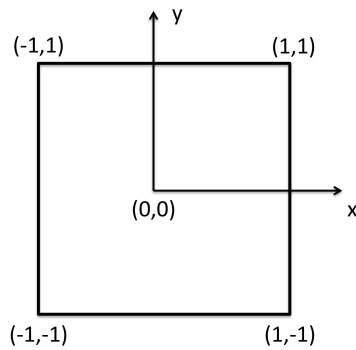
$$u(x, y) = 0 \quad \text{on} \quad \Gamma$$

We wish to use the FEM to determine $u(x, y)$ on the domain Ω.

1. Show that it is sufficient to solve the problem on 1/8-th of the domain only to determine the solution everywhere in Ω.

2. Mesh this deduced domain with four linear triangular elements (justify).

Figure 4.30   Triangular element subject to boundary loads.
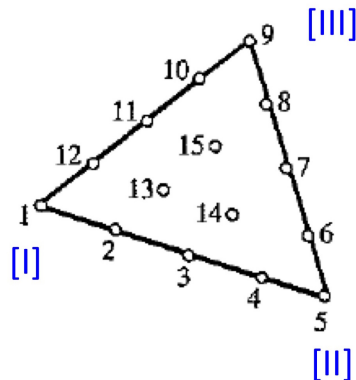
Figure 4.31   2D FEM to solve Poisson's equation

3. Solve the FEM problem on the reduced domain (i.e. calculate the unknown nodal values of the primary variable).

4. Post-process the results of the FEM model (i.e. calculate the unknown boundary integrals of the secondary variable).

4.12   Determine the Lagrange interpolation polynomials for:
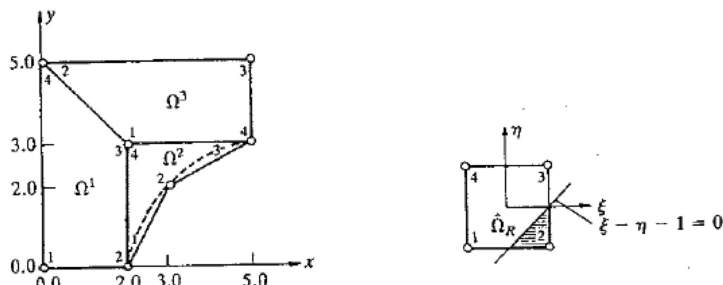
- a triangular element that has two nodes per side ($k = 2$)

- a triangular element that has three nodes per side ($k = 3$)

- a triangular element that has four nodes per side ($k = 4$)

4.13   Determine the interpolation function Ψ_{14} for the triangular element shown in Figure 4.32. *Assume that nodes on the sides of the element are equally spaced.*

Figure 4.32   A higher-order triangular element. Image taken from [18]

4.14   Calculate the Jacobian of each of the three elements of the mesh shown in Figure 4.33. Explain whether the geometry and numbering conventions are acceptable or not.

Figure 4.33   Meshing problem requiring calculating the Jacobian. Image taken from [18]

4.15   Determine the conditions on the location of node 3 of the quadrilateral element shown in Figure 4.34.
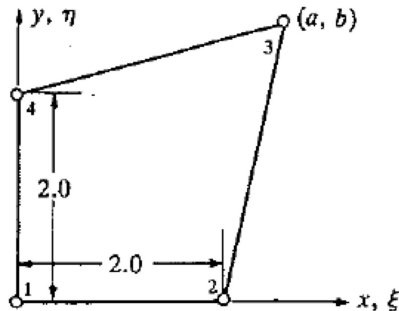
Figure 4.34   Finding an acceptable element shape. Image taken from [18]

4.16   Consider the isoparametric quadrilateral element shown iFigure 4.35. Use the Gauss-Legendre numerical integration scheme of the lowest order possible to calculate the following integrals:

$$S_{ij}^{00} = \int_{\Omega} \Psi_i(x, y)\Psi_j(x, y) dx dy$$

$$S_{ij}^{12} = \int_{\Omega} \frac{\partial \Psi_i(x, y)}{\partial x} \frac{\partial \Psi_i(x, y)}{\partial y} dx dy$$
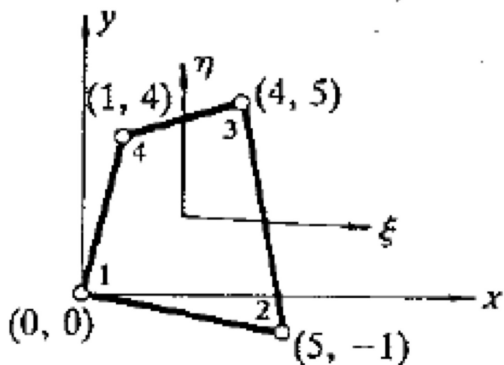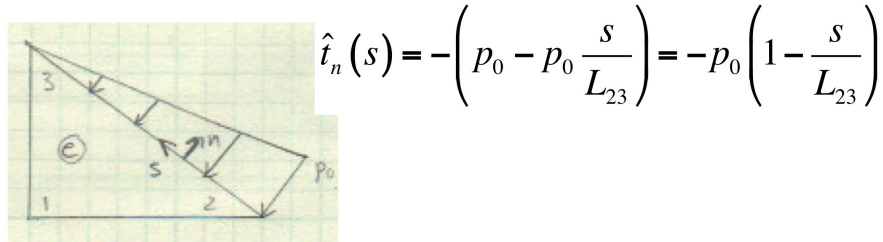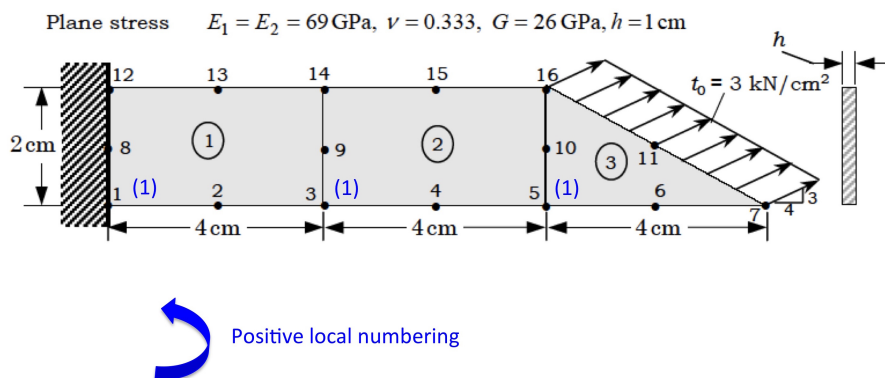
Figure 4.35   Evaluating integrals defined on an element of irregular shape. Image taken from [18]

4.17   Show that the weak formulation of a plane elasticity problem takes the form given in Equations 4.195 and 4.196.

4.18   For the Finite Element in plane elasticity shown in Figure 4.36, determine the surface load vector $\{Q_e\}$.

$$\hat{t}_n(s) = -\left(p_0 - p_0 \frac{s}{L_{23}}\right) = -p_0\left(1 - \frac{s}{L_{23}}\right)$$

Figure 4.36   Calculation of boundary integrals in plane elasticity.

4.19   In the plane stress problem shown in Figure 4.37, determine the horizontal compo-
nent of the load vector at node 16 (Q_{16x}) and the vertical component of the load vector at
node 11 (Q_{11y}).

Figure 4.37   Calculation of boundary integrals in plane elasticity.

PART II

DEFORMATION AND FLOW IN POROUS MEDIA

CHAPTER 5

ELEMENTS OF PORO-ELASTICITY

5.1 Single-phase Newtonian fluid flow in a rigid solid skeleton

5.1.1 Equation of continuity of the fluid
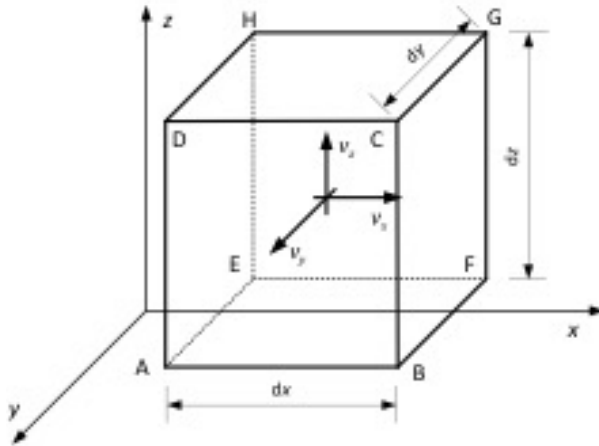
Consider the elementary soil volume shown in Figure 5.1. This volume contains solid soil particles and a single-phased fluid (say, liquid water). The fluid must satisfy the condition of continuity, or mass balance equation, which states that the net mass or weight flow of fluid into or out of a geometrically circumscribed volume in a given time interval must be equal to the storage or loss of storage of fluid in the volume in the interval.

Let us express the continuity condition for the elementary soil volume shown in Figure 5.1, in which the velocity vector of the fluid at the center of the element is noted v. Noting ρ_w the mass density of the fluid, the mass flux of the fluid through the face ADHE is:

$$\left[\rho_w \, v_x - \frac{\partial}{\partial x} \left(\rho_w \, v_x \right) \frac{dx}{2} \right] dy \, dz \tag{5.1}$$

Similarly, the mass flux of fluid through the face BCGF is:

$$\left[\rho_w \, v_x + \frac{\partial}{\partial x} \left(\rho_w \, v_x \right) \frac{dx}{2} \right] dy \, dz \tag{5.2}$$

Figure 5.1   Elementary soil volume: a single-phased incompressible Newtonian fluid flows through a non-deformable solid skeleton. Image taken from [2].

As a result, the net mass of water entering or leaving the element through faces ADHE and BCGF is given by the difference between the above two fluxes, namely:

$$\left[\frac{\partial}{\partial x} \left(\rho_w \, v_x \right) \right] dx \, dy \, dz \tag{5.3}$$

Similarly, for a component of flow that will take place in the z-direction with velocity v_y at the center of the element, the net mass flux parallel to the y-axis is:

$$\left[\frac{\partial}{\partial y} \left(\rho_w \, v_y \right) \right] dx \, dy \, dz \tag{5.4}$$

And lastly, a component of flow that will take place in the y-direction with velocity v_z at the center of the element, the net mass flux parallel to the z-axis is

$$\left[\frac{\partial}{\partial z} \left(\rho_w \, v_z \right) \right] dx \, dy \, dz \tag{5.5}$$

Based on the equations above, the rate of mass storage or loss of fluid in the element will be given by the sum of the net weight fluxes parallel to the three Cartesian axes, i.e.

$$\frac{\partial M}{\partial t} = \left[\frac{\partial}{\partial x} \left(\rho_w \, v_x \right) + \frac{\partial}{\partial y} \left(\rho_w \, v_y \right) + \frac{\partial}{\partial z} \left(\rho_w \, v_z \right) \right] dx \, dy \, dz \tag{5.6}$$

where M is the mass of fluid stored in the volume $dxdydz$. Equation 5.6 is the equation of continuity, which represents the conservation of matter during the flow process. In equation 5.6, $\frac{\partial M}{\partial t}$ takes into account the storage change due to compression of the soil, water, and gas constituents of the soil. The relative magnitudes of the different component storage amounts vary widely for a given soil. If the soil is almost or completely saturated, the change in the gas volume may be neglected. Since this is usually the case in nature, the change of storage in an elemental soil volume is principally due to the compressibility of the soil skeleton and the pore water. At shallow depth only relatively shallow depths (up

to 10 meters) are important to the problem, the fluid compressibility is usually negligible. In addition, the soil itself may be relatively incompressible, for instance if it consists of a dense granular material. In the event that the soil structure and pore fluid may reasonably be assumed to be incompressible, and that no gas exists in the pores, there will be no change in fluid storage in any soil element during the flow process, and equation 5.6 becomes:

$$\frac{\partial}{\partial x}\left(\rho_w \, v_x\right) + \frac{\partial}{\partial y}\left(\rho_w \, v_y\right) + \frac{\partial}{\partial z}\left(\rho_w \, v_z\right) = 0 \tag{5.7}$$

Equation 5.7 is the general equation of continuity of flow when the change in storage is zero; it therefore describes flow conditions which do not change in time and is referred to as a steady-state equation.

5.1.2 Momentum balance equation

According to the previous chapters, the momentum balance equation of a solid:

$$\boldsymbol{div\sigma} + \boldsymbol{f} = \rho \, \boldsymbol{a}(\boldsymbol{x}, t) \tag{5.8}$$

in which $\boldsymbol{\sigma}$ is the stress tensor, $\boldsymbol{f}$ is the body force, ρ is the mass density of the solid and $\boldsymbol{a}$ is the acceleration of the solid at a given point and at a given time. Similarly, the fluid balance of momentum is:

$$\boldsymbol{div}(p_w \boldsymbol{\delta}) + \boldsymbol{f_w} = \rho_w \, \boldsymbol{a_w}(\boldsymbol{x}, t) \tag{5.9}$$

in which p_w is the fluid pore pressure, $\boldsymbol{\delta}$ is the second-order identity tensor, $\boldsymbol{f_w}$ is the body force that applies to the fluid, ρ_w is the mass density of the fluid and $\boldsymbol{a_w}$ is the acceleration of the fluid at a given point and at a given time. In the following, we neglect the gavitational forces that apply on the fluid, so that $\boldsymbol{f_w}$ represents the force exerted by the soil skeleton on the fluid to resist the flow in the soil capillary.

Let us assume that the pore fluid is Newtonian. A Newtonian fluid is a fluid in which the viscous stresses arising from its flow, at every point, are linearly proportional to the local strain rate. The force that resists the flow in the soil capillary, due to the fluid's viscosity, is noted $\boldsymbol{f_w}$ and is thus expressed as:

$$\boldsymbol{f_w} = -\mu_w \, \nabla^2(\boldsymbol{v}) \tag{5.10}$$

in which μ_w is the dynamic viscosity of the fluid, expressed in $Pa.s$ (or $kg.m^{-1}.s^{-1}$). Now combining equations 5.9 and 5.10 and assuming that the acceleration of the fluid is zero, one gets:

$$\nabla^2(\boldsymbol{v}) = \frac{1}{\mu_w} \nabla p_w \tag{5.11}$$

Developping equation 5.11 in a Cartesian coordinate system, one gets:

$$\left(\frac{\partial^2}{\partial x^2} + \frac{\partial^2}{\partial y^2} + \frac{\partial^2}{\partial z^2}\right) v_j = \frac{1}{\mu_w} \frac{\partial p_w}{\partial j}, \quad j = x, y, z \tag{5.12}$$
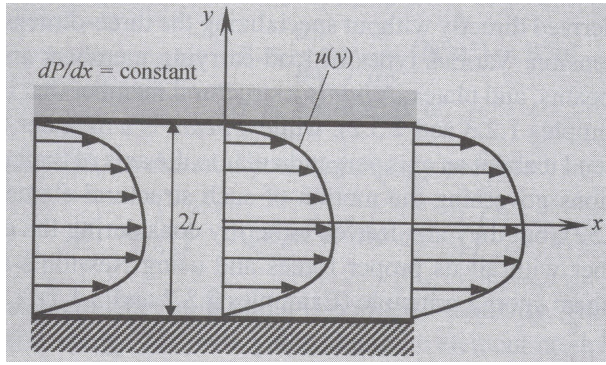
5.1.3 1D fluid flow in a pipe

It is instructive to apply equation 5.12 to the problem of 1D flow through a rigid pipe. Let us consider the pipe shown in Figure 5.2, oriented along the x-axis. Equation 5.12 reduces

to the following governing equation in 1D:

$$\mu_w \frac{d^2 v_x}{dy^2} = \frac{dp_w}{dx}, \quad \mu_w \frac{d^2 v_x}{dy^2} = f(y) \tag{5.13}$$

Assuming that the gradient of pore pressure is a known function of y, one can solve for $v_x(y)$. Solving equation 5.13 allows determining the shape of the flow front illustrated in Figure 5.2.

Figure 5.2   1D Newtonian fluid flow through a rigid pipe. Image taken from [18].

Using the same principles as for the elastic solid, the problem can be solved by the Finite Element Method, starting with the variational formulation. Using the Galerkin method, the discretized variational formulation on a single finite element with N degrees of freedom is expressed as:

$$\forall i, j = 1..N, \quad \left[\int_{y_1}^{y_2} \mu_w \frac{d\Psi_i}{dy} \frac{d\Psi_j}{dy} dy \right] v_{xj} = -\int_{y_1}^{y_2} \Psi_i(y) f(y) dy + Q_i \tag{5.14}$$

in which Ψ_j is the interpolation function relative to the jth degree of freedom ("node"). The last term on the right-hand side emerges due to the integration by part:

$$Q \equiv \mu_w \frac{dv_x}{dy}$$

5.1.4   2D fluid flow for an irrotational fluid

When individual parcels of a frictionless incompressible fluid initially at rest cannot be caused to rotate, the fluid is said to be irrotationnal. Mathematically, this condition translates into:

$$curl(\boldsymbol{v}) = \nabla \times \boldsymbol{v} = \boldsymbol{0} \tag{5.15}$$

In Cartesian coordinates, the 2D version of equation 5.15 is:

$$\frac{\partial v_x}{\partial y} - \frac{\partial v_y}{\partial x} = 0 \tag{5.16}$$

In cylindrical coordinates:

$$\frac{1}{r} \left(\frac{\partial v_r}{\partial \theta} - \frac{\partial (r\, v_\theta)}{\partial r} \right) = 0 \tag{5.17}$$

According to Equation 5.6, the continuity condition (or mass conservation equation) in 2D is:

$$\frac{\partial M}{\partial t} = \left[\frac{\partial}{\partial x} \left(\rho_w \, v_x \right) + \frac{\partial}{\partial y} \left(\rho_w \, v_y \right) \right] dx \, dy \tag{5.18}$$

For an incompressible fluid, this equation becomes:

$$\frac{\partial v_x}{\partial x} + \frac{\partial v_y}{\partial y} = 0 \tag{5.19}$$

In cylindrical coordinates, this translates into:

$$\frac{\partial v_r}{\partial r} + \frac{1}{r} \frac{\partial v_\theta}{\partial \theta} = 0 \tag{5.20}$$

We introduce the stream function Ψ, defined such that:

$$v_x = \frac{\partial \Psi}{\partial y}, \qquad v_y = -\frac{\partial \Psi}{\partial x} \tag{5.21}$$

$$v_r = \frac{1}{r} \frac{\partial \Psi}{\partial \theta}, \qquad v_\theta = -\frac{\partial \Psi}{\partial r} \tag{5.22}$$

And we introduce the potential function Φ, defined such that:

$$v_x = -\frac{\partial \Phi}{\partial x}, \qquad v_y = -\frac{\partial \Phi}{\partial y} \tag{5.23}$$

$$v_r = -\frac{\partial \Phi}{\partial r}, \qquad v_\theta = -\frac{1}{r} \frac{\partial \Phi}{\partial \theta} \tag{5.24}$$

Combining equations 5.16 and 5.21 or equations 5.17 and 5.22, one gets:

$$\nabla^2 \Psi = 0 \tag{5.25}$$

Combining equations 5.16 and 5.23 or equations 5.17 and 5.24, one gets:

$$\nabla^2 \Phi = 0 \tag{5.26}$$

In equations 5.25 and 5.26, we have:

$$\nabla^2 = \frac{\partial^2}{\partial x^2} + \frac{\partial^2}{\partial y^2} \tag{5.27}$$

$$\nabla^2 = \frac{\partial^2}{\partial r^2} + \frac{1}{r} \frac{\partial}{\partial r} + \frac{1}{r^2} \frac{\partial^2}{\partial \theta^2} \tag{5.28}$$

By construction, equal stream lines and equipotential lines are orthogonal:
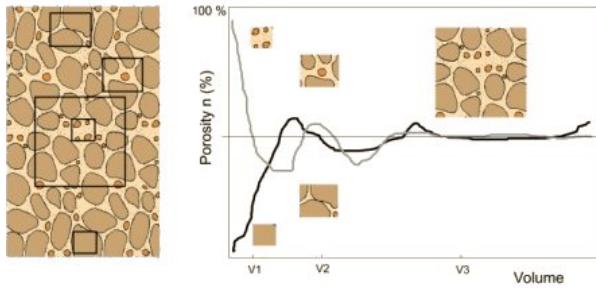
$$-\frac{\partial \Phi}{\partial x} = \frac{\partial \Psi}{\partial y}, \qquad \frac{\partial \Phi}{\partial y} = \frac{\partial \Psi}{\partial x} \tag{5.29}$$

The problem of fluid flow in 2D can be expressed in terms of only own unknown, the stream function Ψ, or, equivalently, the potential function Φ, instead of two unknowns v_x and v_y (or v_r and v_θ). Formulations in Ψ and Φ are equivalent but the boundary conditions for Ψ and Φ are different. The FEM for plane elasticty presented in the previous chapters can easily be adapted to 2D problems of fluid flow with only one dependent variable.

5.2 Mechanics of a deformable solid skeleton filled with one fluid phase

5.2.1 Mathematical description of the porous medium

Porous media are composite materials made of solid, liquid and gas constituents. Field variables are defined by phase (solid, liquid, gas) or by species (mineral in the solid, water/oil/other in the liquid phase, air/vapor/other in the gas phase). Poromechanical variables of the composite porous medium as a whole are average functions of space and time. In space, poromechanical variables are averaged at the scale of a Representative Elementary Volume (REV) of material. The REV is the minimum volume above which the average poromechanical variables of interest are stable. Figure 5.3 illustrates the concept of REV for porosity. Typically, the REV characteristic dimension is 2 orders of magnitude larger than that of the microscopic inhomogeneities (e.g. grains, pores).

Figure 5.3 Concept of REV: the average field variables of interest (here, porosity) do not vary if the averages are calculated over the REV or a volume larger than the REV. Image taken from [7].

A constituent in a particular phase is a "constituent" (for instance, liquid water and vapor are two constituents of the same species). Consider a REV with j constituents. For the jth constituent, we define:

- Volume average of variable $\xi^{(j)}$:

$$\overline{\xi^{(j)}}(\mathbf{x}, t) = \frac{1}{V_{REV}} \int_{V_{REV}} \xi^{(j)}(\mathbf{x}, t)\gamma^{(j)}(\mathbf{x}, t)dV_m \qquad (5.30)$$

- Mass average of variable ξ

$$\langle \xi^{(j)} \rangle(\mathbf{x}, t) = \frac{\int_{V_{REV}} \rho(\mathbf{x}, t)\xi^{(j)}(\mathbf{x}, t)\gamma^{(j)}(\mathbf{x}, t)dV_m}{\int_{V_{REV}} \rho(\mathbf{x}, t)\gamma^{(j)}(\mathbf{x}, t)dV_m} \qquad (5.31)$$

In which:

$$\begin{aligned} \gamma^{(j)}(\mathbf{x}, t) &= 1, \quad \mathbf{x} \in V_{REV} \\ \gamma^{(j)}(\mathbf{x}, t) &= 0, \quad \mathbf{x} \notin V_{REV} \end{aligned} \qquad (5.32)$$
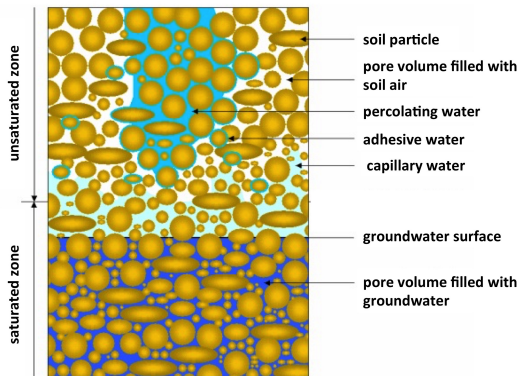
V_m is the characteristic volume of a heterogeneity. ρ is the mass density of the material locate at $\mathbf{x}$ at time t.

In this course, we study dry porous media (solid skeleton and voids filled with air), saturated porous media (typically, a solid skeletong filled with liquid water) and unsaturated porous media (typically, a REV made of a solid skeleton, liquid water and air). The

Table 5.1   Common poromechanical variables.

	State Variable Primary Var.	Driving force Secondary Var.	Energy density	Example constitutive law
Solid	$\mathbf{u}(\mathbf{x}, t)$	$\boldsymbol{\sigma}'(\mathbf{x}, t)$	$\boldsymbol{\sigma}'(\mathbf{x}, t) : \nabla^{sym}\mathbf{u}(\mathbf{x}, t)$	elastic / poroelastic
Water	$p_w(\mathbf{x}, t)$	$\mathbf{q_w}(\mathbf{x}, t)$	$\mathbf{q_w}(\mathbf{x}, t) \cdot \nabla p_w(\mathbf{x}, t)$	Darcy's law
Air	$p_a(\mathbf{x}, t)$	$\mathbf{q_a}(\mathbf{x}, t)$	$\mathbf{q_a}(\mathbf{x}, t) \cdot \nabla p_a(\mathbf{x}, t)$	modified Darcy's law
Heat	$T(\mathbf{x}, t)$	$\mathbf{q_h}(\mathbf{x}, t)$	$\mathbf{q_h}(\mathbf{x}, t) \cdot \nabla T(\mathbf{x}, t)$	Fourier's law

Essential b.c.	Natural b.c.
Dirichlet b.c.	Neuman b.c.

different forms of water in a typical soil REV are shown in Figure 5.4. Momentum balance equations are typically expressed by phase (e.g., solid, liquid, gaz) or for multi-phase components (e.g., liquid+gaz, solid+liquid+gaz). Mass and heat conservation equations are expressed by species (e.g., solid, water, air). Note that two non-miscible fluids are considered as two different phases. A mixture of dry air and vapor is usually considered as a unique phase.

Figure 5.4   The different forms of water in an unsaturated soil. Image taken from [19].

Each constituent is represented by a state variable (primary variable) and a driving force (secondary variable), related to one another by a constitutve equation. Table 5.1 gives an overview of the variables that are the most commonly used in geomechanics. Boundary conditions (b.c.) are imposed either on the state variable (essential b.c.) or on the driving force (natural b.c.), not on both. Momentum balance equations, mass conservation equations and heat conservation equations are solved for the state variables under given initial and boundary conditions (see Section 5.2.2 for more details on the governing equations of a porous medium).

5.2.2 Governing equations of the two-phase isothermal medium

Let us consider a REV made of solid grains and pores filled with liquid water. The balance of momentum of the REV as a whole is:

$$\mathbf{div}\boldsymbol{\sigma} + \mathbf{f} = (1 - \phi)\,\mathbf{a_s}(\mathbf{x}, t) + \phi\,\mathbf{a_w}(\mathbf{x}, t) \tag{5.33}$$

The balance of momentum of the liquid is:

$$\mathbf{div}\,(p_w\boldsymbol{\delta}) + \mathbf{f_w} = \phi\,\mathbf{a_w}(\mathbf{x}, t) \tag{5.34}$$

$\boldsymbol{\sigma}, p_w$: REV stress tensor, water pore pressure
$\mathbf{f}, \mathbf{f_w}$: volume forces applied to the REV, to the water constituent
$\mathbf{a_s}, \mathbf{a_w}$: solid acceleration, water acceleration
ϕ: porosity (pore volume fraction)
$\boldsymbol{\delta}$: second-order identity tensor

In static problems, in the absence of external forces applied to the REV and neglecting gravity effects, the balance of momentum of the REV as a whole is:

$$\mathbf{div}\boldsymbol{\sigma}' - \alpha\nabla p_w = \mathbf{0} \tag{5.35}$$

The balance of momentum of the liquid is:

$$\nabla p_w + \mathbf{R_w} \cdot \mathbf{v_{ws}} = \mathbf{0} \tag{5.36}$$

$\boldsymbol{\sigma}' = \boldsymbol{\sigma} + \alpha\,p_w$: effective stress
$\alpha = 1 - K/K_s$: Biot's coefficient
K, K_s: bulk moduli of the solid skeleton, of the solid phase
$\mathbf{R_w}$: resistance to the water flow in the solid pores
$\mathbf{v_{ws}}$: flow velocity of water relative to the solid skeleton

For a linear isotropic elastic solid skeleton, the constitutive relation is:

$$\boldsymbol{\sigma}' = \mathbf{D_e} : \boldsymbol{\epsilon} = \left(K - \frac{2}{3}G\right)\epsilon_v\boldsymbol{\delta} + 2G\boldsymbol{\epsilon} \tag{5.37}$$

The pores of common geomaterials are small enough to assume that the liquid flow in these pores is laminar. We will come back to this statement in Section 5.3. As a result, the resistance to the water flow in the solid pores can be expressed by means of Darcy's law, as follows:

$$\mathbf{R_w}^{-1} = \frac{\mathbf{K_w}}{\phi\,\mu_w} \tag{5.38}$$

$\mathbf{D_e}$: solid skeleton stiffness tensor
K, G: bulk, shear moduli of the solid skeleton
$\mathbf{K_w}$: water permeability tensor
μ_w: water viscosity
ϵ_v: volumetric deformation: $\epsilon_v = Tr(\boldsymbol{\epsilon})$

Combining momentum balance equations and constitutive equations, we get:

- The momentum balance equation for the REV as a whole:

$$\mathbf{div}\boldsymbol{\sigma}' - \alpha\nabla p_w = \mathbf{0} \tag{5.39}$$

$$\boldsymbol{\sigma}' = \mathbf{D_e} : \boldsymbol{\epsilon} = \left(K - \frac{2}{3}G\right)\epsilon_v\boldsymbol{\delta} + 2G\boldsymbol{\epsilon} \tag{5.40}$$

$$\mathbf{D_e} : \nabla\boldsymbol{\epsilon} - \alpha\nabla p_w = \mathbf{0} \tag{5.41}$$

- The momentum balance equation for the liquid phase:

$$\nabla p_w + \mathbf{R_w} \cdot \mathbf{v_{ws}} = \mathbf{0} \tag{5.42}$$

$$\mathbf{R_w}^{-1} = \frac{\mathbf{K_w}}{\phi\mu_w} \tag{5.43}$$

$$\mathbf{v_{ws}} = -\frac{\mathbf{K_w}}{\phi\mu_w} \cdot \nabla p_w \tag{5.44}$$

Using average mass densities at the scale of the REV, and noting that the time derivative in reference to a moving particle of phase π is:

$$\frac{D^\pi f(\mathbf{x},t)}{Dt} = \frac{\partial f(\mathbf{x},t)}{\partial t} + \mathbf{v}_\pi \cdot \nabla f(\mathbf{x},t) \tag{5.45}$$

The mass balance of the solid constituent becomes:

$$\frac{\partial(1-\phi)\rho_s}{\partial t} + div\left((1-\phi)\rho_s\,\mathbf{v_s}(\mathbf{x},t)\right) = 0, \qquad \mathbf{v_s}(\mathbf{x},t) = \frac{\partial\mathbf{u}(\mathbf{x},t)}{\partial t} \tag{5.46}$$

$$\frac{D^s(1-\phi)\rho_s(\mathbf{x},t)}{Dt} - \frac{\partial\mathbf{u}(\mathbf{x},t)}{\partial t}\cdot\nabla\left((1-\phi)\rho_s(\mathbf{x},t)\right) + div\left((1-\phi)\rho_s\,\frac{\partial\mathbf{u}(\mathbf{x},t)}{\partial t}\right) = 0 \tag{5.47}$$

The mass balance of water becomes:

$$\frac{\partial(\phi\,\rho_w)}{\partial t} + div\left(\phi\rho_w\,\mathbf{v}_w\right) = 0 \tag{5.48}$$

$$\frac{D^w\phi\rho_w(\mathbf{x},t)}{Dt} - \mathbf{v_w}(\mathbf{x},t)\cdot\nabla\left(\phi\rho_w\right) + div\left(\phi\rho_w\,\mathbf{v}_w\right) = 0 \tag{5.49}$$

Noting that, for any scalar β and any vector $\mathbf{v}$, we have:

$$div\left(\beta\,\mathbf{v}\right) = \mathbf{v}\cdot\nabla\beta + \beta\,div\left(\mathbf{v}\right) \tag{5.50}$$

- The mass balance of the solid constituent can finally be expressed as:

$$\frac{D^s(1-\phi)\rho_s(\mathbf{x},t)}{Dt} + (1-\phi)\rho_s\,div\left(\frac{\partial\mathbf{u}(\mathbf{x},t)}{\partial t}\right) = 0 \tag{5.51}$$

- The mass balance of water is expressed as:

$$\frac{D^w \phi \rho_w(\mathbf{x}, t)}{Dt} + \phi \rho_w \, div\,(\mathbf{v}_w) = 0 \tag{5.52}$$

To summarize, the governing equations for a liquid-saturated porous medium are:

- Balance of momentum for REV as a whole:

$$\mathbf{D_e} : \nabla \epsilon - \alpha \nabla p_w = \mathbf{0} \tag{5.53}$$

$$\mathbf{D_e} : \nabla^2 \boldsymbol{u} - \alpha \nabla p_w = \mathbf{0} \tag{5.54}$$

- Balance of momentum for water:

$$\mathbf{v_{ws}} = -\frac{\mathbf{K_w}}{\phi \mu_w} \cdot \nabla p_w \tag{5.55}$$

- Mass balance of the solid constituent:

$$\frac{D^s (1 - \phi) \rho_s(\mathbf{x}, t)}{Dt} + (1 - \phi) \rho_s \, div\left(\frac{\partial \mathbf{u}(\mathbf{x}, t)}{\partial t}\right) = 0 \tag{5.56}$$

- Mass balance of water:

$$\frac{D^w \phi \rho_w(\mathbf{x}, t)}{Dt} + \phi \rho_w \, div\,(\mathbf{v}_w) = 0 \tag{5.57}$$

The unknowns of the problem are the state variables $\boldsymbol{u}$ (the displacement field) and p_w (the pore pressure). One can see that the system of equations above depends on other unknowns: ϕ, ρ_s, ρ_w, $\mathbf{v}_w$ and $\mathbf{v_{ws}}$. Further developments are needed to express ϕ, ρ_s, ρ_w, $\mathbf{v}_w$ and $\mathbf{v_{ws}}$ as functions of $\boldsymbol{u}$ and p_w and reduce the system of equations above to two equations, and solve for the displacement ad pore pressure fields. Below, we provide the corresponding derivations.

The mass balance of the solid constituent is:

$$\frac{D^s (1 - \phi) \rho_s(\mathbf{x}, t)}{Dt} + (1 - \phi) \rho_s \, div\left(\frac{\partial \mathbf{u}(\mathbf{x}, t)}{\partial t}\right) = 0 \tag{5.58}$$

$$\frac{(1 - \phi)}{\rho_s} \frac{D^s \rho_s}{Dt} - \frac{D^s \phi}{Dt} + (1 - \phi) \, div\mathbf{v_s} = 0 \tag{5.59}$$

The mass balance of water is:

$$\frac{D^w \phi \rho_w}{Dt} + \phi \rho_w \, div\mathbf{v_w} = 0 \tag{5.60}$$

$$\frac{D^s \phi \rho_w}{Dt} + \mathbf{v_{ws}} \cdot \nabla(\phi \rho_w) + \phi \rho_w \, div\mathbf{v_{ws}} + \phi \rho_w \, div\mathbf{v_s} = 0 \tag{5.61}$$

$$\frac{D^s\phi}{Dt} + \frac{\phi}{\rho_w}\frac{D^s\rho_w}{Dt} + \frac{\mathbf{v_{ws}}}{\rho_w}\cdot\nabla(\phi\rho_w) + \phi\,div\mathbf{v_{ws}} + \phi\,div\mathbf{v_s} = 0 \tag{5.62}$$

Summing equations 5.59 and 5.62, we get:

$$\frac{(1-\phi)}{\rho_s}\frac{D^s\rho_s}{Dt} + div\mathbf{v_s} + \frac{\phi}{\rho_w}\frac{D^s\rho_w}{Dt} + \frac{1}{\rho_w}\,div\,(\phi\rho_w\mathbf{v_{ws}}) = 0 \tag{5.63}$$

Time derivative of the water density is:

$$\frac{D^s\rho_w}{Dt} = \frac{D^w\rho_w}{Dt} - \mathbf{v_{ws}}\cdot\nabla\rho_w \tag{5.64}$$

Noting K_w^* the bulk modulus of water, water compressibility is expressed as:

$$\frac{D^s\rho_w}{Dt} = \frac{\rho_w}{K_w^*}\frac{D^w p_w}{Dt} - \mathbf{v_{ws}}\cdot\nabla\rho_w \tag{5.65}$$

Hence: we have:

$$\frac{(1-\phi)}{\rho_s}\frac{D^s\rho_s}{Dt} + div\mathbf{v_s} + \frac{\phi}{K_w^*}\frac{D^w p_w}{Dt} - \frac{\phi}{\rho_w}\mathbf{v_{ws}}\cdot\nabla\rho_w + \frac{1}{\rho_w}\,div\,(\phi\rho_w\mathbf{v_{ws}}) = 0 \tag{5.66}$$

$$\frac{(1-\phi)}{\rho_s}\frac{D^s\rho_s}{Dt} + div\mathbf{v_s} + \frac{\phi}{K_w^*}\frac{D^w p_w}{Dt} - \frac{\phi}{K_w^*}\mathbf{v_{ws}}\cdot\nabla p_w + \frac{1}{\rho_w}\,div\,(\phi\rho_w\mathbf{v_{ws}}) = 0 \tag{5.67}$$

$$\frac{(1-\phi)}{\rho_s}\frac{D^s\rho_s}{Dt} + div\mathbf{v_s} + \frac{\phi}{K_w^*}\frac{D^s p_w}{Dt} + \frac{1}{\rho_w}\,div\,(\phi\rho_w\mathbf{v_{ws}}) = 0 \tag{5.68}$$

The time derivative of the solid density is:

$$\frac{D^s\rho_s}{Dt} = \frac{D^s Tr\boldsymbol{\sigma^*}}{Dt}\frac{\partial\rho_s}{\partial Tr\boldsymbol{\sigma^*}} + \frac{D^s p_w}{Dt}\frac{\partial\rho_s}{\partial p_w} \tag{5.69}$$

with $\boldsymbol{\sigma^*} = \boldsymbol{\sigma} - p_w\boldsymbol{\delta}$. We choose linear constitutive laws for the mechanical behavior of the solid skeleton:

$$\frac{D^s\rho_s}{Dt} = \frac{\rho_s}{K_s}\frac{D^s p_w}{Dt} - \frac{\rho_s}{3(1-\phi)K_s}\frac{D^s Tr\boldsymbol{\sigma^*}}{Dt} \tag{5.70}$$

$$\frac{D^s\rho_s}{Dt} = \frac{\rho_s}{K_s}\frac{D^s p_w}{Dt} - \frac{\rho_s}{3(1-\phi)K_s}\frac{D^s Tr\boldsymbol{\sigma}}{Dt} - \frac{\rho_s}{(1-\phi)K_s}\frac{D^s p_w}{Dt} \tag{5.71}$$

We now use the linear isotropic elasticity law:

$$Tr\boldsymbol{\sigma} = Tr\boldsymbol{\sigma'} - 3\alpha\,p_w = 3K\epsilon_v - 3\alpha\,p_w \tag{5.72}$$

$$\frac{D^s\rho_s}{Dt} = \frac{\rho_s}{K_s}\frac{D^s p_w}{Dt} - \frac{\rho_s K}{(1-\phi)K_s}div\mathbf{v_s} + \frac{\rho_s\alpha}{(1-\phi)K_s}\frac{D^s p_w}{Dt} - \frac{\rho_s}{(1-\phi)K_s}\frac{D^s p_w}{Dt} \tag{5.73}$$

We finally get:

$$\frac{(1-\phi)}{\rho_s}\frac{D^s\rho_s}{Dt} = -(1-\alpha)\,div\mathbf{v_s} + \frac{(\alpha-\phi)}{K_s}\frac{D^s p_w}{Dt} \tag{5.74}$$

Now combining equations 5.68 and 5.74, we get:

$$\left(\frac{(\alpha - \phi)}{K_s} + \frac{\phi}{K_w^*}\right)\frac{D^s p_w}{Dt} + \alpha \, div\mathbf{v_s} = -\frac{1}{\rho_w} \, div\left(\phi\rho_w\mathbf{v_{ws}}\right) \qquad (5.75)$$

With the momentum balance equation of water:

$$\mathbf{v_{ws}} = -\frac{\mathbf{K_w}}{\phi\mu_w} \cdot \nabla p_w \qquad (5.76)$$

... we get:

$$\left(\frac{(\alpha - \phi)}{K_s} + \frac{\phi}{K_w^*}\right)\frac{D^s p_w}{Dt} + \alpha \, div\left(\frac{\partial\mathbf{u}}{\partial t}\right) = \frac{1}{\rho_w}\frac{\mathbf{K_w}}{\mu_w}div\left(\rho_w\nabla p_w\right) \qquad (5.77)$$

In undrained conditions, $\nabla\rho_w = \mathbf{0}$ (uniform water pressure distribution).In drained conditions, $\nabla\rho_w = \mathbf{0}$ if the permeability of the soil is high enough.Therefore, the combination of the water momentum balance equation, the solid mass conservation equation and the water mass conservation equation provides:

$$\left(\frac{(\alpha - \phi)}{K_s} + \frac{\phi}{K_w^*}\right)\frac{D^s p_w}{Dt} + \alpha \, div\left(\frac{\partial\mathbf{u}}{\partial t}\right) = \frac{\mathbf{K_w}}{\mu_w}\nabla^2 p_w \qquad (5.78)$$

... which can be solved for the fields of displacements $\mathbf{u}$ and water pore pressure p_w if combined with the momentum balance equation:

$$\mathbf{D_e} : \nabla^2\boldsymbol{u} - \alpha\nabla p_w = \mathbf{0} \qquad (5.79)$$

For a non-viscous elastic porous solid that contains no water ($p_w = 0$), the field of displacements is obtained by solving:

$$\mathbf{D_e} : \nabla^2\boldsymbol{u} = \mathbf{0} \qquad (5.80)$$

and the porosity change is: $\Delta\phi = \epsilon_v = Tr\left(\nabla^{sym}\mathbf{u}\right)$

5.3   Darcy's law and the permeability tensor

5.3.1   From Darcy's law to the Laplace's equation

In Section 5.2.2, we saw that the general form of Darcy's law is:

$$\mathbf{R_w}^{-1} = \frac{\mathbf{K_w}}{\phi\,\mu_w} \qquad (5.81)$$

and that the momentum balance equation of water is

$$\mathbf{v_{ws}} = -\frac{\mathbf{K_w}}{\phi\mu_w} \cdot \nabla p_w \qquad (5.82)$$

Darcy carried out experiments on the flow of water through porous sand filter beds, as a result of which he determined that the superficial velocity of flow was directly related to the pressure gradient through the bed by a constant of proportionality which included both the

soil and water properties. In most hydraulic and soil engineering work, it is conventional to refer to fluid pressures in terms of heads, that is, in terms of the static height of a column of fluid which would result in a given pressure at a point. Thus, instead of referring to a fluid pressure p, where p is expressed in e.g. pounds per square foot, we use the term fluid pressure head denoted by the symbol h_p. Pressure and pressure head are related through the unit weight of the fluid, namely:

$$h_p = \frac{p}{\gamma_w} \tag{5.83}$$

for the case of an incompressible fluid, and

$$h_p = \int \frac{dp}{\gamma_w} \tag{5.84}$$

if compressibility must be taken into account. The equations for superficial velocity may then be expressed as follows:

$$
\begin{aligned}
v_x &= -k_x \frac{\partial h_p}{\partial x} \tag{5.85}\\[2mm]
v_y &= -k_y \frac{\partial h_p}{\partial y}\\[2mm]
v_z &= -k_z \frac{\partial h_p}{\partial z}
\end{aligned}
$$

In these equations, the minus sign indicates that velocity is measured positively in the direction of decreasing pressure. k_x, k_y and k_z are the hydraulic conductivities in directions x, y and z. It can be seen that such a term implicitly involves the unit weight and viscosity of the pore fluid, besides accounting for the size and geometry of the pores of the soil through which flow is taking place. In other engineering research fields (i.e. petroleum engineering) where fluid flow through porous media is of interest, discrimination is made between the fluid and medium properties, so that, for example:

$$k_x = \frac{\gamma_w \, K_x}{\mu} \tag{5.86}$$

where K_x is the permeability in the x-direction, which is a function of the porous medium, and μ is the viscosity of the pore fluid. In the following, we use the capital letter K to refer to the permeability tensor, and we use k to refer to the hydraulic conductivity. Equations 5.85 describe the velocity in terms of the first and third applied force systems used to obtain the Navier-Stokes equations, that is to say, the internal pressure gradients and the fluid viscosity, but do not take into account possible body forces. In soil mechanics work, as mentioned above, the principal body force of interest is gravity, which can be included in the equations in the following way:

$$
\begin{aligned}
v_x &= -k_x \left[\frac{\partial h_p}{\partial x} - \frac{F_x}{g_w} \right] \tag{5.87}\\[3mm]
v_y &= -k_y \left[\frac{\partial h_p}{\partial y} - \frac{F_y}{g_w} \right]\\[3mm]
v_z &= -k_z \left[\frac{\partial h_p}{\partial z} - \frac{F_z}{g_w} \right]
\end{aligned}
$$

where the quantities F_x, F_y and F_z represent the body forces per unit volume due to gravity in the x-, y-, and z-directions respectively. It will be observed that no consideration has been given to the directions in which the axes have been taken, so that gravity-force components may exist in all directions. In their present form, the terms in parentheses in equations 5.87 are inconvenient for further manipulation, and it would be more useful to express both pressure and gravity forces in one derivative with respect to direction. This can be done by considering the height h_e of any fluid element above an arbitrary zero datum plane. The potential energy per unit mass of the fluid with respect to the datum is h_e, and the force required to move the mass at constant pressure in anyone direction will be given by the derivative of the energy with respect to the direction. Since this force is required to overcome the gravitational body force on the mass, we can write:

$$\frac{F_x}{g_w} = -\frac{\partial h_e}{\partial x} \qquad (5.88)$$

$$\frac{F_y}{g_w} = -\frac{\partial h_e}{\partial y}$$

$$\frac{F_z}{g_w} = -\frac{\partial h_e}{\partial z}]$$

where the negative sign is assigned to denote that the force acts in the direction opposite to gravity. Substituting equations 5.88 into 5.87, the superficial velocity can be expressed as follows:

$$v_x = -k_x \frac{\partial h}{\partial x} \qquad (5.89)$$

$$v_y = -k_y \frac{\partial h}{\partial y}$$

$$v_z = -k_z \frac{\partial h}{\partial z}$$

in which $h = h_p + h_e$ is the total pressure head. If the solid grains and the fluid are both incompressible, the general flow equation 5.78 can be re-written as:

$$k_x \frac{\partial^2 h}{\partial x^2} + k_y \frac{\partial^2 h}{\partial y^2} + k_z \frac{\partial^2 h}{\partial z^2} = 0 \qquad (5.90)$$

Equation 5.90 is frequently called the Laplace's equation (of fluid flow). In a steady-state problem, flow takes place in a region with fixed boundaries at which the flow or head conditions are imposed. The solution to the problem consists of finding a function $h(x, y, z)$ which satisfies the Laplace's equation inside the region and which conforms to the conditions imposed along the edges of the region. At the boundaries of such domains, the specified condition may be one of three kinds:

(i) A potential boundary along which the total head is constant: $h = H$ (constant);

(ii) An impervious boundary of normal $\boldsymbol{n}$, along which the fluid is constrained to flow: $\frac{\partial h}{\partial \boldsymbol{n}} = \boldsymbol{0}$ (no flow across the boundary);

(iii) A free surface boundary along which flow takes place, and where the total head at each point is equal to the height of the point above the assumed datum plane since the pressure in the fluid is equal to the external (usually atmospheric) pressure: $\frac{\partial h}{\partial \boldsymbol{n}} = \mathbf{0}$ and $h = f(z)$ (when the z-axis is directed vertically).

5.3.2 Limitations of Darcy's law

As can be readily seen, flow through soils as described by Darcy's law is a viscous phenomenon similar to that on which Hagen-Poiseuille's law is based. A dimensional analysis of the related parameters indicates that the pressure drop over the length of a tube (or a length of porous medium) is (among other relationships) a function of the dimensionless Reynolds number Re:

$$Re = \frac{\gamma_w}{g} \frac{\overline{v}_s \, d}{\mu} \tag{5.91}$$

where $\overline{v}_s$ is the average velocity and d is the diameter of the tube. Reynolds first investigated fluid flow through tubes and found that under certain conditions laminar or smooth flow breaks down and turbulence begins. These conditions are characterized by a limiting value of Re equal, in tube flow, to about 2,000, although the value in a particular experiment depends on environmental conditions. Below this value the flow is smooth, above it, it is turbulent. Descriptions of many investigations on laminar, transitional, and turbulent flows in pipes are given in the literature (e.g.,Dryden, 1948). In such studies the flow occurred in parallel-walled tubes without divergences or breaks in the continuity of the walls. This is obviously not the case in soils, where the diameter of a continuous pore may vary quite abruptly from point to point in the medium. The fluid velocity will also change rapidly as it progresses through the soil, and we may therefore expect, since the conditions under which the transition from smooth to turbulent flow takes place in pipes in laboratory investigations are not adhered to, that the transition in soil may not be characterized by the same Reynolds number. In any event, contrlling the Reynolds number is difficult, because it involves some values of velocity and pore diameter. If one uses the apparent velocity given by Darcy's law and a grain diameter, d, given by the expression:

$$d = \sqrt[3]{\frac{\sum n_s d_s^3}{\sum n_s}} \tag{5.92}$$

in which n_s is the number of grains of diamter d_s occurring in the soil, then it is found that Darcy's law holds up to values of Reynolds number of the order of unity. The pore diameter is thus not directly expressed, but instead an average grain diameter is used. Even if this value of Reynolds number is only very broadly applicable, there is probably an uncertainty of at least an order of magnitude about its accuracy (Scheidegger, 1957). If, in the determination of Reynolds number, the effective diameter of the soil d_{10} is used, the limiting Reynolds number is found to be in the range $3 < Re < 10$. As pointed out by Muscat (1946), under normally encountered pressure differences in soils, Darcy's law appears to be valid at least up to the size range of medium to coarse sands. For turbulent flow in coarse soils or under high heads, Scheidegger (1957) presents various dynamic formulas, which may be applied to water flow through, say, the coarse sections of rock-filled dams. Note also that the streaming potential generated by flow, particularly in finer-grained soils, could give rise to small counter-flows along the pore walls in a direction opposite to that of the main flows, and it may therefore be expected that deviations from Darcy's law would be encountered in extremely fine-grained (cohesive) soils. It has been

suggested that, as a result of physicochemical interactions between the soil and water in clays, seepage will not occur until a certain limiting gradient i_0 of total head is surpassed (Poluvarinova-Kochina P. Y., 1952) so that the first equation 5.89 for example, would be rewritten as follows:

$$v_x = -k_x \left[\frac{\partial h}{\partial x} - i_0 \cdot e_x \right] \tag{5.93}$$

The limiting gradient i_0 depends on both the structure and the void ratio of the soil and may be as large as 20 to 30 in very dense clays. This revision of Darcy's law is not generally employed, although the effect it describes may not be negligible in certain soils, particularly if, and this is usually the case, the gradients in the pore water in laboratory tests are much higher than those generated in the same soil in the field. Theoretical and experimental investigations of the effect of the revised law, equation 5.93, on transient flow processes have been carried out by Florin (1951), who was especially interested in the comparison of field behaviors with predicted quantities based on laboratory tests. Apart from this effect, one may expect variations to arise in the character of fluid flow if the dimensions of the pore spaces become generally of the same order of magnitude as the mean molecular free path length of the fluid. These path lengths are, nevertheless, extremely small in fluids such as water, and a breakdown in Darcy's law from such an effect even in cohesive soils only occurs when the pore fluid is a gas, a circumstance with which we are not concerned.

5.3.3   Permeability in anisotropic geomaterials
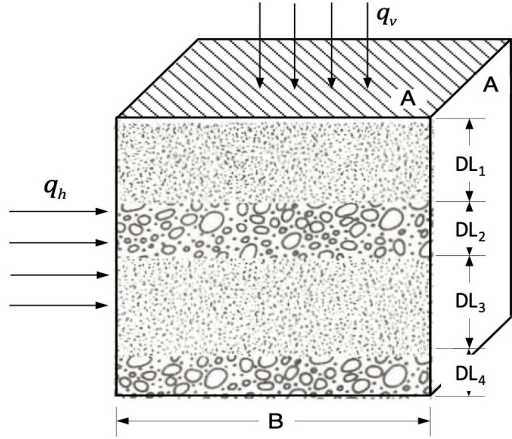
Since most soils are formed by settling on a horizontal surface, stratification or layering occurs through changes in the grain size or in the character of the depositional material. Thus soils are, for the most part, laid down in alternate layers of fine and coarse particles as shown in Figure 5.5. The resulting sediment may be a clay with silt, sand, or coarser or finer clay lenses, or may consist essentially of a granular soil containing layers of silt or clay. A particular deposit of this type is known as a varved clay and is thought to have been built up in glacial lakes as a result of summer and winter climatic changes. The rapid turbulent stream flow of spring and summer bring down all size ranges of the soil from the terrain through which they pass. The coarser sizes settle out rapidly, even in the possibly turbulent lake water, whereas the finer clay sizes remain in suspension, probably in a dispersed state, in the largely salt-free snow and ice melt water. In winter the freezing of the lake surface gives rise to calmer conditions of subsurface water movement so that the fine particles settle out. As a result the deposits formed are strongly stratified, with highly anisotropic properties of permeability, deformability, and shear strength.

In anisotropic soils, the horizontal hydraulic conductivity is greater than the vertical one. This observation may be explained as follows. In Figure 5.5, thehydraulic conductivity of the fine particles is taken to be k_f, that of the coarser material k_c, both being the same in all directions. The thicknesses of the various layers can be taken to be DL_1, DL_2, DL_3, etc. The quantity of flow q_v, which may occur in a vertical direction through a cross-sectional area of soil A is then:

$$q_v = k_f \frac{Dh_1}{DL_1} A = k_c \frac{Dh_2}{DL_2} A = k_f \frac{Dh_3}{DL_3} A = k_f \frac{Dh_4}{DL_4} A, \text{ etc.} \tag{5.94}$$

so that:

$$Dh_1 = \frac{q_v DL_1}{K_f A}, \, Dh_2 = \frac{q_v DL_2}{K_c A}, \text{ etc.} \tag{5.95}$$

Figure 5.5 Flow through anisotropic soil. Image taken from [2].

where Dh_1, Dh_2 are head losses in the layers. If the overall head loss is h, and the total thickness is L, then the quantity of flow can also be written:

$$q_v = k_v \frac{h}{L} A \qquad (5.96)$$

In other words:

$$k_v = \frac{q_v L}{hA} \qquad (5.97)$$

Now, $h = Dh_1 + Dh_2 + Dh_3 + ...$, so that by combining the two above equations, we get:

$$k_v = \frac{Lq_v}{\left(\frac{q_v}{A}\right)\left[\frac{DL_1}{k_f} + \frac{DL_2}{k_c} + \frac{DL_3}{k_f} + \frac{DL_4}{k_c} + ...\right] A} = \frac{L}{\left[\frac{DL_1}{k_f} + \frac{DL_2}{k_c} + \frac{DL_3}{k_f} + \frac{DL_4}{k_c} + ...\right]} \qquad (5.98)$$

This expression, which represents a harmonic mean hydraulic conductivity, is analogous to that for electrical conductivities in series.

If water flows horizontally through a cross-sectional area A of the soil (assumed to be large when compared to the layer thicknesses) of unit depth perpendicular to the paper, then the quantity of flow, q_h, is given by the expression:

$$q_h = k_f \frac{h}{B} DL_1 + k_c \frac{h}{B} DL_2 + k_f \frac{h}{B} DL_3 + k_c \frac{h}{B} DL_4 + ... \qquad (5.99)$$

If $q_h = k_h \frac{h}{B} A$, where B is the width of the region, noting that $A = 1 \times L$, then we have:

$$k_h = \frac{1}{L} \left[k_f DL_1 + k_c DL_2 + k_f DL_3 + k_c DL_4 + ... \right] \qquad (5.100)$$

namely the arithmetic mean value, corresponding to the total electrical conductivity of a parallel array of electrical conductivities. In soils in which the hydraulic conductivity varies from place to place, an average hydraulic conductivity will lie between the arithmetic and harmonic mean values of the permeabilities, weighted according to the related

volumes of soil.

When the directional permeabilities are not equal, but the soil is orthotropic, a convenient substitution may be made which simplifies the problem considerably. One or two (in the three-dimensional case) of the axes may be transformed by the substitutions:

$$x_t = \left[\frac{k_z}{k_x}\right]^{1/2} x \tag{5.101}$$

$$y_t = \left[\frac{k_z}{k_y}\right]^{1/2} y$$

where x_t and y_t are new coordinate axes aligned in the same direction as the former ones, but with all dimensions altered by the substitution. The Laplace's equation(Equation 5.90) is now expressed as:

$$k_z \frac{\partial^2 h}{\partial x_t^2} + k_z \frac{\partial^2 h}{\partial y_t^2} + k_z \frac{\partial^2 h}{\partial z^2} = 0 \tag{5.102}$$

so that:

$$\frac{\partial^2 h}{\partial x_t^2} + \frac{\partial^2 h}{\partial y_t^2} + \frac{\partial^2 h}{\partial z^2} = 0 \tag{5.103}$$

Barron (1948) has presented a technique for transforming non-homogeneous anisotropic flow regions into equivalent non-homogeneous isotropic sections for greater ease of solution. If a problem deals with two or more soils whose hydraulic conductivities are $k_{min,1}$, $k_{max,1}$ and $k_{min,2}$, $k_{max,2}$, and for which the axes of the maximum and minimum permeabilities for the layers are not parallel, Barron transforms the layers by equation 5.101. Nonetheless, this will usually mean that originally corresponding points on the boundaries between layers are separated, and Barron brings them together by changing the scale of one or more layers to attain correspondence.
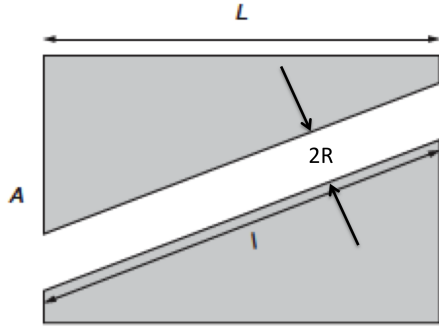
5.3.4   Link between permeability and microstructure

Darcy's law resulted from experimental observations; many attempts have been made to achieve a theoretical confirmation and to determine values of permeability from theoretical considerations of the size of the soil grains and size and shape of the pore spaces through which flow occurs. Many of these investigations have begun from the Hagen-Poiseuille equation for viscous flow through a small capillary tube of radius R, see Figure 5.6.

The average flow velocity through the tube $\overline{v}_s$ is:

$$\overline{v}_s = -\frac{R^2}{8\mu}\frac{dp}{dl} \tag{5.104}$$

A model may then be postulated to consist of a bundle of such tubes arranged in parallel with a ratio of pore cross section to total area n, to simulate the porosity of a soil, in which case, $\overline{v}_s$ represents a seepage velocity. Noting the similarity of equations 5.85 and 5.110, one can write an expression for the coefficient of permeability involving the diameter of the tubes, the porosity of the bundle, and the viscosity of the fluid. This expression can be used to attempt to predict the permeability of a given soil. Nonetheless, in practical applications, there are some differences between the model and soil that become immediately obvious:

Figure 5.6   Viscous fluid flow throug a capillary. Image taken from [15]

not only is it very difficult to specify the "diameter" of the pores, but one encounters even greater difficulties in measuring it, since the pores vary greatly in size and may not, indeed, be continuous throughout the porous medium; generally, the flow in the soil from entrance to exit does not take place in parallel streams. Although the pore size may be related to the dimensions of the grains composing the soil, there can be no unique relationship since the same collection of grains can be arranged in various assemblages containing different pore sizes. Thus, in attempted correlations between models and nature, some form of average pore diameter is sought. The concept of average pore diameter was first introduced in the model of Kozeny and Carman, explained below.

The flux in the pipe shown in Figure 5.6 is:

$$q = -\frac{\pi R^4}{8\eta}\frac{\Delta p}{l} \tag{5.105}$$

According to Darcy's law:

$$q = -K\frac{A}{\eta}\frac{\Delta p}{L} \tag{5.106}$$

The effective permeability for the block is therefore:

$$K = -\frac{\pi R^4}{8A}\frac{L}{l} = -\frac{\pi R^4}{8A\tau}\frac{A}{\eta}\frac{\Delta p}{L} \tag{5.107}$$

in which τ is a tortuosity factor. The porosity is calculated as follows:

$$\phi = \frac{\pi R^2 l}{AL} = \frac{\pi R^2}{A}\tau \tag{5.108}$$

Assitionally, the specific surface area (pore surface area divided by the sample volume) is:

$$S = \frac{2\pi Rl}{AL} = \frac{2\pi R\tau}{A} = \frac{\pi R^2 \tau}{A}\frac{2}{R} = \frac{2\phi}{R} \tag{5.109}$$

From there, we establish the so-called Kozeny-Carman relation:

$$K = \frac{1}{2}\frac{\phi^3}{S^2\tau^2} = \frac{\phi}{8\tau^2}R^2 \tag{5.110}$$

This relation is exact for pipes that have a circular cross section. Since the actual path of fluid flow through the medium is not straight but extremely winding and twisted, various tortuosity factors have been proposed to account for the difference in length between the flow path of an average water molecule and the distance in a straight line through the medium. Other models have been suggested incorporating changes in the cross-sectional area of the tubes to allow for the varying pore diameter in a prototype region. So, in more general terms, Kozeny-Carman permeability model can be stated as:

$$\kappa = B\frac{\phi^3}{S^2\tau^2} = \frac{\phi}{8\tau^2}R^2 \tag{5.111}$$

where B is geometric factor that accounts for the irregularities of pore shapes [15]. For an elliptical cross-section:

$$K = \frac{1}{4}\frac{b^2}{1+(b/a)^2}\frac{\phi}{\tau} = \frac{1}{2}\frac{\phi^3}{S^2\tau^2} \tag{5.112}$$

For a square cross-section:

$$K == 0.562\frac{\phi^3}{S^2\tau^2} \tag{5.113}$$
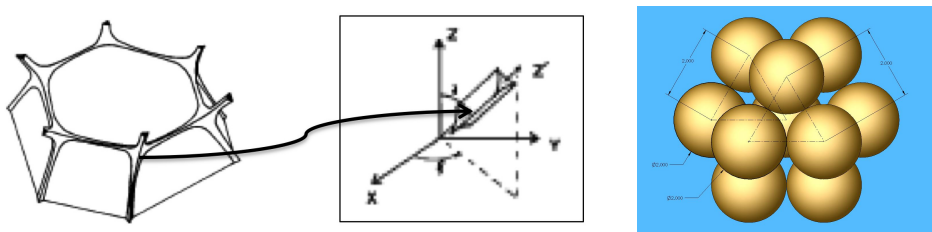
For a triangular cross-section (Figure 5.7):

$$K = \frac{\phi a^2}{80\tau^2} = 0.6\frac{\phi^3}{S^2\tau^2} \tag{5.114}$$

For a packing of identical spheres of diameter d (Figure 5.7):

$$K = \frac{1}{72}\frac{\phi^3}{(1-\phi)^2\tau^2}d^2 \tag{5.115}$$

The assumptions implicit in the various models and their drawbacks are thoroughly dis-
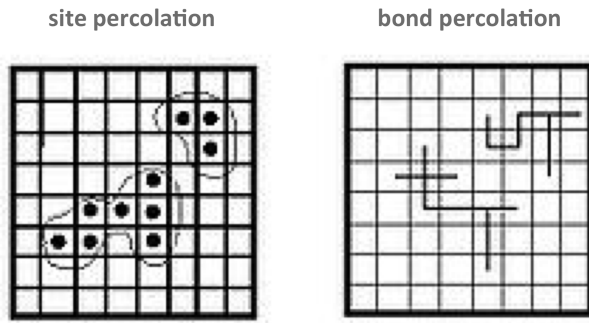
Figure 5.7   Different pore geometries. Left: pores of triangular section. Right: pores within a packing of identical spheres.

cussed by Scheidegger (1957), who points out that the natural heterogeneity of porous media on a small scale suggests mathematical approaches based on disorder rather than order. In other words, Scheidegger proposes statistical analyses of flow in granular soils. In a qualitative analysis along this line, he considers the motion of a small "parcel" of fluid through the pores of the material. This element of volume is small enough so that it does not separate or break up in the flow process. Scheidegger, by considering the probability of a displacement of this parcel in a certain time interval, arrives at an equation corresponding to Darcy's law. Broadbent and Hammersley (1957) have also adopted this approach and
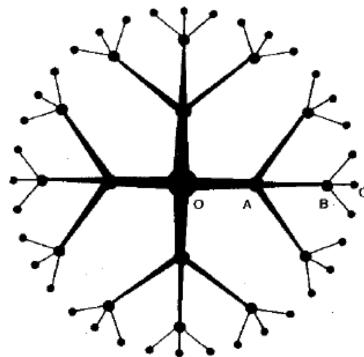
further distinguish between diffusion processes, in which the randomness is inherent in the fluid, and percolation processes, in which the flow is characterized by the random nature of the medium through which flow occurs. Further investigations in this direction would appear to hold promise because of their fundamentally sounder approach to the problem.

In the late 80's, some models were proposed to relate permeability to flow paths. Below the percolation threshold ($p > p_c$), there exists several clusters (flow paths) of variable sizes, see Figure 5.8. We note S the average cluster size. Above the percolation threshold, there exists an infinite cluster (connected flow path). We note P the fraction of sites connected to the infinite cluster. Usually, impossible to get an analytical solution for S and P, unless strong assumptions are made on the topology of the network. In Bethe lattice

Figure 5.8 Percolation theory and connectivity of the flow path. Image taken from *Wikipedia, 2014.*

(Figure 5.9), each site is connected by z neighbors, where z is the network coordination number. Let us pick a site, e.g. O: O is connected to $z = 4$ sites A_i. Each of these sites A_i is connected to $z - 1 = 3$ new sites. A site or a bond is occupied with a probability p. The reader is invited to solve the problems at the end of this chapter to calcualte the percolation threshold and the fraction of sites that are part of the infinite cluster.

Figure 5.9 Bethe Lattice with $z = 4$. Image taken from [11].

5.4 Consolidation problems

5.4.1 The general equation of consolidation

According to Laplace's equation (Equation 5.90):

$$k_x \frac{\partial^2 h}{\partial x^2} + k_y \frac{\partial^2 h}{\partial y^2} + k_z \frac{\partial^2 h}{\partial z^2} = 0 \tag{5.116}$$

Recall that this equation was derived from the following expression:

$$\gamma_w \left[k_x \frac{\partial^2 h}{\partial x^2} + k_y \frac{\partial^2 h}{\partial y^2} + k_z \frac{\partial^2 h}{\partial z^2} \right] = \frac{\partial W}{\partial t} \tag{5.117}$$

where the net weight flux of water into or out of a soil element was equated to the rate of storage of water, $\frac{\partial W}{\partial t}$, in the element. Nonetheless, if either the porous medium or the fluid (or both) are compressible, then there will be fluid storage or loss during flow. Until now, we have established a system of axes and have fixed an element of volume in space with reference to these axes in order to discuss the flow of fluid through the element. However, if this element includes soil solids and the soil is compressing, there will be a flow of soil solids as well as water through the element as time progresses. Therefore, in a rigorous analysis, we must eventually develop another equation, similar to the expression:

$$\left[\frac{\partial(\gamma_w v_x)}{\partial x} + \frac{\partial(\gamma_w v_y)}{\partial y} + \frac{\partial(\gamma_w v_z)}{\partial z} \right] dx dy dz = \frac{\partial W}{\partial t} \tag{5.118}$$

to express the change of storage of soil solids in the fixed volume element in terms of the weight flux of solids through its boundaries. Since Darcy's law has been given for fluid flowing through an assemblage of stationary soil grains, the superficial velocity of the fluid $v_{x,y,z}$ is actually measured with respect to the soil. If the soil is moving, $v_{x,y,z}$ needs to be reformulated with respect to a fixed-volume element in space. In most cases in practice, the velocity of the moving soil grains is so small that it is negligible with respect to fluid velocities, although its existence has been taken into account by Florin (1948) in a study of water flow in a compressing soil. Thus, the analysis as it develops here does not consider the soil grains to move with relation to the fixed volumetric element in space, although, in fact, the problem is formulated to evaluate the movement or settlement of the soil. The process of transient flow of water (or other fluids) through a soil structure which compresses or expands in time is called consolidation in soil mechanics, although the word has another meaning in the related discipline of geology.

5.4.2 Terzaghi's consolidation equation in 1D and 2D

Let us consider a column of soil in which the solid grains and the pore fluid are incompressible (note that the solid skeletong remains compressible). According to Subsection 5.2.2, the governing equation for the solid phase is

$$-\alpha \boldsymbol{\nabla} (p_w) + \mathbf{D_e} : \boldsymbol{\nabla}\boldsymbol{\epsilon} = 0 \tag{5.119}$$

and the governing equation for the liquid phase is:

$$\left(\frac{\alpha - n}{K_s} + \frac{n}{K_w} \right) \dot{p}_w + \alpha \, \dot{\epsilon}_v = \frac{1}{\mu_w} \mathbf{k} : \boldsymbol{\nabla}^2 p_w \tag{5.120}$$

We note:

$$S = \frac{\alpha - n}{K_s} + \frac{n}{K_w} \tag{5.121}$$

Assuming that the solid phase is linear elastic, we have:

$$\frac{\partial p_w}{\partial t} = \frac{\alpha m_v}{S + \alpha^2 m_v} \frac{\partial \sigma_{zz}}{\partial t} + \frac{k}{\mu_w(S + \alpha^2 m_v)} \frac{\partial^2 p_w}{\partial z^2} \tag{5.122}$$
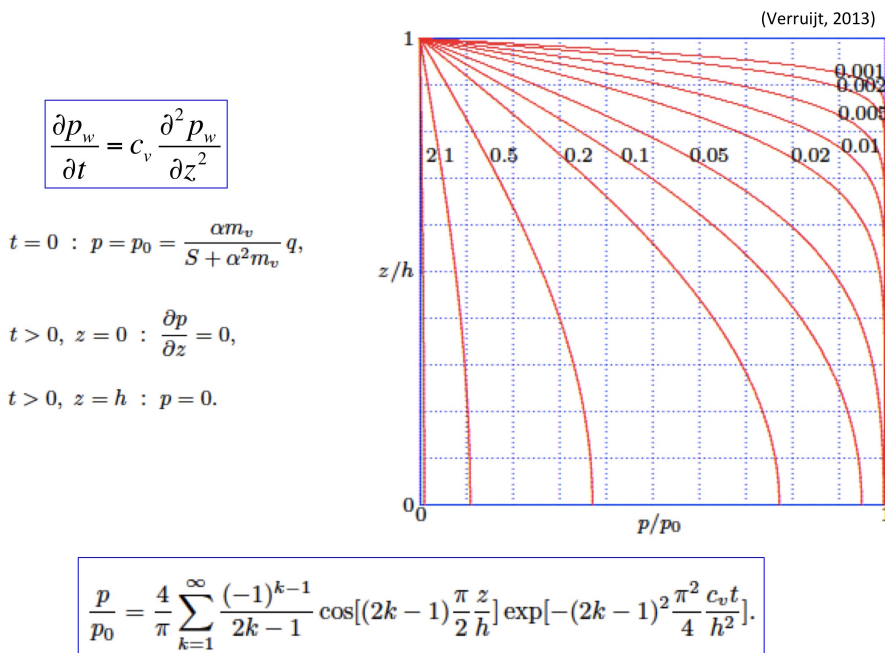
in which m_v is the volume compressibility factor, defined as:

$$m_v = \frac{1}{1 + e} \frac{\partial e}{\partial \sigma'} \tag{5.123}$$

where e is the void ratio (ratio of the volume of voids over the volume of solid in the soil column), and $\sigma' = \sigma - p_w$ is the so-called Terzaghi's effective stress (here, in 1D). For t¿0, the vertical stress σ_{zz} is maintained constant, so that the pore pressure is governed by the following equation:

$$\frac{\partial p_w}{\partial t} = \underbrace{\frac{k}{\mu_w(S + \alpha^2 m_v)}}_{c_v} \frac{\partial^2 p_w}{\partial z^2} \tag{5.124}$$

Equation 5.124 is known as the Terzaghi's consolidation equation. The solution of Terzaghi's consolidation equation is plotted in Figure 5.10.

(Verruijt, 2013)

$$\boxed{\frac{\partial p_w}{\partial t} = c_v \frac{\partial^2 p_w}{\partial z^2}}$$

$$t = 0 \; : \; p = p_0 = \frac{\alpha m_v}{S + \alpha^2 m_v} q,$$

$$t > 0, \; z = 0 \; : \; \frac{\partial p}{\partial z} = 0,$$

$$t > 0, \; z = h \; : \; p = 0.$$

$$\boxed{\frac{p}{p_0} = \frac{4}{\pi} \sum_{k=1}^{\infty} \frac{(-1)^{k-1}}{2k-1} \cos[(2k-1)\frac{\pi}{2}\frac{z}{h}] \exp[-(2k-1)^2 \frac{\pi^2}{4} \frac{c_v t}{h^2}].}$$
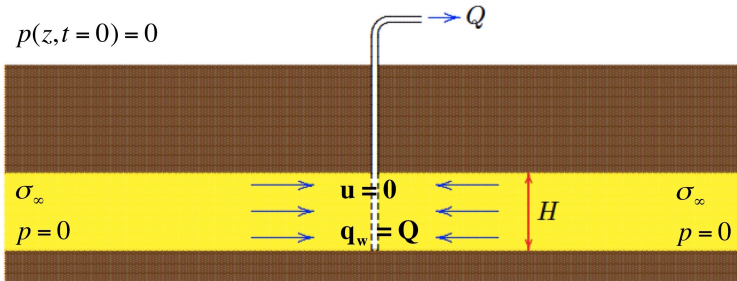
Figure 5.10   Analytical solution of Terzaghi's consolidation equation.
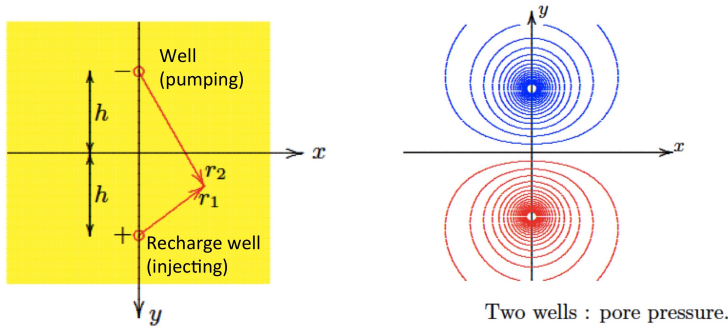
For the problem of radial flow to the well shown in Figure 5.11, the consolidation equation is:

$$\frac{\partial p_w}{\partial t} = c_v \left(\frac{\partial^2 p_w}{\partial r^2} + \frac{1}{r} \frac{\partial p_w}{\partial r} \right) \tag{5.125}$$

If one well is used for injection and another well is used for extraction, the distribution of pore pressure in the subsurfce is as shown in Figure 5.12.

Figure 5.11 Well in an infinite confined aquifer, Theis-Jacob model. Image taken from [20].

Figure 5.12 Consolidation around two wells. Image taken from [20].

5.5 Thermo-elastic behavior of unsaturated porous media

5.5.1 Governing equations

Let us consider a Representative Elementary Volume (REV) of soil that is made of solid grains, liquid (water) and gas (mixture of air and vapor). We consider that the REV can be subjected to stress or displacement perturbations, water and gas pore pressure perturbations and temperature perturbations. Assuming that weight is the only external body force applied to the REV, the momentum balance equation of the REV is:

$$\mathbf{div}\boldsymbol{\sigma} + (1-n)\rho_s(\mathbf{g} - \mathbf{a_s}) + nS_w\rho_w(\mathbf{g} - \mathbf{a_w}) + nS_g\rho_g(\mathbf{g} - \mathbf{a_g}) = 0 \qquad (5.126)$$

Isolating the solid phase, we get:

$$\mathbf{div}\left[\boldsymbol{\sigma}' - \boldsymbol{\delta}(1-n)(S_w\,p_w + S_g\,p_g)\right] + (1-n)\rho_s(\mathbf{g} - \mathbf{a_s}) + \mathbf{f_{ws}} + \mathbf{f_{gs}} = 0 \qquad (5.127)$$

The net stress applied to the solid skeleton is defined as:

$$\boldsymbol{\sigma}' = \boldsymbol{\sigma} + \boldsymbol{\delta}(S_w\,p_w + S_g\,p_g) \qquad (5.128)$$

The fluid pressure contributing to the compressibility of the grains is:

$$-\boldsymbol{\delta}(1-n)(S_w\,p_w + S_g\,p_g) \tag{5.129}$$

The force applied by the liquid flowing in the porous solid skeleton is:

$$\mathbf{f_{ws}} = \mathbf{R_w}\eta_w\mathbf{v_{ws}} = nS_w\mathbf{R_w}\mathbf{v_{ws}} \tag{5.130}$$

The force applied by the gas flowing in the porous solid skeleton is:

$$\mathbf{f_{gs}} = \mathbf{R_g}\eta_g\mathbf{v_{wg}} \tag{5.131}$$

The momentum balance equation of the solid phase is:

$$\mathbf{div}[\boldsymbol{\sigma}' - \boldsymbol{\delta}\,(1-n)(S_wp_w + S_gp_g)] \quad + \quad (1-n)\rho_s\mathbf{g} \tag{5.132}$$
$$-(1-n)\rho_s\mathbf{a_s} + \mathbf{R_w}\eta_w\mathbf{v_{ws}} \quad + \quad \mathbf{R_g}\eta_g\mathbf{v_{wg}} = 0$$

with:

$\boldsymbol{\sigma}'$	Net stress [Pa]	(5.133)
$\boldsymbol{\delta}$	Second-order identity tensor [-]	
n	Porosity [-]	
S_w, S_g	Degree of saturation of liquid water, gas mixture [-]	
p_w, p_g	Pore pressure of liquid water, gas mixture [Pa]	
ρ_s	Solid mass density [kg/m^3]	
$\mathbf{g}$	Gravity acceleration field [m/s^2]	
$\mathbf{a_s}$	Acceleration of the solid phase [m/s^2]	
$\mathbf{R_w}, \mathbf{R_g}$	Flow dissipation term for liquid, gas [Pa.s/m^2]	
η_w, η_g	Volume fraction of liquid, gas in the REV [-]	
$\mathbf{v_{ws}}, \mathbf{v_{wg}}$	Velocity of the liquid in reference to solid, gas [m/s]	

We neglect the gradients of fluids velocity and the effects of phase change.Th balance of momentum of liquid water is:

$$\mathbf{v_{ws}} = \mathbf{R_w}^{-1} : (-\mathbf{grad}(p_w) + \rho_w(\mathbf{g} - \mathbf{a_s} - \mathbf{a_{ws}})) \tag{5.134}$$

The balance of momentum of the gas mixture is:

$$\mathbf{v_{gs}} = \mathbf{R_g}^{-1} : (-\mathbf{grad}(p_g) + \rho_g(\mathbf{g} - \mathbf{a_s} - \mathbf{a_{gs}})) \tag{5.135}$$

with:

$$\mathbf{v_{ws}}, \mathbf{v_{gs}} \quad \text{Velocity of the liquid, gas in reference to solid [m/s]} \quad (5.136)$$

$\mathbf{R_w}, \mathbf{R_g}$	Flow dissipation term for liquid, gas [Pa.s/m^2]
p_w, p_g	Pore pressure of liquid water, gas mixture [Pa]
ρ_w, ρ_g	Mass density of liquid, gas [kg/m^3]
$\mathbf{g}$	Gravity acceleration field [m/s^2]
$\mathbf{a_s}$	Acceleration of the solid phase [m/s^2]
$\mathbf{a_{ws}}, \mathbf{a_{gs}}$	Acceleration of liquid, gas in reference to solid [m/s^2]
η_x	Volume fraction of phase x in REV [-]
$\mathbf{k}$	Permeability [m^2]
μ_x	Dynamic viscosity of phase x [Pa.s]
T	Temperature [K]

We recall that the time derivative of a function $f(\mathbf{x}, t)$ in reference to moving phase π (with velocity $\mathbf{v}^\pi$) is:

$$\frac{D^\pi f(\mathbf{x}, t)}{Dt} = \frac{\partial f(\mathbf{x}, t)}{\partial t} + \mathbf{grad} f \cdot \mathbf{v}^\pi \qquad (5.137)$$

As a result, the mass balance equation of the solid phase is expressed as:

$$\frac{(1-n)}{\rho_s} \frac{D^s \rho_s}{Dt} - \frac{D^s n}{Dt} + (1-n) div \mathbf{v_s} = 0 \qquad (5.138)$$

with:

n	Porosity [-]	(5.139)
ρ_s	Solid mass density [kg/m^3]	
$\mathbf{v_s}$	Velocity field of the solid phase in the REV [m/s]	

The quantity of liquid water lost through evaporation per unit time per unit volume is:

$$\rho_w e^w(\rho) = -\dot{m} \qquad (5.140)$$

so that the mass balance equation of the liquid phase is:

$$\left(\frac{\alpha-n}{K_s}(S_w)^2 + \frac{nS_w}{K_w} \right) \frac{D^s p_w}{Dt} + \frac{\alpha-n}{K_s} S_w S_g \frac{D^s p_g}{Dt} + \alpha S_w div \mathbf{v_s} \qquad (5.141)$$

$$- \beta_{sw} \frac{D^s T}{Dt} + \left(\frac{\alpha-n}{K_s} p_w S_w - \frac{\alpha-n}{K_s} p_g S_w + n \right) \frac{D^s S_w}{Dt}$$

$$+ \frac{1}{\rho_w} div \left(n S_w \rho_w \mathbf{v_{ws}} \right) = -\frac{\dot{m}}{\rho_w}$$

with:

$\beta_s, \beta_w \beta_g$	Thermal expansion coefficient of solid, liquid, gas [K^{-1}]	(5.142)
β_{sw}	$\beta_{sw} = S_w[(\alpha - n)\beta_s + n\beta_w]$	
K_s, K_w	Compression modulus of solid, water [Pa]	

If grains are incompressible, $\alpha = 1$ and $1/K_s \to 0$, and the mass balance equation of the liquid phase reduces to:

$$\frac{nS_w}{K_w}\frac{D^s p_w}{Dt} + S_w div\mathbf{v_s} - \beta_{sw}\frac{D^s T}{Dt} + n\frac{D^s S_w}{Dt} \tag{5.143}$$

$$+ \frac{1}{\rho_w}div\left(nS_w\rho_w\mathbf{v_{ws}}\right) = -\frac{\dot{m}}{\rho_w}$$

Now, the mass balance equation of the gas phase is written as:

$$\frac{\alpha-n}{K_s}S_w S_g\frac{D^s p_w}{Dt} + \frac{\alpha-n}{K_s}(S_g)^2\frac{D^s p_g}{Dt} - \left(n + \frac{\alpha-n}{K_s}p_c S_g\right)\frac{D^s S_w}{Dt} \tag{5.144}$$

$$- \beta_s(\alpha-n)S_g\frac{D^s T}{Dt} + \alpha S_g div\mathbf{v_s} + \frac{nS_g}{\rho_g}\frac{D^s}{Dt}\left[\frac{1}{R\theta}(p_a M_a + p_v M_w)\right]$$

$$+ \frac{1}{\rho_g}div(nS_g\rho_g\mathbf{v_{gs}}) = +\frac{\dot{m}}{\rho_g}$$

We introduce the Kelvin-Laplace law - for the Relative Humidity (RH) in the pores:

$$RH = \frac{p_v}{p_{vs}} = exp\left(\frac{p_c M_w}{\rho_w R\theta}\right) \tag{5.145}$$

with:

p_v, p_{vs}	Vapor pressure, water vapor saturation pressure [Pa]	(5.146)
p_c	$p_c = p_g - p_w :$ Capillary pressure [Pa]	
M_w, M_a	Molar mass of liquid water, gaseous air [kg/mol]	
R	Universal gas constant : $R = 8.3144598 J.mol^{-1}.K^{-1}$	
θ	Absolute temperature [K]	
$\mathbf{v_{gs}}$	Velocity field of the gas phase in reference to the solid [m/s]	

If grains are incompressible, $\alpha = 1$ and $1/K_s \to 0$, and the mass balance equation of the gas phase reduces to:

$$-n\frac{D^s S_w}{Dt} - \beta_s(\alpha-n)S_g\frac{D^s T}{Dt} + S_g div\mathbf{v_s} + \frac{nS_g}{\rho_g}\frac{D^s}{Dt}\left[\frac{1}{R\theta}(p_a M_a + p_v M_w)\right] \tag{5.147}$$

$$+ \frac{1}{\rho_g}div(nS_g\rho_g\mathbf{v_{gs}}) = +\frac{\dot{m}}{\rho_g}$$

The quantity of liquid water lost through evaporation per unit time per unit volume being:

$$\rho_w e^w(\rho) = -\dot{m} \tag{5.148}$$

the energy balance equation is expressed as:

$$(\rho C_p)_{eff}\frac{\partial T}{\partial t} + \left(\rho_w C_p^w\mathbf{v_w} + \rho_g C_p^g\mathbf{v_g}\right)\cdot\mathbf{grad}(T) \tag{5.149}$$

$$-div\left(\chi_{eff}\mathbf{grad}(T)\right) = -\dot{m}\Delta H_{vap}$$

with:

$$\rho_x C_p^x \qquad \text{Heat capacity of the x-th phase [J/K]} \qquad\qquad (5.150)$$

$$(\rho C_p)_{eff} \qquad (\rho C_p)_{eff} = \rho_s C_p^s + \rho_w C_p^w + \rho_g C_p^g$$

$$\chi_x \qquad \text{Thermal conductivity of hte x-th phase [W.m}^{-1}.\text{K}^{-1}]$$

$$\chi_{eff} \qquad \chi_{eff} = \chi_{dry}\left(1 + 4\frac{nS_w p_w}{(1-n)\rho_s}\right)$$

$$\Delta H_{vap} \qquad \Delta H_{vap} = H_v - H_w$$

$$\qquad\qquad \text{Difference between vapor and liquid water enthalpy [J]}$$

To close the formulation, one needs to introduce constitutive relationships. For the solid phase, we use the concept of effective stress:

$$\begin{aligned}
\boldsymbol{\sigma}'' &= \mathbf{D_e} : \boldsymbol{\epsilon} & (5.151) \\
\boldsymbol{\sigma}'' &= \boldsymbol{\sigma} + \alpha\boldsymbol{\delta}\left(S_w p_w + S_g p_g\right) \\
\alpha &= 1 - \frac{K_s}{K}
\end{aligned}$$

...not to be confused with the net stress:

$$\boldsymbol{\sigma}' = \boldsymbol{\sigma} + \boldsymbol{\delta}\left(S_w p_w + S_g p_g\right) \qquad\qquad (5.152)$$

The heat flux is given by Fourier's law:

$$\begin{aligned}
\mathbf{q_h} &= -\chi_{eff}\mathbf{grad}(T) & (5.153) \\
\chi_{eff} &= \chi_{dry}\left(1 + 4\frac{nS_w p_w}{(1-n)\rho_s}\right)
\end{aligned}$$

The transport of water (x=w) and gas (x=g) is assumed to be laminar, so that Darcy's law can be applied:

$$\eta_x \overline{\mathbf{v}}_{\mathbf{xs}} = \frac{k_{rx}\mathbf{k}}{\mu_x} \cdot (-\mathbf{grad}p_x + \rho_x \mathbf{g}) \qquad\qquad (5.154)$$
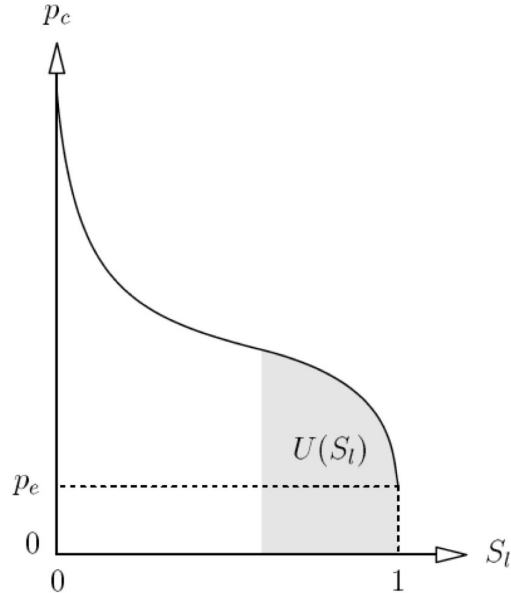
in which k_{rx} is the relative permeability. An additional relationship is needed to relate the relative permeabilities to the saturation degree (ratio between the volume of liquid water over the total volume of pores) and the pore pressures. This is the topic of the next subsection.

5.5.2   The water retention curve (WRC)

The capillary pressure p_c is defined as the difference between the gas pore pressure and the liquid pore pressure:

$$p_c = p_g - p_w \qquad\qquad (5.155)$$

The curve that relates the capillary pressure to the water saturation degree is called the "water retention curve" (WRC). Figure 5.13 shows a schematic WRC. The WRC is typically monotonic; the capillary pressure decreases when the water saturation degree increases.

Figure 5.13   Water retention curve and interfacial energy. Image taken from [5].

The minimal value of the capillary pressure is the air entry pressure, noted p_e. When $p_c > p_e$, S_w starts decreasing when p_c increases. Brooks & Corey's model provides the following expressions for the relative permeability and the capillary pressure:

$$\eta_x \overline{\mathbf{v}}_{\mathbf{xs}} = \frac{k_{rx}\mathbf{k}}{\mu_x} \cdot (-\mathbf{grad}p_x + \rho_x \mathbf{g}) \tag{5.156}$$

$$k_{rw} = (S_e)^{(2+3\lambda)/\lambda}$$

$$k_{rg} = (1 - S_e)^2 (1_{(}S_e)^{(2+\lambda)/\lambda})$$

$$p_c = \frac{p_b}{(S_e)^{1/\lambda}}$$

$$S_e = \frac{S_w - S_{wc}}{1 - S_{wc}}$$

with:

$$p_b \qquad \text{Bubbling pressure [Pa]} \tag{5.157}$$

$$S_{wc} \qquad \text{Residual (irreducible) degree of saturation [-]}$$

$$\lambda \qquad \text{Pore size distribution index [-]}$$

van Genucthen's WRC is described as follows:

$$S_w = \left(1 + \left(\frac{p_c}{A}\right)^n\right)^{-1+1/n} \tag{5.158}$$

in which n and A are positive model parameters.

Brutsaert's model assumes the following equation for the WRC:

$$S_w = \left(1 + \left(\frac{p_c}{A}\right)^n\right)^{-1} \tag{5.159}$$

in which n and A are positive model parameters.

In the case of an experiment with no deformation and no temperature change, the expression of the REV free energy is of the form [5]:

$$\Psi_s = \Phi_0 \, U(S_w) \tag{5.160}$$

in which:

$$U(S_w) = \int_{S_w}^1 p_c(s)ds \tag{5.161}$$

Φ_0 is the initial porosity of the REV and $U(S_w)$ is the energy of the interfaces in the REV (solid/liquid, solid/gas and liquid/gas interfaces). In isothermal conditions, the equation of the WRC is of the form $p_c = p_c(S_w)$. From Equation 5.161, the WRC equation can also be written as:

$$p_c = -\frac{dU}{dS_w} \tag{5.162}$$

$U(S_w)$ can be understood as the work that needs to be provided to the interfaces to bring the specimen from a state of full saturation ($S_w = 1$) to the current saturation (S_w), per unit of porous space $\Phi_0 d\Omega$. The interfacial energy can be expressed as:

$$\Phi_0 \, U = \gamma_{sw}\omega_{sw} + \gamma_{sg}\omega_{sg} + \gamma_{lw}\omega_{lw} - \gamma_{sl}\omega_s \tag{5.163}$$

with $\omega_s = \omega_{sl} + \omega_{sg}$, and in which the subscripts s, w and g refer to the solid, liquid and gaseous phases respectively. γ is an interfacial energy, and ω_β is the fraction of interface of type β ($\beta = sl, sg, lg$). The same analysis can be done in non-isothermal conditions (see [5]).

The WRC can be determined experimentally, by drying the pores while controlling the capillary pressure. For materials with a low permeability, such as clays and concretes, this method is quite limited, because the capillary pressure that needs to be applied to empty the pores is too high. In practice, the WRC can be determined experimentally for saturations above 90%. Under that value, it is necessary to know the sorption isotherm. In a sorption experiment, the specimen is in equilibrium under a constant temperature, and under a controlled relative humidity:
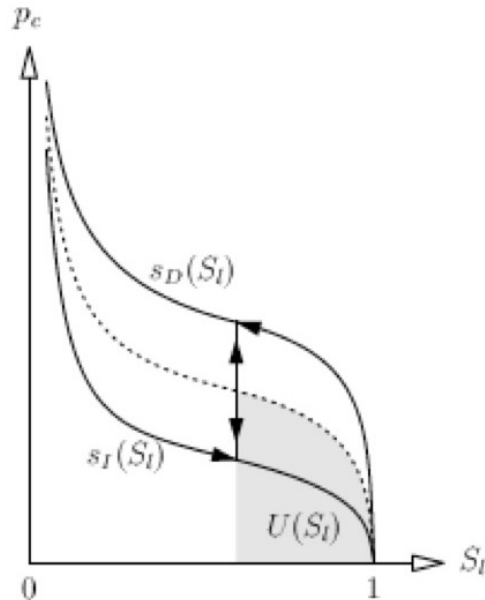
$$h_r = \frac{p_v}{p_{vs}} \tag{5.164}$$

in which p_v is the vapor pressure and p_{vs} is the vapor pressure in a saturated saline solution. It is possible to control h_r by controlling the concentration of the saline solution. The sorption isotherm is then obtained: $h_r = h_r(S_w)$. The gas mixture in the specimen is in equilibrium with the atmostphere, so that $p_l - p_{atm}$ is the opposite of the capillary pressure. The thermodynamic equilibrium between liquid water and vapor is thus [5]:

$$-p_c = \rho_w \frac{RT}{M_v} \ln(h_r) \tag{5.165}$$

in which M_v is the mass per mole of vapor ($M_v = 18g/mol$). Equation 5.165 shows that the WRC can be found indirectly by measuring S_w while controlling h_r.

When the specimen is subjected to reversible transformations, the WRC is bilateral, i.e. the same curve holds for drying and wetting paths. However, the WRC exhibits hysteresis in most soils and rocks. Let us start from a dry state (S_w small, p_c high). When p_c decreases, the point (S_w, p_c) follows the so-called imbibition (or wetting) curve: $p_c = s_I(S_w)$. Once $S_w = 100\%$, if p_c is increased, (S_w, p_c) follows the so-called draining curve: $p_c = s_D(S_w)$. The curves s_I and s_D are different. For a given capillary pressure, the degree of saturation is smaller during the imbibition path than during the draining path. Both curves form a reproducible hysteretic loop. If the variation of p_c is reversed, the point (S_w, p_c) switches from one curve to the other, as shown in Figure 5.14 (line of equation $S_w = cst$). The positivity of the dissipated interface energy is expressed as:
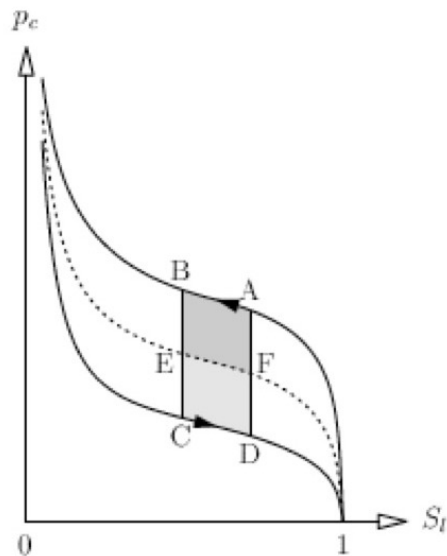
Figure 5.14   Water retention curve during a draining path and during an inmbibition path (solid lines) the curve $-\frac{\partial U}{\partial S_w}$ (dashed line) is inside the hysteretic loop. The area under that curve (in grey) represents the variation of interfacial energy per unit of porous volume, $U(S_w)$. Image taken from [5].

$$-\Phi_0 \left(p_c + \frac{\partial U}{\partial S_w} \right) dS_w \geq 0 \tag{5.166}$$

If the transformation is reversible, then the energy dissipated is zero and $-\Phi_0 p_c dS_w$ is equal to the variation of interfacial energy $\Phi_0 U$. In case of hysteresis, the relation $U(S_w) = \int_{S_w}^{1} p_c(s)ds$ no longer holds. The equation above informs on the value of the thermodynamic force $-\frac{\partial U}{\partial S_w}$ that is conjugated to S_w. We have:

$$s_I \leq -\frac{\partial U}{\partial S_w} \leq s_D \tag{5.167}$$

In other words, the point $(S_w, -\frac{\partial U}{\partial S_w})$ in the plane (S_w, p_c) describes a curve that is between the imbibition and draining WRC. The area of that curve represents the interfacial energy $U(S_w)$, as illustrated in Figure 5.14. The energy dissipated during a draining path (AB in Figure 5.15) is, therefore, equal to the area of the surface comprosed between the draining curve and the curve of equation $-\frac{\partial U}{\partial S_w}(S_w)$. Similarly, the energy dissipated during an imbibition path (CD in Figure 5.15) is the area of the surface comprised between the imbibition curve and the curve of equation $-\frac{\partial U}{\partial S_w}(S_w)$. During a cycle (ABCD), the energy dissipated is thus equal to the area of the surface comprised between the draining curve and the imbibition curve.

Figure 5.15   During a draining path (AB), the energy dissipated is equal to the area ABEF. During an imbibition path (CD), the energy dissipated is equal to the area CDFE. Image taken from [5].

PROBLEMS

5.1   [FEM for 1D steady fluid flow] Consider the steady laminar flow of a viscous in-compressible fluid with constant density in a long annular region between two coaxial cylinders of radii R_i and R_0 (see Figure 5.16). The differential equation for this case is given by:

$$-\frac{1}{r}\frac{d}{dr}\left(r\,\mu\,\frac{dw}{dr}\right) = f_0, \quad f_0 = \frac{P_1 - P_2}{L}$$

where w is the velocity along the cylinders (i.e., the z component of velocity), μ is the vis-cosity, L is the length of the region along the cylinders in which the flow is fully developed, and P_1 and P_2 are the pressures at $z = 0$ and $z = L$, respectively (P_1 and P_2 represent the combined effect of static pressure and gravitational force). The boundary conditions are:

$$w(r = R_0) = w(r = R_i) = 0$$

1. Write the weak formulation of the problem.

2. Consider two linear elements over the segment $[R_0,\ R_i]$. Write the two elementary equations that govern the problem, using Ritz method.

3. Assemble and condense the system of equations.

4. Solve the system of finite element equations for the primary variable and write the expression of approximate solution over the segment $[R_0,\ R_i]$.

5. Post-process the finite element results to calculate the unknown nodal secondary vari-ables.

6. Repeat questions 2 and 3 with one quadratic element. Do not solve.

5.2   [FEM for 2D steady fluid flow] Consider the irrotational flow of an ideal fluid about a circular cylinder with its axis perpendicular to the plane of flow, which takes place between two long horizontal walls (see figure 5.17). The governing equation is:
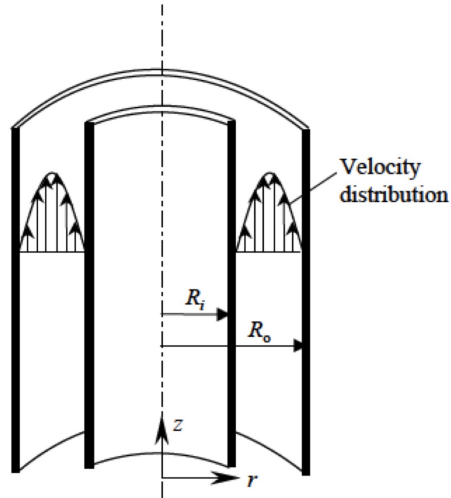
$$-\nabla^2 u = 0 \tag{5.168}$$

Is it more computationally efficient to model the flow problem with the stream function ($u = \Psi$) or the flow potential ($u = \Phi$)?
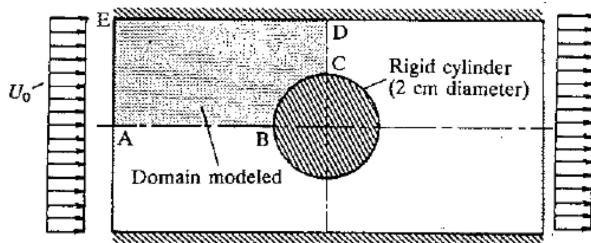
5.3   [FEM for 2D steady fluid flow] Consider the groundwater flow problem governed by the following equation:

$$-\frac{\partial}{\partial x}\left(a_{11}\frac{\partial \Phi}{\partial x}\right) - \frac{\partial}{\partial y}\left(a_{22}\frac{\partial \Phi}{\partial y}\right) = f(x,y) \tag{5.169}$$
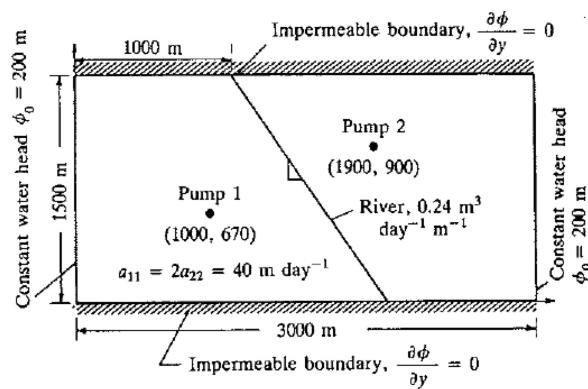
Two pumps are used to extract the water brought by a river, modeled as a lineic fluid source. The boundary and loading conditions are shown in the Figure 5.18. Propose a FEM model made of linear triangular elements to approximate the distribution of water fluxes.

Figure 5.16   Viscous incompressible fluid flow in an annular area.

Figure 5.17   Flow around a non-penetrable obstacle in 2D. Image taken from [18].

Figure 5.18   Seepage problem in 2D. Image taken from [18].

5.4   To account for a percolation porosity, the following modified Kozeny-Carman relation was established:

$$K = B\frac{(\phi - \phi_c)^3}{(1 + \phi_c - \phi)^2}d^2$$

1. Calculate the permeability of a sandstone sample which has porosity 0.32 and an average grain size of 100 μm. Assume $B = 15$ and $\phi_c = 0.035$.

2. Compare the permeabilities κ_1 and κ_2 of two sandstones that have the same porosity and pore microstructure, but different average grain sizes, $d_1 = 80\mu m$ and $d_2 = 240\mu m$.

5.5   We recall that the 1D laminar flow in a pipe of circular cross-section of radius r is:

$$q = -\frac{\pi r^4}{8\eta}\frac{\Delta p}{L}$$
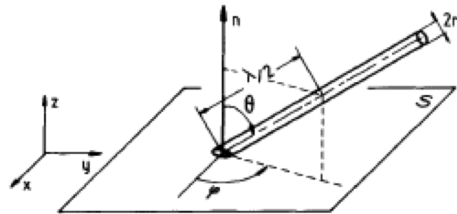
In a tubular pore of circular cross-section, with radius r, Darcy's law is expressed as:

$$q = -K\frac{A}{\eta}\frac{\Delta p}{L} = K\frac{\pi r^2}{\eta}\frac{\Delta p}{L}$$

Consider a unit rock volume that contains N tubular pores of circular cross-section, following an isotropic distribution, with a radius size distribution $p(r)$. Show that the intrinsic permeability K has the following expression:

$$\kappa = \frac{\Phi}{8}\frac{1}{\int_0^\infty f(r)dr}\int_0^\infty r^2 f(r)dr$$

In which Φ is the porosity of the rock sample, and in which the radius volume frequency $f(r)$ is defined as $f(r) = N L \pi r^2 p(r)$.

Figure 5.19   Pipe model: Unit section S intercepts pipes of various orientations (θ, ϕ), radius r and length λ. $\bar{l}$ is the average spacing between two pipes. Image taken from [10]

5.6   Show that for the pipe model illustrated in Figure 5.19, the intrinsic permeability above the percolation threshold has the following expression:

$$K = \frac{\pi}{32} \frac{\overline{\lambda r^4}}{\bar{l}^3}$$

in which $\overline{\lambda}$ is the average capillary length and $\overline{r}$ is the average capillary radius. *Assume that the distribution of capillaries centers along the z-axis is homogeneous and isotropic, and that the probability density functions of r, λ, θ and ϕ are isotropic and statistically independent.*

5.7   Consider the Bethe Lattice shown in Figure 5.9.

1. What is the percolation threshold p_c for this network?

2. What is the average number of sites T to which the origin is connected through a single branch A ? *(T is the average size of the cluster for each branch).*

3. Determine the form of the relationship that links S to p and p_c.

4. Determine P, the fraction of sites that are part of the infinite cluster. *Introduce Q, the probability that a path starting from the origin is interrupted somewhere.*
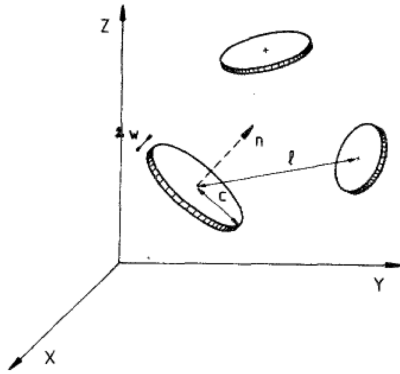
5.8   Consider a geomaterial in which the pores are penny-shaped, with the geometric parameters explained in Figure 5.20.

1. Calculate the value of l (average distance between fractures) at the percolation threshold. Assume that the fractures are disk shaped and of radius $c = 200\mu m$. *Assume that each fracture is a site that is part of a Bethe lattice.*

2. Calculate the maximum value of permeability for a population of identical fractures with radius $c = 200\mu m$ and aperture $w = 1\mu m$. <u>Given</u>: The permeability of a network of penny-shaped fractures is:

$$k = \frac{4\pi}{15} f \frac{\overline{w^3} \overline{c^2}}{\bar{l}^3}$$

In which f is the portion of fractures that form an infinite cluster, and $\overline{x}^n$ is the n-th moment of probability of the variable x.

5.9   Prove the axis-symmetric consolidation equation (Equation 5.125).

Figure 5.20   Flow in a network of penny-shaped pores. Image taken from [10].

5.10   Consider a rock specimen filled with oil (mass density ρ_n, pressure p_n, saturation degree S_n) and water (mass density ρ_w, pressure p_w, saturation degree S_w). The specimen is cylindrical, with impermeable lateral boundaries. The specimen is subjected to a constant water flow at the base. The initial saturation degree of oil is $S_n^0 = 0.8$. We assume that fluid flow is purely 1D and occurs only in the direction of the axis of the specimen. The capillary pressure is assumed to be negligible, i.e. $\forall z$, $p_n(z) = p_w(z) = p(z)$. The porosity of the specimen is assumed to remain constant.

1. Provide the governing equations of the water and oil phases.

2. Assume that the fluids are incompressible. Show that the sum of the fluid velocities $v(z) = v_n(z) + v_w(z)$ is uniform throughout the sample, i.e. that $v(z)$ does not depend on the position z in the sample.

3. Show that:
$$\frac{dp}{dz} = \frac{-v(z) + (K_w\rho_w/\mu_w + K_n\rho_n/\mu_n)\,g}{K_w/\mu_w + K_n/\mu_n}$$

Explain why dp/dz only depends on S_w.

5.11   The capillary rise in a tube can be calculated by using Jurin's equation:

$$\gamma_w\, h = p_n - p_w$$

and Laplace's equation:

$$p_n - p_w = \frac{2t_{n/w}\cos\theta_w}{r}$$

in which h is the height of the capillary rise, γ_w is the specific weight of the wetting fluid in the tube (e.g., water), p_w is the pressure of the wetting fluid (water), p_n is the pressure of the non-wetting fluid (e.g., air), r is the radius of the tube, $t_{n/w}$ is the surface tension in the meniscus (e.g., at the water/air interface) and θ_w is the wetting angle, i.e. the angle that exists between the normal to the tube wall and the tangent to the meniscus. For a water/air meniscus under ambient temperature, we have $t_{n/w} = 75$ mN/m. The porous network inside a soil specimen is often modeled as a distribution of capillary tubes that are parallel to each other and that are not connected to one another, so that the equations of Jurin and Laplace can be applied. With this assumption in mind, let us consider a cylindrical soil specimen, 5 cm in diameter and 100 cm in height, made of solid grains, liquid water and gaseous air. The soil porous network is modeled by the bundle of tubes described in Table 5.2. Furthermore, it is assumed that the tubes are perfectly wettable, i.e., $\theta_w = 0^o$.

1. Calculate the porosity of the specimen.

2. Express the capillary rise in a single tube of diameter D (in symbolic formula). Calculate the capillary rise h in each type of tube listed in Table 5.2.

3. Express the relationship between the capillary pressure and the degree of saturation in water of the specimen. Plot the Water Retention Curve of the specimen.

Table 5.2   Porous network modeled as a bundle of tubes

Tube diameter (μm)	Number of tubes
0.1	500
0.5	1,000
1	5,000
5	50,000
10	100,000
50	50,000
100	5,000
500	1,000
1000	500

5.12   Let us consider two non-deformable cylinders of radius R and of length 1 m in the direction orthogonal to the sheet of paper (see Figure 5.21). At the contact between the two cylinders, a water meniscus exists. We assume that the material that makes the cylinders is perfectly wettable, i.e., $\theta_w = 0$. The meniscus section is an arc of circle of radius r. The width of the meniscus relative to the axis that links the two centers of the cylinders is noted l.
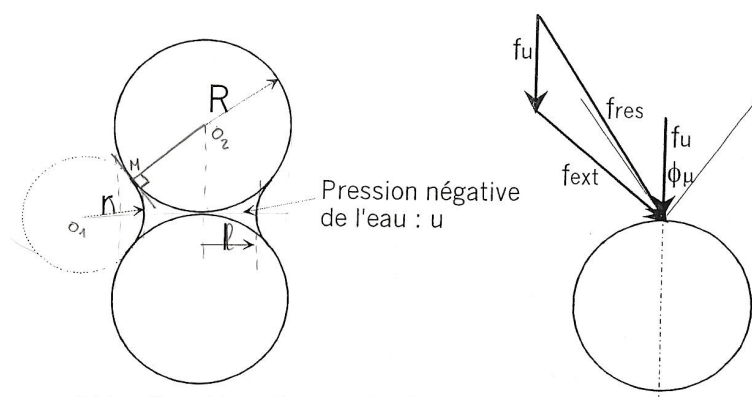
1. Calculate l as a function of r and R. Derive the relation between the water capillary pressure in the meniscus, R and $\alpha = R/r$. From there, calculate the attraction force f_u between the two cylinders because of the presence of the meniscus (provide the expression of f_u as a function of α and R).

2. Generalize the result found in question 1 above to a regular cubic packing of cylinders. Give the expression of the effective stress. What are the limitations of this model?

3. Calculate the porosity, void ratio and dry specific weight of the material (assuming a regular cubic packing). Assume $\rho_s = 27$ kN/m^3 (for the solid grains).

4. The capillary cohesion is defined as:

$$c_s = \sigma'_n \tan \Phi'$$

in which Φ' is the friction angle and σ'_n is the normal component of the effective stress (where here, the normal direction is the direction of the segment that links the centers of both cylinders). Calculate the capillary cohesion of the medium as a function of the water capillary pressure, for a friction angle of 30°. Plot the variations of the cohesion for $R = 1\mu m$.

5. Calculate the increase in material strength in the vertical direction as a function of the capillary pressure. Assume hte following:

   ▪ The stress path is triaxial (σ_H=cst);
   ▪ The external forces are given as: $f_{ext} = 2R \times \left(0.75\sigma_v^2 + 0.25\sigma_h^2\right)$;
   ▪ The orientation angle of the external forces compared to the vertical is given as: $\delta_{ext} = 60 - arctan(0.577 \times (\sigma_H/\sigma_v))$ (in degrees);
   ▪ The material strength of the dry medium is 100 kPa, which corresponds to an external force oriented by an angle of 30° compared to the vertical (normal).

   To proceed with the calculation, assume a value of σ_v and calculate the capillary force such that σ_v reaches the material strength.

Figure 5.21 The menisci between two solid cylinders and the corresponding inter-granular forces. Image taken after Fleureau's course notes.

CHAPTER 6

FINITE ELEMENT METHOD IN PORO-ELASTICITY

6.1 1D eigenvalue and transient problems

6.1.1 Eigenvalue problems

6.1.1.1 Governing equations

Consider a differential equation that includes both space and time derivatives of the dependent variable, as follows:

$$A_x\left(u(x,t)\right) + B_t\left(u(x,t)\right) = f(x,t) \tag{6.1}$$

in which A_x is a linear operator with space derivatives and B_t is a linear operator with time derivatives. Since the differential operators are linear, it is possible to find the overall solution of the PDE by summing the solution to the homogeneous differential equation (without right-hand side member) and a particular solution of the actual differential equation at stake:

$$A_x\left(u_p(x,t)\right) + B_t\left(u_p(x,t)\right) = f(x,t) \tag{6.2}$$

$$A_x\left(u_h(x,t)\right) + B_t\left(u_h(x,t)\right) = 0 \tag{6.3}$$

With linear operators:

$$u(x,t) = u_p(x,t) + u_h(x,t) \tag{6.4}$$

The problem is now to solve for $u_h(x,t)$. Often, the space and time variables are separated, and the solution is sought in the form:

$$u_h(x,t) = U_1(x)\,U_2(t) \tag{6.5}$$

u_h satisfies the homogeneous governing equation, and with linear operators:

$$A_x \left(U_1(x) \, U_2(t) \right) \; = \; -B_t \left(U_1(x) \, U_2(t) \right) \tag{6.6}$$

$$-\frac{1}{U_1(x)} A_x \left(U_1(x) \right) \; = \; \frac{1}{U_2(t)} B_t \left(U_2(t) \right) \tag{6.7}$$

In the equation above, the left-hand side is a function of space only, while the right-hand side is a function of time only. So the equality can only hold if both sides of the equality are constants.

If the time operator B_t is a time derivative or order 1, then the PDE is said to be parabolic (e.g. problem of heat transfer). The solution is then of the form:

$$-\frac{1}{U_1(x)} A_x \left(U_1(x) \right) \; = \; \frac{1}{U_2(t)} B_t \left(U_2(t) \right) \; = \; -\lambda, \quad \lambda > 0 \tag{6.8}$$

$$U_2(t) \; = \; A \, exp(-\lambda \, t) \tag{6.9}$$

If the time operator B_t is a time derivative or order 2, then the PDE is said to be hyperbolic (e.g. problem of bar or beam vibration). The solution is then of the form:

$$-\frac{1}{U_1(x)} A_x \left(U_1(x) \right) \; = \; \frac{1}{U_2(t)} B_t \left(U_2(t) \right) \; = \; -\omega^2 \tag{6.10}$$

$$U_2(t) \; = \; A \, exp(-i\omega \, t) \tag{6.11}$$

For both parabolic and hyperbolic equations:

$$U_2(t) \, A_x \left(U_1(x) \right) \; + U_1(x) \, B_t \left(U_2(t) \right) \; = \; 0$$

For parabolic equations:

$$A \, exp(-\lambda \, t) \, A_x \left(U_1(x) \right) \; + U_1(x) \, cst \, A \, (-\lambda) \, exp(-\lambda \, t) \; = \; 0 \tag{6.12}$$

$$\frac{1}{cst} A_x \left(U_1(x) \right) \; = \; \lambda \, U_1(x) \tag{6.13}$$

For example, for a problem of 1D het transfer:

$$-\frac{1}{\rho \, c \, A_{section}} \frac{d}{dx} \left(k \, A_{section} \frac{d \, U_1(x)}{dx} \right) \; = \; \lambda \, U_1(x) \tag{6.14}$$

For hyperbolic equations:

$$A \, exp(-i\omega \, t) \, A_x \left(U_1(x) \right) \; + U_1(x) \, cst \, A \, \left(-\omega^2 \right) \; exp(-i\omega \, t) \; = \; 0 \tag{6.15}$$

$$\frac{1}{cst} A_x \left(U_1(x) \right) \; = \; \omega^2 \, U_1(x) \tag{6.16}$$

For example, for the motion of a bar:

$$-\frac{1}{\rho \, A_{section}} \frac{d}{dx} \left(E \, A_{section} \frac{d U_1(x)}{dx} \right) \; = \; \omega^2 \, U_1(x) \tag{6.17}$$

The general form of an eigenvalue equation is:

$$A(u) = \beta B(u) \tag{6.18}$$

in which A and B are operators, generally linear, and β is an eigenvalue. Each eigenvalue defines an eigenmode, and each u associated with an eigenvalue is called an eigenvector (or eigenfunction):

$$\Rightarrow \quad U_1(x) = C\cos(\alpha x) + D\sin(\alpha x) \tag{6.19}$$

In a matrix form:

$$([A] - \beta[B])\{U_1\} = \{0\} \tag{6.20}$$

To get non-trivial solutions $\{U_1\}$:

$$det\left([A] - \beta[B]\right) = 0 \tag{6.21}$$

The equation above can be solved for the eigenvalues β_i. There is one solution $\{U_1\}$ per mode:

$$\forall i, \quad ([A] - \beta_i[B])\{U_1\} = \{0\} \tag{6.22}$$

From there, it is possible to solve for the eigenvectors, i.e., for the α_i coefficients.

6.1.1.2 Eigenvalue problem with a parabolic equation

Consider the following governing equation, for 1D heat transfer:

$$-\frac{d}{dx}\left(a(x)\frac{dU_1}{dx}\right) + c(x)U_1(x) = \lambda\, c_0(x)\, U_1(x) \tag{6.23}$$

The weak formulation is:

$$\forall w \simeq \delta U_1, \ \int_{x_a}^{x_b} \frac{dw}{dx}\left(a(x)\frac{dU_1}{dx} + c(x)w(x)U_1(x)\right) dx - \lambda \int_{x_a}^{x_b} c_0(x)\, w(x)U_1(x)dx$$

$$= \left[w(x)a(x)\frac{dU_1}{dx}\right]_{x_a}^{x_b} = \left[w(x)Q(x)\right]_{x_a}^{x_b}$$

$$\tag{6.24}$$

Using a Finite Element model based on Ritz method:

$$([K^e] - \lambda[M^e])\{U_1\} = \{Q\} \tag{6.25}$$

Stiffness Matrix: $\quad K_{ij}^e = \displaystyle\int_{x_e}^{x_{e+1}} \left(a(x)\frac{d\Psi_i}{dx}\frac{d\Psi_j}{dx} + c(x)\Psi_i(x)\Psi_j(x)\right) dx \tag{6.26}$

Mass Matrix: $\quad M_{ij}^e = \displaystyle\int_{x_e}^{x_{e+1}} \left(c_0(x)\Psi_i(x)\Psi_j(x)\right) dx$

- If the i-th primary variable is imposed, the i-th equation is deleted from the system of condensed equations.

- If a connectivity condition is imposed, $\overline{Q} = 0$.

- If the i-th secondary variable is imposed, usually a mixed condition of the type $\overline{Q} = A\left(\overline{U_1}\right)$ is imposed. The term $A\left(\overline{U_1}\right)$ is moved to the left hand side and A is integrated in the stiffness matrix.

Therefore the system of condensed equations is expressed as:

$$\left([\widehat{K}] - \lambda[\widehat{M}]\right)\{U_1\} = \{0\} \tag{6.27}$$

The number of eigenvalues λ increases with the number of degrees of freedom (d.o.f.):

$$det\left([\widetilde{K}] - \lambda[\widehat{M}]\right) = 0 \tag{6.28}$$

For each mode M:

$$U_1{}^M(x) = \Sigma_{j=1}^N U_1{}_j^M \Psi_j(x) \tag{6.29}$$

6.1.1.3 Eigenvalue problem with a hyperbolic equation

Consider the governing equation of a beam vibration problem:

$$\rho A_{section}\frac{\partial^2 w}{\partial t^2} - \rho I\frac{\partial^4 w}{\partial t^2 \partial x^2} + \frac{\partial^2}{\partial x^2}\left(EI\frac{\partial^2 w}{\partial x^2}\right) = q(x,t) \tag{6.30}$$

The homogeneous solution is:

$$w_h(x,t) = U_1(x)\,exp(-i\omega t) \tag{6.31}$$

The governing equation in space is:

$$-\omega^2\,\rho\,A_{section}\,U_1(x) + \omega^2\,\rho\,I\frac{d^2 U_1(x)}{dx^2} + \frac{\partial^2}{\partial x^2}\left(EI\frac{\partial^2 U_1(x)}{\partial x^2}\right) = 0 \tag{6.32}$$

The Finite Element model takes the following form:

$$\left([K^e] - \omega^2[M^e]\right)\{U_1\} = \{Q\} \tag{6.33}$$

The stiffness matrix is:

$$K_{ij}^e = \int_{x_e}^{x_{e+1}} EI\frac{d^2\Psi_i}{dx^2}\frac{d^2\Psi_j}{dx^2}dx \tag{6.34}$$

The mass matrix is:

$$M_{ij}^e = \int_{x_e}^{x_{e+1}}\left(\rho\,A_{section}\Psi_i(x)\Psi_j(x) - \rho\,I\frac{d\Psi}{dx}\frac{d\Psi}{dx}\right)dx \tag{6.35}$$

The vector of secondary variables is obtained after two integrations by parts:

$$Q_i = \left[\Psi_i(x)\frac{d}{dx}\left(EI\frac{d^2 U_1(x)}{dx^2}\right) - \omega^2\,\rho\,I\,\Psi_i(x)U_1(x)\right]_{x_e}^{x_{e+1}} - \left[EI\frac{d\Psi_i}{dx}\frac{d^2 U_1(x)}{dx^2}\right]_{x_e}^{x_{e+1}} \tag{6.36}$$

6.1.2 Transient problems

6.1.2.1 Decoupled formulation

Consider now that the nodal values at functions of time, i.e. that the d.o.f. are transient. That happens when the systems is not free nor forced, for instance when intermittent loads are applied. Then, a transient regime occurs before the steady state, previously treated as

an eigenvalue problem. An interpolation in both space and time is needed to approximate $u(x, t)$. Two options are possible to develop the FEM model:

- Coupled Formulation: interpolation functions depending on space and time:

$$u(x,t) \simeq u^e_{FEM}(x,t) = \Sigma^N_{j=1} \widehat{u}^e_j \widehat{\Psi}^e_j(x,t) \tag{6.37}$$

- Decoupled Formulation: interpolation performed every time step with interpolation functions depending on space only:

$$u(x,t) \simeq u^e_{FEM}(x,t) = \Sigma^N_{j=1} u^e_j(t) \Psi^e_j(x) \tag{6.38}$$

FE models are mostly based on decoupled formulations, and are therefore formulated in two steps:

1. Discretization in Space:

$$\forall t_s \in [0,\, t], \quad u^e_j(x, t_s) = \Sigma^N_{j=1} u^e_j(t_s) \Psi^e_j(x) \tag{6.39}$$

$$t_s = s\,\Delta t \tag{6.40}$$

2. Discretization in Time - often based on Finite Difference schemes.

A decoupled formulation can be used when:

- The exact solution can be expressed as:

$$u(x,t) = f(x)g(t) \tag{6.41}$$

- For a fine time discretization, i.e. for a small Δt (stability condition).

6.1.2.2 Space discretization
The typical governing equation is:

$$-\frac{\partial}{\partial x}\left(a\frac{\partial u}{\partial x}\right) + \frac{\partial^2}{\partial x^2}\left(b\frac{\partial^2 u}{\partial x^2}\right) + c_0\,u + c_1\frac{\partial u}{\partial t} + c_2\frac{\partial^2 u}{\partial t^2} = f(x,t) \tag{6.42}$$

There are terms requiring 1 integration by parts and terms requiring 2 integrations by parts. The primary variables are u, $\frac{\partial u}{\partial x}$. The secondary variables are:

$$Q^1 = -a\frac{\partial u}{\partial x} + \frac{\partial}{\partial x}\left(b\frac{\partial^2 u}{\partial x^2}\right) \tag{6.43}$$

$$Q^2 = -b\frac{\partial^2 u}{\partial x^2}$$

The weak formulation is of the form:

$$\forall w \sim \delta u, \qquad 0 = \int_{x_a}^{x_b}\left(a\frac{\partial w}{\partial x}\frac{\partial u(x,t)}{\partial x} + b\frac{\partial^2 w}{\partial x^2}\frac{\partial^2 u(x,t)}{\partial x^2}\right) dx$$

$$+ \int_{x_a}^{x_b}\left(c_0 w(x)u(x,t) + c_1 w(x)\frac{\partial u(x,t)}{\partial t} + c_2 w(x)\frac{\partial^2 u(x,t)}{\partial t^2}\right) dx \tag{6.44}$$

$$- \int_{x_a}^{x_b} w(x)f(x,t)dx - Q^1_1 w(x_a) + Q^1_2 w(x_b) - Q^2_1\frac{\partial w}{\partial x}(x_a) + Q^2_2\frac{\partial w}{\partial x}(x_b)$$

For a given time t_s, the Finite Element model with Ritz Method is:

$$0 = \left[\int_{x_a}^{x_b} \left(a\frac{d\Psi_i}{dx}\frac{d\Psi_j}{dx} + b\frac{d^2\Psi_i}{dx^2}\frac{d^2\Psi_j}{dx^2} + c_0\Psi_i(x)\Psi_j(x)\right) dx\right] u_j(t_s)$$

$$+\left[\int_{x_a}^{x_b} c_1\Psi_i(x)\Psi_j(x)dx\right]\frac{du_j}{dt}(t_s) , + \left[\int_{x_a}^{x_b} c_2\Psi_i(x)\Psi_j(x)dx\right]\frac{d^2u_j}{dt^2}(t_s) \qquad (6.45)$$

$$-\int_{x_a}^{x_b}\Psi_i(x)f(x,t_s)dx - Q_1^1 w(x_a) + Q_2^1 w(x_b) - Q_1^2\frac{\partial w}{\partial x}(x_a) + Q_2^2\frac{\partial w}{\partial x}(x_b)$$

In a matrix form: $[K]\{u\} + [C]\{\dot{u}\} + [M]\{\ddot{u}\} = \{F + Q\}$ \qquad (6.46)

Parabolic Equations: $[K]\{u\} + [M^1]\{\dot{u}\} = \{F + Q\}$ \qquad (6.47)

in which $[K]$ is the stiffness matrix, $[M]$ is the mass matrix, and $[C]$ is the damping matrix, assumed to be zero in the following.

6.1.2.3   Time discretization for parabolic equations

A typical time-dependent parabolic equation encountered in engineering is:

$$a\frac{du(t)}{dt} + bu(t) = f(t), \quad 0 < t < T, \quad u(t = 0) = u_0 \qquad (6.48)$$

Note that initial conditions required in order to solve the problem. The time discretization process is done with an α-family of approximation (this is a Finite Difference type of approximation):

$$(1 - \alpha)\dot{u}_s + \alpha\dot{u}_{s+1} = \frac{u_{s+1} - u_s}{\Delta t_{s+1}}, \quad 0 \le \alpha \le 1 \qquad (6.49)$$

The time discretization can be understood as an approximation of a weighted average of the derivatives by a linear interpolation of the dependent variable in time. Assuming that the mass matrix $[M]$ does not depend on time, the weak formulation at two distinct times t_s and t_{s+1} is obtained as follows:

$$\begin{cases} [M]\{\dot{u}\}_s + [K]_s\{u\}_s = \{F + Q\}_s \\ \\ [M]\{\dot{u}\}_{s+1} + [K]_{s+1}\{u\}_{s+1} = \{F + Q\}_{s+1} \end{cases} \qquad (6.50)$$

Using the FDM interpolation of the time derivatives:

$$[M]\left(\alpha\{\dot{u}\}_{s+1} + (1-\alpha)\{\dot{u}\}_s\right) = [M]\frac{1}{\Delta t_{s+1}}\left(\{u\}_{s+1} - \{u\}_s\right) \qquad (6.51)$$

The resulting equation system is:

$$\Delta t_{s+1}\left(\alpha\{F + Q\}_{s+1} - \alpha[K]_{s+1}\{u\}_{s+1}\right)$$

$$\qquad (6.52)$$

$$+\Delta t_{s+1}\left((1-\alpha)\{F + Q\}_s - (1-\alpha)[K]_s\{u\}_s\right) = [M]\left(\{u\}_{s+1} - \{u\}_s\right)$$

The equations are solved by using a time marching scheme: Given u, F and Q at all times ¡ t_s, we determine u at time t_{s+1} with:

$$([M] + \alpha \Delta t_{s+1}[K]_{s+1}) \{u\}_{s+1} =$$

$$([M] - (1 - \alpha)\Delta t_{s+1}[K]_s) \{u\}_s \tag{6.53}$$

$$+\Delta t_{s+1} (\alpha\{F + Q\}_{s+1} + (1 - \alpha)\{F + Q\}_s)$$

- The preceding numerical scheme is said to be consistent with the problem $[M]\{\dot{u}\}_s + [K]_s\{u\}_s = \{F+Q\}_s$ if the round-off and truncation errors tend to 0 when $\Delta t \to 0$.

- The numerical solution accuracy is measured by norms of the difference between the exact and approximate solutions.

- A time-approximation scheme is said to be convergent if for a fixed time t_s, the numerical value $\{u\}_s$ converges to its value $\{u(t_s)\}$ when $\Delta t \to 0$.

A numerical scheme is said to be stable if the approximate solution remains bounded even for high times. Stability accounts for the accumulation of errors while computing the current solution (at t_s) from anterior solutions ($t < t_s$). To find out in which conditions a FEM model is stable, consider the solution in the steady state. At this point, loads imposed do not depend on time and the time marching scheme writes:

$$([M] + \alpha \Delta t_{s+1}[K]_{s+1}) \{u\}_{s+1} = ([M] - (1 - \alpha)\Delta t_{s+1}[K]_s) \{u\}_s \tag{6.54}$$

In addition, the approximation solution in the steady state is expressed as:

$$u_{FEM}(x,t) = \sum_{k=1}^{M} \left(\sum_{j=1}^{N} U_j^k \Psi_j(x) \right) exp(-\lambda_k t) \tag{6.55}$$

in which M is the number of modes and N is the interpolation order. In particular, the monomodal approximation writes:

$$u_{FEM}(x,t) = \sum_{j=1}^{N} U_j^1 \Psi_j(x) exp(-\lambda_1 t) \tag{6.56}$$

in which:

$$([K] - \lambda_1[M]) \{u^1\} = \{0\} \tag{6.57}$$

So that, at all times:

$$[K] \{u^1\} exp(-\lambda_1 t) = \lambda_1[M] \{u^1\} exp(-\lambda_1 t) \tag{6.58}$$

At times t_s and t_{s+1}:

$$[K] \{u^1\}_s = \lambda_1[M] \{u^1\}_s, \quad [K] \{u^1\}_{s+1} = \lambda_1[M] \{u^1\}_{s+} \tag{6.59}$$

Using a constant time step, a constant stiffness matrix and a constant mass matrix, and injecting in the steady state time marching scheme:

$$(1 + \alpha\lambda_1\Delta t) [M]\{u\}_{s+1} = (1 - (1 - \alpha)\lambda_1\Delta t) [M]\{u\}_s \tag{6.60}$$

Since the mass matrix is invertible, we get that the FEM model is stable if, and only if:

$$\left| \frac{1 + (\alpha - 1)\lambda_1 \Delta t}{1 + \alpha \lambda_1 \Delta t} \right| < 1 \tag{6.61}$$

Since $0 \leq \alpha \leq 1$ and $\lambda_1 > 0$ (λ_1 is a physical entity that depends on impedance terms), we see that the FEM model is unconditionally stable if $\alpha \geq 1/2$. If $\alpha < 1/2$, the scheme is automatically stable if $1 + (\alpha - 1)\lambda_1 \Delta t > 0$ (but this happens rarely in physical problems). If $\alpha < 1/2$ and $1 + (\alpha - 1)\lambda_1 \Delta t \leq 0$, the stability criterion is:

$$\Delta t < \frac{2}{(1 - 2\alpha)\lambda_1} = \Delta_{crit} \tag{6.62}$$

For approximations with more that one mode, note that the subsequence eigenvalues λ_j are smaller than λ_1, so that if the stability criterion $\Delta t < \frac{2}{(1-2\alpha)\lambda_1}$ is satisfied, we have $\Delta t < \frac{2}{(1-2\alpha)\lambda_j}$ for all modes j. In other words, for $\alpha < 1/2$, the FEM model is conditionally stable and the stability criterion is:

$$\Delta t < \frac{2}{(1 - 2\alpha)\lambda_{max}} = \Delta_{crit} \tag{6.63}$$

where λ_{max} is the largest eigenvalue of the associated eigenvalue problem (steady state).

6.1.2.4 Time discretization for hyperbolic equations

Hyperbolic Equations contain time-derivatives of order 2. The most common time discretization scheme is the so-called Newmark's Scheme, which can be stated as follows:

$$\begin{cases} \{u\}_{s+1} = \{u\}_s + \Delta t \{\dot{u}\}_s + \frac{1}{2} (\Delta t)^2 \{\ddot{u}\}_{s+\gamma} \\ \\ \{\dot{u}\}_{s+1} = \{\dot{u}\}_s + \Delta t \{\ddot{u}\}_{s+\alpha} \end{cases} \tag{6.64}$$

with:

$$\{\ddot{u}\}_{s+\theta} = (1 - \theta)\{\ddot{u}\}_s + \theta\{\ddot{u}\}_{s+1} \tag{6.65}$$

The general Form of the matrix equation after time discretization is:

$$[\widehat{K}]_{s+1}\{u\}_{s+1} = \{\widehat{F}\}_{s,s+1} \tag{6.66}$$

$$\begin{cases} [\widehat{K}]_{s+1} = [K]_{s+1} + coef_M * [M]_{s+1} + coef_C * [C]_{s+1} \\ \\ \{\widehat{F}\}_{s,s+1} = \{F\}_{s+1} + [M]_{s+1}\{A\}_s + [C]_{s+1}\{B\}_s \end{cases} \tag{6.67}$$

$$\begin{cases} \{A\}_s = coef_{A1}\{u\}_s + coef_{A2}\{\dot{u}\}_s + coef_{A3}\{\ddot{u}\}_s \\ \\ \{B\}_s = coef_{B1}\{u\}_s + coef_{B2}\{\dot{u}\}_s + coef_{B3}\{\ddot{u}\}_s \end{cases} \tag{6.68}$$

This system of equations needs to be solved for the unknown $\{u\}$ at time t_s from the dependent variables $\{u\}$, $\{\dot{u}\}$ and $\{\ddot{u}\}$ determined at previous time steps. The stability conditions are more difficult to establish. Here, they are given without proof, as follows:

- for $\alpha = 1/2$:

- – if $\gamma = 1/2$: constant-average acceleration method, stable
- – if $\gamma = 1/3$: linear acceleration method, conditionally stable
- – if $\gamma = 0$: central difference method, conditionally stable

- for $\alpha = 3/2$:

  - – if $\gamma = 8/5$: Galerkin method, stable
  - – if $\gamma = 2$: backward method, stable

For $\alpha \geq 1/2$ and $\gamma < \alpha$:

$$\Delta t < \Delta t_{crit} = \left[\frac{1}{2} \omega_{max}^2 (\alpha - \gamma) \right]^{-1/2} \tag{6.69}$$

$$\left([K] - \omega^2 [M] \right) \{u\} = \{F + Q\} \tag{6.70}$$

6.1.2.5 Numerical techniques to expedite calculations

For parabolic equations:

$$([M] + \alpha \Delta t_{s+1} [K]_{s+1}) \{u\}_{s+1} =$$

$$([M] - (1 - \alpha) \Delta t_{s+1} [K]_s) \{u\}_s \tag{6.71}$$

$$+ \Delta t_{s+1} (\alpha \{F + Q\}_{s+1} + (1 - \alpha) \{F + Q\}_s)$$

For $\alpha = 0$:

$$[M]\{u\}_{s+1} = ([M] - \Delta t_{s+1} [K]_s) \{u\}_s + \Delta t_{s+1} \{F + Q\}_s \tag{6.72}$$

If $[M]$ is diagonal:

$$u_i(t_{s+1}) = \frac{1}{M_{ii}} \left(M_{ii} u_i(t_s) - \Delta t \sum_{j=1}^{N} K_{ij} u_j t_s \right) + \frac{\Delta t}{M_{ii}} (F_s + Q_s) \tag{6.73}$$

In general, weighted integral formulations lead to symmetric, positive-definite, non-diagonal mass matrices (called consistent mass matrices). But there are techniques to diagonalize the mass matrix:

- Row sum lumping:

$$M_{ii}^L = \sum_{j=1}^{N} M_{ij}^C = \sum_{j=1}^{N} \int_{x_a}^{x_b} \rho \Psi_i(x) \Psi_j(x) dx = \int_{x_a}^{x_b} \rho \Psi_i(x) \left(\sum_{j=1}^{N} \Psi_j(x) \right) dx = \int_{x_a}^{x_b} \rho \Psi_i(x) dx$$
$$\tag{6.74}$$

  The same matrix operators are applied simultaneously to the left and right hand sides of the time marching scheme. For linear elements:

$$[M^C] = \frac{\rho h_e}{6} \begin{bmatrix} 2 & 1 \\ 1 & 2 \end{bmatrix} \Rightarrow [M^L] = \frac{\rho h_e}{2} \begin{bmatrix} 1 & 0 \\ 0 & 1 \end{bmatrix} \tag{6.75}$$

- Proportional lumping:

$$M_{ii}^L = \frac{\int_{x_a}^{x_b} \rho dx}{\sum_{i=1}^{N} \int_{x_a}^{x_b} \rho \Psi_i(x)\Psi_i(x)dx} \int_{x_a}^{x_b} \rho \Psi_i(x)\Psi_i(x)dx, \quad M_{ij}^L = 0 \text{ for } i \neq j \tag{6.76}$$

6.2   Flow of viscous incompressible fluids

6.2.1   Governing equations

- We assume that the flow is slow so that inertial effects are negligible:

$$\mathbf{v} \cdot \nabla(\mathbf{v}) \simeq \mathbf{0} \tag{6.77}$$

- The fluid is assumed to be viscous, i.e. $\mu \neq 0$, and the following constitutive equations hold:

$$\sigma_{xx} = \tau_{xx} - P, \quad \sigma_{yy} = \tau_{yy} - P, \quad \sigma_{xy} = \tau_{xy} \tag{6.78}$$

$$\tau_{xx} = 2\mu \frac{\partial v_x}{\partial x}, \quad \tau_{yy} = 2\mu \frac{\partial v_y}{\partial y}, \quad \tau_{xx} = \mu \left(\frac{\partial v_x}{\partial y} + \frac{\partial v_y}{\partial x} \right) \tag{6.79}$$

It is impossible to simplify the momentum equation into:

$$\frac{\rho}{2} \left(v_x^2 + v_y^2 \right) + \widehat{P} = 0 \tag{6.80}$$

- The fluid is assumed to be incompressible, i.e. $\rho = cst$ and:

$$\frac{\partial \rho}{\partial t} = 0 \tag{6.81}$$

The 2 equations of momentum conservation are:

$$\begin{cases} \rho \frac{\partial v_x}{\partial t} - \frac{\partial \sigma_{xx}}{\partial x} - \frac{\partial \sigma_{xy}}{\partial y} - f_x = 0 \\[3mm] \rho \frac{\partial v_y}{\partial t} - \frac{\partial \sigma_{xy}}{\partial x} - \frac{\partial \sigma_{yy}}{\partial y} - f_y = 0 \end{cases} \tag{6.82}$$

The fluid mass conservation (continuity equation) is expressed as:

$$\frac{\partial v_x}{\partial x} + \frac{\partial v_y}{\partial y} = 0 \tag{6.83}$$

The boundary conditions are of the form:

- primary variables: v_x, v_y

- secondary variables: t_x, t_y

$$t_x = \sigma_{xx} n_x + \sigma_{xy} n_y, \qquad t_y = \sigma_{xy} n_x + \sigma_{yy} n_y \tag{6.84}$$

In general, the initial conditions are of the form:

$$v_x(x, y, 0) = v_x^0(x, y), \qquad v_y(x, y, 0) = v_y^0(x, y) \tag{6.85}$$

We develop a Finite Element model based on a decoupled formulation:

$$\forall t_s \in [0,\, t], \quad v_x(x, y, t_s) = \sum_{j=1}^{N_x} v_{x\,j}^{\,e}(t_s)\Psi_j(x, y) \tag{6.86}$$

$$\forall t_s \in [0,\, t], \quad v_y(x, y, t_s) = \sum_{j=1}^{N_y} v_{y\,j}^{\,e}(t_s)\Phi_j(x, y) \tag{6.87}$$

6.2.2 Space discretization

The weak formulation is obtained as follows:

- Weighted Integral Statement:

$$\int_\Omega w_1 \left[-\frac{\partial}{\partial x}\left(2\mu\frac{\partial v_x}{\partial x} - P\right) - \mu\frac{\partial}{\partial y}\left(\frac{\partial v_x}{\partial y} + \frac{\partial v_y}{\partial x}\right)\right] dxdy$$

$$+ \int_\Omega \rho w_1 \dot{v}_x(t_s) dxdy - \int_\Omega w_1 f_x dxdy = 0 \tag{6.88}$$

$$\int_\Omega w_2 \left[-\mu\frac{\partial}{\partial x}\left(\frac{\partial v_x}{\partial y} + \frac{\partial v_y}{\partial x}\right) - \frac{\partial}{\partial y}\left(2\mu\frac{\partial v_y}{\partial y} - P\right)\right] dxdy$$

$$+ \int_\Omega \rho w_2 \dot{v}_y(t_s) dxdy - \int_\Omega w_2 f_y dxdy = 0 \tag{6.89}$$

- Integration by Parts:

$$\int_\Omega \left[\frac{\partial w_1}{\partial x}\left(2\mu\frac{\partial v_x}{\partial x} - P\right) + \mu\frac{\partial w_1}{\partial y}\left(\frac{\partial v_x}{\partial y} + \frac{\partial v_y}{\partial x}\right)\right] dxdy$$

$$+ \int_\Omega \rho w_1 \dot{v}_x(t_s) dxdy - \int_\Omega w_1 f_x dxdy \tag{6.90}$$

$$- \oint_\Gamma w_1 \left[\left(2\mu\frac{\partial v_x}{\partial x} - P\right)n_x + \mu\left(\frac{\partial v_x}{\partial y} + \frac{\partial v_y}{\partial x}\right)n_y\right] ds = 0$$

$$\int_\Omega \left[\mu\frac{\partial w_2}{\partial x}\left(\frac{\partial v_x}{\partial y} + \frac{\partial v_y}{\partial x}\right) + \frac{\partial w_2}{\partial y}\left(2\mu\frac{\partial v_y}{\partial y} - P\right)\right] dxdy$$

$$+ \int_\Omega \rho w_2 \dot{v}_y(t_s) dxdy - \int_\Omega w_2 f_y dxdy \tag{6.91}$$

$$- \oint_\Gamma w_2 \left[\mu\left(\frac{\partial v_x}{\partial y} + \frac{\partial v_y}{\partial x}\right)n_x + \left(2\mu\frac{\partial v_y}{\partial y} - P\right)n_y\right] ds = 0$$

- Boundary Conditions:

$$\forall w_1(x, y) \sim \delta v_x(x, y, t_s), \quad \int_\Omega \left[\frac{\partial w_1}{\partial x}\left(2\mu\frac{\partial v_x}{\partial x} - P\right) + \mu\frac{\partial w_1}{\partial y}\left(\frac{\partial v_x}{\partial y} + \frac{\partial v_y}{\partial x}\right)\right] dxdy$$

$$+ \int_\Omega \rho w_1 \dot{v}_x(t_s) dxdy - \int_\Omega w_1 f_x dxdy - \oint_\Gamma w_1 t_x ds = 0 \tag{6.92}$$

$$\forall w_2(x,y) \sim \delta v_y(x,y,t_s), \quad \int_\Omega \left[\frac{\partial w_2}{\partial y} \left(2\mu \frac{\partial v_y}{\partial y} - P \right) + \mu \frac{\partial w_2}{\partial y} \left(\frac{\partial v_x}{\partial y} + \frac{\partial v_y}{\partial x} \right) \right] dxdy$$

$$+ \int_\Omega \rho w_2 \dot{v}_y(t_s) dxdy - \int_\Omega w_2 f_y dxdy - \oint_\Gamma w_2 t_y ds = 0 \tag{6.93}$$

Now, if we try to write the weak formulation of the mass conservation equation, the weighted integral statement is:

$$\int_\Omega w_3 \left(\frac{\partial v_x}{\partial x} + \frac{\partial v_y}{\partial y} \right) dxdy = 0 \tag{6.94}$$

in which:

$$w_3 \left(\frac{\partial v_x}{\partial x} + \frac{\partial v_y}{\partial y} \right) dxdy \equiv \mathbf{power} \tag{6.95}$$

so $w_3(x,y) \sim \pm \delta P$. We cannot balance the orders of the derivatives, so an integration by parts will not be helpful. There is no boundary integral and therefore, P is not a primary variable. We thus have 2 primary variables (v_x, v_y) for 3 independent nodal variables (v_x, v_y, P) in 3 independent governing equations. So 3 sets of interpolation functions are needed. The nodal variables are all independent, i.e. none of them is the derivative of another, so Lagrange polynomials are needed. Variables v_x and v_y are the same physical entity (velocities), and so they require the same interpolation order. According to the differentiability requirements in the weak formulation, the minimum order of the interpolation polynomials is 1 for v_x and v_y (linear) and 0 for P (constant over each element). We note:

$$v_x^e(x,y,t_s) \simeq \sum_{j=1}^N v_{xj}^e(t_s) \Psi_j(x,y) \tag{6.96}$$

$$v_y^e(x,y,t_s) \simeq \sum_{j=1}^N v_{yj}^e(t_s) \Psi_j(x,y) \tag{6.97}$$

$$P^e(x,y,t_s) \simeq \sum_{j=1}^M P_j^e(t_s) \Phi_j(x,y) = \sum_{j=1}^M P_j^e(t_s) \Phi_j \tag{6.98}$$

If the Ψ_j functions are linear and if the Φ_j function is a constant, the matrix form of the Ritz Finite Element equations is given in Figure 6.1. Another way to write the Finite Element equations is as follows:

$$\begin{cases} [M]\{\dot{\Delta}\} + [K^{11}]\{\Delta\} + [K^{12}]\{P\} = \{F^1\} + \{Q^1\} \\[2mm] [K^{21}]\{\Delta\} = \{0\} \end{cases} \tag{6.99}$$

$$[M] = \int_{\Omega_e} \rho[\Psi]^T[\Psi]dxdy, \quad [K^{11}] = \int_{\Omega_e} [\Psi]^T[B]^T \begin{bmatrix} 2\mu & 0 & 0 \\ 0 & 2\mu & 0 \\ 0 & 0 & \mu \end{bmatrix} [B][\Psi]dxdy \tag{6.100}$$

$$\begin{bmatrix} 2[S^{11}]+[S^{22}] & [S^{21}] & -[S^{10}] \\ [S^{12}] & [S^{11}]+2[S^{22}] & -[S^{20}] \\ -[S^{10}]^T & -[S^{20}]^T & [0] \end{bmatrix} \begin{Bmatrix} \{v_x\} \\ \{v_y\} \\ \{P\} \end{Bmatrix}$$

$$+ \begin{bmatrix} [M] & [0] & [0] \\ [0] & [M] & [0] \\ [0] & [0] & [0] \end{bmatrix} \begin{Bmatrix} \{\dot{v}_x\} \\ \{\dot{v}_y\} \\ \{\dot{P}\} \end{Bmatrix} = \begin{Bmatrix} \{F^1\} \\ \{F^2\} \\ \{0\} \end{Bmatrix}$$

$$M_{ij} = \int_{\Omega_e} \rho \psi_i^e \psi_j^e \, dx \, dy$$

$$S_{ij}^{\alpha\beta} = \int_{\Omega_e} \mu \frac{\partial \psi_i^e}{\partial x_\alpha} \frac{\partial \psi_j^e}{\partial x_\beta} \, dx \, dy \; ; \quad \alpha, \beta = 1, 2$$

$$S_{iJ}^{\alpha 0} = \int_{\Omega_e} \mu \frac{\partial \psi_i^e}{\partial x_\alpha} \phi_J^e \, dx \, dy \; ; \quad \alpha = 1, 2$$

$$F^1 = \int_{\Omega_e} \psi_i^e f_x \, dx \, dy + \oint_{\Gamma_e} \psi_i^e t_x \, ds$$

$$F^2 = \int_{\Omega_e} \psi_i^e f_y \, dx \, dy + \oint_{\Gamma_e} \psi_i^e t_y \, ds$$

Figure 6.1 Ritz Finite Element model for a 2D problem of incompressible viscous fluid flow. Image taken from [18].

$$[K^{12}] = \int_{\Omega_e} \left(\left\{ \begin{matrix} \partial/\partial x \\ \partial/\partial y \end{matrix} \right\}^T [\Psi] \right)^T \{\Phi\}^T dxdy \tag{6.101}$$

$$[K^{21}] = \int_{\Omega_e} \{\Phi\} \left(\left\{ \begin{matrix} \partial/\partial x \\ \partial/\partial y \end{matrix} \right\}^T [\Psi] \right) dxdy \tag{6.102}$$

$$\{F^1\} = \int_{\Omega_e} [\Psi]^T \left\{ \begin{matrix} f_x \\ f_y \end{matrix} \right\} dxdy, \quad \{Q^1\} = \oint_{\Gamma_e} [\Psi]^T \left\{ \begin{matrix} t_x \\ t_y \end{matrix} \right\} ds \tag{6.103}$$

Here, we have a mixed velocity-pressure formulation. A classical way to solve this kind of problem is to use the continuity equation that applies on the pressure as a constraint and to solve equations that only depend on the degrees of freedom. This technique is called the penalty method; it is basically a minimization method. Below, we explain how to use the penalty method for a 2D problem of incompressible viscous fluid flow.

With the weight functions $w_1 \sim \delta v_x$, $w_2 \sim \delta v_y$ and $w_3 \sim \delta P$, the weak formulation may be written as:

$$\begin{cases} B_t(\mathbf{w}, \mathbf{v}) + B_v(\mathbf{w}, \mathbf{v}) - \overline{B}_p(\mathbf{w}, P) = l(\mathbf{w}) \\ \\ -B_p(w_3, \mathbf{v}) = 0 \end{cases} \tag{6.104}$$

$$\{\mathbf{w}\} = \begin{Bmatrix} w_1 \\ w_2 \end{Bmatrix}, \quad \{\mathbf{v}\} = \begin{Bmatrix} v_x \\ v_y \end{Bmatrix}, \quad \{\mathbf{f}\} = \begin{Bmatrix} f_x \\ f_y \end{Bmatrix}, \quad \{\mathbf{t}\} = \begin{Bmatrix} t_x \\ t_y \end{Bmatrix} \quad (6.105)$$

$$B_t(\mathbf{w}, \mathbf{v}) = \int_{\Omega_e} \rho\{\mathbf{w}\}^T\{\dot{\mathbf{v}}\}d\mathbf{x}, \quad B_v(\mathbf{w}, \mathbf{v}) = \int_{\Omega_e} \{[B]\{\mathbf{w}\}\}^T[C_\mu]\{[B]\{\mathbf{v}\}\}d\mathbf{x} \quad (6.106)$$

$$\overline{B}_p(\mathbf{w}, P) = \int_{\Omega_e} [\{\partial/\partial x,\, \partial/\partial y\}\{\mathbf{w}\}]^T P d\mathbf{x} \quad (6.107)$$

$$B_p(w_3, \mathbf{v}) = \int_{\Omega_e} w_3\,[\{\partial/\partial x,\, \partial/\partial y\}\{\mathbf{v}\}]d\mathbf{x} \quad (6.108)$$

$$l(\mathbf{w}) = \int_{\Omega_e} \{\mathbf{w}\}^T\{\mathbf{f}\}d\mathbf{x} + \oint_{\Gamma_e} \{\mathbf{w}\}^T\{\mathbf{t}\}ds \quad (6.109)$$

In a steady state problem:

$$\begin{cases} B_v(\mathbf{w}, \mathbf{v}) - \overline{B}_p(\mathbf{w}, P) = l(\mathbf{w}) \\[2mm] -B_p(w_3, \mathbf{v}) = 0 \end{cases} \quad (6.110)$$

$w_1 \sim \delta v_x$, $w_2 \sim \delta v_y$, and $\frac{\partial v_x}{\partial x} + \frac{\partial v_y}{\partial y} = 0$, so $\frac{\partial w_1}{\partial x} + \frac{\partial w_2}{\partial y} = 0$ and $\overline{B}_p(\mathbf{w}, P) = 0$, and finally $B_v(\mathbf{w}, \mathbf{v}) = l(\mathbf{w})$. Moreover, since $B_v(\mathbf{w}, \mathbf{v})$ is symmetric, the problem boils down to minimizing $I_v(\mathbf{v}) = \frac{1}{2}B_v(\mathbf{v}, \mathbf{v}) - l(\mathbf{v})$ with $B_p(w_3, \mathbf{v}) = 0\ \forall w_3$, i.e. with $G(\mathbf{v}) = \frac{\partial v_x}{\partial x} + \frac{\partial v_y}{\partial y} = 0$. The problem can thus be formulated as:
Minimize $I_L(\mathbf{v}, \lambda)$ defined as:

$$I_L(\mathbf{v}, \lambda) = I_v(\mathbf{v}) + \int_{\Omega_e} \lambda G(\mathbf{v})dxdy \quad (6.111)$$

in which λ is a Lagrange multiplier. The miimization imposes:

$$\delta I_L = \delta_{v_x}I_L + \delta_{v_y}I_L + \delta_\lambda I_L = 0 \quad (6.112)$$

$$\Rightarrow \quad \delta_{v_x}I_L = 0, \quad \delta_{v_y}I_L = 0, \quad \delta_\lambda I_L = 0 \quad (6.113)$$

After some computations:

$$\begin{cases} B_v(\delta\mathbf{v}, \mathbf{v}) + \overline{B}_p(\delta\mathbf{v}, \lambda) = l(\delta\mathbf{v}) \\[2mm] B_p(\delta\lambda, \mathbf{v}) = 0 \end{cases} \quad (6.114)$$

The penalty model is similar to the Lagrange problem:

$$I_P(\mathbf{v}) = I_v(\mathbf{v}) + \frac{\gamma_e}{2}\int_{\Omega_e} [G(\mathbf{v})]^2 d\mathbf{x} \quad (6.115)$$

in which γ_e is a penalty parameter, typically chosen as $10^4\mu \le \gamma_e \le 10^{12}\mu$. A constraint is thus included in a least-squares sense. The problem is to minimize $I_P(\mathbf{v})$: *in function of variations of $\mathbf{v}$ only*:

$$\delta I_P = \delta_{v_x}I_P + \delta_{v_y}I_P = 0 \quad (6.116)$$

After some computations:

$$B_p(\delta\mathbf{v}, \mathbf{v}) = l(\delta\mathbf{v}) \tag{6.117}$$

Two integral equations are gathered in one vector equation because the constraint is already included in the penalty function. Comparing the weak formulations obtained with both methods leads to:

$$\lambda = \gamma_e \left(\frac{\partial v_x}{\partial x} + \frac{\partial v_y}{\partial y} \right) \equiv -P \tag{6.118}$$

It is therefore possible to post-compute the pressure distribution from the minimization coefficient. The weak formulation can be expressed in terms of the velocities only. For instance, the weak formulation of a transient problem with the penalty method, in which the continuity condition is included in the momentum equilibrium equations, is:

$$
\begin{cases}
0 = \int_{\Omega_e} \left[\rho\delta v_x \frac{\partial v_x}{\partial t} + 2\mu \frac{\partial(\delta v_x)}{\partial x} \frac{\partial v_x}{\partial x} + \mu \frac{\partial(\delta v_x)}{\partial y} \left(\frac{\partial v_x}{\partial y} + \frac{\partial v_y}{\partial x} \right) \right] dxdy \\[2mm]
+ \int_{\Omega_e} \left[\gamma_e \frac{\partial(\delta v_x)}{\partial x} \left(\frac{\partial v_x}{\partial x} + \frac{\partial v_y}{\partial y} \right) \right] dxdy - \int_{\Omega_e} \delta v_x \, f_x \, dxdy - \oint_{\Gamma_e} \delta v_x \, t_x \, ds \\[4mm]
0 = \int_{\Omega_e} \left[\rho\delta v_y \frac{\partial v_y}{\partial t} + 2\mu \frac{\partial(\delta v_y)}{\partial y} \frac{\partial v_y}{\partial y} + \mu \frac{\partial(\delta v_y)}{\partial x} \left(\frac{\partial v_x}{\partial y} + \frac{\partial v_y}{\partial x} \right) \right] dxdy \\[2mm]
+ \int_{\Omega_e} \left[\gamma_e \frac{\partial(\delta v_y)}{\partial y} \left(\frac{\partial v_x}{\partial x} + \frac{\partial v_y}{\partial y} \right) \right] dxdy - \int_{\Omega_e} \delta v_y \, f_y \, dxdy - \oint_{\Gamma_e} \delta v_y \, t_y \, ds
\end{cases}
\tag{6.119}
$$

The Finite Element equations can be expressed as two matrix equations by blocks:

$$
\begin{bmatrix} [M] & [0] \\ [0] & [M] \end{bmatrix} \begin{Bmatrix} \{\dot{v}_x\} \\ \{\dot{v}_y\} \end{Bmatrix} + \begin{bmatrix} [K^{11}] & [K^{12}] \\ [K^{21}] & [K^{22}] \end{bmatrix} \begin{Bmatrix} \{v_x\} \\ \{v_y\} \end{Bmatrix} = \begin{Bmatrix} \{F^1\} \\ \{F^2\} \end{Bmatrix} \tag{6.120}
$$

The stiffness blocks represent couplings between the derivatives in x and y:

$$K_{ij}^{11} = 2 \int_{\Omega_e} \mu \frac{\partial\Psi_i}{\partial x} \frac{\partial\Psi_j}{\partial x} dxdy + \int_{\Omega_e} \mu \frac{\partial\Psi_i}{\partial y} \frac{\partial\Psi_j}{\partial y} dxdy + \int_{\Omega_e} \gamma_e \frac{\partial\Psi_i}{\partial x} \frac{\partial\Psi_j}{\partial x} dxdy \tag{6.121}$$

$$K_{ij}^{22} = \int_{\Omega_e} \mu \frac{\partial\Psi_i}{\partial x} \frac{\partial\Psi_j}{\partial x} dxdy + 2 \int_{\Omega_e} \mu \frac{\partial\Psi_i}{\partial y} \frac{\partial\Psi_j}{\partial y} dxdy + \int_{\Omega_e} \gamma_e \frac{\partial\Psi_i}{\partial y} \frac{\partial\Psi_j}{\partial y} dxdy \tag{6.122}$$

$$K_{ij}^{12} = \int_{\Omega_e} \mu \frac{\partial\Psi_i}{\partial y} \frac{\partial\Psi_j}{\partial x} dxdy + \int_{\Omega_e} \gamma_e \frac{\partial\Psi_i}{\partial x} \frac{\partial\Psi_j}{\partial y} dxdy \tag{6.123}$$

$$K_{ij}^{21} = \int_{\Omega_e} \mu \frac{\partial\Psi_i}{\partial x} \frac{\partial\Psi_j}{\partial y} dxdy + \int_{\Omega_e} \gamma_e \frac{\partial\Psi_i}{\partial y} \frac{\partial\Psi_j}{\partial x} dxdy \tag{6.124}$$

Note that there is no space derivative in the mass matrix nor in the force vector:

$$M_{ij} = \int_{\Omega_e} \rho\Psi_i\Psi_j dxdy \tag{6.125}$$

$$F_i^1 = \int_{\Omega_e} \Psi_i f_x dxdy + \oint_{\Gamma_e} \Psi_i t_x \, ds \tag{6.126}$$

$$F_i^2 = \int_{\Omega_e} \Psi_i f_y dxdy + \oint_{\Gamma_e} \Psi_i t_y \, ds \tag{6.127}$$

6.2.3 Time discretization

The final form of the FE matrix equations obtained with the penalty method is as follows:

$$\forall t_s \in [0,\, t], \quad [M]_s\{\dot{\Delta}\}_s + [K]_s\{\Delta\}_s = \{F\}_s \tag{6.128}$$

Since the governing equatino is parabolic, the time discretizatin is handled with a α-family of approximation. Assuming that the mass matrix does not depend on time:

$$([M] + \alpha\Delta t\, [K]_{s+1})\,\{\Delta\}_{s+1} =$$

$$\tag{6.129}$$

$$([M] - (1-\alpha)\Delta t\, [K]_s)\,\{\Delta\}_s + \alpha\Delta t\{F\}_{s+1} + (1-\alpha)\Delta t\{F\}_{s+1}$$

In the mixed FE model, the matrix equations contain zeroes, see Figure 6.1. As a result, the mass matrix equation cannot be inverted, the computations require a lot of iterations and convergence is difficul to reach. It is then advisable to eliminate the equations in P. In the mixed FE model:

$$\begin{cases} [M]\{\dot{\Delta}\} + [K_{11}]\{\Delta\} + [K_{12}]\{P\} = \{F_1\} + \{Q_1\} \\[2mm] [K_{21}]\{\Delta\} = \{0\} \end{cases} \tag{6.130}$$

In the penalty model:

$$[M]\{\dot{\Delta}\} + ([K_{11}] + [K^p])\,\{\Delta\} = \{F_1\} + \{Q_1\} \tag{6.131}$$

in which a "Penalty Stiffness" was introduced, as follows:

$$[K^p] = \int_{\Omega_e} \gamma_e \left(\left\{\begin{array}{c} \partial/\partial x \\ \partial/\partial y \end{array}\right\}^T [\Psi]\right)^T \left(\left\{\begin{array}{c} \partial/\partial x \\ \partial/\partial y \end{array}\right\}^T [\Psi]\right) d\mathbf{x} \tag{6.132}$$

In the penalty method, the pressure variable does not apprea explicitly in the continuity equation. The system of equations is time-singular in pressure. As a result, it is impossible to use explicit time-integration methods.

In a steady state, the penalty FEM equations are:

$$([K_{11}] + [K^p])\,\{\Delta\} = \{F_1\} + \{Q_1\} \tag{6.133}$$

with:

$$[K^p] = \int_{\Omega_e} \gamma_e \left(\left\{\begin{array}{c} \partial/\partial x \\ \partial/\partial y \end{array}\right\}^T [\Psi]\right)^T \left(\left\{\begin{array}{c} \partial/\partial x \\ \partial/\partial y \end{array}\right\}^T [\Psi]\right) d\mathbf{x} \tag{6.134}$$

The constraint $[K^p]\{\Delta^e\}$ has to be as small as possible; γ_e is chosen large to reach a better accuracy through the minimization process:

$$10^4\mu \leq \gamma_e \leq 10^{12}\mu$$

If γ_e is really huge, $[K_{11}]$ becomes negligible compared to $[K^p]$:

$$[K^p]\{\Delta\} \simeq \{F_1\} + \{Q_1\} \tag{6.135}$$

If $[K^p]$ is non-singluar (invertible), then $\{\Delta\} \simeq 0$ and the momentum equations are not satisfied. The problem is said to be over-constrained (or "locked"). So the idea is to force $[K^p]$ to be singular, and invert $[K_{11}] + [K^p]$ (which will be non-singular because $[K_{11}]$ is non-singular). We then obtained a reduced integration, because the numerical integration of $[K^p]$ is done with one order less than necessary to get the exact estimation of the matrix. In steady state, the pore pressure field is calcualted as follows:

- in a Mixed FE Model: from the interpolation formulas.

$$P^e(x, y) \simeq \sum_{j=1}^{M} P_j \Phi_j(x, y) \tag{6.136}$$

- in a Penalty Model: from the mass conservation "constraint":

$$P_\gamma^e(x, y) \simeq -\gamma \sum_{j=1}^{N} \left(\frac{\partial \Psi_j}{\partial x} v_{xj} + \frac{\partial \Psi_j}{\partial y} v_{yj} \right) \tag{6.137}$$

The stress field is obtained from the velocities and pressures, as follows:

$$\sigma_{xx}^e \simeq 2\mu \sum_{j=1}^{N} \frac{\partial \Psi_j}{\partial x} v_{xj} - P^e(x, y), \quad \sigma_{yy}^e \simeq 2\mu \sum_{j=1}^{N} \frac{\partial \Psi_j}{\partial y} v_{yj} - P^e(x, y) \tag{6.138}$$

$$\sigma_{xy}^e \simeq \mu \sum_{j=1}^{N} \left(\frac{\partial \Psi_j}{\partial y} v_{xj} + \frac{\partial \Psi_j}{\partial x} v_{yj} \right) \tag{6.139}$$

6.3   FEM for deformable porous media saturated with one fluid phase

6.3.1   Weak formulation

The governing equations that describe the behavior of a deformable porous medium filled with a single fluid phase were explained in Section 5.2. The summary of the strong formulation is as follows:

Governing equation for the solid phase:

$$-\alpha \boldsymbol{\nabla} (p_w) + \mathbf{D_e} : \boldsymbol{\nabla}\boldsymbol{\epsilon} = 0 \tag{6.140}$$

Governing equation for the liquid phase:

$$\left(\frac{\alpha - n}{K_s} + \frac{n}{K_w} \right) \frac{D^s p_w}{Dt} + \alpha \frac{\partial \epsilon_v}{\partial t} = \frac{1}{\mu_w} \mathbf{k} : \boldsymbol{\nabla}^2 p_w \tag{6.141}$$

Boundary conditions:

$$\begin{aligned}
\mathbf{u} &= \widehat{\mathbf{u}} \quad \text{on } \Gamma_u \tag{6.142} \\
p_w &= \widehat{p}_w \quad \text{on } \Gamma_w \\
\boldsymbol{\sigma} \cdot \mathbf{n} &= \widehat{\mathbf{t}} \quad \text{on } \Gamma_u^q \\
\widehat{q}_w &= -\left(\frac{\rho_w}{\mu_w} \mathbf{k} : \boldsymbol{\nabla} p_w \right) \cdot \mathbf{n} \quad \text{on } \Gamma_w^q
\end{aligned}$$

Initial conditions:

$$\begin{aligned}\mathbf{u} &= \mathbf{u_0} \quad \text{on } \Gamma \text{ and in } \Omega \text{ at t=0} \\ p_w &= p_{w0} \quad \text{on } \Gamma \text{ and in } \Omega \text{ at t=0}\end{aligned} \tag{6.143}$$

The weak formulation for the solid phase, starting from the governing equation in the x-direction, is obtained as follows. The weighted integral statement is:

$$\forall w \sim \delta u_x, \quad \int_\Omega \left(-\alpha\, w\, \boldsymbol{\nabla}\, (p_w) + w\, \mathbf{D_e} : (\boldsymbol{\nabla})^2\, \mathbf{u} \right) \cdot \mathbf{e_x} dV = 0 \tag{6.144}$$

Using the divergence theorem, the integration by parts yields:

$$\forall w \sim \delta u_x, \quad \int_\Omega \left(-\alpha\boldsymbol{\nabla} w\, p_w + \boldsymbol{\nabla} w \cdot \mathbf{D_e} : \boldsymbol{\nabla}\mathbf{u} \right) \cdot \mathbf{e_x} dV \tag{6.145}$$

$$= \oint_\Gamma w\left(\mathbf{D_e} : \boldsymbol{\epsilon} - \alpha p_w \boldsymbol{\delta} \right) : \left(\mathbf{n} \otimes \mathbf{e_x} \right) dS$$

Lastly, the boundary conditions are applied:

$$\forall w \sim \delta u_x, \quad \int_\Omega \left(-\alpha\boldsymbol{\nabla} w\, p_w + \boldsymbol{\nabla} w \cdot \mathbf{D_e} : \boldsymbol{\nabla}\mathbf{u} \right) \cdot \mathbf{e_x} dV = \int_{\Gamma_u^q} w\, \boldsymbol{\sigma} : \left(\mathbf{n} \otimes \mathbf{e_x} \right) dS \tag{6.146}$$

$$\forall w \sim \delta u_x, \quad \int_\Omega \left(-\alpha\boldsymbol{\nabla} w\, p_w + \boldsymbol{\nabla} w \cdot \mathbf{D_e} : \boldsymbol{\nabla}\mathbf{u} \right) \cdot \mathbf{e_x} dV = \int_{\Gamma_u^q} w\, \widehat{t}_x dS \tag{6.147}$$

The weak formulation for the solid phase in the other directions of space is obtained in the same way. For the liquid phase, the weighted integral statement is:

$$\forall w* \sim \delta p_w, \quad \int_\Omega (w*) \left(\frac{\alpha-n}{K_s} + \frac{n}{K_w} \right) \dot{p}_w dV \tag{6.148}$$

$$+ \int_\Omega (w*)\, \alpha\, \nabla\dot{\mathbf{u}} : \boldsymbol{\delta}\, dV = \int_\Omega (w*)\, \frac{1}{\mu_w}\mathbf{k} : \boldsymbol{\nabla}^2 p_w\, dV$$

Using the divergence theorem, the integration by parts yields:

$$\forall w* \sim \delta p_w, \quad \int_\Omega (w*) \left(\frac{\alpha-n}{K_s} + \frac{n}{K_w} \right) \dot{p}_w dV + \int_\Omega (w*)\, \alpha\, \nabla\dot{\mathbf{u}} : \boldsymbol{\delta}\, dV \tag{6.149}$$

$$+ \int_\Omega \boldsymbol{\nabla}(w*)\, \frac{1}{\mu_w}\mathbf{k} : \boldsymbol{\nabla} p_w\, dV = \oint_\Gamma (w*)\frac{1}{\mu_w}\mathbf{k} : \boldsymbol{\nabla} p_w\, \mathbf{n}\, dS$$

Lastly, boundary conditions are applied as follows:

$$\forall w* \sim \delta p_w, \quad \int_\Omega (w*) \left(\frac{\alpha-n}{K_s} + \frac{n}{K_w} \right) \dot{p}_w dV + \int_\Omega (w*)\, \alpha\, \nabla\dot{\mathbf{u}} : \boldsymbol{\delta}\, dV \tag{6.150}$$

$$+ \int_\Omega \boldsymbol{\nabla}(w*)\, \frac{1}{\mu_w}\mathbf{k} : \boldsymbol{\nabla} p_w\, dV = - \int_{\Gamma_w^q} (w*)\frac{1}{\rho_w}\widehat{q}_w\, dS$$

The overall weak formulation can be written in a matrix form, as follows:

$$\int_\Omega \{\delta\mathbf{u}\}^T [L]^T [D_e][L]\{\mathbf{u}\}dV - \int_\Omega \{\delta\mathbf{u}\}^T [L]^T \{\mathbf{m}\}\alpha p_w dV = \int_{\Gamma_u^q} \{\delta\mathbf{u}\}^T \{\widehat{\mathbf{t}}\}dS \tag{6.151}$$

$$\int_{\Omega} \delta p_w \, S \, \dot{p}_w \, dV + \int_{\Omega} \delta p_w \, \alpha \, \{\mathbf{m}\}^T [L] \{\dot{\mathbf{u}}\} \, dV + \int_{\Omega} \{\boldsymbol{\nabla}(\delta p_w)\}^T \frac{1}{\mu_w} [k] \{\boldsymbol{\nabla} p_w\} \, dV \quad (6.152)$$

$$= - \int_{\Gamma_w^q} \delta p_w \frac{1}{\rho_w} \widehat{q}_w \, dS$$

in which:

$$S = \left(\frac{\alpha - n}{K_s} + \frac{n}{K_w} \right) \quad (6.153)$$

$$\{\mathbf{m}\}^T = \{1\,1\,1\,0\,0\,0\}^T \quad (6.154)$$

and:

$$\{\boldsymbol{\epsilon}\} = [\mathbf{L}]\{\mathbf{u}\} \quad (6.155)$$

with:

$$[L] = \begin{bmatrix} \frac{\partial}{\partial x} & 0 & 0 \\[2mm] 0 & \frac{\partial}{\partial y} & 0 \\[2mm] 0 & 0 & \frac{\partial}{\partial z} \\[2mm] \frac{\partial}{\partial y} & \frac{\partial}{\partial x} & 0 \\[2mm] 0 & \frac{\partial}{\partial z} & \frac{\partial}{\partial y} \\[2mm] \frac{\partial}{\partial z} & 0 & \frac{\partial}{\partial x} \end{bmatrix} \quad (6.156)$$

6.3.2 Space discretization

Displacements and pore pressure are approximated with two different families of interpolation functions, as follows:

$$\mathbf{u}^{(\mathbf{e})} = \sum_{k=1}^{N_1} \mathbf{u_k} \Psi_k(x, y, z), \quad p^{(e)} = \sum_{k=1}^{N_2} p_{w,k} \Phi_k(x, y, z) \quad (6.157)$$

$$\left\{ u_x^{(e)}, \, u_y^{(e)}, \, u_z^{(e)} \right\} = \{\Psi_1 \, \Psi_2 \dots \Psi_{N_1}\}^T \begin{bmatrix} u_{x,1} & u_{y,1} & u_{z,1} \\ u_{x,2} & u_{y,2} & u_{z,2} \\ \dots & \dots & \dots \\ u_{x,N_1} & u_{y,N_1} & u_{z,N_1} \end{bmatrix} \quad (6.158)$$

$$\left\{ u_x^{(e)}, \, u_y^{(e)}, \, u_z^{(e)} \right\} = \{N_u\}^T \begin{bmatrix} u_{x,1} & u_{y,1} & u_{z,1} \\ u_{x,2} & u_{y,2} & u_{z,2} \\ \dots & \dots & \dots \\ u_{x,N_1} & u_{y,N_1} & u_{z,N_1} \end{bmatrix} \quad (6.159)$$

$$p_w^{(e)} = \{\Phi_1 \, \Phi_2 \dots \Phi_{N_2}\}^T \begin{Bmatrix} p_{w,1} \\ p_{w,2} \\ \dots \\ p_{w,N2} \end{Bmatrix} = \{N_p\}^T \begin{Bmatrix} p_{w,1} \\ p_{w,2} \\ \dots \\ p_{w,N_2} \end{Bmatrix} \quad (6.160)$$

For the solid phase:

$$\int_\Omega \{N_u\}^T [L]^T [D_e][L]\{N_u\}\{\mathbf{u_k}\}dV \; - \int_\Omega \{N_u\}^T [L]^T \{\mathbf{m}\}\alpha\{N_p\}\{p_{w,k}\}dV \quad (6.161)$$

$$= \int_{\Gamma_u^q} \{N_u\}^T \{\widehat{\mathbf{t}}\}dS$$

For the liquid phase:

$$\int_\Omega \{N_p\}^T S \{N_p\}\{\dot{p}_{w,k}\}\,dV \; + \int_\Omega \{N_p\}^T \alpha \{\mathbf{m}\}^T [L]\{N_u\}\{\dot{\mathbf{u}}_k\}\,dV \qquad (6.162)$$

$$+ \int_\Omega \{\boldsymbol{\nabla} N_p\}^T \frac{1}{\mu_w}[k]\{\boldsymbol{\nabla} N_p\}\{p_{w,k}\}\,dV \; = \; - \int_{\Gamma_w^q} \{N_p\}^T \frac{1}{\rho_w}\widehat{q}_w \, dS$$

The matrix Finite Element equations after space discretization are:

$$\begin{bmatrix} [\mathbf{K_e}] & -[\mathbf{Q}] \\ [\mathbf{0}] & [\mathbf{H}] \end{bmatrix} \begin{Bmatrix} \{\mathbf{u_k}\} \\ \{p_{w,k}\} \end{Bmatrix} + \begin{bmatrix} [\mathbf{0}] & [\mathbf{0}] \\ [\mathbf{Q}]^T & [\mathbf{S}] \end{bmatrix} \begin{Bmatrix} \{\dot{\mathbf{u}}_k\} \\ \{\dot{p}_{w,k}\} \end{Bmatrix} = \begin{Bmatrix} \{\mathbf{f_u}\} \\ \{f_p\} \end{Bmatrix} \quad (6.163)$$

$$[\mathbf{K_e}] \;=\; \int_\Omega \{N_u\}^T [L]^T [D_e][L]\{N_u\}dV \qquad (6.164)$$

$$[\mathbf{H}] \;=\; \int_\Omega \{\boldsymbol{\nabla} N_p\}^T \frac{1}{\mu_w}[k]\{\boldsymbol{\nabla} N_p\}dV$$

$$[\mathbf{Q}] \;=\; \int_\Omega \{N_u\}^T [L]^T \{\mathbf{m}\}\alpha\{N_p\}dV$$

$$[\mathbf{S}] \;=\; \int_\Omega \{N_p\}^T S \{N_p\}dV$$

$$\{\mathbf{f_u}\} \;=\; \int_{\Gamma_u^q} \{N_u\}^T \{\widehat{\mathbf{t}}\}dS$$

$$\{f_p\} \;=\; - \int_{\Gamma_w^q} \{N_p\}^T \frac{1}{\rho_w}\widehat{q}_w \, dS$$

The mass matrix is not symmetric. Below is a technique that can be used to restore the symmetry of the matrix. For the solid phase:

$$-\frac{\partial}{\partial t}\left[\int_\Omega \{N_u\}^T [L]^T [D_e][L]\{N_u\}\{\mathbf{u_k}\}dV\right] \qquad (6.165)$$

$$-\frac{\partial}{\partial t}\left[- \int_\Omega \{N_u\}^T [L]^T \{\mathbf{m}\}\alpha\{N_p\}\{p_{w,k}\}dV\right] \;=\; -\frac{\partial}{\partial t}\left[\int_{\Gamma_u^q} \{N_u\}^T \{\widehat{\mathbf{t}}\}dS\right]$$

$$-\underbrace{\frac{\partial [\mathbf{K_e}]}{\partial \mathbf{u}}}_{[\mathbf{K_T}]}\{\dot{\mathbf{u}}_k\} + [\mathbf{Q}]\{\dot{p}_{w,k}\} \;=\; -\{\dot{\mathbf{f}}_u\} \qquad (6.166)$$

For the liquid phase:

$$[\mathbf{H}]\{p_{w,k}\} + [\mathbf{Q}]^T\{\dot{\mathbf{u}}_k\} + [\mathbf{S}]\{\dot{p}_{w,k}\} \;=\; \{f_p\} \qquad (6.167)$$
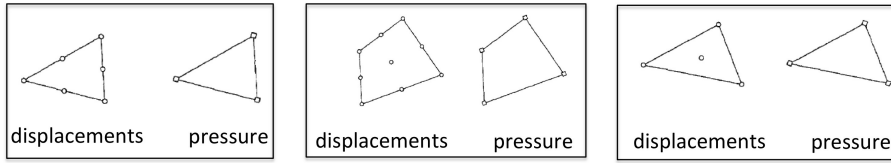
Therefore, we get:

$$\begin{bmatrix} [\mathbf{0}] & [\mathbf{0}] \\ [\mathbf{0}] & [\mathbf{H}] \end{bmatrix} \left\{ \begin{array}{c} \{\mathbf{u_k}\} \\ \{p_{w,k}\} \end{array} \right\} + \begin{bmatrix} -[\mathbf{K_T}] & [\mathbf{Q}] \\ [\mathbf{Q}]^T & [\mathbf{S}] \end{bmatrix} \left\{ \begin{array}{c} \{\dot{\mathbf{u}}_k\} \\ \{\dot{p}_{w,k}\} \end{array} \right\} = \left\{ \begin{array}{c} -\{\dot{\mathbf{f}}_u\} \\ \{f_p\} \end{array} \right\} \quad (6.168)$$

In the undrained limit state, when $\mathbf{H} \simeq \mathbf{0}$ and $\mathbf{S} \simeq \mathbf{0}$:

$$\begin{bmatrix} -[\mathbf{K_T}] & [\mathbf{Q}] \\ [\mathbf{Q}]^T & [\mathbf{0}] \end{bmatrix} \left\{ \begin{array}{c} \{\dot{\mathbf{u}}_k\} \\ \{\dot{p}_{w,k}\} \end{array} \right\} = \left\{ \begin{array}{c} -\{\dot{\mathbf{f}}_u\} \\ \{f_p\} \end{array} \right\} \quad (6.169)$$

- The equation in the second row can only be solved if $\text{rank}[\mathbf{Q}]^T \geq N_2$.

- The equation in the first row can only be solved if $\text{rank}[\mathbf{K_T}] \geq N_2$, i.e. if $N_1 \geq N_2$.

- As a result, the interpolation order for the displacement field has to be greater than that of the pore pressure field (See Figure 6.2).


Figure 6.2 Allowed interpolations for modeling a deformable porous solid filled with one fluid phase.

6.3.3 Time discretization

The time discretization scheme is as follows:

$$\left(\frac{d[\mathbf{X}]}{dt} \right)_{n+\theta} = \frac{[\mathbf{X}]_{n+1} - [\mathbf{X}]_n}{\Delta t} \qquad [\mathbf{X}]_{n+\theta} = (1-\theta)[\mathbf{X}]_n + \theta\,[\mathbf{X}]_{n+1} \quad (6.170)$$

The FE matrix equations before time discretization are:

$$[\mathbf{K_e}]\{\mathbf{u_k}\}_{n+\theta} - [\mathbf{Q}]\{p_{w,k}\}_{n+\theta} = \{\mathbf{f_u}\}_{n+\theta} \quad (6.171)$$

$$\Delta t[\mathbf{H}]\{p_{w,k}\}_{n+\theta} + \Delta t[\mathbf{Q}^T]\{\dot{\mathbf{u}}_k\}_{n+\theta} + \Delta t[\mathbf{S}]\{\dot{p}_{w,k}\}_{n+\theta} = \Delta t\{f_p\}_{n+\theta} \quad (6.172)$$

After time discretization, the FE equations are:

$$\theta[\mathbf{K_e}]_{n+\theta}\{\mathbf{u_k}\}_{n+1} - \theta[\mathbf{Q}]_{n+\theta}\{p_{w,k}\}_{n+1} \quad (6.173)$$
$$= (\theta-1)[\mathbf{K_e}]_{n+\theta}\{\mathbf{u_k}\}_n + (1-\theta)[\mathbf{Q}]_{n+\theta}\{p_{w,k}\}_n + \{\mathbf{f_u}\}_{n+\theta}$$

$$\theta\Delta t[\mathbf{H}]_{n+\theta}\{p_{w,k}\}_{n+1} + [\mathbf{Q}^T]_{n+\theta}\{\mathbf{u_k}\}_{n+1} + [\mathbf{S}]_{n+\theta}\{p_{w,k}\}_n \quad (6.174)$$
$$= -(1-\theta)\Delta t[\mathbf{H}]_{n+\theta}\{p_{w,k}\}_n + [\mathbf{Q}^T]_{n+\theta}\{\mathbf{u_k}\}_n + [\mathbf{S}]_{n+\theta}\{p_{w,k}\}_n + \Delta t\{f_p\}_{n+\theta}$$

The time marching scheme can be stated as follows:

$$
\begin{bmatrix} \theta[\mathbf{K_e}] & -\theta[\mathbf{Q}] \\ [\mathbf{Q}^T] & [\mathbf{S}] + \theta\Delta t[\mathbf{H}] \end{bmatrix}_{n+\theta} \left\{ \begin{array}{c} \{\mathbf{u_k}\} \\ \{p_{w,k}\} \end{array} \right\}_{n+1} =
$$

$$
\begin{bmatrix} (\theta-1)[\mathbf{K_e}] & (1-\theta)[\mathbf{Q}] \\ [\mathbf{Q}^T] & [\mathbf{S}] - (1-\theta)\Delta t[\mathbf{H}] \end{bmatrix}_{n+\theta} \left\{ \begin{array}{c} \{\mathbf{u_k}\} \\ \{p_{w,k}\} \end{array} \right\}_n + \left\{ \begin{array}{c} \{\mathbf{f_u}\} \\ \Delta t\{f_p\} \end{array} \right\}_{n+\theta}
$$

(6.175)

In steady state, there is no more coupling between the mechanical and hydraulic equations:

$$
\begin{bmatrix} [\mathbf{K_e}] & -[\mathbf{Q}] \\ [\mathbf{0}] & [\mathbf{H}] \end{bmatrix} \left\{ \begin{array}{c} \{\mathbf{u_k}\} \\ \{p_{w,k}\} \end{array} \right\} + \begin{bmatrix} [\mathbf{0}] & [\mathbf{0}] \\ [\mathbf{Q}]^T & [\mathbf{S}] \end{bmatrix} \left\{ \begin{array}{c} \{\dot{\mathbf{u}}_k\} \\ \{\dot{p}_{w,k}\} \end{array} \right\} = \left\{ \begin{array}{c} \{\mathbf{f_u}\} \\ \{f_p\} \end{array} \right\}
$$

(6.176)

$$
\Rightarrow \quad \begin{bmatrix} [\mathbf{K_e}] & -[\mathbf{Q}] \\ [\mathbf{0}] & [\mathbf{H}] \end{bmatrix} \left\{ \begin{array}{c} \{\mathbf{u_k}\} \\ \{p_{w,k}\} \end{array} \right\} = \left\{ \begin{array}{c} \{\mathbf{f_u}\} \\ \{f_p\} \end{array} \right\}
$$

(6.177)

6.3.4 Stability criteria

The time marching scheme on the symmetric FE equations is:

$$
\begin{bmatrix} -[\mathbf{K_T}] & [\mathbf{Q}] \\ [\mathbf{Q}^T] & [\mathbf{S}] + \theta\Delta t[\mathbf{H}] \end{bmatrix}_{n+\theta} \left\{ \begin{array}{c} \{\mathbf{u_k}\} \\ \{p_{w,k}\} \end{array} \right\}_{n+1} =
$$

$$
\begin{bmatrix} -[\mathbf{K_T}] & [\mathbf{Q}] \\ [\mathbf{Q}^T] & [\mathbf{S}] - (1-\theta)\Delta t[\mathbf{H}] \end{bmatrix}_{n+\theta} \left\{ \begin{array}{c} \{\mathbf{u_k}\} \\ \{p_{w,k}\} \end{array} \right\}_n + \Delta t \left\{ \begin{array}{c} \{\dot{\mathbf{f}}_u\} \\ \{f_p\} \end{array} \right\}_{n+\theta}
$$

(6.178)

which is of the form:

$$
([\mathbf{B}] + \theta\Delta t[\mathbf{C}])\,\{\mathbf{X}\}_{n+1} = ([\mathbf{B}] - (1-\theta)\Delta t[\mathbf{C}])\,\{\mathbf{X}\}_n + \Delta t\{\mathbf{F}\}_{n+\theta}
$$

(6.179)

For $\{\mathbf{F}\} = \{\mathbf{0}\}$, we have $\{\mathbf{X}\}_{n+1} = \lambda\{\mathbf{X}\}_n$. So the system is stable only if: $|\lambda| < 1$.

Let us note μ_1, μ_2,..., μ_m the distinct complex eigenvalues of $[\mathbf{B}]^{-1}[\mathbf{C}]$, and $\{\mathbf{\Psi}\}_j$ the corresponding eigenvectors. For $j = 1..m$:

$$
(1 + \mu_j\theta\Delta t)\,\{\mathbf{\Psi}\}_j^T\{\mathbf{X}\}_{n+1} = (1 - \mu_j(1-\theta)\Delta t)\,\{\mathbf{\Psi}\}_j^T\{\mathbf{X}\}_n
$$

(6.180)

Stability is ensured if and only if $|\lambda| < 1$. Conditions of stability are detailed in Figure 6.3.

Note that for a hyperbolic governing equation with a damping term, the Finite Element equaitons after time discretization are:

$$
\begin{bmatrix} M & 0 \\ 0 & 0 \end{bmatrix} \left\{ \begin{array}{c} \ddot{u} \\ \ddot{p} \end{array} \right\} + \begin{bmatrix} C & 0 \\ Q^T & S \end{bmatrix} \left\{ \begin{array}{c} \dot{u} \\ \dot{p} \end{array} \right\} + \begin{bmatrix} K & -Q \\ 0 & H \end{bmatrix} \left\{ \begin{array}{c} u \\ p \end{array} \right\} = -\left\{ \begin{array}{c} f \\ q \end{array} \right\}
$$

(6.181)

$$\left| \frac{1 - (1 - \theta)\Delta t \mu_j}{1 + \theta \Delta t \mu_j} \right| < 1 \tag{3.58}$$

for $j = 1, \ldots, m$. By writing $\mathrm{Re}[\mu_j] = \mu_R$ and $\mathrm{Im}[\mu_j] = \mu_I$, inequality (3.58) can be recast as

$$-2\mu_R < (2\theta - 1)(\mu_R^2 + \mu_I^2)\Delta t \tag{3.59}$$

1. Assume that $\theta > 1/2$. If $\mu_R > 0$ the condition given by (3.59) is satisfied for all Δt and μ_I, thus ensuring unconditional stability of equation (3.49). If $\mu_R \leq 0$ the condition given by (3.59) leads to a conditional stability with a requirement of the form

$$\Delta t > \frac{-2}{2\theta - 1} \frac{\mu_R}{(\mu_R^2 + \mu_I^2)} \tag{3.60}$$

   which results in lower bounds for the time step length Δt.
2. Assume that $\theta < 1/2$. Conditional stability is achieved for

$$\Delta t < \frac{2}{1 - 2\theta} \frac{\mu_R}{(\mu_R^2 + \mu_I^2)} \tag{3.60}$$

   with an upper bound for the time step length Δt. Only when $\mu_R \leq 0$ is (3.49) unstable.

Figure 6.3   Stability criteria for a Finite Element model of deformable porous solid filled one fluid phase. Image taken from [**?**].

The time discretization scheme is [26]:

$$\begin{aligned}
p_{n+1} &= p_n + (1-\theta)\Delta t \dot{p}_n + \theta \Delta t \dot{p}_{n+1} \tag{6.182}\\
\Delta p_{n+1} &= \Delta t \dot{p}_n + \theta \Delta t \Delta \dot{p}_{n+1}\\[4pt]
\dot{\mathbf{u}}_{n+1} &= \dot{\mathbf{u}}_n + (1-\beta_1)\Delta t \ddot{\mathbf{u}}_n + \beta_1 \Delta t \ddot{\mathbf{u}}_{n+1}\\
\Delta \dot{\mathbf{u}}_{n+1} &= \Delta t \ddot{\mathbf{u}}_n + \beta_1 \Delta t \Delta \ddot{\mathbf{u}}_{n+1}\\[4pt]
\mathbf{u}_{n+1} &= \mathbf{u}_n + \Delta t \dot{\mathbf{u}}_n + \frac{1}{2}\Delta t^2 \ddot{\mathbf{u}}_n + \frac{1}{2}\beta_2 \Delta t^2 \Delta \ddot{\mathbf{u}}_{n+1}\\
\Delta \mathbf{u}_{n+1} &= \Delta t \dot{\mathbf{u}}_n + \frac{1}{2}\Delta t^2 \ddot{\mathbf{u}}_n + \frac{1}{2}\beta_2 \Delta t^2 \Delta \ddot{\mathbf{u}}_{n+1}
\end{aligned}$$

Writing FEM equations in terms of variations of dofs, at time $n + 1$:

$$\begin{aligned}
\mathbf{M}\Delta\ddot{\mathbf{u}}_{n+1} + \mathbf{C}\Delta\dot{\mathbf{u}}_{n+1} + \mathbf{K}\Delta\mathbf{u}_{n+1} - \mathbf{Q}\Delta\mathbf{p}_{n+1} + \mathbf{f}_{n+1} &= \mathbf{0} \tag{6.183}\\
\mathbf{Q}^T\Delta\dot{\mathbf{u}}_{n+1} + \mathbf{S}\Delta\dot{\mathbf{p}}_{n+1} + \mathbf{H}\Delta\mathbf{p}_{n+1} + \mathbf{q}_{n+1} &= \mathbf{0}
\end{aligned}$$

with:

$$\begin{aligned}
\Delta p_{n+1} &= \Delta t \dot{p}_n + \theta \Delta t \Delta \dot{p}_{n+1} \tag{6.184}\\
\Delta \dot{\mathbf{u}}_{n+1} &= \Delta t \ddot{\mathbf{u}}_n + \beta_1 \Delta t \Delta \ddot{\mathbf{u}}_{n+1}\\
\Delta \mathbf{u}_{n+1} &= \Delta t \dot{\mathbf{u}}_n + \frac{1}{2}\Delta t^2 \ddot{\mathbf{u}}_n + \frac{1}{2}\beta_2 \Delta t^2 \Delta \ddot{\mathbf{u}}_{n+1}
\end{aligned}$$

$$\left(\mathbf{M} + \beta_1 \Delta t \mathbf{C} + \frac{1}{2}\beta_2 \Delta t^2 \mathbf{K}\right)\Delta\ddot{\mathbf{u}}_{n+1} - \theta\Delta t\mathbf{Q}\Delta\dot{\mathbf{p}}_{n+1} + \mathbf{F}_n = \mathbf{0} \qquad (6.185)$$

$$\mathbf{Q}^T\beta_1\Delta t\Delta\ddot{\mathbf{u}}_{n+1} + (\mathbf{S} + \theta\Delta t\mathbf{H})\Delta\dot{\mathbf{p}}_{n+1} + \mathbf{Q}_n = \mathbf{0}$$

$$\frac{1}{\beta_1\Delta t}\left(\mathbf{M} + \beta_1\Delta t\mathbf{C} + \frac{1}{2}\beta_2\Delta t^2\mathbf{K}\right)\beta_1\Delta t\Delta\ddot{\mathbf{u}}_{n+1} - \mathbf{Q}\theta\Delta t\Delta\dot{\mathbf{p}}_{n+1} + \mathbf{F}_n = \mathbf{0} (6.186)$$

$$-\mathbf{Q}^T\beta_1\Delta t\Delta\ddot{\mathbf{u}}_{n+1} - \left(\frac{1}{\theta\Delta t}\mathbf{S} + \mathbf{H}\right)\theta\Delta t\Delta\dot{\mathbf{p}}_{n+1} - \mathbf{Q}_n = \mathbf{0}$$

$\mathbf{F}_n$ and $\mathbf{Q}_n$ depend on variables at time n and on predictable force terms. We now have a symmetric matrix. We can solve for $\Delta\ddot{\mathbf{u}}_{n+1}$ and $\Delta\dot{\mathbf{p}}_{n+1}$:

$$\begin{bmatrix} \frac{1}{\beta_1\Delta t}\left(\mathbf{M} + \beta_1\Delta t\mathbf{C} + \frac{1}{2}\beta_2\Delta t^2\mathbf{K}\right) & -\mathbf{Q} \\ -\mathbf{Q}^T & -\left(\frac{1}{\theta\Delta t}\mathbf{S} + \mathbf{H}\right) \end{bmatrix}\left\{\begin{array}{c} \beta_1\Delta t\Delta\ddot{\mathbf{u}}_{n+1} \\ \theta\Delta t\Delta\dot{\mathbf{p}}_{n+1} \end{array}\right\} = \left\{\begin{array}{c} \mathbf{F}_n \\ \mathbf{Q}_n \end{array}\right\}$$

$$(6.187)$$

Stability is unconditional when [26]:

$$\beta_2 \geq \beta_1, \quad \beta_1 \geq \frac{1}{2}, \quad \theta \geq \frac{1}{2} \qquad (6.188)$$

6.3.5 Partitioned systems of equations

Different space interpolation schemes can be considered for different degrees of freedom. In the same way, different time interpolation schemes can be used for different degrees of freedom. Degrees of freedom can be gathered based on physical meaning (e.g., displacements vs. pore pressure) or based on any other mathematical consideration (e.g. stability on certain parts of the mesh). Let us consider a general parabolic matrix equation:

$$[\mathbf{C}]\{\dot{\mathbf{a}}\} + [\mathbf{K}]\{\mathbf{a}\} + \{\mathbf{f}\} = \{\mathbf{0}\} \qquad (6.189)$$

which is partitioned into two (or more) families of degrees of freedom, as follows:

$$\begin{bmatrix} \mathbf{C}_{11} & \mathbf{C}_{12} \\ \mathbf{C}_{21} & \mathbf{C}_{22} \end{bmatrix}\left\{\begin{array}{c} \dot{\mathbf{a}}_1 \\ \dot{\mathbf{a}}_2 \end{array}\right\} + \begin{bmatrix} \mathbf{K}_{11} & \mathbf{K}_{12} \\ \mathbf{K}_{21} & \mathbf{K}_{22} \end{bmatrix}\left\{\begin{array}{c} \mathbf{a}_1 \\ \mathbf{a}_2 \end{array}\right\} + \left\{\begin{array}{c} \mathbf{f}_1 \\ \mathbf{f}_2 \end{array}\right\} = \left\{\begin{array}{c} \mathbf{0} \\ \mathbf{0} \end{array}\right\} \qquad (6.190)$$

with the two following time discretization schemes:

$$\mathbf{a}_1 = \mathbf{a}_{1n} + \tau\boldsymbol{\alpha}_1 \qquad (6.191)$$
$$\mathbf{a}_2 = \mathbf{a}_{2n} + \tau\boldsymbol{\alpha}_2$$

Inserting the above into each of the partitions and using different weight functions:

$$\mathbf{C}_{11}\boldsymbol{\alpha}_1 + \mathbf{C}_{12}\boldsymbol{\alpha}_2 + \mathbf{K}_{11}\left(\mathbf{a}_{1n} + \theta\Delta t\boldsymbol{\alpha}_1\right) + \mathbf{K}_{12}\left(\mathbf{a}_{2n} + \theta\Delta t\boldsymbol{\alpha}_2\right) + \mathbf{f}_1 = \mathbf{0} (6.192)$$
$$\mathbf{C}_{21}\boldsymbol{\alpha}_1 + \mathbf{C}_{22}\boldsymbol{\alpha}_2 + \mathbf{K}_{21}\left(\mathbf{a}_{1n} + \overline{\theta}\Delta t\boldsymbol{\alpha}_1\right) + \mathbf{K}_{12}\left(\mathbf{a}_{2n} + \overline{\theta}\Delta t\boldsymbol{\alpha}_2\right) + \mathbf{f}_2 = \mathbf{0} (6.193)$$

- Thre is unconditional stability of the whole system only if $\theta \geq 1/2, \overline{\theta} \geq 1/2$.

- There is conditional stability id $\Delta t \leq \Delta t_{crit}$ for each partitioned system considered without its coupling terms.

The principle of the implicit-explicit partition is as follows:

- Noting h is the element size, the critical time step is proportional to h^2 for a parabolic governing equation, and proportional to h for a hyperbolic governing equation.

- If a single explicit scheme were to be used with very small elements occurring in one partition, the time step would become too small to ensure computational efficiency.

- Therefore it may be advantageous to use an explicit scheme for a part of the domain with larger elements while maintaining an unconditionally stable algorithm with the same time step in the partition in which elements are small (or very stiff).

- For this reason, implicit-explicit partitions are frequently used.

If a parabolic equation is split into an implicit (I) system and an explicit (E) system:

$$[\mathbf{C}_I]\{\dot{\mathbf{a}}_I\} + [\mathbf{C}_E]\{\dot{\mathbf{a}}_E\} + [\mathbf{K}_I]\{\mathbf{a}_I\} + [\mathbf{K}_E]\{\mathbf{a}_E\} + \{\mathbf{f}\} = \{\mathbf{0}\} \tag{6.194}$$

Vectors $\{\mathbf{a}_E\}$ and $\{\mathbf{a}_I\}$ are obtained iteratively [26].

- Calculation of implicit vector of d.o.f. at time $n+1$, iteration j:

$$(\mathbf{a}_I)_{(n+1)}^{(j)} = (\mathbf{a}_I)_{(n)} + (1-\theta)\Delta t(\dot{\mathbf{a}}_I)_{(n)} + \theta\Delta t(\dot{\mathbf{a}}_I)_{(n+1)}^{(j)} \tag{6.195}$$

- Calculation of explicit vector of d.o.f. at time $n+1$, iteration j:

$$(\mathbf{a}_E)_{(n+1)}^{(j)} = (\mathbf{a}_E)_{(n)} + (1-\theta)\Delta t(\dot{\mathbf{a}}_E)_{(n)} + \theta\Delta t(\dot{\mathbf{a}}_E)_{(n+1)}^{(j-1)} \tag{6.196}$$

At time $n+1$, iteration j, the system of equations can be written in the form:

$$([\mathbf{C}_I] + \theta\Delta t[\mathbf{K}_I])\{(\dot{\mathbf{a}}_I)_{(n+1)}^{(j)}\} + [\mathbf{C}_E]\{(\dot{\mathbf{a}}_E)_{(n+1)}^{(j)}\} + \{\mathbf{F}\}_{(n+1)}^{(j-1)} = \{\mathbf{0}\} \tag{6.197}$$

in which $\{\mathbf{F}\}_{(n+1)}^{(j-1)}$ depends on variables obtained at time n or at iteration $j-1$. There is unconditional stability for the implicit part if $\theta \geq 0.5$. There is conditional stability for the explicit part if $\Delta t < \Delta t_{crit}$ (which depends on element size).

Partitioned systems of equations are typically resolved in a staggered fashion. For instance, consider the following partition:

$$\begin{bmatrix} \mathbf{C}_{11} & \mathbf{0} \\ \mathbf{0} & \mathbf{C}_{22} \end{bmatrix} \begin{Bmatrix} \dot{\mathbf{a}}_1 \\ \dot{\mathbf{a}}_2 \end{Bmatrix} + \begin{bmatrix} \mathbf{K}_{11} & \mathbf{K}_{12} \\ \mathbf{K}_{21} & \mathbf{K}_{22} \end{bmatrix} \begin{Bmatrix} \mathbf{a}_1 \\ \mathbf{a}_2 \end{Bmatrix} + \begin{Bmatrix} \mathbf{f}_1 \\ \mathbf{f}_2 \end{Bmatrix} = \begin{Bmatrix} \mathbf{0} \\ \mathbf{0} \end{Bmatrix} \tag{6.198}$$

where $\mathbf{a}_1$ and $\mathbf{a}_2$ are discretized in time with the same parameter θ. A staggered algorithm will solve the first and second partitions separately. The unknowns the first system ($\mathbf{a}_1$) are obtained iteratively with assumed values of the unknowns of the second system ($\mathbf{a}_2$), and vice versa:

1. Assume $\mathbf{a}_2 = \bar{\mathbf{a}}_2 = \mathbf{a}_{2n}$.

2. Solve the fist equation for α_1, with $\mathbf{a}_1 = \mathbf{a}_{1n} + \tau\alpha_1$:

$$\mathbf{C}_{11}\alpha_1 + \mathbf{K}_{11}(\mathbf{a}_{1n} + \theta\Delta t\alpha_1) = -\mathbf{f}_1 - \mathbf{K}_{12}\mathbf{a}_{2n} \qquad (6.199)$$

3. Use the value of α_1 to solve the second equation for α_2:
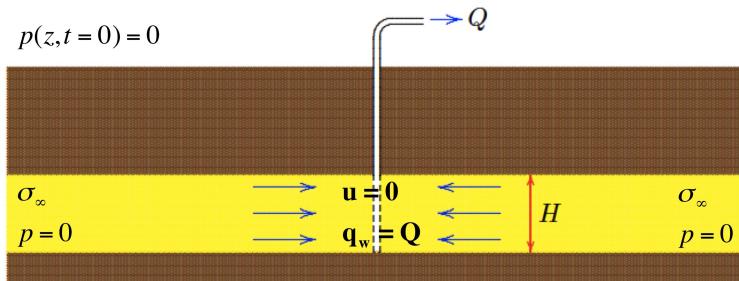
$$\mathbf{C}_{22}\alpha_2 + \mathbf{K}_{22}(\mathbf{a}_{2n} + \theta\Delta t\alpha_2) = -\mathbf{f}_2 - \mathbf{K}_{21}(\mathbf{a}_{1n} + \theta\Delta t\alpha_1) \qquad (6.200)$$

4. Repeat 2. and 3. until convergence is reached.

This scheme is unconditionnally stable if $\theta \geq 1/2$. Accuracy is lost in the staggering process, but the scheme converges and is more computationally efficient (it allows parallel computing for instance).

6.3.6 Infinite elements (for aquifer problems)

Aquifer problems such as the one shown in Figure 6.4 require modeling "infinite aquifers" in very large domains, which involves high computational costs. If the domain size is reduced accuracy decreases. In transient problems, some errors only emerge after a certain time and therefore, truncating the domain is sometimes acceptable for studies of flow in the short term. Alternatively, infinite elements (IE) can be used.

Well in infinite confined aquifer, Theis-Jacob model.

Figure 6.4   Radial flow to a well in an infinite confined aquifer. Image taken from [20].

Decay function finite elements are defined with 2D interpolation functions $\Psi(x, y)$ that are maintained in one direction (e.g., x), and multiplied by a decay function in the other (e.g., y). At node i for instance:

$$\Phi_i(x, y) = \Psi_i(x, y) \times f_i(y) \qquad (6.201)$$

with $\Phi_i(x_i, y_i) = 1$ and $\Phi_i \to_\infty \lambda$ (where λ is the far field condition). Some examples of far field functions are given below:

$$f_i(y) = exp\left(\frac{y_i - y}{L}\right), y \geq 0 \qquad (6.202)$$

$$f_i(y) = \left[\frac{y_i - y_0}{y - y_0}\right]^n \qquad (6.203)$$

Mapped Infinite Elements (MIE) map a finite domain into an infinite domain, thanks to well-chosen interpolation functions. An example is given in 1D in Figure 6.5. The element in the actual coordinate system (x) has inifinite dimensions while the mater element in the reference coordinate system (ξ) has length 2. The coordinate x is mapped as:

$$x(\xi) = M_1(\xi)x_1 + M_2(\xi)x_2, \quad M_1(\xi) = \frac{-2\xi}{1-\xi}, \quad M_2(\xi) = \frac{1+\xi}{1-\xi} \tag{6.204}$$
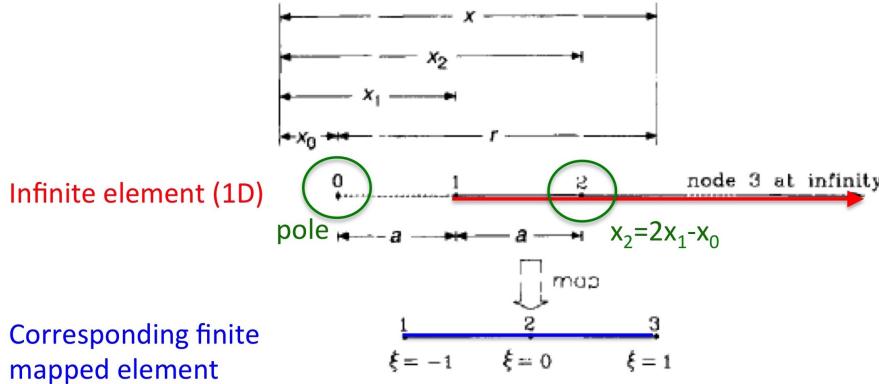
in which the weight functions satisfy the partition of unity:

$$M_1(\xi) + M_2(\xi) = 1 \tag{6.205}$$

We have:

$$\xi = 1 - \frac{2a}{x - (x_1 - a)} = 1 - \frac{2a}{r}, \quad a = x_2 - x_1 = x_1 - x_0 \tag{6.206}$$

The field variables (displacements, pressures, temperatures) are then interpolated using

Figure 6.5 Principle of a Mapped Infinite Element.

the standard interpolation functions:

$$U(\xi) = \sum_{i=1}^{n+1} N_i(\xi)U_i = \alpha_0 + \alpha_1\xi + \alpha_2\xi^2 + ... + \alpha_n\xi^n \tag{6.207}$$

Using Equation 6.206, we can express the field variable as a function of the global coordinate r:
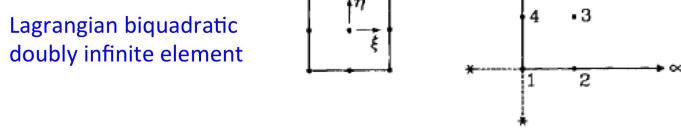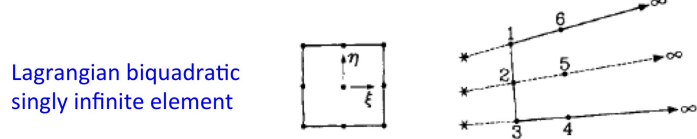
$$U(r) = \beta_0 + \frac{\beta_1}{r} + \frac{\beta_2}{r^2} + ... + \frac{\beta_n}{r^n} \tag{6.208}$$

The mapping functions for 2D MIEs are givent in Figure 6.6.

6.4 FEM for deformable non-isothermal unsaturated porous media

6.4.1 Balance equations

In the following, we consider a REpresentattive Elementary Volume (REV) made of a solid skeleton (s) + liquid water (w) + water vapor (v) + gaseous dry air (a). We note (g) the

Lagrangian biquadratic singly infinite element

Lagrangian biquadratic doubly infinite element

$$\hat{M}_1(\xi,\eta) = M_1(\xi)N_1(\eta) \qquad \hat{M}_2(\xi,\eta) = M_1(\xi)N_2(\eta) \qquad \hat{M}_3(\xi,\eta) = M_1(\xi)N_3(\eta)$$
$$\hat{M}_4(\xi,\eta) = M_2(\xi)N_3(\eta) \qquad \hat{M}_5(\xi,\eta) = M_2(\xi)N_2(\eta) \qquad \hat{M}_6(\xi,\eta) = M_2(\xi)N_1(\eta)$$

Figure 6.6   Mapped Infinite Elements in 2D.

with gas mixture vapor (v) + air (a). Assuming that weight is the only external body force applied to the REV, the REV momentum balance equation is:

$$\mathbf{div}\boldsymbol{\sigma} + (1-n)\rho_s(\mathbf{g} - \mathbf{a_s}) + nS_w\rho_w(\mathbf{g} - \mathbf{a_w}) + nS_g\rho_g(\mathbf{g} - \mathbf{a_g}) = 0 \qquad (6.209)$$

Isolating the solid phase:

$$\mathbf{div}\left[\boldsymbol{\sigma}' - \boldsymbol{\delta}(1-n)(S_w\, p_w + S_g\, p_g)\right] + (1-n)\rho_s(\mathbf{g} - \mathbf{a_s}) + \mathbf{f_{ws}} + \mathbf{f_{gs}} = 0 \qquad (6.210)$$

The net stress applied to the solid skeleton is defined as:

$$\boldsymbol{\sigma}' = \boldsymbol{\sigma} + \boldsymbol{\delta}(S_w\, p_w + S_g\, p_g) \qquad (6.211)$$

Fluid pressure contributing to the compressibility of the grains:

$$-\boldsymbol{\delta}(1-n)(S_w\, p_w + S_g\, p_g)$$

The force applied by the liquid flowing in the porous solid skeleton is:

$$\mathbf{f_{ws}} = \mathbf{R_w}\eta_w\mathbf{v_{ws}} = nS_w\mathbf{R_w}\mathbf{v_{ws}}$$

The force applied by the gas flowing in the porous solid skeleton is:

$$\mathbf{f_{gs}} = \mathbf{R_g}\eta_g\mathbf{v_{wg}} \qquad (6.212)$$

The momentum balance equation for the solid phase is thus:

$$\mathbf{div}[\boldsymbol{\sigma}' - \boldsymbol{\delta}\,(1-n)(S_wp_w + S_gp_g)] \quad + \quad (1-n)\rho_s\mathbf{g} \qquad (6.213)$$
$$-(1-n)\rho_s\mathbf{a_s} + \mathbf{R_w}\eta_w\mathbf{v_{ws}} \quad + \quad \mathbf{R_g}\eta_g\mathbf{v_{wg}} = 0$$

with:

$\boldsymbol{\sigma}'$	Net stress [Pa]
$\boldsymbol{\delta}$	Second-order identity tensor [-]
n	Porosity [-]
S_w, S_g	Degree of saturation of liquid water, gas mixture [-]
p_w, p_g	Pore pressure of liquid water, gas mixture [Pa]
ρ_s	Solid mass density [kg/m^3]
$\mathbf{g}$	Gravity acceleration field [m/s^2]
$\mathbf{a_s}$	Acceleration of the solid phase [m/s^2]
$\mathbf{R_w}$, $\mathbf{R_g}$	Flow dissipation term for liquid, gas [Pa.s/m^2]
η_w, η_g	Volume fraction of liquid, gas in the REV [-]
$\mathbf{v_{ws}}$, $\mathbf{v_{wg}}$	Velocity of the liquid in reference to solid, gas [m/s]

We neglect the gradients of fluids velocity and the effects of phase change. The balance of momentum of liquid water is:

$$\mathbf{v_{ws}} = \mathbf{R_w}^{-1} : (-\mathbf{grad}(p_w) + \rho_w(\mathbf{g} - \mathbf{a_s} - \mathbf{a_{ws}})) \qquad (6.214)$$

The balance of momentum of the gas mixture is:

$$\mathbf{v_{gs}} = \mathbf{R_g}^{-1} : (-\mathbf{grad}(p_g) + \rho_g(\mathbf{g} - \mathbf{a_s} - \mathbf{a_{gs}})) \qquad (6.215)$$

with:

$\mathbf{v_{ws}}$, $\mathbf{v_{gs}}$	Velocity of the liquid, gas in reference to solid [m/s]
$\mathbf{R_w}$, $\mathbf{R_g}$	Flow dissipation term for liquid, gas [Pa.s/m^2]
p_w, p_g	Pore pressure of liquid water, gas mixture [Pa]
ρ_w, ρ_g	Mass density of liquid, gas [kg/m^3]
$\mathbf{g}$	Gravity acceleration field [m/s^2]
$\mathbf{a_s}$	Acceleration of the solid phase [m/s^2]
$\mathbf{a_{ws}}$, $\mathbf{a_{gs}}$	Acceleration of liquid, gas in reference to solid [m/s^2]

We define:

$$\mathbf{R_x}^{-1} = \frac{1}{\eta_x} \frac{\mathbf{k}}{\mu_x}(\rho_x, \eta_x, T), \quad x = w, g \qquad (6.216)$$

with:

η_x	Volume fraction of phase x in REV [-]
$\mathbf{k}$	Permeability [m^2]
μ_x	Dynamic viscosity of phase x [Pa.s]
T	Temperature [K]

The mass balance equation of the solid phase is expressed as:

$$\frac{(1-n)}{\rho_s}\frac{D^s\rho_s}{Dt} - \frac{D^s n}{Dt} + (1-n)div\mathbf{v_s} = 0 \tag{6.217}$$

with:

n	Porosity [-]
ρ_s	Solid mass density [kg/m^3]
$\mathbf{v_s}$	Velocity field of the solid phase in the REV [m/s]

in which it is reminded that the time derivative of a function $f(\mathbf{x}, t)$ in reference to a moving phase π (with velocity $\mathbf{v}^\pi$) is:

$$\frac{D^\pi f(\mathbf{x},t)}{Dt} = \frac{\partial f(\mathbf{x},t)}{\partial t} + \mathbf{grad}f \cdot \mathbf{v}^\pi \tag{6.218}$$

The quantity of liquid water that is lost through evaporation per unit time per unit volume is:

$$\rho_w e^w(\rho) = -\dot{m} \tag{6.219}$$

Hence the mass balance equation of the liquid phase is:

$$\left(\frac{\alpha-n}{K_s}(S_w)^2 + \frac{nS_w}{K_w}\right)\frac{D^s p_w}{Dt} + \frac{\alpha-n}{K_s}S_wS_g\frac{D^s p_g}{Dt} + \alpha S_w div\mathbf{v_s} \tag{6.220}$$

$$-\beta_{sw}\frac{D^s T}{Dt} + \left(\frac{\alpha-n}{K_s}p_w S_w - \frac{\alpha-n}{K_s}p_g S_w + n\right)\frac{D^s S_w}{Dt} \tag{6.221}$$

$$+\frac{1}{\rho_w}div\left(nS_w\rho_w\mathbf{v_{ws}}\right) = -\frac{\dot{m}}{\rho_w}$$

with:

β_s, β_w β_g	Thermal expansion coefficient of solid, liquid, gas [K^{-1}]
β_{sw}	$\beta_{sw} = S_w[(\alpha-n)\beta_s + n\beta_w]$
K_s, K_w	Compression modulus of solid, water [Pa]

Note that if grains are incompressible, $\alpha = 1$ and $1/K_s \to 0$, and the mass balance equation of the liquid phase is simplified into:

$$\frac{nS_w}{K_w}\frac{D^s p_w}{Dt} + S_w div\mathbf{v_s} - \beta_{sw}\frac{D^s T}{Dt} + n\frac{D^s S_w}{Dt} \tag{6.222}$$

$$+\frac{1}{\rho_w}div\left(nS_w\rho_w\mathbf{v_{ws}}\right) = -\frac{\dot{m}}{\rho_w}$$

The mass balance equation of the gas phase is expressed as:

$$\frac{\alpha-n}{K_s}S_wS_g\frac{D^s p_w}{Dt} + \frac{\alpha-n}{K_s}(S_g)^2\frac{D^s p_g}{Dt} - \left(n + \frac{\alpha-n}{K_s}p_c S_g\right)\frac{D^s S_w}{Dt} \tag{6.223}$$

$$-\beta_s(\alpha-n)S_g\frac{D^s T}{Dt} + \alpha S_g div\mathbf{v_s} + \frac{nS_g}{\rho_g}\frac{D^s}{Dt}\left[\frac{1}{R\theta}(p_a M_a + p_v M_w)\right]$$

$$+\frac{1}{\rho_g}div(nS_g\rho_g\mathbf{v_{gs}}) = +\frac{\dot{m}}{\rho_g}$$

The Kelvin-Laplace law (for the Relative Humidity (RH) in the pores) states that:

$$RH = \frac{p_v}{p_{vs}} = exp\left(\frac{p_c M_w}{\rho_w R\theta}\right)$$ (6.224)

with:

p_v, p_{vs}	Vapor pressure, water vapor saturation pressure [Pa]
p_c	$p_c = p_g - p_w$: Capillary pressure [Pa]
M_w, M_a	Molar mass of liquid water, gaseous air [kg/mol]
R	Universal gas constant : $R = 8.3144598 J.mol^{-1}.K^{-1}$
θ	Absolute temperature [K]
$\mathbf{v_{gs}}$	Velocity field of the gas phase in reference to the solid [m/s]

If grains are incompressible, $\alpha = 1$ and $1/K_s \to 0$ and the mass balance equation of the gas phase is simplified into:

$$-n\frac{D^s S_w}{Dt} - \beta_s(\alpha - n)S_g\frac{D^s T}{Dt} + S_g div\mathbf{v_s} + \frac{nS_g}{\rho_g}\frac{D^s}{Dt}\left[\frac{1}{R\theta}(p_a M_a + p_v M_w)\right]$$ (6.225)
$$+\frac{1}{\rho_g}div(nS_g\rho_g\mathbf{v_{gs}}) = +\frac{\dot{m}}{\rho_g}$$

Lastly, the energy balance equation is:

$$(\rho C_p)_{eff}\frac{\partial T}{\partial t} + \left(\rho_w C_p^w \mathbf{v_w} + \rho_g C_p^g \mathbf{v_g}\right) \cdot \mathbf{grad}(T)$$ (6.226)

$$-div\left(\chi_{eff}\mathbf{grad}(T)\right) = -\dot{m}\Delta H_{vap}$$

with:

$\rho_x C_p^x$	Heat capacity of the x-th phase [J/K]
$(\rho C_p)_{eff}$	$(\rho C_p)_{eff} = \rho_s C_p^s + \rho_w C_p^w + \rho_g C_p^g$
χ_x	Thermal conductivity of hte x-th phase [W.m^{-1}.K^{-1}]
χ_{eff}	$\chi_{eff} = \chi_{dry}\left(1 + 4\dfrac{nS_w p_w}{(1-n)\rho_s}\right)$
ΔH_{vap}	$\Delta H_{vap} = H_v - H_w$
	Difference between vapor and liquid water enthalpy [J]

6.4.2   Constitutive equations

The relationships between the primary and secondary variables are given by the constitutive equations. Below are common constitutive models. For the solid phase, we use the

concept of effective stress, and:

$$\begin{aligned}
\boldsymbol{\sigma}'' &= \mathbf{D_e} : \boldsymbol{\epsilon} \\
\boldsymbol{\sigma}'' &= \boldsymbol{\sigma} + \alpha\boldsymbol{\delta}\left(S_w p_w + S_g p_g\right) \\
\alpha &= 1 - \frac{K_s}{K}
\end{aligned}$$

(6.227)

...not to be confused with the net stress:

$$\boldsymbol{\sigma}' = \boldsymbol{\sigma} + \boldsymbol{\delta}\left(S_w p_w + S_g p_g\right)$$

(6.228)

For the heat flux, we typically use Fourier's law:

$$\begin{aligned}
\mathbf{q_h} &= -\chi_{eff}\mathbf{grad}(T) \\
\chi_{eff} &= \chi_{dry}\left(1 + 4\frac{nS_w p_w}{(1-n)\rho_s}\right)
\end{aligned}$$

(6.229)

(6.230)

For hte transport of water (x=w) and gas (x=g) in laminar flow, a common choice is Darcy's law with Brooks & Corey's relative permeability and water retention curve:

$$\begin{aligned}
\eta_x \overline{\mathbf{v}}_{\mathbf{xs}} &= \frac{k_{rx}\mathbf{k}}{\mu_x} \cdot \left(-\mathbf{grad}p_x + \rho_x\mathbf{g}\right) \\
k_{rw} &= (S_e)^{(2+3\lambda)/\lambda} \\
k_{rg} &= (1 - S_e)^2(1_{(}S_e)^{(2+\lambda)/\lambda}) \\
p_c &= \frac{p_b}{(S_e)^{1/\lambda}} \\
S_e &= \frac{S_w - S_{wc}}{1 - S_{wc}}
\end{aligned}$$

(6.231)

(6.232)

(6.233)

(6.234)

(6.235)

with

p_b	Bubbling pressure [Pa]
S_{wc}	Residual (irreducible) degree of saturation [-]
λ	Pore size distribution index [-]

6.4.3   Weak formulation

The derivation of the weak formulation is lengthy because the governing equations are coupled. Here, we provide the weak formulation without prrof. The interested reader is referred to [14, 25] for more details.

For the momentum balance equation of the three-phase REV, noting $L^T\sigma = \text{div }\sigma$

$$\int_{\Omega} (Lw)^T \sigma \, d\Omega = \int_{\Omega} w^T \rho g \, d\Omega + \int_{\Gamma_d^q} w^T \bar{t} \, d\Gamma$$

Primary variables are interpolated from their nodal values. Introducing the vectors of interpolation functions:

$$\mathbf{u} = \mathbf{N}_u \bar{\mathbf{u}} \qquad p^w = \mathbf{N}_p \bar{\mathbf{p}}^w \qquad p^g = \mathbf{N}_p \bar{\mathbf{p}}^g \qquad T = \mathbf{N}_t \bar{\mathbf{T}}$$

We get:

$$\int_{\Omega} (L\mathbf{N}_u)^T \sigma'' d\Omega - \int_{\Omega} \alpha \mathbf{m}^T (S_w p^w \mathbf{N}_p + S_g p^g \mathbf{N}_p) \, d\Omega = \int_{\Omega} \mathbf{N}_u^T \rho g \, d\Omega + \int_{\Gamma_u^q} \mathbf{N}_u^T \bar{t} \, d\Gamma$$

For the mass conservation equation of water:

$$\int_{\Omega} \mathbf{w}^{*T} \left[\left(\frac{\alpha - n}{K_s} S_w (\rho^{gw} S_g + \rho^w S_w) + \rho^w S_w \frac{n}{K_w} \right) \frac{\partial p^w}{\partial t} \right.$$
$$\left. + \frac{\alpha - n}{K_s} S_g (\rho^{gw} S_g + \rho^w S_w) \frac{\partial p^g}{\partial t} \right] d\Omega$$
$$+ \int_{\Omega} \mathbf{w}^{*T} \left[\alpha (\rho^{gw} S_g + \rho^w S_w) \mathbf{m}^T L \frac{\partial \mathbf{u}}{\partial t} - S_w \beta_{swg} \frac{\partial T}{\partial t} + S_g n \boxed{\frac{\partial}{\partial t} \left(\frac{M_w}{\theta R} p^{gw} \right)} \right] d\Omega$$
$$+ \int_{\Omega} \mathbf{w}^{*T} \left\{ \left[\frac{\alpha - n}{K_s} (\rho^{gw} S_g p^c + \rho^w S_w p^w - \rho^w S_w p^c) + n(\rho^w - \rho^{gw}) \right] \frac{\partial S_w}{\partial t} \right\} d\Omega$$
$$- \int_{\Omega} (\nabla \mathbf{w}^*)^T \left[-\rho^g \frac{M_a M_w}{M_g^2} \mathbf{D}_g \boxed{\nabla \left(\frac{p^{gw}}{p^g} \right)} + \rho^{gw} \frac{k k^{rg}}{\mu^g} (-\nabla p^g + \rho^g g) \right] d\Omega$$
$$- \int_{\Omega} (\nabla \mathbf{w}^*)^T \left[\rho^w \frac{k k^{rw}}{\mu^w} (-\nabla p^w + \rho^w g) \right] d\Omega$$
$$+ \int_{\Gamma_u^q} \mathbf{w}^{*T} [q^w + q^{gw} + \beta_c (\rho^{gw} - \rho^{gw}_{\infty})] d\Gamma = 0$$

With:
$$\boxed{\frac{\partial}{\partial t} \left(\frac{M_w}{\theta R} p^{gw} \right) = \frac{M_w}{\theta R} \frac{\partial p^{gw}}{\partial p^c} \left(\frac{\partial p^g}{\partial t} - \frac{\partial p^w}{\partial t} \right) + \frac{M_w}{\theta R} \left(\frac{\partial p^{gw}}{\partial T} - \frac{p^{gw}}{\theta} \right) \frac{\partial T}{\partial t}}$$
$$\nabla \left(\frac{p^{gw}}{p^g} \right) = \frac{\nabla p^{gw}}{p^g} - \frac{p^{gw}}{(p^g)^2} \nabla p^g = \frac{1}{p^g} \frac{\partial p^{gw}}{\partial p^c} (\nabla p^g - \nabla p^w) - \frac{p^{gw}}{(p^g)^2} \nabla p^g$$

$$\int_{\Omega} \mathbf{N}_p^{\mathrm{T}}\left[\left(\frac{\alpha-n}{K_s}S_w(\rho^{gw}S_g+\rho^wS_w)+\rho^wS_w\frac{n}{K_w}\right)\mathbf{N}_p\frac{\partial\bar{\mathbf{p}}^w}{\partial t}\right.$$

$$\left.+\frac{\alpha-n}{K_s}S_g(\rho^{gw}S_g+\rho^wS_w)\mathbf{N}_p\frac{\partial\bar{\mathbf{p}}^g}{\partial t}\right]d\Omega$$

$$+\int_{\Omega}\mathbf{N}_p^{\mathrm{T}}\left[\alpha(\rho^{gw}S_g+\rho^wS_w)\mathbf{m}^{\mathrm{T}}\mathbf{L}\mathbf{N}_u\frac{\partial\bar{\mathbf{u}}}{\partial t}-S_w\beta_{sgw}\mathbf{N}_t\frac{\partial\bar{\mathbf{T}}}{\partial t}\right.$$

$$\left.+S_gn\frac{M_w}{\theta R}\frac{\partial p^{gw}}{\partial p^c}\mathbf{N}_p\left(\frac{\partial\bar{\mathbf{p}}^g}{\partial t}-\frac{\partial\bar{\mathbf{p}}^w}{\partial t}\right)\right]d\Omega+\int_{\Omega}\mathbf{N}_p^{\mathrm{T}}\left[S_gn\frac{M_w}{\theta R}\left(\frac{\partial p^{gw}}{\partial T}-\frac{p^{gw}}{\theta}\right)\mathbf{N}_t\frac{\partial\bar{\mathbf{T}}}{\partial t}\right]d\Omega$$

$$+\int_{\Omega}\mathbf{N}_p^{\mathrm{T}}\left\{\begin{bmatrix}\frac{\alpha-n}{K_s}(\rho^{gw}S_gp^c+\rho^wS_wp^w-\rho^wS_wp^c)+n(\rho^w-\rho^{gw})\end{bmatrix}\\\left(\frac{\partial S_w}{\partial p^c}\mathbf{N}_p\frac{\partial\bar{\mathbf{p}}^g}{\partial t}-\frac{\partial S_w}{\partial p^c}\mathbf{N}_p\frac{\partial\bar{\mathbf{p}}^w}{\partial t}+\frac{\partial S_w}{\partial T}\mathbf{N}_t\frac{\partial\bar{\mathbf{T}}}{\partial t}\right)\end{bmatrix}\right\}d\Omega$$

$$-\int_{\Omega}(\nabla\mathbf{N}_p)^{\mathrm{T}}\left\{-\rho^g\frac{M_aM_w}{M_g^2}\mathbf{D}_g\left[\frac{1}{p^g}\frac{\partial p^{gw}}{\partial p^c}(\nabla\mathbf{N}_p\bar{\mathbf{p}}^g-\nabla\mathbf{N}_p\bar{\mathbf{p}}^w)-\frac{p^{gw}}{(p^g)^2}\nabla\mathbf{N}_p\bar{\mathbf{p}}^g\right]\right\}d\Omega$$

$$-\int_{\Omega}(\nabla\mathbf{N}_p)^{\mathrm{T}}\left\{\rho^{gw}\frac{kk^{rg}}{\mu^g}(-\nabla\mathbf{N}_p\bar{\mathbf{p}}^g+\rho^g\mathbf{g})\right\}d\Omega$$

$$-\int_{\Omega}(\nabla\mathbf{N}_p)^{\mathrm{T}}\left[\rho^w\frac{kk^{rw}}{\mu^w}(-\nabla\mathbf{N}_p\bar{\mathbf{p}}^w+\rho^w\mathbf{g})\right]d\Omega$$

$$+\int_{\Gamma_g^q}\mathbf{N}_p^{\mathrm{T}}[q^w+q^{gw}+\beta_c(\rho^{gw}-\rho_\infty^{gw})]d\Gamma=0$$

For the mass conservation equation of gas, with $\rho^{ga}=\rho^g-\rho^{gw}$

$$\int_{\Omega}\mathbf{w}^{\bullet\mathrm{T}}\left[\frac{\alpha-n}{K_s}S_wS_g\rho^{ga}\frac{\partial p^w}{\partial t}+\frac{\alpha-n}{K_s}S_g^2\rho^{gu}\frac{\partial p^g}{\partial t}-\left(\frac{\alpha-n}{K_s}S_gp^c+n\right)\rho^{ga}\boxed{\frac{\partial S_w}{\partial t}}\right.$$

$$\left.-\rho^{ga}\beta_{sg}\frac{\partial T}{\partial t}\right]d\Omega+\int_{\Omega}\mathbf{w}^{\bullet\mathrm{T}}\left[\alpha S_g\rho^{ga}\mathbf{m}^{\mathrm{T}}L\frac{\partial\mathbf{u}}{\partial t}+S_gn\frac{\partial}{\partial t}\left(\frac{p^{ga}M_a}{\theta R}\right)\right]d\Omega$$

$$-\int_{\Omega}(\nabla\mathbf{w}^{\bullet})^{\mathrm{T}}\left\{\left[\rho^{ga}\frac{kk^{rg}}{\mu^g}(-\nabla p^g+\rho^g\mathbf{g})\right]+\left[\rho^g\frac{M_aM_w}{M_g^2}\mathbf{D}_g\nabla\boxed{\left(\frac{p^{gw}}{p^g}\right)}\right]\right\}d\Omega$$

$$+\int_{\Gamma_g^q}\mathbf{w}^{\bullet\mathrm{T}}q^{ga}d\Gamma=0$$

With:

$$\frac{\partial S_w}{\partial t}=\frac{\partial S_w}{\partial p^c}\frac{\partial p^c}{\partial t}+\frac{\partial S_w}{\partial T}\frac{\partial T}{\partial t}=\frac{\partial S_w}{\partial p^c}\frac{\partial p^g}{\partial t}-\frac{\partial S_w}{\partial p^c}\frac{\partial p^w}{\partial t}+\frac{\partial S_w}{\partial T}\frac{\partial T}{\partial t}$$

$$\frac{\partial}{\partial t}\left(\frac{M_w}{\theta R}p^{gw}\right)=\frac{M_w}{\theta R}\frac{\partial p^{gw}}{\partial p^c}\left(\frac{\partial p^g}{\partial t}-\frac{\partial p^w}{\partial t}\right)+\frac{M_w}{\theta R}\left(\frac{\partial p^{gw}}{\partial T}-\frac{p^{gw}}{\theta}\right)\frac{\partial T}{\partial t}$$

$$\nabla\left(\frac{p^{gw}}{p^g}\right)=\frac{\nabla p^{gw}}{p^g}-\frac{p^{gw}}{(p^g)^2}\nabla p^g=\frac{1}{p^g}\frac{\partial p^{gw}}{\partial p^c}(\nabla p^g-\nabla p^w)-\frac{p^{gw}}{(p^g)^2}\nabla p^g$$

$$\frac{\partial}{\partial t}\left(\frac{p^{ga}M_a}{\theta R}\right)=\frac{\partial}{\partial t}\left[\frac{(p^g-p^{gw})M_a}{\theta R}\right]$$

$$=\frac{M_a}{\theta R}\frac{\partial p^g}{\partial t}-\frac{M_a}{\theta^2R}\frac{\partial T}{\partial t}-\frac{M_w}{\theta R}\frac{\partial p^{gw}}{\partial p^c}\left(\frac{\partial p^g}{\partial t}-\frac{\partial p^w}{\partial t}\right)$$

$$-\frac{M_w}{\theta R}\left(\frac{\partial p^{gw}}{\partial T}-\frac{p^{gw}}{\theta}\right)\frac{\partial T}{\partial t}$$

$$
\int_{\Omega} \mathbf{N}_p^{\mathrm{T}} \left[\frac{\alpha - n}{K_s} S_w S_g \rho^{gu} \mathbf{N}_p \frac{\partial \bar{\mathbf{p}}^w}{\partial t} + \frac{\alpha - n}{K_s} S_g^2 \rho^{gu} \mathbf{N}_p \frac{\partial \bar{\mathbf{p}}^g}{\partial t} - \rho^{gu} \beta_{sg} \mathbf{N}_t \frac{\partial \bar{\mathbf{T}}}{\partial t} \right] d\Omega
$$

$$
- \int_{\Omega} \mathbf{N}_p^{\mathrm{T}} \left[\left(\frac{\alpha - n}{K_s} S_g p^c + n \right) \rho^{gu} \left(\frac{\partial S_w}{\partial p^c} \mathbf{N}_p \frac{\partial \bar{\mathbf{p}}^g}{\partial t} - \frac{\partial S_w}{\partial p^c} \mathbf{N}_p \frac{\partial \bar{\mathbf{p}}^w}{\partial t} + \frac{\partial S_w}{\partial T} \mathbf{N}_t \frac{\partial \bar{\mathbf{T}}}{\partial t} \right) \right] d\Omega
$$

$$
+ \int_{\Omega} \mathbf{N}_p^{\mathrm{T}} \left[\alpha S_g \rho^{gu} \mathbf{m}^{\mathrm{T}} \mathbf{L} \mathbf{N}_u \frac{\partial \bar{\mathbf{u}}}{\partial t} + S_g n \frac{M_a}{\theta R} \mathbf{N}_p \frac{\partial \bar{\mathbf{p}}^g}{\partial t} - S_g n \frac{M_a}{\theta^2 R} \mathbf{N}_t \frac{\partial \bar{\mathbf{T}}}{\partial t} \right] d\Omega
$$

$$
- \int_{\Omega} \mathbf{N}_p^{\mathrm{T}} \left[S_g n \frac{M_w}{\theta R} \left(\frac{\partial p^{gw}}{\partial T} - \frac{p^{gw}}{\theta} \right) \mathbf{N}_t \frac{\partial \bar{\mathbf{T}}}{\partial t} \right] d\Omega
$$

$$
+ \int_{\Omega} \mathbf{N}_p^{\mathrm{T}} \left[-S_g n \frac{M_w}{\theta R} \frac{\partial p^{gw}}{\partial p^c} \mathbf{N}_p \frac{\partial \bar{\mathbf{p}}^g}{\partial t} + S_g n \frac{M_w}{\theta R} \frac{\partial p^{gw}}{\partial p^c} \mathbf{N}_p \frac{\partial \bar{\mathbf{p}}^w}{\partial t} \right] d\Omega
$$

$$
- \int_{\Omega} (\nabla \mathbf{N}_p)^{\mathrm{T}} \left[\rho^{gu} \frac{\mathbf{k} k^{rg}}{\mu^g} (-\nabla \mathbf{N}_p \bar{\mathbf{p}}^g + \rho^g \mathbf{g}) \right] d\Omega + \int_{\Gamma_g^q} \mathbf{N}_p^{\mathrm{T}} q^{gu} d\Gamma
$$

$$
- \int_{\Omega} (\nabla \mathbf{N}_p)^{\mathrm{T}} \left\{ \rho^g \frac{M_a M_w}{M_g^2} \mathbf{D}_g \left[\frac{1}{p^g} \frac{\partial p^{gw}}{\partial p^c} (\nabla \mathbf{N}_p \bar{\mathbf{p}}^g - \nabla \mathbf{N}_p \bar{\mathbf{p}}^w) - \frac{p^{gw}}{(p^g)^2} \nabla \mathbf{N}_p \bar{\mathbf{p}}^g \right] \right\} d\Omega = 0
$$

For the energy conservation equation:

$$
\int_{\Omega} \mathbf{w}^{\circ \mathrm{T}} (\rho C_p)_{\mathrm{eff}} \frac{\partial T}{\partial t} d\Omega + \int_{\Omega} (\nabla \mathbf{w}^{\circ})^{\mathrm{T}} \chi_{\mathrm{eff}} \nabla T d\Omega
$$

$$
+ \int_{\Omega} \mathbf{w}^{\circ \mathrm{T}} \left\{ \left[n S_w \rho^w C_p^w \frac{\mathbf{k} k^{rw}}{\mu^w} (-\nabla p^w + \rho^w \mathbf{g})^{\mathrm{T}} \right. \right.
$$

$$
\left. + n S_g \rho^g C_p^g \frac{\mathbf{k} k^{rg}}{\mu^g} (-\nabla p^g + \rho^g \mathbf{g}) \right] \cdot \nabla T \right\} d\Omega
$$

$$
+ \int_{\Omega} \mathbf{w}^{\circ \mathrm{T}} \Delta H_{\mathrm{vap}} \left\{ -\rho^w \left(\frac{\alpha - n}{K_s} S_w^2 + S_w \frac{n}{K_w} \right) \frac{\partial p^w}{\partial t} \right.
$$

$$
\left. - \rho^w \frac{\alpha - n}{K_s} S_g S_w \frac{\partial p^g}{\partial t} - \alpha \rho^w S_w \mathbf{m}^{\mathrm{T}} \mathbf{L} \frac{\partial \mathbf{u}}{\partial t} \right\} d\Omega
$$

$$
+ \int_{\Omega} \mathbf{w}^{\circ \mathrm{T}} \Delta H_{\mathrm{vap}} \left\{ \beta_{sw} \frac{\partial T}{\partial t} - \rho^w \left[\frac{\alpha - n}{K_s} S_w p^w - \frac{\alpha - n}{K_s} S_w p^g + n \right] \boxed{\frac{\partial S_w}{\partial t}} \right\} d\Omega
$$

$$
+ \int_{\Omega} (\nabla \mathbf{w}^{\circ})^{\mathrm{T}} \Delta H_{\mathrm{vap}} \left[\rho^w \frac{\mathbf{k} k^{rw}}{\mu^w} (-\nabla p^w + \rho^w \mathbf{g}) \right] d\Omega
$$

$$
+ \int_{\Gamma_T^q} \mathbf{w}^{\circ \mathrm{T}} [q^{\mathrm{T}} + \alpha_c (T - T_\infty)] d\Gamma = 0
$$

With:
$$
\boxed{\frac{\partial S_w}{\partial t} = \frac{\partial S_w}{\partial p^c} \frac{\partial p^c}{\partial t} + \frac{\partial S_w}{\partial T} \frac{\partial T}{\partial t} = \frac{\partial S_w}{\partial p^c} \frac{\partial p^g}{\partial t} - \frac{\partial S_w}{\partial p^c} \frac{\partial p^w}{\partial t} + \frac{\partial S_w}{\partial T} \frac{\partial T}{\partial t}}
$$

$$
\int_{\Omega} \mathbf{N}_t^{\mathrm{T}} (\rho C_p)_{\text{eff}} \mathbf{N}_t \frac{\partial \bar{\mathbf{T}}}{\partial t} d\Omega + \int_{\Omega} (\nabla \mathbf{N}_t)^{\mathrm{T}} \chi_{\text{eff}} \nabla \mathbf{N}_t \bar{\mathbf{T}} d\Omega
$$

$$
+ \int_{\Omega} \mathbf{N}_t^{\mathrm{T}} \left\{ \left[n S_w \rho^w C_p^w \frac{k k^{rw}}{\mu^w} (-\nabla p^w + \rho^w \mathbf{g})^{\mathrm{T}} + n S_g \rho^g C_p^g \frac{k k^{rg}}{\mu^g} (-\nabla p^g + \rho^g \mathbf{g}) \right] \cdot \nabla \mathbf{N}_t \bar{\mathbf{T}} \right\} d\Omega
$$

$$
+ \int_{\Omega} \mathbf{N}_t^{\mathrm{T}} \Delta H_{\text{vap}} \left\{ -\rho^w \left(\frac{\alpha - n}{K_s} S_w^2 + S_w \frac{n}{K_w} \right) \mathbf{N}_p \frac{\partial \bar{\mathbf{p}}^w}{\partial t} - \rho^w \frac{\alpha - n}{K_s} S_g S_w \mathbf{N}_p \frac{\partial \bar{\mathbf{p}}^g}{\partial t} \right\} d\Omega
$$

$$
- \int_{\Omega} \mathbf{N}_t^{\mathrm{T}} \Delta H_{\text{vap}} \alpha \rho^w S_w \mathbf{m}^{\mathrm{T}} \mathbf{L} \mathbf{N}_u \frac{\partial \bar{\mathbf{u}}}{\partial t} d\Omega
$$

$$
+ \int_{\Omega} \mathbf{N}_t^{\mathrm{T}} \Delta H_{\text{vap}} \left\{ \begin{array}{l} \beta_{sw} \mathbf{N}_t \frac{\partial \bar{\mathbf{T}}}{\partial t} - \rho^w \left[\frac{\alpha - n}{K_s} S_w p^w - \frac{\alpha - n}{K_s} S_w p^g + n \right] \\[2mm] \left(\frac{\partial S_w}{\partial p^c} \mathbf{N}_p \frac{\partial \bar{\mathbf{p}}^g}{\partial t} - \frac{\partial S_w}{\partial p^c} \mathbf{N}_p \frac{\partial \bar{\mathbf{p}}^w}{\partial t} + \frac{\partial S_w}{\partial T} \mathbf{N}_t \frac{\partial \bar{\mathbf{T}}}{\partial t} \right) \end{array} \right\} d\Omega
$$

$$
+ \int_{\Omega} (\nabla \mathbf{N}_t)^{\mathrm{T}} \Delta H_{\text{vap}} \left[\rho^w \frac{k k^{rw}}{\mu^w} (-\nabla \mathbf{N}_p \bar{\mathbf{p}}^w + \rho^w \mathbf{g}) \right] d\Omega
$$

$$
+ \int_{\Gamma_t^T} \mathbf{N}_t^{\mathrm{T}} [q^{\Gamma} + \alpha_c (T - T_{\infty})] d\Gamma = 0
$$

In a **matrix form**, component by component:

$$
\mathbf{K}_c \frac{\partial \bar{\mathbf{u}}}{\partial t} + \mathbf{K}_{tc} \frac{\partial \bar{\mathbf{T}}}{\partial t} - C_{sw} \frac{\partial \bar{\mathbf{p}}^w}{\partial t} - C_{sg} \frac{\partial \bar{\mathbf{p}}^g}{\partial t} = \frac{\partial \mathbf{f}^u}{\partial t}
$$

$$
\mathbf{C}_{ws} \frac{\partial \bar{\mathbf{u}}}{\partial t} + \mathbf{P}_{ww} \frac{\partial \bar{\mathbf{p}}^w}{\partial t} + \mathbf{C}_{wg} \frac{\partial \bar{\mathbf{p}}^g}{\partial t} + \mathbf{C}_{wt} \frac{\partial \bar{\mathbf{T}}}{\partial t} + \mathbf{H}_{ww} \bar{\mathbf{p}}^w + \mathbf{K}_{wg} \bar{\mathbf{p}}^g = \mathbf{f}^w
$$

$$
\mathbf{C}_{gs} \frac{\partial \bar{\mathbf{u}}}{\partial t} + \mathbf{C}_{gw} \frac{\partial \bar{\mathbf{p}}^w}{\partial t} + \mathbf{P}_{gg} \frac{\partial \bar{\mathbf{p}}^g}{\partial t} + \mathbf{C}_{gt} \frac{\partial \bar{\mathbf{T}}}{\partial t} + \mathbf{K}_{gw} \bar{\mathbf{p}}^w + \mathbf{H}_{gg} \bar{\mathbf{p}}^g = \mathbf{f}^g
$$

$$
\mathbf{C}_{ts} \frac{\partial \bar{\mathbf{u}}}{\partial t} + \mathbf{C}_{tw} \frac{\partial \bar{\mathbf{p}}^w}{\partial t} + \mathbf{C}_{tg} \frac{\partial \bar{\mathbf{p}}^g}{\partial t} + \mathbf{P}_{tt} \frac{\partial \bar{\mathbf{T}}}{\partial t} + \mathbf{K}_{tw} \bar{\mathbf{p}}^w + \mathbf{H}_{tt} \bar{\mathbf{T}} = \mathbf{f}^t
$$

Coupled matrix FEM equation:

$$
\begin{bmatrix} \mathbf{0} & \mathbf{0} & \mathbf{0} & \mathbf{0} \\ \mathbf{0} & \mathbf{H}_{ww} & \mathbf{K}_{wg} & \mathbf{0} \\ \mathbf{0} & \mathbf{K}_{gw} & \mathbf{H}_{gg} & \mathbf{0} \\ \mathbf{0} & \mathbf{K}_{tw} & \mathbf{0} & \mathbf{H}_{tt} \end{bmatrix} \begin{Bmatrix} \bar{\mathbf{u}} \\ \bar{\mathbf{p}}^w \\ \bar{\mathbf{p}}^g \\ \bar{\mathbf{T}} \end{Bmatrix} + \begin{bmatrix} \mathbf{K}_T & -\mathbf{C}_{sw} & -\mathbf{C}_{sg} & \mathbf{K}_{tT} \\ \mathbf{C}_{ws} & \mathbf{P}_{ww} & \mathbf{C}_{wg} & \mathbf{C}_{wt} \\ \mathbf{C}_{gs} & \mathbf{C}_{gw} & \mathbf{P}_{gg} & \mathbf{C}_{gt} \\ \mathbf{C}_{ts} & \mathbf{C}_{tw} & \mathbf{C}_{tg} & \mathbf{P}_{tt} \end{bmatrix} \frac{\partial}{\partial t} \begin{Bmatrix} \bar{\mathbf{u}} \\ \bar{\mathbf{p}}^w \\ \bar{\mathbf{p}}^g \\ \bar{\mathbf{T}} \end{Bmatrix} = \begin{Bmatrix} \frac{\partial \mathbf{f}^u}{\partial t} \\ \mathbf{f}^w \\ \mathbf{f}^g \\ \mathbf{f}^t \end{Bmatrix}
$$

PROBLEMS

6.1   Consider plane wall of thickness L, initially at a uniform temperature T_0, which has both surfaces suddenly exposed to a fluid at temperature T_∞. The governing differential equation is:

$$k\frac{\partial^2 T}{\partial x^2} = \rho c_0 \frac{\partial T}{\partial t}$$

The initial condition is $T(x, 0) = T_0$ and we consider two sets of boundary conditions:

Set 1: $T(0, t) = T_\infty, \quad T(L, t) = T_\infty$

Set 2: $T(0, t) = T_\infty, \quad \left[k\frac{\partial T}{\partial x} + \beta(T - T_\infty)\right]_{x=L} = 0$

Approximate the solution with two linear Finite Elements. Solve for the unknown temperatures and heat fluxes.

6.2   Consider a uniform beam of rectangular cross section (B×H), fixed at $x = 0$ and free at $x = L$. We use the Euler-Bernouilli beam theory. Neglecting the rotary inertia term, the governing equation for beam deflection is:

$$\rho A \frac{\partial^2 w}{\partial t^2} + \frac{\partial^2}{\partial x^2}\left[EI\frac{\partial^2 w}{\partial x^2}\right] = q(x, t)$$

The boundary conditions are:

$$W(0) = 0, \quad \frac{dW}{dx} = 0, \quad \left[EI\frac{d^2 W}{dx^2}\right]_{x=L} = 0, \quad \left[EI\frac{d^3 W}{dx^3}\right]_{x=L} = 0$$

Determine the first two flexural frequencies of the beam by using the minimum number of Euler-Bernouilli beam elements.

6.3   Consider a uniform bar of cross-sectional area A, modulus of elasticity E, mass density m, and length L. The axial displacement under the action of time-dependent axial forces is governed by the wave equation:
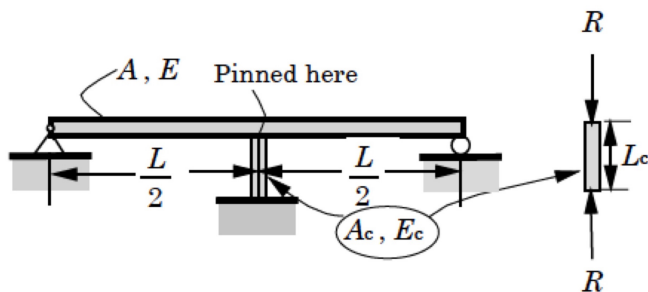
$$\frac{\partial^2 u}{\partial t^2} = a^2 \frac{\partial^2 u}{\partial x^2}, \quad a = \left(\frac{E}{m}\right)^{1/2}$$

Determine the transient response [i.e., find u(x, t)] of the bar when the end x = 0 is fixed and the end x = L is subjected to a force P_0. Assume zero initial conditions. Use one linear element to approximate the spatial variation of the solution, and solve the resulting ordinary differential equation in time exactly to obtain:

$$u_2(x, t) = \frac{P_0 L}{AE}\frac{x}{L}(1 - cos\alpha t), \quad \alpha = \sqrt{3}\frac{a}{L}$$

6.4   Consider a simply supported beam (of Young's modulus E, mass density ρ, area of cross section A, second moment of area about the axis of bending I, and length L) with an elastic support at the center of the beam (see Figure 6.7). Determine the fundamental natural frequency using the minimum number of Euler-Bernoulli beam elements. It is reminded that in Euler-Bernouilli beam theory, if the rotary inertia term is neglected, the governing equation for beam deflection is:

$$\rho A \frac{\partial^2 w}{\partial t^2} + \frac{\partial^2}{\partial x^2}\left[EI\frac{\partial^2 w}{\partial x^2}\right] = q(x,t)$$

Figure 6.7   Beam vibration problem

6.5   Consider the transient heat conduction problem governed by the following equation:

$$\frac{\partial u}{\partial t} - \frac{\partial^2 u}{\partial x^2} = 0, \quad 0 < x < 1$$

with boundary conditions:

$$u(0,t) = 0, \quad \frac{\partial u}{\partial x}(1,t) = 0$$

and initial condition:

$$u(x,0) = 1$$

where u is the non-dimensionalized temperature. Discuss the stability of the FEM model for one linear element and for two linear elements.

6.6   We wish to determine the transverse motion of a beam clamped at both ends and subjected to an initial deflection, by using Euler-Bernouilli theory. The governing equation is:

$$\frac{\partial^2 w}{\partial t^2} + \frac{\partial^4 w}{\partial x^4} = 0, \quad 0 < x < 1$$

with the following boundary conditions:

$$w(0,t) = 0, \quad \frac{\partial w}{\partial x}(0,t) = 0, \quad w(1,t) = 0, \quad \frac{\partial w}{\partial x}(1,t) = 0$$

and the following initial conditions:

$$w(x,0) = sin\pi x - \pi x(1-x), \quad \frac{\partial w}{\partial t}(x,0) = 0$$
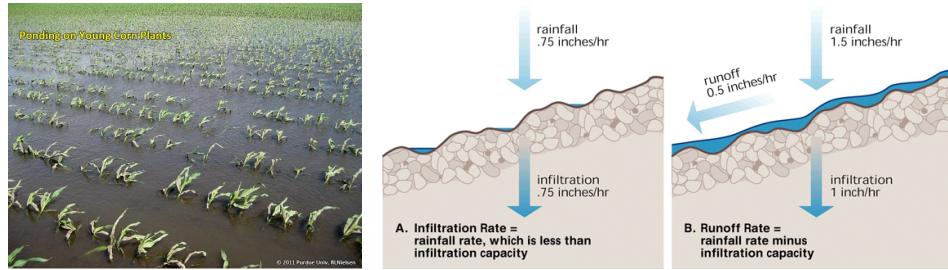
Establish a stability criterion with the lowest number of Euler-Bernouilli beam elements possible.

6.7   Establish a stability criterion for the 1D consolidation problem. Assume that there is drainage at the top and and that the bottom boundary is impermeable.
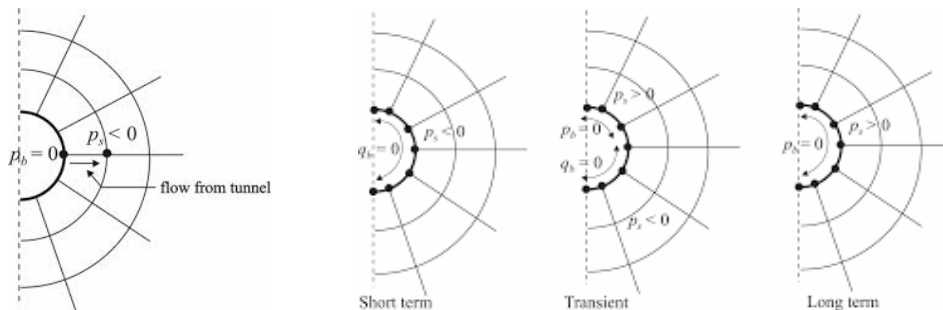
6.8   Dual boundary conditions occur in flow problems in which a pressurized fluid reservoir is in contact with the domain under study:

- If the pore pressure at the boundary is more tensile (i.e. lower) than a prescribed value p_*, then one needs to apply a fluid flow $\bar{q}_n$ at the boundary.

- If the pore pressure at the boundary is more compressive (i.e. greater) than the prescribed value p_*, then one needs to impose the pore pressure p_* at all nodes of the boundary.

Figure 6.8 on the left hand-side shows the example of ponding, for which such boundary conditions are necessary. Explain how you would use the dual boundary condition for a problem of rainfall (Figure 6.8 on the right hand-side) and for a problem of tunnel excavation in a water saturated rock mass (Figure 6.9).
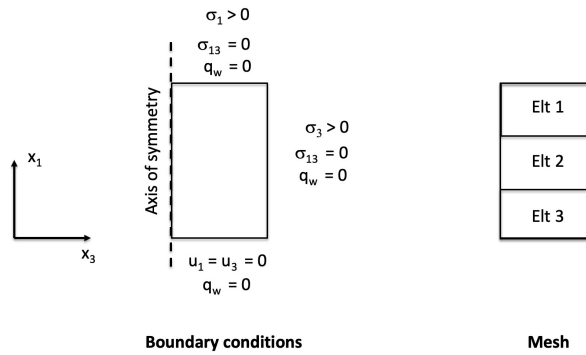

Figure 6.8   Problems in which a dual boundary condition is needed: ponding (left) and rainfall (right).


Figure 6.9   Problem in which a dual boundary condition is needed: tunnel excavation.

6.9   Consider a triaxial compression test performed on a water-saturated soil specimen, as shown in Figure 6.10. The experiment is undrained, and axis-symmetry is assumed. The soil is assumed to be linear elastic. Biot's hydro-mechanical constitutive relationships hold.

- Write the strong formulation of the problem (introduce as many constitutive parameters as necessary).

- Write the weak formulation of the problem (in cylindrical coordinates).

- The specimen is modeled with three rectangular elements, as shown in Figure 6.10. Calculate the elementary stiffness of each element, assuming that the displacement field is interpolated with quadratic polynomials, and the pore pressure field is interpolated with linear polynomials.

- Assemble the elementary equations established in question 2 above.

- Discretize the assembled equations in time. Provide the conditions in which the time marching scheme is stable.

- Introduce the boundary conditions in the Finite Element equations, condense the system of equations if possible, and solve it for the primary variables.

- Post-process the secondary variables.
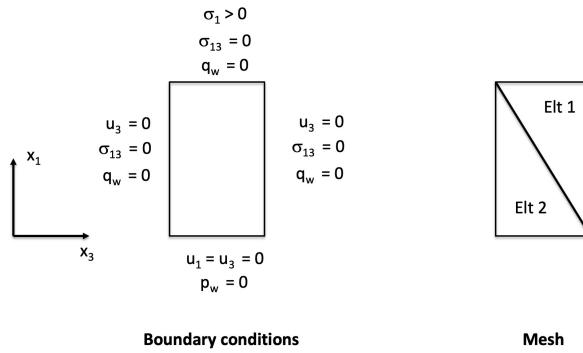
Figure 6.10   Finite Element model of undrained triaxial compression test performed on water-saturated soil

6.10   Consider an oedometer test performed on a water-saturated soil specimen, as shown in Figure 6.11. The specimen is drained at the bottom and it is studied in plane strain. The soil is assumed to be linear elastic. Biot's hydro-mechanical constitutive relationships hold.

- Write the strong formulation of the problem (introduce as many constitutive parameters as necessary).

- Write the weak formulation of the problem.

- The specimen is modeled with two triangular elements, as shown in Figure 6.11. Calculate the elementary stiffness of each element, assuming that the displacement field

is interpolated with quadratic polynomials, and the pore pressure field is interpolated with linear polynomials.

- Assemble the elementary equations established in question 2 above.

- Discretize the assembled equations in time. Provide the conditions in which the time marching scheme is stable.

- Introduce the boundary conditions in the Finite Element equations, condense the system of equations if possible, and solve it for the primary variables.

- Post-process the secondary variables.

Figure 6.11 Finite Element model of drained oedometric test performed on water-saturated soil

6.11 Consider an oedometer test performed on a partially saturated soil specimen, as shown in Figure 6.12. The specimen is drained at the bottom and it is studied in plane strain. The soil is assumed to be linear elastic.

- Write the strong formulation of the problem (introduce as many constitutive parameters as necessary).

- Write the weak formulation of the problem.

- The specimen is modeled with two triangular elements, as shown in Figure 6.12. Calculate the elementary stiffness of each element, assuming that the displacement field is interpolated with quadratic polynomials, and the pore pressure fields is interpolated with linear polynomials.

- Assemble the elementary equations established in question 2 above.

- Discretize the assembled equations in time. Provide the conditions in which the time marching scheme is stable.

- Introduce the boundary conditions in the Finite Element equations, condense the system of equations if possible, and solve it for the primary variables.

- Post-process the secondary variables.
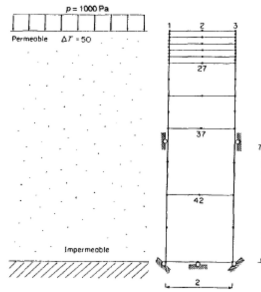
Figure 6.12   Finite Element model of drained oedometric test performed on partially saturated soil
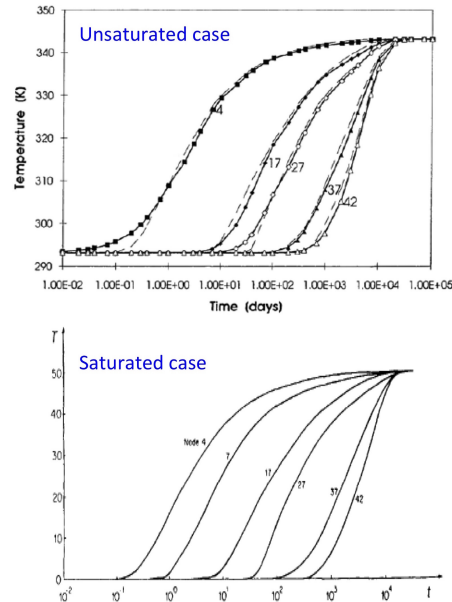
6.12   We use the FEM to compare two one-dimensional consolidation experiments (see the column of soil in Figure 6.13):

1. $S_{w0} = 0.92$ (homogeneous initial partial saturation) with a capillary pressure - water saturation curve independent of temperature;

2. $S_{w0} = 0.92$ (homogeneous initial partial saturation), with a capillary pressure - water saturation curve that depends on temperature.
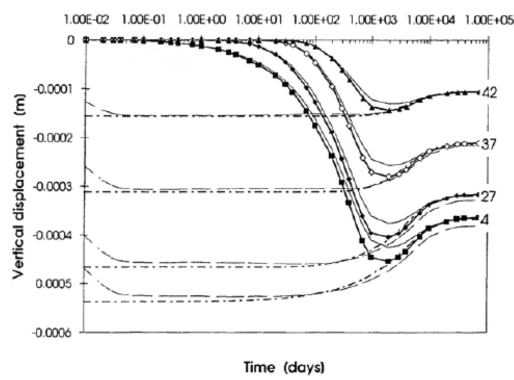
A Brooks & Corey relationship is assumed between the capillary pressure, the saturation degree and the relative permeability. The solid grains and the water are assumed to be incompressible. The boundary conditions are the following: no lateral displacement or heat flux on lateral boundaries; at the top: uniform stress, T=343.15 K, $p_g = p_{atm}$ and p_c chosen to ensure $S_w = 0.92$; no vertical displacement and no heat flux on the bottom boundary. The same results were obtained with 9 and 18 8-noded isoparametric elements with a 3x3 Gaussian integration scheme. The time step was 0.01 days for the first 100 steps, and then the time step was multiplied by 10 every 100 time steps, until 10^7 days elapsed. Comment on the results obtained in Figures 6.14-6.17 (in particular, explain the difference between the profiles obtained in the saturated and unsaturated cases).


Figure 6.13   Unsaturated soil consolidation under non isothermal conditions
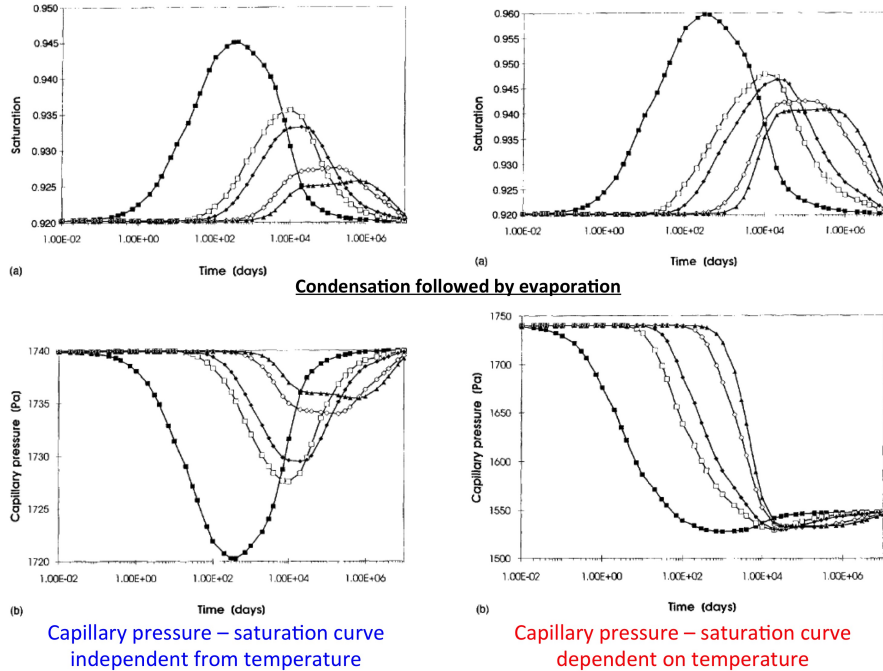
Figure 6.14   Unsaturated consolidation: temperature profiles
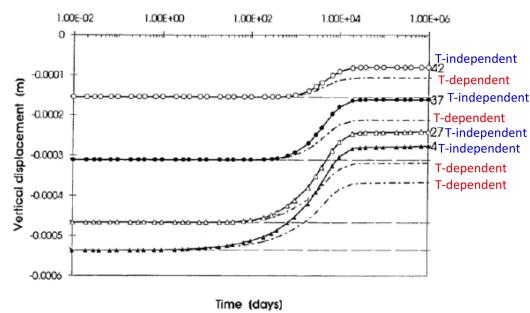
Comparison between the saturated case (solid lines) and the second partially saturated case (chain dots): heavy lines are the present solution; light lines are the solution of Schrefler *et al.* [22]. The numbers on the curves are the nodal points selected within the mesh

Figure 6.15   Unsaturated consolidation: displacement profiles, comparison between saturated and unsaturated cases

Condensation followed by evaporation

Capillary pressure – saturation curve
independent from temperature

Capillary pressure – saturation curve
dependent on temperature

Figure 6.16   Unsaturated consolidation: water retention curves


Figure 6.17   Unsaturated consolidation: displacement profiles, comparison between the two unsaturated models (WRC that depends/does not depend on temperature)

PART III

YIELD AND FAILURE
OF GEOMATERIALS

CHAPTER 7

FUNDAMENTAL PRINCIPLES OF PLASTICITY

Before the theory of plastic stress-strain relations was developed for metals by de Saint-Venant and Levt in the 1870s, the concept of perfect plasticity had already been used to solve geotechnical stability problems involving earth pressures and retaining walls by Coulomb (1770s) and Rankine (1850s). However, without a stress-strain relation, it is not possible to use the theory of plasticity to estimate deformation [23]. This is why in the early stage of the development of soil mechanics and geotechnical engineering, almost all the calculations were concerned with the stability of structures and earthworks. In these analyses, the soil was considered to be a rigid-perfectly plastic solid, and simple calculations led to an estimate of the maximum load the structure can sustain before collapse. In Chapter **??**, we will learn how to use some basic assumptions of perfect plasticity to prevent the collapse of earth structures. In Chapter 8, we will use plasticity stress-strain relationships to predict soil non-elastic stiffness and deformation. Below, we recall basic principles of plasticity [12].

7.1 Basic components of a plasticity model

The first and fundamental assumption of plasticity theory is that the strains can be decomposed into additive elastic and plastic components:

$$\epsilon_{ij} = \epsilon_{ij}^e + \epsilon_{ij}^p \tag{7.1}$$

The elastic strains ϵ_{ij}^e can be specified by any of the means used for elasticity, as discussed in Chapter 3. The rules used to define the plastic strains have become well established over

many years, but they are based on empirical observation, first of metals and later of many other materials. The concept of a yield surface is introduced. This is a surface in stress space, defined through a yield function by $f(\sigma_{ij}, ...) = 0$. For the time being, we shall just consider this as a function of the stresses, although later we shall consider cases where it is also a function of other variables.

Changes in plastic strain can occur only if the stress point lies on the yield surface, so that:

$$f(\sigma_{ij}) = 0 \tag{7.2}$$

If the stress point falls within the yield surface (which is conventionally defined as the region where $f(\sigma_{ij}) < 0$), then no plastic strain increments occur, and the response is incrementally elastic. We refer to this region as "within" the yield surface, even for the quite common cases where the surface is not closed in stress space. Stress states outside the yield surface, i. e. for which $f(\sigma_{ij}) > 0$, are not attainable.

When yield occurs at a particular point on the yield surface, it is found empirically for many materials (at least to a first approximation) that the ratios between the plastic strain components are fixed, irrespective of the stress increments. One way of defining this mathematically is to define a flow rule, in which the ratio of strain increments is related directly to the stress state. This method is sometimes used for models that involve just two dimensions of stress, but for more complex cases, it becomes very cumbersome, and the ratios between the strain increments are defined instead by a plastic potential, from which the flow rule can be derived. The plastic potential, like the yield surface, is a function of the stresses and other variables, and is usually written $g(\sigma_{ij}, ...) = 0$. The direction of the plastic strain increment is then defined as normal to the plastic potential:

$$\dot{\epsilon}_{ij}^{p} = \lambda \frac{\partial g(\sigma_{ij}, ...)}{\partial \sigma_{ij}} \tag{7.3}$$

In metal plasticity, it is usual for the yield function $f(\sigma_{ij}, ...) = 0$ and the plastic potential $g(\sigma_{ij}, ...) = 0$ to be identical functions. This important case is called *associated flow* or *normality* (in the sense that the plastic strain increments are normal to the yield surface, and not in the sense that normal means that this represents the usual behaviour of materials). For some materials, notably soils, the empirical evidence for non-associated flow is so overwhelming that it is essential to address this more complex case.
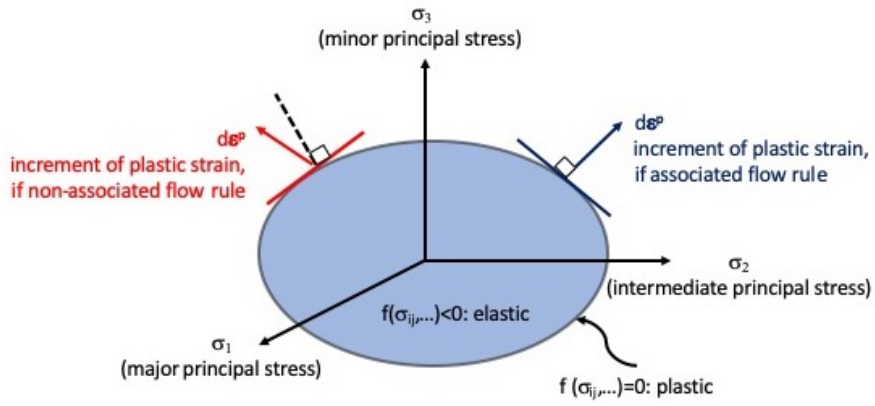
Figure 7.1 summarizes the basic components of a plasticity model, which can be completely defined by the following assumptions:

- Decomposition of the strain into elastic and plastic components;

- Definition of the elastic strains that requires specification of a single scalar function;

- Definition of a yield surface $f(\sigma_{ij}, ...) = 0$;

- Definition of a plastic potential $g(\sigma_{ij}, ...) = 0$.

The complete stress conditions for plastic and elastic behavior [23] may be stated as:

$$\text{Elastic:} \quad f(\sigma_{ij}, ...) = 0 \text{ or } \frac{\partial f}{\partial \sigma_{ij}} d\sigma_{ij} < 0 \text{ (if unloading)} \tag{7.4}$$
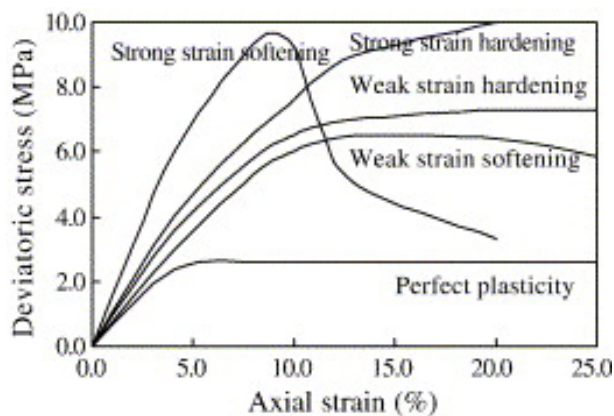
$$\text{Plastic:} \quad f(\sigma_{ij}, ...) = 0 \text{ and } \frac{\partial f}{\partial \sigma_{ij}} d\sigma_{ij} = 0$$

Figure 7.1   The deformation mechanisms inside and on a yield surface plotted in the stress space.

7.2   Principles of perfect plasticity

Figure 7.2 shows typical soil stress-strain curves. The stress-strain behavior of most real soils is characterized by an initial linear portion. Beyond the linear portion of the stress-strain curve, the soil is said to exhibit strain hardening (respectively, strain softening) if the increment of strain is of the same sign (respectively, of opposite sign) as the increment of stress. Most real soils exhibit a peak or failure stress followed by softening to a residual stress ("strong strain softening"). In limit analysis, it is necessary to ignore the strain softening (or work softening) feature of the stress-strain diagram and to take the stress-strain diagram to consist of two straight lines: the linear portion and a horizontal line. A hypothetical material exhibiting this property of continuing plastic flow at constant stress is called *ideally plastic* or *perfectly plastic* material.

**Figure 7.2**   Schematic stress-strain curves for soils. Figure taken from [24].

In perfect plasticity, the yield surface remains fixed in stress space, so there is no hardening (or softening). Thus the yield surface is only a function of the stress $f(\sigma_{ij}) = 0$. The plastic potential will have the form $g(\sigma_{ij}, \boldsymbol{x}) = 0$, where $\boldsymbol{x}$ are the dummy variables

introduced to satisfy the (not strictly necessary) condition that $g = 0$ at each stress point on the yield surface. The incremental stress-strain relationship is obtained by combining the equations below.

The strain decomposition is written in incremental form:

$$\dot{\epsilon}_{ij} = \dot{\epsilon}_{ij}^e + \dot{\epsilon}_{ij}^p \tag{7.5}$$

The elastic strain rates are defined by an elastic stiffness matrix D_{ijkl}^e:

$$\dot{\sigma}_{ij} = D_{ijkl}^e \dot{\epsilon}_{kl}^e \tag{7.6}$$

The yield surface is written in differential form, noting that during any process in which the plastic strains are non-zero, not only is $f = 0$, but also $\dot{f} = 0$. This incremental form of the yield surface is usually referred to as the *consistency condition*:

$$\dot{f} = \frac{df}{d\sigma_{ij}} \dot{\sigma}_{ij} = 0 \tag{7.7}$$

Finally, we need the plastic strain rate ratio, obtained from the plastic potential:

$$\dot{\epsilon}_{ij}^p = \lambda \frac{\partial g}{\partial \sigma_{ij}} \tag{7.8}$$

From the equations above, we get:

$$\dot{\sigma}_{ij} = D_{ijkl}^e (\dot{\epsilon}_{kl} - \dot{\epsilon}_{kl}^p) = D_{ijkl}^e \left(\dot{\epsilon}_{kl} - \lambda \frac{\partial g}{\partial \sigma_{kl}} \right) \tag{7.9}$$

Now combining equations 7.7 and 7.9, we get:

$$\dot{f} = \frac{df}{d\sigma_{ij}} D_{ijkl}^e \left(\dot{\epsilon}_{kl} - \lambda \frac{\partial g}{\partial \sigma_{kl}} \right) = 0 \tag{7.10}$$

which leads to the solution for the plastic multiplier λ:

$$\lambda = \frac{\frac{df}{d\sigma_{ij}} D_{ijkl}^e \dot{\epsilon}_{kl}}{\frac{df}{d\sigma_{pq}} D_{pqrs}^e \frac{\partial g}{\partial \sigma_{rs}}} \tag{7.11}$$

Equation 7.11 is then back-substituted into equation 7.9 to give:

$$\dot{\sigma}_{ij} = D_{ijkl}^e \dot{\epsilon}_{kl} - \frac{\frac{df}{d\sigma_{mn}} D_{mnab}^e \dot{\epsilon}_{ab}}{\frac{df}{d\sigma_{pq}} D_{pqrs}^e \frac{\partial g}{\partial \sigma_{rs}}} D_{ijkl}^e \frac{\partial g}{\partial \sigma_{kl}} \tag{7.12}$$

With some interchanging of the dummy subscripts, this can be rewritten:

$$\dot{\sigma}_{ij} = D_{ijkl}^{ep} \dot{\epsilon}_{kl} \tag{7.13}$$

where D_{ijkl}^{ep} is the elastic-plastic stiffness matrix defined as:

$$D_{ijkl}^{ep} = D_{ijkl}^e - \frac{D_{ijab}^e \frac{\partial g}{\partial \sigma_{ab}} \frac{df}{d\sigma_{mn}} D_{mnkl}^e}{\frac{df}{d\sigma_{pq}} D_{pqrs}^e \frac{\partial g}{\partial \sigma_{rs}}} \tag{7.14}$$

It is important to note that this stiffness matrix is singular, so that it cannot be inverted to give a compliance matrix. This is a feature common to all perfect plasticity models.

To conclude, given the specification of the elastic behaviour, the yield surface, and the plastic potential, the incremental constitutive behaviour can be obtained by applying a purely automatic process to obtain the incremental stress-strain relationship. This is important because no further *ad hoc* assumptions are necessary. Note also that the derivation involves solely matrix manipulation and differentiation. Both processes can be readily carried out using symbolic manipulation packages.

7.3 Plastic hardening and softening

7.3.1 Incremental response for strain hardening

For strain-hardening plasticity, the yield surface is now also a function of the plastic strains, the consistency condition takes the form:

$$\dot{f} = \frac{\partial f}{\partial \sigma_{ij}} \dot{\sigma}_{ij} + \frac{\partial f}{\partial \epsilon_{ij}^p} \dot{\epsilon}_{ij}^p = 0 \tag{7.15}$$

Introducing the flow rule (equation 7.8) in the equation above, one gets:

$$\dot{f} = \frac{\partial f}{\partial \sigma_{ij}} \dot{\sigma}_{ij} + \lambda \frac{\partial f}{\partial \epsilon_{ij}^p} \frac{\partial g}{\partial \sigma_{ij}} = 0 \tag{7.16}$$

It is more convenient in this case to obtain the solution for λ in terms of the stress increment rather than the strain increment (as was used for perfect plasticity):

$$\lambda = -\frac{\frac{\partial f}{\partial \sigma_{ij}} \dot{\sigma}_{ij}}{\frac{\partial f}{\partial \epsilon_{ij}^p} \frac{\partial g}{\partial \sigma_{ij}}} \tag{7.17}$$

The quantity:

$$h = -\frac{\partial f}{\partial \epsilon_{ij}^p} \frac{\partial g}{\partial \sigma_{ij}} \tag{7.18}$$

is often termed the *hardening modulus*, and we can write $\lambda = \frac{1}{h} \frac{\partial f}{\partial \sigma_{ij}} \dot{\sigma}_{ij}$ or $\dot{\epsilon}_{ij}^p = \frac{1}{h} \frac{\partial g}{\partial \sigma_{ij}} \frac{\partial f}{\partial \sigma_{kl}} \dot{\sigma}_{kl}$. The hardening modulus is not a defined parameter of the model, but is derived at a given stress point in terms of the yield function and plastic potential. It is identically zero in a perfect plasticity model. The most convenient way to proceed is to use the elastic compliance matrix:

$$\dot{\epsilon}_{ij}^e = C_{ijkl}^e \dot{\sigma}_{kl} \tag{7.19}$$

so that:

$$\dot{\epsilon}_{ij} = C_{ijkl}^e \dot{\sigma}_{kl} + \dot{\epsilon}_{ij}^p = C_{ijkl}^e \dot{\sigma}_{kl} + \frac{1}{h} \frac{\partial g}{\partial \sigma_{ij}} \frac{\partial f}{\partial \sigma_{kl}} \dot{\sigma}_{kl} \tag{7.20}$$

which leads to:

$$\dot{\epsilon}_{ij} = C_{ijkl}^{ep} \dot{\sigma}_{kl} \tag{7.21}$$

where the elastic-plastic compliance matrix is:

$$C_{ijkl}^{ep} = C_{ijkl}^e + \frac{1}{h} \frac{\partial g}{\partial \sigma_{ij}} \frac{\partial f}{\partial \sigma_{kl}} = C_{ijkl}^e - \frac{\frac{\partial g}{\partial \sigma_{ij}} \frac{\partial f}{\partial \sigma_{kl}}}{\frac{\partial f}{\partial \epsilon_{mn}^p} \frac{\partial g}{\partial \sigma_{mn}}} \tag{7.22}$$

If the stiffness matrix is required, it can be obtained either by numerical inversion of the compliance matrix, or by solving for the plastic multiplier, as before, in terms of the strains. Starting with the consistency condition:

$$\dot{f} = \frac{\partial f}{\partial \sigma_{ij}}\dot{\sigma}_{ij} + \frac{\partial f}{\partial \epsilon^p_{ij}}\dot{\epsilon}^p_{ij} = \frac{\partial f}{\partial \sigma_{ij}}D^e_{ijkl}\left(\dot{\epsilon}_{kl} - \lambda\frac{\partial g}{\partial \sigma_{kl}}\right) + \lambda\frac{\partial f}{\partial \epsilon^p_{ij}}\frac{\partial g}{\partial \sigma_{ij}} = 0 \qquad (7.23)$$

The solution for λ becomes:

$$\lambda = \frac{\frac{\partial f}{\partial \sigma_{ij}}D^e_{ijkl}\dot{\epsilon}_{kl}}{\left(\frac{\partial f}{\partial \sigma_{pq}}D^e_{pqrs} - \frac{\partial f}{\partial \epsilon^p_{rs}}\right)\frac{\partial g}{\partial \sigma_{rs}}} \qquad (7.24)$$

The solution then proceeds exactly as for the perfectly plastic case, except that this time D^e_{ijkl} takes the form:

$$D^{ep}_{ijkl} = D^e_{ijkl} - \frac{D^e_{ijab}\frac{\partial g}{\partial \sigma_{ab}}\frac{\partial f}{\partial \sigma_{mn}}D^e_{mnkl}}{\left(\frac{\partial f}{\partial \sigma_{pq}}D^e_{pqrs} - \frac{\partial f}{\partial \epsilon^p_{rs}}\right)\frac{\partial g}{\partial \sigma_{rs}}} \qquad (7.25)$$

Note that if $\frac{\partial f}{\partial \epsilon^p_{rs}} = 0$, then the equation above reduces to the result for perfect plasticity. However, the equation for compliance, Equation 7.22, becomes singular in the perfectly plastic case.

7.3.2   Isotropic hardening

If the yield surface expands (or contracts) but does not translate as plastic straining occurs, then this is said to be *isotropic hardening* (or softening) [12]. This is illustrated in Figure 7.3.a for a simple one-dimensional material that hardens linearly and isotropically with plastic strain. The material yields at A at a stress c, and during plastic deformation AB, it hardens and the stress increases to c_1. It is then unloaded, and reverse yielding occurs at C when the stress is $-c_1$. Further hardening occurs on CD, so that, when the material is reloaded, the expansion of the yield surface is such that the yield at E occurs above the original curve AB, and further hardening occurs along EF. Figure 7.3.b illustrates isotropic hardening in two dimensions. The surface expands but does not change shape.

   The rule of isotropic hardening assumes that the yield surface maintains its shape, center and orientation, but expands or contracts uniformly about the centre of the yield surface [23]. A yield surface with its centre at the origin may be generally described by the following function:
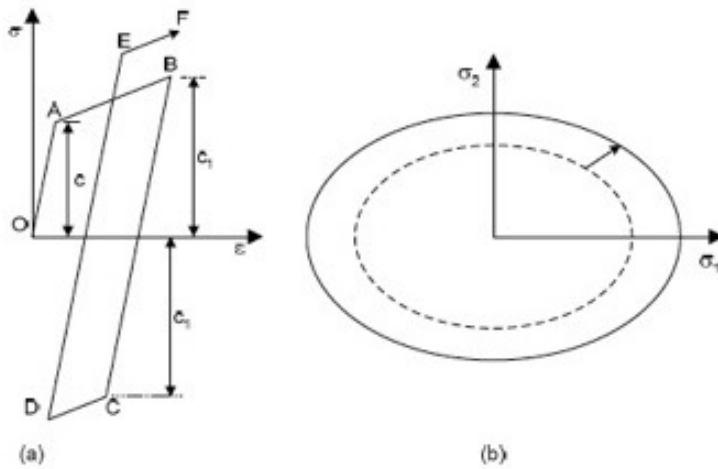
$$f(\sigma_{ij}, \beta) = f_1(\sigma_{ij}) - R(\beta) = 0 \qquad (7.26)$$

where R represents the size of the yield surface, depending on plastic strains through the hardening parameter β. The two earliest and most widely used hardening parameters are the accumulated equivalent plastic strain:

$$\beta = \int\left[\sqrt{\frac{2}{3}}\left(\dot{\epsilon}^p_{ij}\dot{\epsilon}^p_{ij}\right)^{1/2}\right] \qquad (7.27)$$
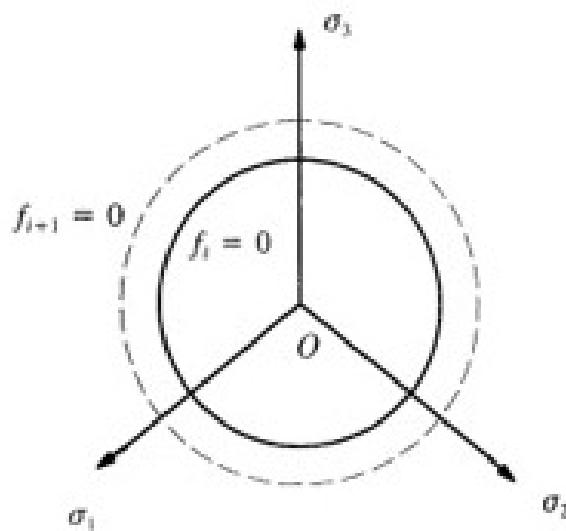
and the plastic work:

$$\beta = \int\left[\sigma_{ij}\dot{\epsilon}^p_{ij}\right] \qquad (7.28)$$

Figure 7.3   Isotropic hardening: (a) stress-strain curve in one dimension; (b) change of size of yield surface in two dimensions. Figure taken from [12].
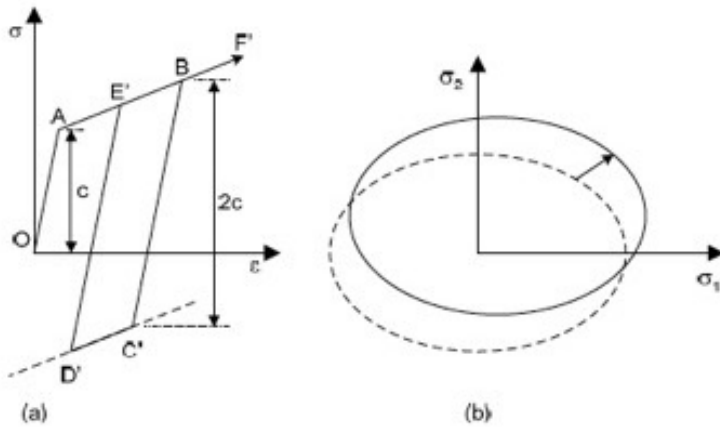
Figure 7.4 shows an example of isotropic hardening where the yield surface is uniformly expanding during the process of plastic flow when a stress increment is applied from step i to i+1. The size of the yield surface at any stage of loading is determined as long as an evolution rule defining the relationship between R and β is defined.


Figure 7.4   Isotropic hardening with uniform expansion of the yield surface. Figure taken from [23].

7.3.3 Kinematic hardening

If the yield surface translates, but does not change size, as plastic strain occurs, then this is said to be kinematic hardening [12]. Figure 7.5.a, which should be contrasted with Figure 7.3.a, shows the response of a simple kinematic hardening material that hardens linearly with plastic strain. The loading curve OAB is identical to that of isotropic hardening, but on unloading from B, yield occurs at C', such that the size of the elastic region is $2c$ (the stress at C' therefore is $c_1 - 2c$). Hardening occurs on reverse loading C'D', but on reloading, yield occurs at E', which falls on the original line AB, and the hardening once again occurs along E'F'. Figure 7.5.b (which should be contrasted with Figure 7.3.b) shows the translation of a yield surface for a kinematic hardening model in two dimensions.


Figure 7.5   Kinetic hardening: (a) stress-strain curve in one dimension; (b) translation of yield surface in two dimensions. Figure taken from [12].

The fact that the yield surface translates in the stress space and its shape and size remain unchanged can be described by writing the initial yield function as [23]:

$$f(\sigma_{ij}, \alpha_{ij}) = f_1(\sigma_{ij} - \alpha_{ij}) - R_0 = 0 \qquad (7.29)$$

where α_{ij} represents the coordinates of the center of the yield surface, which is also known as the back stress. R_0 is a material constant representing the size of the original yield surface. It can be seen that as the back stress α_{ij} changes due to plastic flow, the yield surface translates in the stress space while maintaining its initial shape and size. It is clear now that the formulation of a kinematic hardening model involves assuming an evolution rule of the back stress α_{ij} in terms of ϵ_{ij}^p, σ_{ij} or α_{ij}. The first simple kinematic hardening model was proposed by Prager (1955). This classical model assumes that the yield surface keeps its original shape and size and moves in the direction of plastic strain rate tensor (see Figure 7.6). Mathematically, it can be expressed by the following linear evolution rule:
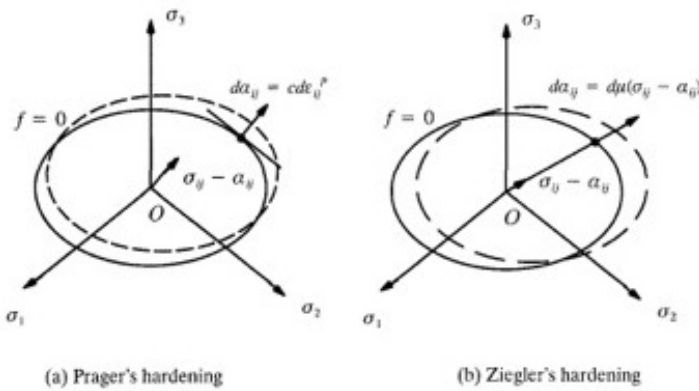
$$\dot{\alpha}_{ij} = c\,\dot{\epsilon}_{ij}^p \qquad (7.30)$$

where c is a material constant. Whilst Prager's model is reasonable for one-dimensional problems, it does not seem to give consistent predictions for two- and three-dimensional cases. The reason is that the yield function takes different forms for one-, two- and three-dimensional cases. To overcome this limitation, Ziegler (1959) suggested that the yield

surface should move in the direction as determined by the vector $\sigma_{ij} - \alpha_{ij}$, see Figure 7.6. Mathematically, Ziegler's model can be expressed as follows:

$$\dot{\alpha}_{ij} = d\mu \left(\sigma_{ij} - \alpha_{ij} \right) \tag{7.31}$$

where $d\mu$ is a material constant.

(a) Prager's hardening   (b) Ziegler's hardening

Figure 7.6   Prager's and Ziegler's kinematic hardening. Figure taken from [23].

7.3.4   Mixed hardening

The term mixed hardening is used to indicate cases when the yield surface not only expands or contracts but also translates in the stress space upon plastic loading (see Figure 7.7). This means that both the centre and size of the yield surface will depend on plastic strain. In this case, the yield function can be expressed by:

$$f(\sigma_{ij}, \alpha_{ij}, \alpha) = f_1(\sigma_{ij} - \alpha_{ij}) - R(\beta) = 0 \tag{7.32}$$
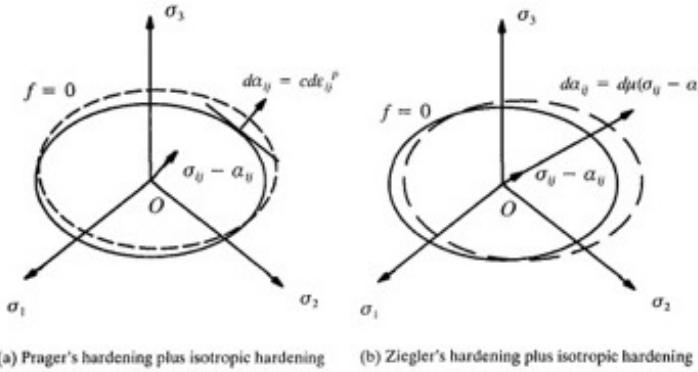
where the size of the yield surface can be assumed to be a function of either plastic strain or plastic work., while either Prager's rule (Equation 7.30) or Ziegler's rule (Equation 7.2) may be used to control the translation of the yield surface upon loading.

7.4   Restrictions on plasticity theories

Two important restrictions on plasticity theories have been applied by many users in the past, and these are discussed below [12]. Both bear a superficial similarity to thermodynamic laws, and both lead to normality relationships, but neither embodies any thermodynamic principles.
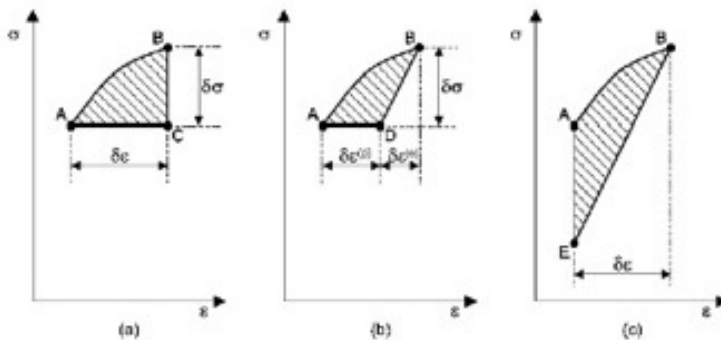
7.4.1   Drucker's Stability Postulate

Drucker (1951) proposed a stability postulate for plastically deforming materials. It can be stated in a variety of equivalent ways, but represents the idea that, if a material is in a given

(a) Prager's hardening plus isotropic hardening   (b) Ziegler's hardening plus isotropic hardening

Figure 7.7   Mixed hardening. Figure taken from [23].

state of stress and some external agency applies additional stresses, then "The work done by the external agency on the displacements it produces must be positive or zero" (Drucker, 1959). If the external agency applies a stress increment $\delta\sigma_{ij}$ that causes additional strains $\delta\epsilon_{ij}$, then the postulate is that $\delta\sigma_{ij}\delta\epsilon_{ij} > 0$ The product $\delta\sigma_{ij}\delta\epsilon_{ij}$ is often called the second order work.

In the one-dimensional case shown in Figure 7.8.a, the postulate states that the area ABC must be positive. Strain-softening behaviour is thus excluded. If the external agency first applies then removes the stress increment $\delta\sigma_{ij}$, such that the additional strain remaining after this stress cycle is $\delta\epsilon_{ij}^p$, then it also follows from the postulate that $\delta\sigma_{ij}\delta\epsilon_{ij}^p \geq 0$. Thus in the one-dimensional case shown in Figure 7.8.b, the area ABD must be zero or positive.

Figure 7.8   One-dimensional illustrations of (a,b) Drucker's postulate and (c) Il'iushin's postulate. Figure taken from [12].

In the one-dimensional case, a strain-softening material is mechanically unstable under stress control, and this is linked to the identification of the Drucker postulate as a "stability postulate". Unfortunately, this has led to the interpretation that a material which does not obey the postulate will exhibit mechanically unstable behavior. The obvious corollary is that a material which is mechanically stable must therefore obey the postulate. The identifi-

cation of the postulate with mechanical stability for the multidimensional case is, however, erroneous. The conclusion that mechanically stable materials must obey Drucker's postulate is therefore equally erroneous

7.4.2 Il'iushin's Postulate of Plasticity

The postulate of plasticity proposed by Il'iushin (1961) is similar to Drucker's postulate, but significantly, it uses a cycle of strain rather than a cycle of stress. It is simply stated as follows. Consider a cycle of strain which, to avoid complications from thermal strains, takes place at constant temperature. It is assumed that the material is in equilibrium throughout, and that the strain (for a sufficiently small region under consideration) is homogeneous. The material is said to be plastic if, during the cycle, the total work done is positive, and is said to be elastic if the work done is zero. The postulate excludes the possibility that the work done might be negative. This is illustrated for the one-dimensional case in Figure 7.8.c, where the postulate states that the area ABE must be non-negative.

The postulate has certain advantages over Drucker's statement because it uses a strain cycle. Drucker's statement depends on consideration of a cycle of stress, which is not attainable in certain cases such as strain softening. On the other hand, almost all materials can always be subjected to a strain cycle. The exceptions are rather unusual materials which exhibit "locking" behavior (in the one-dimensional case this involves a response in which an increase in stress results in a decrease in strain). Such materials rather odd and conceptual. A more significant limitation is Il'iushin's assumption that the strain is homogeneous. It may well be that for some cases (e. g. strain-softening behavior), homogeneous strain is not possible, and bifurcation must occur.

PROBLEMS

7.1   Derive the stress-strain relationship for the Drucker-Prager elastic-perfectly plastic model, described by the following equations:

$$\dot{\epsilon}_{ij} = \dot{\epsilon}_{ij}^e + \dot{\epsilon}_{ij}^p$$

$$\dot{\sigma}_{ij} = D_{ijkl}^e \dot{\epsilon}_{kl}^e$$

$$f(\sigma_{ij}) = \sqrt{J_2} - \alpha I_1 - k$$

$$g(\sigma_{ij}) = \sqrt{J_2} - \beta I_1$$

in which k, α and β are material constants, with $\alpha \neq \beta$.

7.2   Derive the stress-strain relationship for the mixed hardening elastic-plastic model, described by the following equations:

$$\dot{\epsilon}_{ij} = \dot{\epsilon}_{ij}^e + \dot{\epsilon}_{ij}^p$$

$$\dot{\sigma}_{ij} = D_{ijkl}^e \dot{\epsilon}_{kl}^e$$

$$f(\sigma_{ij}, \alpha_{ij}, \beta) = f_1(\sigma_{ij} - \alpha_{ij}) - R(\beta) = 0$$

$$\beta = \int \left[\sigma_{ij} \dot{\epsilon}_{ij}^p \right]$$

$$\dot{\alpha}_{ij} = d\mu \ (\sigma_{ij} - \alpha_{ij})$$

$$g(\sigma_{ij}, \alpha_{ij}, \beta) = f(\sigma_{ij}, \alpha_{ij}, \beta)$$

CHAPTER 8

PERFECT PLASTICITY IN GEOMECHANICS

8.1 Cohesive soils - Associated flow rule

For cohesive soils [23], the two most widely used plasticity models are those proposed by Tresca (1864) and von Mises (1913) initially for metals. Experience suggests that under undrained conditions, fully saturated cohesive soils (i.e. clay) can be modelled accurately by either Tresca or von Mises plasticity theory.

8.1.1 Tresca model

Tresca's yield criterion is:
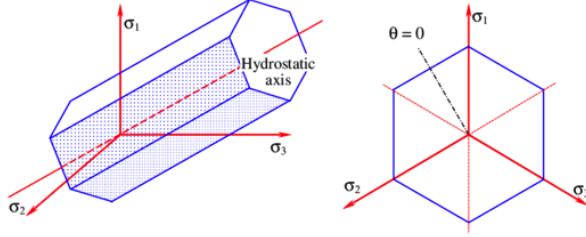
$$f = \sigma_1 - \sigma_3 - 2S_u = 0 \tag{8.1}$$

where the princpal stresses are ordered such that $\sigma_1 \geq \sigma_2 \geq \sigma_3$ and S_u is the undrained shear strength. From a computational point of view, it is more useful to write the above equation in terms of the second invariant of deviatoric stress J_2 and Lode's angle θ_l, as follows:

$$f = \sqrt{J_2}cos\theta_l - S_u = 0 \tag{8.2}$$

As shown in Figure 8.1, The Tresca yield surface is a regular hexagon on a deviatoric plane, and a cylinder with an hexagonal base in the three-dimensional stress space.

When a saturated clay is loaded under undrained conditions, the volume remains constant. As a result it is suitable to adopt an associated plastic flow rule by treating the yield

Figure 8.1 Tresca yield surface in the three-dimensional stress space . Taken from *Taiebat and Carter, 2008, Flow rule effects in the Tresca model.*

function (Equation 8.2) as the plastic potential as well. Therefore:

$$g = \sqrt{J_2}cos\theta_l - S_u = 0 \tag{8.3}$$

The complete relation between a stress rate and a strain rate for an elastic-perfectly plastic solid may be expressed as follows:

$$\dot{\sigma}_{ij} = D^{ep}_{ijkl}\dot{\epsilon}_{kl} \tag{8.4}$$

where the elastic-plastic stiffness matrix D^{ep}_{ijkl} is defined by:

$$D^{ep}_{ijkl} = D^e_{ijkl} - \frac{1}{H}D^e_{ijmn}\frac{\partial g}{\partial \sigma_{mn}}\frac{\partial f}{\partial \sigma_{pq}}D^e_{pqkl} \tag{8.5}$$

in which:

$$H = \frac{\partial f}{\partial \sigma_{ij}}D^e_{ijkl}\frac{\partial g}{\partial \sigma_{kl}} \tag{8.6}$$

To determine the complete stress-strain relation for Tresca materials, we need to determine $\partial f/\partial\sigma_{ij}$ and $\partial g/\partial\sigma_{ij}$, which can be obtained using the chain rule:

$$\frac{\partial f}{\partial \sigma_{ij}} = \frac{\partial f}{\partial J_2}\frac{\partial J_2}{\partial \sigma_{ij}} + \frac{\partial f}{\partial \theta_l}\frac{\partial \theta_l}{\partial \sigma_{ij}} = \frac{cos\theta_l}{2\sqrt{J_2}}\frac{\partial J_2}{\partial \sigma_{ij}} - \sqrt{J_2}sin\theta_l\frac{\partial \theta_l}{\partial \sigma_{ij}} \tag{8.7}$$

$$\frac{\partial g}{\partial \sigma_{ij}} = \frac{\partial g}{\partial J_2}\frac{\partial J_2}{\partial \sigma_{ij}} + \frac{\partial g}{\partial \theta_l}\frac{\partial \theta_l}{\partial \sigma_{ij}} = \frac{cos\theta_l}{2\sqrt{J_2}}\frac{\partial J_2}{\partial \sigma_{ij}} - \sqrt{J_2}sin\theta_l\frac{\partial \theta_l}{\partial \sigma_{ij}} \tag{8.8}$$

where $\partial J_2/\partial\sigma_{ij}$ and $\partial\theta_l/\partial\sigma_{ij}$ are independent of the form of yield functions and plastic potentials as they only depend on the definitions of the second invariant of deviatoric stress and Lode's angle. It is noted from Figure 8.1 that Tresca's yield function and plastic potential are not differentiable at certain corner points.

8.1.2 von Mises model
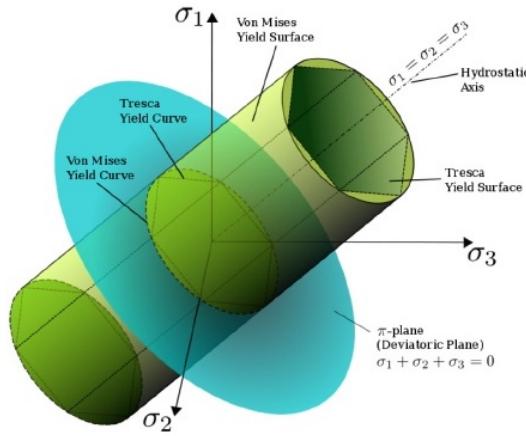
A slightly better alternative to the Tresca yield criterion is the criterion proposed by von Mises (1913). von Mises suggested that yielding occurred when the second invariant of deviatoric stress reached a critical value, von Mises' yield criterion is expressed as follows:

$$f = \sqrt{J_2} - k = 0 \tag{8.9}$$

or:

$$f = (\sigma_1 - \sigma_2)^2 + (\sigma_2 - \sigma_3)^2 + (\sigma_3 - \sigma_1)^2 - 6k^2 = 0 \tag{8.10}$$

where k is the undrained shear strength of the soil in pure shear. As shown in Figure 8.2, the von Mises yield surface is a circle on a deviatoric plane and a cylinder of circular base in the three-dimensional stress space. Like the Tresca yield surface, the von Mises yield criterion does not depend on the mean stress. A physical interpretation of the von Mises yield criterion was that Equation 8.9 implies that yielding begins when the elastic energy of distortion reaches a critical value (Hill, 1950).


Figure 8.2   von Mises and Tresca yield surfaces in the three-dimensional stress space . Taken from *Wikipedia, Dec. 2019*.

By suitably choosing the value of the strength parameter k in Equation 8.9, we can make the von Mises circle pass through the corners of the Tresca hexagon, as shown in Figure 8.2, which happens when:

$$k = \frac{S_u}{cos\theta_l} = \frac{2}{\sqrt{3}}S_u \tag{8.11}$$

By comparing Tresca's and von Mises' yield criteria, it is obvious that the von Mises yield criterion generally implies a slightly higher undrained shear strength. The difference depends on Lode's angle that indicates the direction of shear stress. For undrained loading, the plastic volumetric strain is zero so that an associated flow rule is adequate, namely:

$$g = \sqrt{J_2} - k = 0 \tag{8.12}$$

which, together with Equation 8.9, leads to:

$$\frac{\partial f}{\partial \sigma_{ij}} = \frac{\partial f}{\partial J_2}\frac{\partial J_2}{\partial \sigma_{ij}} = \frac{1}{2\sqrt{J_2}}\frac{\partial J_2}{\partial \sigma_{ij}} \tag{8.13}$$

$$\frac{\partial g}{\partial \sigma_{ij}} = \frac{\partial g}{\partial J_2}\frac{\partial J_2}{\partial \sigma_{ij}} = \frac{1}{2\sqrt{J_2}}\frac{\partial J_2}{\partial \sigma_{ij}} \tag{8.14}$$

8.2   Frictional soils - Non-associated flow rule

For cohesive-frictional soil and rock [23], neither Tresca's nor von Mises' yield criterion is adequate. This is because the key feature of yielding of frictional materials is their mean pressure dependence. In other words, a correct yield criterion for any frictional material would be a function of the first stress invariant or mean pressure. In this respect, the oldest and still the most useful yield criterion for cohesive frictional materials is the empirical proposal made by Coulomb (1773) in his investigations of retaining walls.

8.2.1   Mohr-Coulomb model

The yield criterion proposed by Coulomb (1773) is in terms of shear stress τ and normal stress σ_n acting on a plane. It suggests that the yielding begins as long as the shear stress and the normal stress satisfy the following equation:

$$|\tau| = c + \sigma_n \, tan\phi \tag{8.15}$$

where c and ϕ are the cohesion and internal angle of friction for the soil. In terms of the principal stresses, Coulomb's yield criterion can be expressed by:

$$f = \sigma_1 - \sigma_3 - (\sigma_1 + \sigma_3)sin\phi - 2c\,cos\phi = 0 \tag{8.16}$$

for $\sigma_1 \geq \sigma_2 \geq \sigma_3$. In terms of the stress invariants and Lode's angle, the Mohr-Coulomb yield criterion in Equation 8.16 can be written as:

$$f = \sqrt{J_2} - \frac{m(\theta_l, \phi) \, sin\phi}{3} I_1 - m(\theta_l, \phi) \, c\,cos\phi = 0 \tag{8.17}$$

where

$$m(\theta_l, \phi) = \frac{\sqrt{3}}{\left(\sqrt{3}cos\theta_l + sin\theta_l \, sin\phi\right)} \tag{8.18}$$

Alternatively, Equation 8.17 can also be expressed in terms of the generalised shear stress q and the mean stress p as follows:

$$f = q - \sqrt{3}\,p\,m(\theta_l, \phi) \, sin\phi - \sqrt{3}\,m(\theta_l, \phi) \, c\,cos\phi = 0 \tag{8.19}$$

by noting $q = \sqrt{3J_2}$ and $p = I_1/3$. The shape of the Coulomb's yield surface is similar to that of Tresca in a deviatoric plane. However, the Coulomb's yeild surface forms a cone instead of a cylinder in the three dimensional stress space, as shown in Figure 8.3.

   With the Mohr-Coulomb model, it is often assumed that the plastic potential takes the same form as the yield function (Equation 8.15):
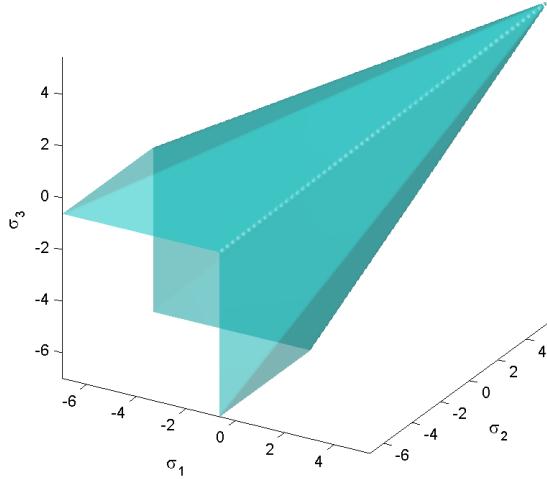
$$g = |\tau| - c - \beta\sigma_n \tag{8.20}$$

Clearly, if $\beta = tan\phi$, then the yield surface and plastic potential are identical and the flow rule becomes associated. In this case, the increment of normal plastic strain is calculated as:

$$\dot{\epsilon}_n^p = \lambda \frac{\partial g}{\partial \sigma_n} = -\lambda \, tan\phi \tag{8.21}$$

and the increment of shear plastic strain is:

$$\dot{\gamma}^p = \lambda \frac{\partial g}{\partial \tau} = sign(\tau)\,\lambda \tag{8.22}$$

Figure 8.3   Coulomb yield surface in the three-dimensional stress space . Taken from *Wikipedia, Dec. 2019.*

The rate of plastic work is then determined as:

$$\dot{W}^p = \sigma_n \dot{\epsilon}_n^p + \tau \dot{\gamma}^p = -\lambda \, \sigma_n \, tan\phi + \lambda |\tau| \tag{8.23}$$

For a perfectly frictional material, $c = 0$ and therefore, from Equation 8.15, $|\tau| - tan\phi\sigma_n = 0$. It follows that for a purely frictional material, $\dot{W}^p = 0$. Thus a "frictional" material with associated flow is not frictional at all. It dissipates no work plastically!

Now consider plastic strains in more detail. It is simple to show from the flow rule that $\dot{\epsilon}_n^p / \dot{\gamma}^p = \beta \, sign(\tau)$. Since λ is a positive multiplier, it also follows that τ and $\dot{\gamma}^p$ have the same sign, so that we can write $\dot{\epsilon}_n^p / \dot{\gamma}^p = \beta \, sign \, (\dot{\gamma}^p)$ or $\dot{\epsilon}_n^p = \beta \, |\dot{\gamma}^p|$. For a positive value of β, the volumetric plastic strain is always positive and the material *dilates*. The apparent frictional strength in an associated material is entirely due to this dilation. More realistically, $\beta < tan\phi$ and $\dot{W}^p = -\lambda \, \sigma_n \, (tan\phi - \beta)$, which is positive because the normal stress is compressive for the material to be frictional: $\sigma_n < 0$. So plastic work if dissipated if $\beta < tan\phi$. For $\beta = 0$, $\dot{\epsilon}_n^p = 0$, and the material deforms at constant volume. The yield surface and flow vectors for the general case are shown in Figure 8.4.

It is often assumed that the plastic potential takes the same form as the yield function but the friction angle is replaced by the dilation angle ψ (which is a smaller angle than the friction angle). Therefore:

$$g = |\tau| - c - \sigma_n \, tan\psi \tag{8.24}$$
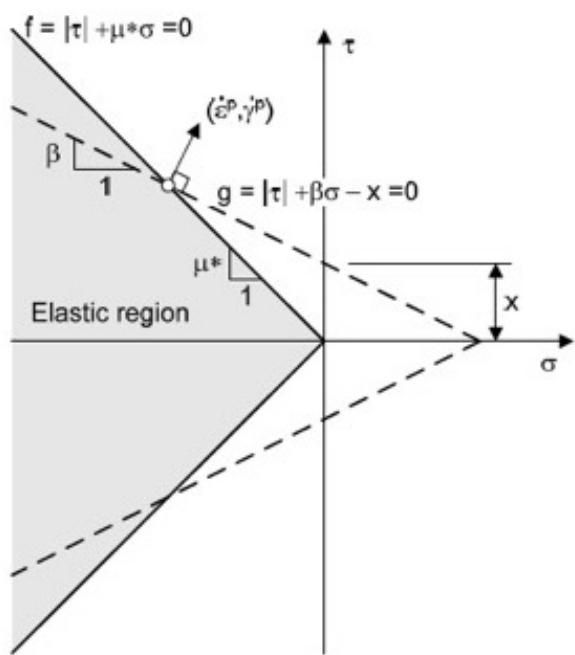
or equivalently:

$$g = \sqrt{J_2} - \frac{m \, (\theta_l, \psi) \, sin\psi}{3} I_1 - m \, (\theta_l, \psi) \, c \, cos\psi = 0 \tag{8.25}$$

where:

$$m(\theta_l, \psi) = \frac{\sqrt{3}}{\left(\sqrt{3}cos\theta_l + sin\theta_l \, sin\psi \right)} \tag{8.26}$$

To link the plastic potential and the yield function, a stress-dilatancy equation must be used which defines the relationship between the angles of friction and dilation. Perhaps

Figure 8.4 Coulomb frictional yield surface and non associated flow rule $(c = 0)$. Taken from [12].

the most successful stress-dilatancy model is that developed by Rowe (1962), which has been further simpHfied by Bolton (1986) as follows:

$$\psi = 1.25 \left(\phi - \phi_{cv} \right) \tag{8.27}$$

where ϕ_{cv} is the angle of friction at the critical state. The above assumption implies a non-associated flow rule as the angles of friction and dilation are not the same.

The differentiation of the yield function and plastic potential with respect to stress can be evaluated by the chain rule:

$$\frac{\partial f}{\partial \sigma_{ij}} = \frac{\partial f}{\partial I_1} \frac{\partial I_1}{\partial \sigma_{ij}} + \frac{\partial f}{\partial J_2} \frac{\partial J_2}{\partial \sigma_{ij}} + \frac{\partial f}{\partial \theta_l} \frac{\partial \theta_l}{\partial \sigma_{ij}} \tag{8.28}$$

$$\frac{\partial g}{\partial \sigma_{ij}} = \frac{\partial g}{\partial I_1} \frac{\partial I_1}{\partial \sigma_{ij}} + \frac{\partial g}{\partial J_2} \frac{\partial J_2}{\partial \sigma_{ij}} + \frac{\partial g}{\partial \theta_l} \frac{\partial \theta_l}{\partial \sigma_{ij}} \tag{8.29}$$

8.2.2 Drucker-Prager model

The von Mises yield criterion is not suitable for modelling the yielding of frictional material as it does not include the effect of mean stress as observed in experiments. To overcome this limitation of the von Mises yield function, Drucker and Prager (1952) proposed the following revised function for frictional soils:

$$f = \sqrt{J_2} - \alpha \, I_1 - k = 0 \tag{8.30}$$

where α and k are material constants. On a deviatoric plane, the equation plots as a circle, as for the von Mises yield surface. However in the three-dimensional principal stress space, the Drucker-Prager yield surface is a cone whilst the von Mises yield surface is an infinitely long cylinder. Figure 8.5 shows the shapes of all the yield surfaces covered so far (Tresca, von Mises, Mohr-Coulomb and Drucker-Prager).

To select the material constants a and k for use in analysis, the Drucker-Prager yield surface is often matched with the Mohr-Coulomb yield surface using a certain criterion. Figure 8.5.F shows such a match (the match is different for major and minor vertices). Mathematically, this condition demands the following relations:

$$\alpha = \frac{2 \, sin\phi}{\sqrt{3} \left(3 - sin\phi \right)} \tag{8.31}$$
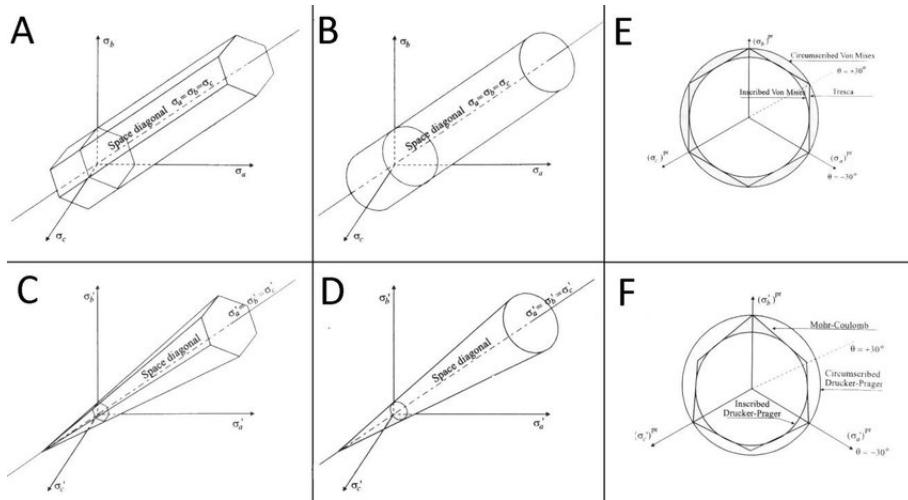
$$k = \frac{6c \, cos\phi}{\sqrt{3} \left(3 - sin\phi \right)} \tag{8.32}$$

As another example, if the Drucker-Prager and Mohr-Coulomb criteria are made to give an identical limit load for a plane strain problem, then the following relationships must hold [23]:

$$\alpha = \frac{tan\phi}{\sqrt{9 + 12tan^2\phi}} \tag{8.33}$$

$$k = \frac{3c}{\sqrt{9 + 12tan^2\phi}} \tag{8.34}$$

Because of its simplicity, the Druclcer-Prager yield criterion has been used quite widely in geotechnical analysis. However experimental research suggests that its circular shape on a

Figure 8.5 Yield surfaces in 3D stress space. A. Tresca yield surface, B. von Mises yield surface, C. Mohr Coulomb yield surface, D. Drucker-Prager yield surface, E. comparison between Tresca and von Mises surfaces in a diaviatoric plane (a plane normal to the space diagonal), and F. comparison between Mohr Coulomb and Drucker-Prager surfaces in a deviatoric plane. Taken from [8].

deivatoric plane does not agree well with experimental data. For this reason care is needed when the Drucker-Prager plasticity model is used in geotechnical analysis.

To complete the formulation of the Drucker-Prager plasticity model, we need to define a plastic potential. As for the case of the Mohr-Coulomb plasticity model, we may adopt a plastic potential that is in the same form as the yield function, namely:

$$g = \sqrt{J_2} - \alpha' I_1 = \text{constant} \tag{8.35}$$

where the angle of friction needed to be replaced by the angle of dilation, and

$$\alpha' = \frac{2sin\psi}{\sqrt{3}\,(3 - sin\psi)} \tag{8.36}$$

in which ψ denotes the angle of dilation.

The differentiation of the yield function and plastic potential with respect to stress can be evaluated by the chain rule:

$$\frac{\partial f}{\partial \sigma_{ij}} = \frac{\partial f}{\partial I_1}\frac{\partial I_1}{\partial \sigma_{ij}} + \frac{\partial f}{\partial J_2}\frac{\partial J_2}{\partial \sigma_{ij}} = -\alpha\frac{\partial I_1}{\partial \sigma_{ij}} + \frac{1}{2\sqrt{J_2}}\frac{\partial J_2}{\partial \sigma_{ij}} \tag{8.37}$$

$$\frac{\partial g}{\partial \sigma_{ij}} = \frac{\partial g}{\partial I_1}\frac{\partial I_1}{\partial \sigma_{ij}} + \frac{\partial g}{\partial J_2}\frac{\partial J_2}{\partial \sigma_{ij}} = -\alpha'\frac{\partial I_1}{\partial \sigma_{ij}} + \frac{1}{2\sqrt{J_2}}\frac{\partial J_2}{\partial \sigma_{ij}} \tag{8.38}$$

8.2.3 Hoek-Brown model

In addition to the linear Mohr-Coulomb yield criterion, a number of researchers have also used non-linear yield criteria to analyse rock mechanics problems. A most popular development has been the empirical non-linear criterion proposed by Hoek and Brown (1980) to

describe the yield and failure behaviour of rock masses [23]. The yield of rock is assumed to be governed by the Hoek and Brown criterion in the following form:

$$f = \sigma_1 - \sigma_3 - \sqrt{m\,Y\,\sigma_3 + s\,Y^2} = 0 \qquad (8.39)$$

where σ_1 and σ_3 are the major and minor principal stresses; Y the uniaxial compressive strength of the intact rock material; and mands are constants depending on the nature of the rock mass and the extent to which it is broken prior to being subjected to the principal stresses σ_1 and σ_3. The Hoek-Brown criterion offers some advantages over other approaches in determining the overall strength of in-situ rock masses because it is based on one simple material property, Y, and rock mass quality data that may be systematically collected and evaluated during site investigation.

For the convenience of numerical applications, the Hoek-Brown criterion may also be expressed in terms of stress invariants by the following equation:
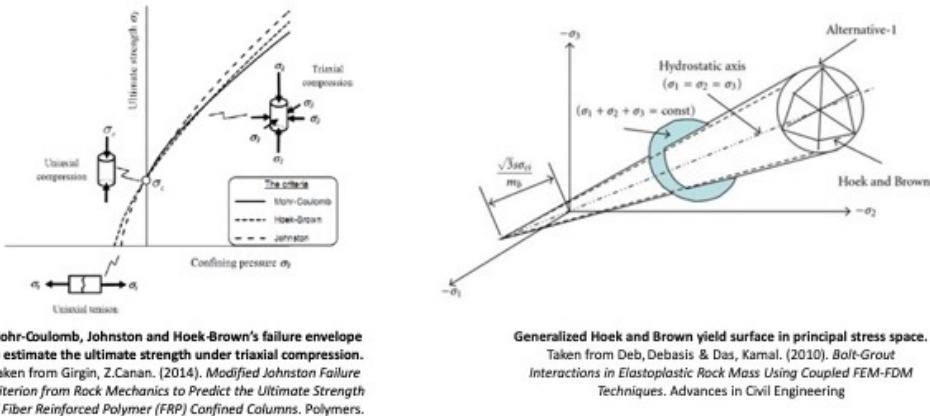
$$f = 4\,J_2\,cos^2\theta_l + g(\theta_l)\sqrt{J_2} - \alpha\,I_1 - k = 0 \qquad (8.40)$$

where:

$$g(\theta_l) = m\,Y\left(cos\theta_l + \frac{sin\theta_l}{\sqrt{3}}\right) \qquad (8.41)$$

$$k = s\,Y^2 \qquad (8.42)$$

Figure 8.6 illustrates the shape of the Hoek and Brown yield surface in 2D and in 3D.

Mohr-Coulomb, Johnston and Hoek-Brown's failure envelope to estimate the ultimate strength under triaxial compression. Taken from Girgin, Z.Canan. (2014). *Modified Johnston Failure Criterion from Rock Mechanics to Predict the Ultimate Strength of Fiber Reinforced Polymer (FRP) Confined Columns. Polymers.*

Generalized Hoek and Brown yield surface in principal stress space. Taken from Deb, Debasis & Das, Kamal. (2010). *Bolt-Grout Interactions in Elastoplastic Rock Mass Using Coupled FEM-FDM Techniques. Advances in Civil Engineering*

Figure 8.6   Hoek and Brown yield surface in 2D and in 3D.

The non-associated flow rule can be obtained by adopting a simplified Hoek-Brown criterion as the plastic potential [23]:

$$g = 3J_2 + \frac{\sqrt{3}m'\,Y}{2}\sqrt{J_2} - \frac{m'\,Y}{3}I_1 = 0 \qquad (8.43)$$

where m' is a reduced Hoek-Brown parameter m. Since the plastic potential is not a function of Lode's angle, it plots as a circle on a deviatoric plane.

The differentiation of the yield function and plastic potential with respect to stress can be evaluated by the chain rule:

$$\frac{\partial f}{\partial \sigma_{ij}} = \frac{\partial f}{\partial I_1}\frac{\partial I_1}{\partial \sigma_{ij}} + \frac{\partial f}{\partial J_2}\frac{\partial J_2}{\partial \sigma_{ij}} + \frac{\partial f}{\partial \theta_l}\frac{\partial \theta_l}{\partial \sigma_{ij}} \tag{8.44}$$

$$\frac{\partial g}{\partial \sigma_{ij}} = \frac{\partial g}{\partial I_1}\frac{\partial I_1}{\partial \sigma_{ij}} + \frac{\partial g}{\partial J_2}\frac{\partial J_2}{\partial \sigma_{ij}} \tag{8.45}$$

PROBLEMS

8.1   A material element is subjected to proportional loading. The principal stresses are given by $(2\sigma, \sigma, 0)$ where σ is an increasing stress value.

1. Find the magnitude of σ where the material begins to yield, according to Tresca's criterion.

2. Adopting the associated flow rule, find also the plastic strain rate $\dot{\epsilon}^p_{ij}$ at onset of yielding expressed in terms of the plastic multiplier $\dot{\lambda}$.

3. If the effective plastic strain rate $\dot{\epsilon}^p_{eff}$ is defined as:

$$\dot{\epsilon}^p_{eff} = \sqrt{\frac{2}{3}\dot{\epsilon}^p_{ij}\dot{\epsilon}^p_{ij}},$$

   how is $\dot{\epsilon}^p_{eff}$ related to $\dot{\lambda}$?

4. Now suppose that the principal stresses are given by $(\sigma, \sigma, 0)$. What problem is encountered is you should determine $\dot{\epsilon}^p_{ij}$?

8.2   The stress at a point is given by:

$$[\sigma_{ij}] = \begin{bmatrix} 30 & 45 & 60 \\ 45 & 20 & 50 \\ 60 & 50 & 10 \end{bmatrix} \text{ MPa}$$

Determine the stress invariants I_1, J_2, J_3 and the Lode angle θ.

8.3   A material is to be loaded to a stress state

$$[\sigma_{ij}] = \begin{bmatrix} 50 & -30 & 0 \\ -30 & 90 & 0 \\ 0 & 0 & 0 \end{bmatrix} \text{ MPa}$$

What should be the minimum uniaxial yield stress of the material so that it does not fail, according to (a) Tresca criterion; (b) von Mises criterion? What do the theories predit when the yield stress of the material is 80MPa?

8.4   A material element is subjected to proportional loading. The principal stresses are given by $(2\sigma, \sigma, 0)$ where σ is an increasing stress value.

1. Find the magnitude of σ where the material begins to yield, according to von Mises's criterion.

2. Adopting the associated flow rule, find also the plastic strain rate $\dot{\epsilon}^p_{ij}$ at onset of yielding expressed in terms of the plastic multiplier $\dot{\lambda}$.

3. If the effective plastic strain rate $\dot{\epsilon}^p_{eff}$ is defined as:

$$\dot{\epsilon}^p_{eff} = \sqrt{\frac{2}{3}\dot{\epsilon}^p_{ij}\dot{\epsilon}^p_{ij}},$$

   how is $\dot{\epsilon}^p_{eff}$ related to $\dot{\lambda}$?

4. Repeat the three questions above when the principal stresses are given by $(\sigma, \sigma, 0)$.

8.5 Prandtl-Reuss equations are obtained by combining Hooke's law with a flow rule that assumes that the plastic strain increments are proportional to the principal deviatoric stresses s_i:

$$\frac{\dot{\epsilon}^p_1}{s_1} = \frac{\dot{\epsilon}^p_2}{s_2} = \frac{\dot{\epsilon}^p_3}{s_3} = \dot{\lambda} \geq 0$$

In Cartesian coordinates, it is common to express the flow rule above in the following alternate form:

$$\frac{\dot{\epsilon}^p_{xx} - \dot{\epsilon}^p_{yy}}{s_{xx} - s_{yy}} = \frac{\dot{\epsilon}^p_{xx} - \dot{\epsilon}^p_{yy}}{\sigma_{xx} - \sigma_{yy}} = \frac{\dot{\epsilon}^p_{yy} - \dot{\epsilon}^p_{zz}}{s_{yy} - s_{zz}} = ... = \dot{\lambda} \geq 0$$

In terms of actual stresses, one can show that:

$$\dot{\epsilon}^p_{xx} = \frac{2}{3}\dot{\lambda}\left[\sigma_{xx} - \frac{1}{2}\left(\sigma_{yy} + \sigma_{zz}\right)\right], \quad \dot{\epsilon}^p_{yy} = \frac{2}{3}\dot{\lambda}\left[\sigma_{yy} - \frac{1}{2}\left(\sigma_{zz} + \sigma_{xx}\right)\right]$$

$$\dot{\epsilon}^p_{zz} = \frac{2}{3}\dot{\lambda}\left[\sigma_{zz} - \frac{1}{2}\left(\sigma_{xx} + \sigma_{yy}\right)\right], \quad \dot{\epsilon}^p_{xy} = \dot{\lambda}\sigma_{xy}, \quad \dot{\epsilon}^p_{yz} = \dot{\lambda}\sigma_{yz}, \quad \dot{\epsilon}^p_{zx} = \dot{\lambda}\sigma_{zx}$$

The Prandtl-Reuss equations are the full elastic-plastic stress-strain relations that are obtained by combining the previous equations with Hooke's law:

$$\dot{\epsilon}_{xx} = \frac{1}{E}\left[\dot{\sigma}_{xx} - \nu\left(\dot{\sigma}_{yy} + \dot{\sigma}_{zz}\right)\right] + \frac{2}{3}\dot{\lambda}\left[\sigma_{xx} - \frac{1}{2}\left(\sigma_{yy} + \sigma_{zz}\right)\right]$$

$$\dot{\epsilon}_{yy} = \frac{1}{E}\left[\dot{\sigma}_{yy} - \nu\left(\dot{\sigma}_{zz} + \dot{\sigma}_{xx}\right)\right] + \frac{2}{3}\dot{\lambda}\left[\sigma_{yy} - \frac{1}{2}\left(\sigma_{zz} + \sigma_{xx}\right)\right]$$

$$\dot{\epsilon}_{zz} = \frac{1}{E}\left[\dot{\sigma}_{zz} - \nu\left(\dot{\sigma}_{xx} + \dot{\sigma}_{yy}\right)\right] + \frac{2}{3}\dot{\lambda}\left[\sigma_{zz} - \frac{1}{2}\left(\sigma_{xx} + \sigma_{yy}\right)\right]$$

$$\dot{\epsilon}_{xy} = \frac{1+\nu}{E}\dot{\sigma}_{xy} + \dot{\lambda}\sigma_{xy}, \quad \dot{\epsilon}_{yz} = \frac{1+\nu}{E}\dot{\sigma}_{yz} + \dot{\lambda}\sigma_{yz}, \quad \dot{\epsilon}_{zx} = \frac{1+\nu}{E}\dot{\sigma}_{zx} + \dot{\lambda}\sigma_{zx}$$

$$\dot{\epsilon}_{ij} = \frac{1+\nu}{E}\dot{\sigma}_{ij} - \frac{\nu}{E}\delta_{ij}\dot{\sigma}_{kk} + \dot{\lambda}s_{ij}$$

Consider the uniaxial straining of a perfectly plastic isotropic von Mises material specimen. There is only one non-zero strain, ϵ_{xx}. One only need consider two stresses, σ_{xx}, σ_{yy}, since $\sigma_{zz} = \sigma_{yy}$ by isotropy.

1. Write down the two relevant Prandtl-Reuss equations.

2. Evaluate the stresses and strains at first yield.

3. For plastic flow, show that $\dot{\sigma}_{xx} = \dot{\sigma}_{yy}$ and that:

$$\frac{\dot{\sigma}_{xx}}{\dot{\epsilon}_{xx}} = \frac{E}{3(1 - 2\nu)}$$

8.6   Mohr-Coulomb's yield criterion:

1. Show that the magnitude of the hydrostatic stress vector is $\rho = \sqrt{3}c\cot\Phi$ for the Mohr-Coulomb yield criterion when the deviatoric stress is zero.

2. Show that, for a Mohr-Coulomb material, $\sin\Phi = (r-1)/(r+1)$ where $r = f_{Yc}/f_{Yt}$ is the compressive to tensile strength ratio.

3. A sample of concrete is subjected to a stress $\sigma_{11} = \sigma_{22} = -p$, $\sigma_{33} = -Ap$ where the constant $A > 1$. Using the Mohr-Coulomb criterion and the result of the previous question, show that the material will not fail provided $A < f_{Yc}/p + r$.

8.7   A material element is subjected to proportional loading. The principal stresses are given by $(2\sigma, \sigma, 0)$ where σ is an increasing stress value.

1. Find the magnitude of σ where the material begins to yield, according to Mohr-Coulomb's criterion.

2. Adopting the associated flow rule, find also the plastic strain rate $\dot{\epsilon}^p_{ij}$ at onset of yielding expressed in terms of the plastic multiplier $\dot{\lambda}$.

3. If the effective plastic strain rate $\dot{\epsilon}^p_{eff}$ is defined as:

$$\dot{\epsilon}^p_{eff} = \sqrt{\frac{2}{3}\dot{\epsilon}^p_{ij}\dot{\epsilon}^p_{ij}},$$

   how is $\dot{\epsilon}^p_{eff}$ related to $\dot{\lambda}$?

4. Now suppose that the principal stresses are given by $(\sigma, \sigma, 0)$. What problem is encountered is you should determine $\dot{\epsilon}^p_{ij}$?

8.8   Durcker-Prager's yield criterion:

1. Show that the magnitude of the hydrostatic stress vector is $\rho = |\rho| = k/\sqrt{3}\alpha$ for the Drucker-Prager yield criterion when the deviatoric stress is zero.

2. Given the yield stresses σ_t and σ_c in uniaxial tension and compression, respectively, find the yield stress in shear resulting from the following yield criteria: (a) Tresca; (b) von Mises; (c) Mohr-Coulomb; (d) Drucker-Prager.

8.9   A material element is subjected to proportional loading. The principal stresses are given by $(2\sigma, \sigma, 0)$ where σ is an increasing stress value.

1. Find the magnitude of σ where the material begins to yield, according to Drucker-Prager's criterion.

2. Adopting the associated flow rule, find also the plastic strain rate $\dot{\epsilon}_{ij}^p$ at onset of yielding expressed in terms of the plastic multiplier $\dot{\lambda}$.

3. If the effective plastic strain rate $\dot{\epsilon}_{eff}^p$ is defined as:

$$\dot{\epsilon}_{eff}^p = \sqrt{\frac{2}{3}\dot{\epsilon}_{ij}^p \dot{\epsilon}_{ij}^p},$$

how is $\dot{\epsilon}_{eff}^p$ related to $\dot{\lambda}$?

4. Repeat the three questions above when the principal stresses are given by $(\sigma, \sigma, 0)$.

8.10   Conventional triaxial compression tests $(\sigma_1, \sigma_2 = \sigma_3)$ were conducted on cylindrical rock specimens. The test results are reported in the following table.

σ_1 (MPa)	$\sigma_2 = \sigma_3$ (MPa)
48.3	1.7
53.7	2.8
56.7	3.4
70.8	6.9
70.9	6.9
94.8	13.8
94.7	13.8
94.9	13.8
115.8	20.7
115.9	20.7

Direct tension tests gace a tensile strength of $\sigma_t = 3.4$ MPa. We want to model the rock strength. Use plots to estimate the failure criterion parameters and discuss the applicability of the (a) Linear Mohr-Coulomb criterion; (b) Non-linear Hoek-Brown criterion.

CHAPTER 9

INTRODUCTION TO THE CRITICAL STATE THEORY

9.1 The need for isotropic hardening in soil plasticity models

When it comes to soil modeling [23], perfect plasticity is limiting. Work-hardening shows potential because both shear and consolidation loading influence the yielding of soils. Accordingly, some authors proposed to include a cap to the Mohr-Coulomb yield surface. Current plastic compaction (or density) can be used as a hardening parameter to determine the evolution of cap surfaces. The introduction of work-hardening into soil mechanics led to the generalization of the family of soil models developed at Cambridge (e.g., the Cam-Clay model). Many more of these models have been proposed since then. A key feature of all these models has been the concept of critical states. The critial state theory (CST) anticipates that an ultimate, perfectly plastic state (the critical state) will be reached after large deformation.

Schofield and Wroth (1968) describe the concept of critical states in the following way: "The kernel of our idea is the concept that soil and other granular materials, if continuously distorted until they flow as a frictional fluid, will come into a well-defined critical state determined by two equations:
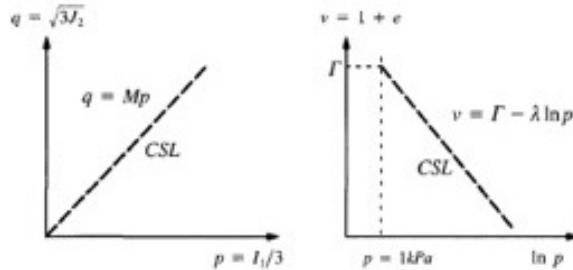
$$q = M\,p \tag{9.1}$$

$$\Gamma = v + \lambda\,ln(p) \tag{9.2}$$

The constants M, Γ and λ represent basic soil material properties and the parameters q, v, and p are defined in due course."

As a result the critical states depend on the mean effective stress p, shear stress q and soil

specific volume v and are shown graphically in Figure **??** as two straight lines (now known as the critical state lines CSL), where e denotes the void ratio.


Figure 9.1   Concept of critical states. Taken from [23].

Schofield and Wroth (1968) further explain that at the critical state, soils behave as a *frictional fluid* so that yielding occurs at constant volume and constant stresses. In other words, the plastic volumetric strain increment is zero at the critical state, since elastic strain increments will be zero due to the constant stress condition at the critical state. Also it was assumed that the critical state lines are unique for a given soil regardless of stress paths used to bring them about from any initial conditions.

9.2   Cam-Clay model (saturated soil)

In the following, we explain how a critical state-based, strain hardening plasticity model can be formulated, taking the Cam-Clay model as an example. For simplicity, we will only present the case of a triaxial test, that is, when two effective principal stresses are equal and the directions of principal stresses are fixed with respect to the material element. The generalization to a general three-dimensional case can be found in [23] (Section 6.10). Assuming compressive stresses and strains as positive, the two effective stress variables normally used in critical state soil mechanics are:

$$p = \frac{1}{3}\left(\sigma_1' + 2\sigma_3'\right), \quad q = \sigma_1' - \sigma_3' \tag{9.3}$$

where σ_1' and σ_3' denote effective vertical and radial stresses respectively. The corresponding strains are:

$$\epsilon_p = \epsilon_1 + 2\epsilon_3, \quad \epsilon_q = \frac{2}{3}\left(\epsilon_1 - \epsilon_3\right) \tag{9.4}$$

9.2.1   Work equation and plastic potential

The plastic work per unit volume of a triaxial sample with the externally applied mean and shear stresses p and q is:

$$\dot{W}_p = p\dot{\epsilon}_p^p + q\dot{\epsilon}_q^p \tag{9.5}$$

where ϵ_p^p and ϵ_q^p are the volumetric and shear plastic strains, respectively. It is assumed that all the plastic work, defined by Equation 9.5, is dissipated entirely in friction, namely:

$$\dot{W}_d = M\, p\, \dot{\epsilon}_q^p \tag{9.6}$$

where M is the ratio of q/p at the critical state. The energy conservation then requires:

$$\dot{W}_p = \dot{W}_d \tag{9.7}$$

which leads to the following work equation for the Cam-Clay model:

$$p\dot{\epsilon}_p^p + q\dot{\epsilon}_q^p = M\,p\,\dot{\epsilon}_q^p \tag{9.8}$$

The above work equation can be rearranged as:

$$\frac{q}{p} + \frac{\dot{\epsilon}_p^p}{\dot{\epsilon}_q^p} = M \tag{9.9}$$

Now let us assume that there exists a plastic potential for the soil that depends on both the mean and shear stresses:

$$g = g(p, q) = 0 \tag{9.10}$$

from which we can write the following:

$$\dot{\epsilon}_p^p = \lambda\,\frac{\partial g}{\partial p}, \quad \dot{\epsilon}_q^p = \lambda\,\frac{\partial g}{\partial q} \tag{9.11}$$

By noting that the plastic strain is normal to the plastic potential, it can be shown that:

$$\frac{\dot{\epsilon}_p^p}{\dot{\epsilon}_q^p} = -\frac{\dot{q}}{\dot{p}} \tag{9.12}$$

By substituting Equation 9.12 into Equation 9.9, we obtain:

$$\frac{q}{p} - \frac{\dot{q}}{\dot{p}} = M \tag{9.13}$$

which may be integrated to give an equation for the plastic potential:

$$g = g(p, q) = \frac{q}{p\,M} + ln\left(\frac{p}{p_0}\right) = 0 \tag{9.14}$$
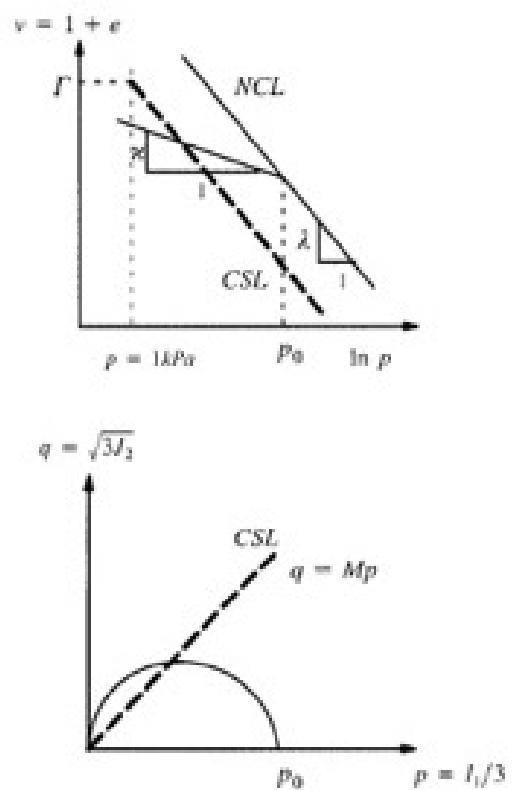
where p_0 is a constant which indicates the size of the plastic potential. Physically, it represents the mean stress when $q/p = 0$, as illustrated in Figure 9.2.

9.2.2 Associated plastic flow rule and yield criterion

In developing the Cam clay model, it was assumed that the soil obeys an associated flow rule so that the yield function is identical to the plastic potential. Hence

$$f = f(p, q, p_0) = \frac{q}{p\,M} + ln\left(\frac{p}{p_0}\right) = 0 \tag{9.15}$$

where p_0 is the preconsolidation pressure (see Figure 9.2) served as the hardening parameter that changes with the plastic strain.

Figure 9.2   The normal consolidation line (NCL), critical state lines (CSL) and yield surface (plastic potential). Taken from [23].

9.2.3   Plastic hardening law - volumetric hardening

It is clear from equation 9.15 that the size of the yield surface is represented by the preconsolidation pressure p_0 (Figure 6.2). In Cam clay, p_0 is assumed to change with the plastic volumetric strain in the following manner:

$$\dot{p}_0 = \frac{v\, p_0}{\lambda - \chi} \dot{\epsilon}_p^p \tag{9.16}$$

where χ is a material constant that represents the slope of elastic loading and unloading lines in a $v - lnp$ plot (see Figure 9.2).

9.2.4   Elastic component of the model

In Cam clay, it was assumed that the bulk modulus is proportional to the mean pressure p:

$$K = \frac{v\, p}{\chi} \tag{9.17}$$

The second elastic constant can be chosen by using either an assumed constant value of Poisson's ratio ν or an assumed constant value of shear modulus G. As it is usually more convenient to specify a value of Poisson's ratio, the shear modulus may therefore be assumed to vary with stress level in the same form as K:

$$G = \frac{3(1 - 2\nu)}{2(1 + \nu)} K \tag{9.18}$$

From a theoretical point of view, it would be preferable to assume a constant value of shear modulus, because the use of a constant Poisson's ratio would lead to a non-conservative model in the sense that it may not conserve energy during closed stress cycles.

9.2.5   The complete stress-strain relation

From equation 9.11 and noting that the hardening parameter p_0 in Cam clay is assumed to depend only on the plastic volumetric strain, we obtain the following equation:

$$\frac{\partial f}{\partial p}\dot{p} + \frac{\partial f}{\partial q}\dot{q} + \frac{\partial f}{\partial p_0}\frac{\partial p_0}{\partial \epsilon_p^p}\lambda\frac{\partial g}{\partial p} = 0 \tag{9.19}$$

The above equation gives the expression for the non-negative plastic multiplier:

$$\lambda = -\frac{\frac{\partial f}{\partial p}\dot{p} + \frac{\partial f}{\partial q}\dot{q}}{\frac{\partial f}{\partial p_0}\frac{\partial p_0}{\partial \epsilon_p^p}\frac{\partial g}{\partial p}} = \frac{1}{K_p}\left(\frac{\partial f}{\partial p}\dot{p} + \frac{\partial f}{\partial q}\dot{q}\right) \tag{9.20}$$

where:

$$K_p = -\frac{\partial f}{\partial p_0}\frac{\partial p_0}{\partial \epsilon_p^p}\frac{\partial g}{\partial p} \tag{9.21}$$

Equation 9.20 can be substituted into equation 9.11 to give the expression for the plastic strain increments:

$$\dot{\epsilon}_p^p = \lambda\frac{\partial g}{\partial p} = \frac{\frac{\partial g}{\partial p}}{K_p}\left(\frac{\partial f}{\partial p}\dot{p} + \frac{\partial f}{\partial q}\dot{q}\right) \tag{9.22}$$

$$\dot{\epsilon}_q^p = \lambda\frac{\partial g}{\partial q} = \frac{\frac{\partial g}{\partial q}}{K_p}\left(\frac{\partial f}{\partial p}\dot{p} + \frac{\partial f}{\partial q}\dot{q}\right) \tag{9.23}$$

By adding the elastic strain increments, we can obtain the following elastic-plastic relations between stress increments and strain increments:

$$\dot{\epsilon}_p = \dot{\epsilon}_p^e + \dot{\epsilon}_p^p = \frac{1}{K}\dot{p} + \frac{\frac{\partial g}{\partial p}}{K_p}\left(\frac{\partial f}{\partial p}\dot{p} + \frac{\partial f}{\partial q}\dot{q}\right) \tag{9.24}$$

$$\dot{\epsilon}_q = \dot{\epsilon}_q^e + \dot{\epsilon}_q^p = \frac{1}{3G}\dot{q} + \frac{\frac{\partial g}{\partial q}}{K_p}\left(\frac{\partial f}{\partial p}\dot{p} + \frac{\partial f}{\partial q}\dot{q}\right) \tag{9.25}$$

For Cam clay, all the differentiations needed to define the incremental stress-strain relations 9.24 and 9.25 are given as follows:

$$\frac{\partial f}{\partial p} = \frac{\partial g}{\partial p} = -\frac{q}{M\,p^2} + \frac{1}{p} \tag{9.26}$$

$$\frac{\partial f}{\partial q} = \frac{\partial g}{\partial q} = \frac{1}{M\,p} \tag{9.27}$$

$$\frac{\partial f}{\partial p_0} = -\frac{1}{p_0} \tag{9.28}$$

$$\frac{\partial p_0}{\partial \epsilon_p^p} = \frac{\lambda - \chi}{v\,p_0} \tag{9.29}$$

PART IV

APPENDICES

APPENDIX A

BIBLIOGRAPHY

REFERENCES

1. Atkinson, J. (1981). An introduction to the mechanics of soils and foundations: through critical state soil mechanics. John Wiley & Sons, New-York.

2. D. Assimaki (2014). Theoretical Geomechanics. CEE 6460 graduate course notes. Georgia Institute of Technology.

3. D. Aubry and P.E. Gautier (2003). Mécanique I. Mécanique des milieux continus. Course notes. Ecole Centrale de Paris.

4. B.H.G. Brady, E.T. Brown (2004). Rock Mechanics for Underground Mining, third edition. Springer.

5. P. Dangla (2010). Introduction à la Mécanique des Milieux Poreux. Course notes. Ecole Nationale des Ponts et Chaussées.

6. L. Dormieux (2006). Mécanique des milieux continus. Course notes. Ecole Nationale des Ponts et Chaussées.

7. echo2.epfl.ch (January 2016)

8. Falkingham, P. (2019). Computer simulation of dinosaur tracks. Ph.D. Thesis.

9. J.M. Gere & B.J. Goodno (2013). Mechanics of Materials, 8th edition, CENGAGE Learning, ISBN-13:9781111577735

10. Y. Gueguen, J. Dienes (1989). Transport properties of rocks from statistics and percolation. Mathematical geology, 21(1), 1-13.

11. Y. Gueguen, V. Palciauskas (1994). Introduction to Rock Physics. Princeton University Press.

12. Houlsby, G. T., & Puzrin, A. M. (2007). Principles of hyperplasticity: an approach to plasticity theory based on thermodynamic principles. Springer Science & Business Media

13. Jaeger, J. C., Cook, N. G., & Zimmerman, R. (2009). Fundamentals of rock mechanics. John Wiley & Sons.

14. Lewis, R. W., Schrefler, B. A. (1998). The finite element method in the static and dynamic deformation and consolidation of porous media. John Wiley.

15. G. Mavko, T. Mukerji, J. Dvorkin (2009). The Rock Physics Handbook: Tools for Seismic Analysis of Porous Media. Cambridge University Press.

16. D. Mohr (2015). Basic notions of fracture mechanics and ductile fracture. Course notes. ETH Zurich.

17. Poulos, H.G. and Davis, E.H. (1974) Elastic Solutions for Soil and Rock Mechanics, Wiley & Sons.

18. Reddy, J. N. (2004). An introduction to the finite element method (Vol. 1221). New York, USA: McGraw-Hill.

19. stadtentwicklung.berlin.de (January 2016)

20. Verruijt, A. (2013). Theory and problems of poroelasticity. Delft University of Technology.

21. Wikipedia, January 2020. Determinant.

22. Wikipedia (2020). Mohr's Circle. wikipedia.org

23. Yu, H. S. (2007). Plasticity and geotechnics (Vol. 13). Springer Science & Business Media

24. Zhang, S., Lai, Y., Sun, Z., & Gao, Z. (2007). Volumetric strain and strength behavior of frozen soils under confinement. Cold regions science and technology, 47(3), 263-270.

25. Zienkiewicz, O. C., Chan, A. H. C., Pastor, M., Schrefler, B. A., Shiomi, T. (1999). Computational geomechanics. Chichester: Wiley.

26. Zienkiewicz, O. C., Taylor, R.L. (2000). The Finite Element Method. Volume 1: The Basis. Butterworth Heinemann, Fifth edition.